Ebola virus replication leading to viral load as a predictor of disease severity and transmission

Thèse

Marc-Antoine De La Vega

Doctorat en microbiologie-immunologie
Philosophiæ doctor (Ph. D.)

Québec, Canada

EBOLA VIRUS REPLICATION LEADING TO VIRAL LOAD AS A PREDICTOR OF DISEASE SEVERITY AND TRANSMISSION

Thèse

Marc-Antoine de La Vega

Sous la direction de :

Gary Kobinger, Ph.D., directeur de recherche

Résumé

Le virus Ebola (EBOV) est l'agent étiologique de la maladie à virus Ebola (MVE), une maladie à progression fulgurante qui peut atteindre des taux de mortalité allant jusqu'à 90%. Malgré le fait que ce virus ait été découvert en 1976, ce n'est pas avant 2014 que le public fut exposé à ses effets dévastateurs, alors que l'épidémie de 2014-2016 qui a frappé l'Afrique de l'Ouest ne soit déclarée une urgence de santé publique à portée internationale, et où plus de 28 000 individus seront touchés principalement en Guinée, au Sierra Leone, et au Libéria, mais également aux États-Unis et en Europe. Une des raisons principales qui fait en sorte que notre compréhension du virus n'évolue pas aussi rapidement que pour d'autres agents pathogènes est qu'EBOV doit être manipulé dans le plus haut niveau de sécurité biologique, c'est-à-dire un laboratoire de niveau de confinement 4. Ce type de laboratoire est rare, et le fait de devoir contenir le virus à l'intérieur de celui-ci complexifie le nombre d'expériences pouvant y être effectué. De plus, aucune intervention prophylactique ou thérapeutique n'a été disponible pendant plus de 40 ans. La majorité des travaux effectués ont donc continuellement cherché à pallier à ce manque. Ainsi, un important travail a été effectué afin de comprendre la nature des réponses immunitaires suite à l'infection, puisque cette dernière peut mieux diriger le développement de mesures efficaces. Cependant, peu d'études se sont penchées sur la caractérisation des propriétés virales basiques, tels que les déterminants viraux associés avec la pathogénèse et la transmission du virus. Dans cette thèse, le rôle spécifique de la charge virale, résultant de la réplication du virus Ebola, est évalué dans un contexte de sévérité de la maladie et de transmission.

Dans un premier temps, un état général des connaissances quant à EBOV et son cycle de vie est présenté, ainsi que de la manière dont le virus se comporte chez l'humain et dans les modèles animaux. Dans le premier chapitre de cette thèse, l'association entre la charge virale et l'issue suite à la maladie est décrite dans un contexte d'une épidémie naturelle chez l'humain. Dans un contexte de diagnostic, la virémie de patients qui se sont présentés à un centre de traitement Ebola a été évaluée, mais de plus amples analyses ont révélées que ceux qui se présentaient avec une virémie moindre étaient plus susceptible de se rétablir, une mesure indirecte de la sévérité de la maladie. Dans le second chapitre, un nouveau modèle de transmission chez le furet est décrit, où la transmission résultant d'un contact direct ou indirect a été évaluée simultanément. Alors que les mâles en contact direct avec un furet infecté ont développé et succombé à la MVE dans un laps de temps correspondant à une infection par leur compagnon de cage en phase terminale, aucune femelle n'a développer la MVE ou possédait une charge virale détectable. Cependant, tous les animaux contacts directs et indirects ont expérimenté une séroconversion à EBOV, suggérant que dans ce modèle une transmission par contact indirect est fréquente, mais résulte en une maladie clinique moins sévère. Finalement, dans le dernier chapitre de cette thèse, le rôle de la charge virale et de la voie d'infection est évalué dans un modèle de primates non-humains.

Dans une série d'expériences indépendantes, une infection intraoesophagienne ou par exposition du visage des animaux à des aérosols n'a pas résulté en une infection clinique ou une virémie. Cependant, les animaux en contact direct avec ceux infecté par aérosol ont tous développé des anticorps spécifiques contre EBOV. Des expériences additionnelles utilisant un modèle d'infection intramusculaire ou intratrachéale suggèrent que la charge virale détermine la transmission d'EBOV dans un contexte d'infection intramusculaire, puisque le seul animal ayant transmis avec succès EBOV à son compagnon de cage était celui démontrant les plus hauts niveaux de virémie et sécrétion virale. Cette transmission est facilitée dans un modèle d'infection intratrachéale, puisqu'elle a été observée de manière consistante entre les animaux infectés et contacts. En effet, la charge virale mesurée dans les sécrétions mucosales des animaux infectés était plus élevée que celle de l'animal ayant transmis EBOV lors de l'infection intramusculaire, suggérant que dans ce modèle d'infection, la charge virale sécrétée est associée avec la transmission d'EBOV.

Abstract

Ebola virus (EBOV) is the etiological agent responsible for Ebola virus disease (EVD), a rapidly progressing infection which has historically reached case fatality rates of up to 90%. Although the virus was first identified in 1976, it was not until 2014 that the general public was exposed to its devastating impacts, as the 2014-2016 West African Ebola outbreak was declared a public health emergency of international concern and affected over 28,000 individuals, mostly in Guinea, Sierra Leone, and Liberia, but also in the United States and Europe. One of the main reasons that hinders our ability to characterize this disease extensively and rapidly is that handling this virus requires the highest level of biosafety containment available, namely biosafety level 4. These facilities are scarce world-wide, and the need to maintain high confinement usually limits the size and volume of the experiments that can be safely performed within. Given that for over 40 years, no medical countermeasures were available, a large proportion of available biosafety level 4 (BSL-4) resources was dedicated to solving this pressing issue. As such, a large amount of important work has focused on understanding the immune responses to infection, as they can better direct the development of efficacious countermeasures. Conversely, little has been done to characterize basic viral properties, such as viral determinants associated with pathogenicity and transmission of this virus. In this thesis, the role of viral loads specifically, as a result of virus replication, is evaluated with regards to pathogenicity and transmission.

In the first section of this document, the current state of knowledge related to EBOV and its life cycle is presented, as well as what is currently known about how the virus behaves in both humans and animal models. In the first chapter of this thesis, the association between viral load and outcome is described from a human outbreak perspective. In the context of diagnostics, viremia of individuals who presented at an Ebola management center was assessed, but a follow-up analysis revealed that individuals who presented for care with a lower viremia better associated with recovery—an indirect measure of disease severity. In the second chapter, a novel ferret model for transmission is described, where transmission resulting from direct and indirect contact could be evaluated simultaneously. While male direct contact animals developed and succumbed to clinical EVD in a timeframe consistent with infection by their terminally-ill challenged cagemate, no female contact animals became viremic or symptomatic. Interestingly, all direct and indirect contact animals seroconverted against EBOV, suggesting that in this model indirect transmission is frequent but results in a less-severe disease. Finally, in the final chapter of this thesis, the role of viral loads, as well as route of infection, was evaluated thoroughly in non-human primates. In a series of independent experiments, intraesophageal and facial aerosol exposure did not result in clinical EVD or viremia, but interestingly, all contact animals from the latter challenge seroconverted. Additional intramuscular or intratracheal challenge studies suggest that viral loads determine transmission of EBOV in an intramuscular challenge, as only the animal exhibiting the highest viral load was

able to transmit EBOV to its contact cagemate. This transmission was found to be facilitated when using an intratracheal route of infection, as transmission was observed consistently from an infected to a naïve cagemate. Interestingly, viral loads as a result of shedding were found to be higher than those of the transmitting animal from the intramuscular challenge, suggesting that in this model, viral load as a result from shedding associate with transmission.

Table of content

List of figures

Supplemental figures:

List of tables

Supplemental tables:

List of abbreviations

AdHu5:	Human type 5 adenovirus
Ag:	Antigen
ALT:	Alanine transaminase
ANOVA:	Analysis of variance
aPTT:	Activated prothrombin time
AST:	Aspartate transaminase
BCL-2:	B-cell lymphoma 2
BDBV:	Bundibugyo virus
BOMV:	Bombali virus
BSL-4:	Biosafety level 4
CCL:	C-C motif chemokine ligand
CDC:	Centers for disease control and prevention
CFR :	Case fatality rate
CI:	Confidence interval
CIHR:	Canadian Institute for Health Research
COPII:	Coat protein complex II
CPK:	Creatine phosphokinase
CSR:	Case survival rate
CT:	Cycle threshold
CTD:	C-terminus domain
DC:	Dendritic cell
DC-SIGN	DC-Specific Intercellular adhesion molecule-3-Grabbing Non-integrin
DMEM:	Dulbecco's modified Eagle's medium
DNA:	Deoxyribonucleic acid
dpi:	Days post-infection
DRC:	Democratic Republic of the Congo
EBOV:	Ebola virus
EDTA:	Ethylenediaminetetraacetic acid
EHF :	Ebola hemorrhagic fever
eIF-2α:	Eukaryotic initiation factor 2 alpha
ELISA:	Enzyme-linked immunosorbent assay
EM:	Electron microscopy
EMA:	European Medicines Agency
EMC:	Ebola management center
ER:	Endoplasmic reticulum
ESCRT:	Endosomal sorting complex required for transport
EVD :	Ebola virus disease
FDA:	Food and drug administration
ffu:	Focus forming units
GA-EBOV:	Guinea pig-adapted EBOV
GEQ:	Genome equivalent copies
GP:	Glycoprotein
HIV:	Human immunodeficiency virus
HUJV:	Huángjiāo virus
ICTV:	International Committee on Taxonomy of Viruses
IDT:	Integrated DNA Technologies
IFA:	Indirect fluorescent antibody
IFN:	Interferon

IFNAR:	Interferon alpha and beta receptor
Ig :	Immunoglobulin
IKKε:	Inhibitor of nuclear factor kappa-B kinase
IL:	Interleukin
i.m.:	Intramuscularly
i.n.:	Intranasally
INR:	International normalized ratio
i.p.:	Intraperitoneally
IPC:	Infection prevention and control
IQGAP1:	IQ Motif Containing GTPase Activating Protein 1
IRF:	Interferon regulatory factor
kb:	Kilobase
kDa:	Kilodalton
KGH:	Kenema general hospital
L:	EBOV Viral polymerase
L-SIGN:	Liver/lymph node-specific intracellular adhesion molecules-3 grabbing non-integrin
LDH:	Lactate dehydrogenase
LLOV:	Lloviu virus
mAb:	Monoclonal antibody
MA-EBOV:	Mouse-adapted Ebola virus
MAP:	Mitogen-activated protein
MARV:	Marburg virus
MDA5:	Melanoma differentiation-associated protein 5
mDC:	Myeloid DC
MHC:	Major histocompatibility complex
MLAV:	Měnglà virus
MoH:	Ministry of health
mRNA:	messenger RNA
MSF:	Médecins Sans Frontières
NCBI:	National Center for Biotechnology Information
NHP:	Non-human primate
NK:	Natural killer
NML:	National microbiology laboratory
NP:	Nucleoprotein
NPC1:	Niemann-Pick C1
nt:	Nucleotide
ORF:	Open reading frame
PACT:	PKR activator protein
PAMP:	Pathogen-associated molecular patterns
PBS:	Phosphate buffered saline
PCR:	Polymerase chain reaction
PEVDS:	Post-EBOV disease syndrome
PFU:	Plaque forming units
PHAC:	Public Health Agency of Canada
PKR:	Protein kinase R
PP1:	Protein phosphatase 1
PP2A-B56:	Protein phosphatase 2A-B56 domain
PPE:	Personal protective equipment
PPV:	Positive predictive value
PS:	Phosphatidylserine
qPCR:	Quantitative PCR

RAVV:	Ravn virus
RBBP6:	Retinoblastoma-binding protein 6
RDT:	Rapid diagnostic test
RESTV:	Reston virus
RIG-I:	Retinoic acid-inducible gene I
RNA:	Ribonucleic acid
RNAi:	Ribonucleic acid interference
RNP:	Ribonucleoprotein
ROC:	Receiver operating characteristic
RT-PCR:	Reverse transcription PCR
s.c.:	Subcutaneously
SD:	Standard deviation
sGP:	Secreted glycoprotein
ssGP:	Small secreted glycoprotein
STAT1:	Signal transducer and activator of transcription 1
SUDV:	Sudan virus
TAFV:	Taï Forest virus
TBK1:	TANK-binding kinase 1
$TCID_{50}$:	Median tissue culture infectious dose
TCR:	T cell receptor
TIM-1:	T-cell immunoglobulin and mucin domain 1
TNFα:	Tumour necrosis factor alpha
TLR:	Toll-like receptor
USA:	United States of America
UTR:	Untranslated region
VP:	Viral protein
VSV:	Vesicular stomatitis virus
WHO:	World health organization
WT:	Wild-type
XILV:	Xīlǎng virus

To my loving parents,

Acknowledgement

Throughout the last few years, I've come to the realization that none of this endeavour could have been possible without the support of numerous individuals. First and foremost, I would like to thank my supervisor and mentor Gary Kobinger. You have taught me about the importance of communication, collaboration, open science, and data sharing through your involvement with health emergency responses and the World Health Organization. Conversely, you have also taught me about independence as not everyone I may meet during my career may be as supportive as you have showed me to be. You have taught me that innovation and change can be challenging to implement in the current system, but perseverance and good science will eventually pay off. However, what I'm most grateful for is the diversity of experiences and skills I've got to witness and learn by your side, something that very few graduate students I've met can say. I had the opportunity of being involved in fundamental, translational, pre-clinical, and clinical work. I was trained to work within laboratories of all four biosafety levels. You had me involved in numerous projects that are unrelated to this thesis, but have been critical in expanding my horizons, making me understand that there is more to a graduate program than the project right in front you. Most importantly, you brought me out into the field—four times in Africa for Ebola outbreak response and training, and countless more times all around Canada during the COVID-19 pandemic to assist with diagnostics—away from the comfort of petri dishes, where I could witness what the viruses that we spend so much time studying were actually capable of. I had the opportunity of meeting amazing people along the way, both locally and internationally, and if at 23 years old, landing alone at three o'clock in the morning in Conakry, Guinea, amidst the largest Ebola outbreak ever recorded doesn't build character, I don't know what will. Thank you for having faith in me and to keep offering me opportunities to help me grow as a person and a scientist.

Next, I would like to thank Dr. Darryl Falzarano, as an external examiner, and Dr. Mariana Baz and Dr. Sachiko Sato, as internal examiners, to have accepted to review this work on such short notice. Your input on this work will be invaluable in furthering my development as a scientist.

Switching universities during the middle of my graduate studies has brought its fair share of challenges, but it also means you get to meet even more amazing individuals and scientists along the way. While they cannot all be singled out—that would be a whole thesis on its own—I would like to thank everyone from Special Pathogens who has helped me at one point or another. Kaylie, Geoff, Anders, Kevin, Bello and Derek, thank you for helping out with experiments. Qiu, Wong, Fausth, Trina, and Jonathan, thank you the countless revisions to manuscripts and presentations, as well as scientific discussions. Learning from you has been a privilege I wish will never stop.

Finally, my sanity would not be at the level it currently is if it was not for the constant support of family and friends. Mom and dad, thank you for always supporting me at every level. I am aware of how lucky I have been in all this and thanks to you, I could always focus on my studies without having to worry about anything else. It is now time for you to enjoy retirement, knowing that I have made it to the finish line and that you will have one more diploma to hang in the stairs back home. To my Winnipeg Squad, thank you for making my time there so enjoyable. I have never hidden the fact that Winterpeg was far from being my favorite city, but one thing is true, ‘’Friendly Manitoba’’ is an accurate statement. Whether it was cabins, weddings, or long nights out, they will always be remembered and for you guys, I would not mind going back to Winnipeg. Last but not least, to all my friends back at home in Quebec, thank you for being there whenever I needed to unwind. Whether it was in person or online, you made me feel like I was never alone, wherever I might have been in the world. Thank you for picking me up at airports, offering me a place to stay, or entertaining me through your crazy plans.

Even though I plan to keep on moving all around the globe, I’m happy to know that I won’t have to do it alone, and that family and friends back home will be there to support me.

Foreword

These past few years of graduate studies have been anything but typical. However, one element that has remained constant throughout these years and has always brought me a feeling of accomplishment is my contribution to various fields, through the publication of peer-reviewed articles. Indeed, since 2014, I have contributed as a first author to seven publications—three data papers and four reviews—and as a co-author, I have contributed to 13 publications—11 data papers, one review and one book chapter. Furthermore, I have two additional first author data papers in preparation—one of those being presented in this thesis as chapter 3—, as well a four co-author data papers. Finally, I have also had the opportunity of getting deployed to the Democratic Republic of the Congo twice, to Guinea, and to Burundi in order to assist Médecins Sans Frontières or the World Health Organization with Ebola virus disease outbreak response, either as support for diagnostics, or for training purposes.

In the context of this thesis, the three main chapters have been generated through the insertion of published and unpublished manuscripts, for which details regarding publication status and authorship are described below.

Chapter 1: Ebola viral load at diagnosis associates with patient outcome and outbreak evolution.

This article was received by *The Journal of Clinical Investigation* on June 8th 2015, accepted on September 28th 2015, and published online on November 9th 2015. Of note, the data used in this article was generated by members of the Special Pathogens group (National Microbiology Laboratory, Winnipeg, MB), as part of diagnostic support to *Médecins Sans Frontières (MSF)* during the months of July to December 2014, during the 2014-2016 West African Ebola outbreak. Two members from the group were deployed for periods of 5 weeks, in rotations, to Sierra Leone, where data was generated in the field as part of diagnostic activities. However, for insurance purposes, students were not allowed to deploy as part of these rotations, hence why I was unable to generate the data myself.

For this publication, as first author, I had the main responsibility of study design, writing the first draft of manuscript, handle the edits from the co-authors, and using the database prepared by colleagues, I've also generated Figure 1A-C, Figure 2A-B, Figure 3, and Figure 5. Grazia Caleo, the co-first author, is an MSF epidemiologist which had the responsibility, along with Anja Wolz and Jane Greig to prepare the database that would be used for analysis, as MSF was in control of the medical information regarding patients. Jonathan Audet assisted with generating Table 1, Figure 4, and all statistical analyses. He also provided assistance in the redaction of the first draft, and along with Robert A. Kozak, handled the revisions from reviewers as I was at the time deployed to Guinea to support outbreak response, under MSF. The data itself was generated by Xiangguo Qiu, James I. Brooks, Allen Grolla, Darwyn Kobasa, James E. Strong and Gary P. Kobinger. Steven Kern

provided assistance by generating Figure 2C. Armand Sprecher assisted with the study design and, along with Kamalini Lokuge, Antonino Di Caro, Giuseppe Ippolito, and Michel Van Herp, provided valuable comments regarding the conclusions of the manuscript. Gary Kobinger also assisted with study design and editing the manuscript. Finally, David K. Kargbo and Brima Kargbo were members of the Ministry of Health in Sierra Leone which facilitated the use of the data for publication.

Chapter 2: Modeling Ebola virus transmission using ferrets.

This article was received by *mSphere* on June 6th 2018, accepted for publication on October 8th 2018, and published online on October 31st 2018. Of note, for obvious biosafety reasons, part of this work had to be conducted inside a biosafety level (BSL) 4 laboratory (BSL4), where the handling of sharps and the inactivation of samples so that they can be analyzed inside a biosafety level 2 laboratory, can only be done by trained individuals, tasks for which I did not receive the appropriate training to perform myself.

For this publication, as first author, I was involved in study design, performed the daily husbandry of animals inside BSL4, assisted qualified individuals with sample collection on the required days, had the main responsibility of writing the manuscript, and generated the data for all figures and supplemental material, except for Figure 4. Geoff Soule performed the ELISAs that generated the data for Figure 4, and along with Kaylie N. Tran and Shihua He, assisted with sample processing inside the BSL4 laboratory for their use inside a biosafety level 2 laboratory. Kevin Tierney is the animal technician which collected the samples from the animals. Gary Wong, Xiangguo Qiu, and Gary Kobinger helped with data analysis and manuscript editing.

Chapter 3: Role of key infectivity parameters in the transmission of Ebola virus Makona in macaques.

This manuscript has not been peer reviewed yet, but was submitted to *The Journal of Infectious Diseases* on June 10th 2021 and has been under review by the editors since June 23rd 2021. Similar to the ferret study above, the majority of the experiments regarding this study were performed inside a BSL4 laboratory. Given the highly demanding nature of non-human primates, a fact that is amplified under BSL4 conditions, sample collection days necessitate the majority of team members to be available and inside the BSL4 laboratory. This allows efficient processing of the animals and samples, while respecting the limited amount of time an individual is allowed to spend consecutively inside a BSL4 facility. Of note, I was not personally trained to enter the BSL4 laboratory at the time, hence could not participate in sample collection directly.

For this publication, as first author, I had the main responsibility of generating all figures, measuring viral loads by PCR inside a biosafety level 2 laboratory (supplemental figures 3, 6, and 8) and writing the first draft of the manuscript. Gary Wong and Gary Kobinger provided assistance with editing the manuscript, and were involved, along with Haiyan Wei, Shihua He, Alexander Bello, Hugues Fausther-Bovendo, Jonathan Audet, Kevin Tierney, Kaylie Tran, Geoff Soule, Trina Racine, James E. Strong, and Xiangguo Qiu, in sample collection inside the

BSL4 laboratory. Geoff Soule also conducted the ELISA for Figure 1, Supplemental Table 1, and Supplemental Figure 5. Finally, Trina Racine performed the live virus titration required for Figure 3, 4, and 5, based on samples positive by PCR, once I had moved to Université Laval and lost access to the BSL4 facility.

Introduction

Nomenclature and taxonomy

Proper nomenclature for filoviruses regarding the United States National Center for Biotechnology Information (NCBI) database should be based on the following template: <virus name>(/<strain>)/<isolation host-suffix>/<country of sampling>/<year of sampling>/<genetic variant designation>-<isolate designation>. Regarding <isolation host-suffix>, the isolation host should be written in the format ''first letter of the host genus name.full name of species descriptor'', such as ''H.sapiens'' if the virus was originally isolated from a clinical case. The suffix represents whether the sequence is coming from an unpassaged sample (-wt), a virus isolated in tissue culture (-tc), represents a genomic fragment (-frag), is no longer available for laboratory studies anymore (-hist), or was adapted experimentally to cells or animals it would not naturally be able to infect (-lab)[1–3]. The genus *Ebolavirus* is currently composed of six species: *Bombali ebolavirus*, *Bundibugyo ebolavirus*, *Reston ebolavirus*, *Sudan ebolavirus*, *Taï Forest ebolavirus* and *Zaire ebolavirus*, each represented by a single member; Bombali virus (BOMV), Bundibugyo virus (BDBV), Reston virus (RESTV), Sudan virus (SUDV), Taï Forest virus (TAFV) and Ebola virus (EBOV), respectively (Figure 1: Taxonomy of members of the Filoviridae family). *Ebolavirus* is part of the *Filoviridae* family, under the *Mononegavirales* order. According to the International Committee on Taxonomy of Viruses (ICTV), this order has always stood on its own but a recent proposal to unify all negative-sense ribonucleic acid (RNA) viruses under a common phylum, in order to replace the unofficial Baltimore classification, has been made. As of July 2018, the *Mononegavirales* order is now a member of the *Monjiviricetes* class under the subphylum *Haploviricotina*, which in turn is part of the unifying phylum *Negarnaviricota*. The *Filoviridae* family also includes two other genera that are genetically closely related to *Ebolavirus*, *Cuevavirus* and *Marburgvirus*. These genera are represented by a single

Realm: *Riboviria*
Kingdom: *Orthornavirae*
Phylum: *Negarnaviricota*
Subphylum: *Haploviricotina*
Class: *Monjiviricetes*
Order: *Mononegavirales*
Family: *Filoviridae*
Genus: *Cuevavirus*
Species: *Lloviu cuevavirus*
Virus: Lloviu virus (LLOV)
Genus: *Dianlovirus*
Species: *Mengla dianlovirus*
Virus: Měnglà virus (MLAV)
Genus: *Ebolavirus*
Species: *Bombali ebolavirus*
Virus: Bombali virus (BOMV)
Species: *Bundibugyo ebolavirus*
Virus: Bundibugyo virus (BDBV)
Species: *Reston ebolavirus*
Virus: Reston virus (RESTV)
Species: *Sudan ebolavirus*
Virus: Sudan virus (SUDV)
Species: *Tai Forest ebolavirus*
Virus: Taï Forest virus (TAFV)
Species: *Zaire ebolavirus*
Virus: Ebola virus (EBOV)
Genus: *Marburgvirus*
Species: *Marburg marburgvirus*
Virus: Marburg virus (MARV)
Virus: Ravn virus (RAVV)
Genus: *Striavirus*
Species: *Xilang striavirus*
Virus: Xīlàng virus (XILV)
Genus: *Thamnovirus*
Species: *Huangjiao thamnovirus*
Virus: Huángjiāo virus (HUJV)

Figure 1: Taxonomy of members of the Filoviridae *family*

species each, *Lloviu cuevavirus* and *Marburg marburgvirus*, respectively. The former consists of a single representative, Lloviu virus (LLOV), while the latter is represented by two distinct viruses, Marburg virus (MARV) and Ravn virus (RAVV)[3,4]. Recent genomic screenings of various animal species are, however, in the process of expanding the *Filoviridae* family. Indeed, BOMV was recently identified following the screening of little free-tailed (*Chaerephon pumilus*) and Angolan free-tailed bats (*Mops condylurus*) in 2018 in Sierra Leone, and is described as a sixth species of the *Ebolavirus* genus[5]. Two other filoviruses, initially described as Wēnlǐng frogfish filovirus and the Wēnlǐng thamnaconus septentrionalis filovirus, were identified following the screening of a striated frogfish (*Antennarius striatus*) and a filefish (*Thamnaconus septentrionalis*), respectively. These are described as members of novel species of two new genera of *Filoviridae*, *Striavirus* and *Thamnovirus*. The Wēnlǐng frogfish filovirus has since been renamed Xīlǎng virus (XILV) and is the sole representative of the *Xilang striavirus* genus, while the Wēnlǐng thamnaconus septentrionalis filovirus was renamed Huángjiāo virus (HUJV) and is the sole representative of the *Huangjiao thmanovirus* genus[6,7]. Finally, a novel filovirus, the Měnglà virus (MLAV), was sequenced in a *Rousettus* bat in China. Phylogenetic analysis revealed that MLAV could constitute a novel genus of *Filoviridae*[8].

Virus structure

Morphology

The prefix filo-, in Filoviridae, is derived from the Latin noun filum which is defined as a thread, filament or string. EBOV, similar to other filoviruses, is no exception and possesses a filamentous morphology. Although fairly consistent in width, averaging 80-100 nm, EBOV particles can vary greatly in length and shape such as simple, branched, U- or 6-shaped[9,10]. A striking feature of EBOV is that three different virion structures have been described so far. Single virions average approximately 1000 nm and contain a single copy of the genome (Figure 2: Schematic of Ebola virus structure

Figure 3: Schematic representation of a typical EBOV genomeFigure 4). However, more complex structures have been described as polyploid and therefore contain several copies of the EBOV genome, a number that can reach as high as 20. These structures therefore considerably extend the length of the viral particle to 20 µm or longer, and can be found in two different configurations—linked or continuous. Continuous particles are enveloped, single nucleocapsids that contain two or more copies of the genome, whereas linked particles are described as containing two or more individual genome nucleocapsids that are enveloped together[11,12].

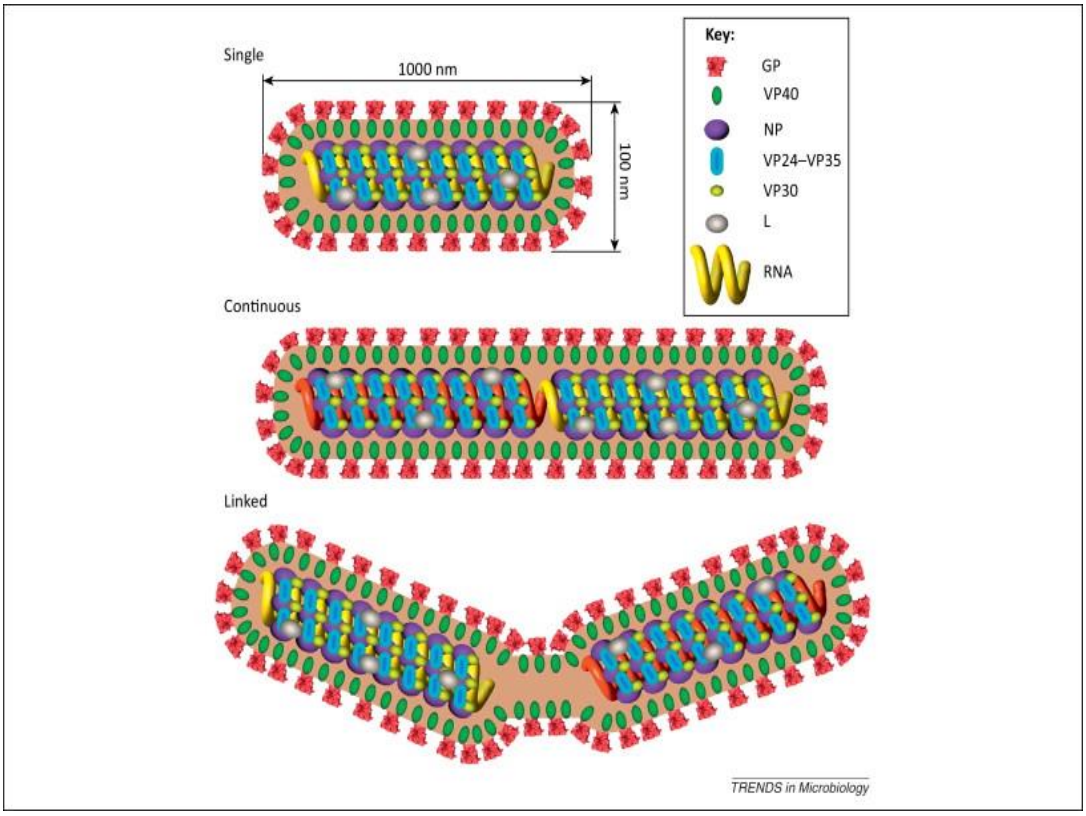

Figure 2: Schematic of Ebola virus structure

Reprinted from *Trends in Microbiology*, Vol 21, Booth T. F. *et al*., How do filovirus filaments bend without breaking?, Pages 583-593, Crown copyright © 2013, with permission from Elsevier.

Genome organization

The EBOV genome consists of a non-segmented, linear, negative-sense and single-stranded RNA that is approximately 19 kilobases (kb) in length[13]. It is organized in the following order: a conserved 3' non-coding region followed by seven genes, which encode a total of nine proteins, and is terminated by a conserved 5' non-coding region. From 3' to 5', the genes are ordered as followed: nucleoprotein (NP), viral protein (VP) 35 (VP35), VP40, glycoprotein/soluble glycoprotein/small soluble glycoprotein ($GP_{1,2}$/sGP/ssGP), VP30, VP24, and the viral polymerase (L). Genes are separated by intergenic regions, but on three occasions possess overlapping start and stop sites, located between VP35 and VP40, GP/sGP/ssGP and VP30, as well as VP24 and L (Figure 5: Schematic representation of a typical EBOV genome

The model genome used for this figure is the genome of the reference isolate Ebola virus/H.sapiens-tc/COD/1976/Yambuku-Mayinga. Created with BioRender.com

Figure 6: Ebola virus genome structure and life cycle.Figure 7). Each EBOV gene is flanked by a transcription start signal, consisting of a conserved 12 nucleotides (nt) sequence (3'-CU[C/A]CUUCUAAUU-5') and a consensus stop signal (3'-UAAUUCUUUUU[U]-5')[14–16].

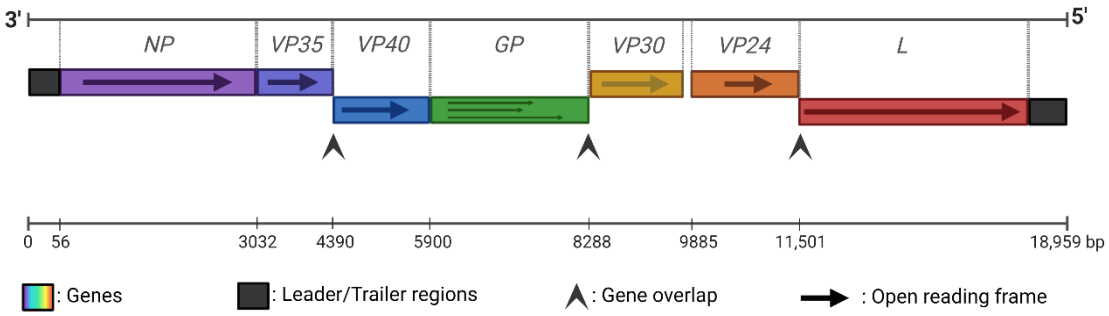

Figure 5: Schematic representation of a typical EBOV genome

The model genome used for this figure is the genome of the reference isolate Ebola virus/H.sapiens-tc/COD/1976/Yambuku-Mayinga. Created with BioRender.com

Viral proteins

As mentioned previously, the first protein encoded by the EBOV genome is NP[17]. Its calculated molecular weight is 83.3-85 kilodaltons (kDa) but the observed molecular weight is actually closer to 104-115 kDa, initially thought to be due to post-translational modifications such as O-glycosylation and sialyation[18]. However, additional studies revealed that this aberrant migration was rather due to two regions of the COOH-terminal domain, namely amino acids 439-492 and 589-739[19]. Indeed, mass spectrometry analysis of NP in reductive elimination experiments, which allows detection of glycans at the picomolar level, could not detect any carbohydrate modifications. The NP is a key element of the ribonucleoprotein (RNP) complex, essential for transcription and replication. It physically binds to both VP30 and VP35, as well as RNA, protecting it from degradation. It forms a helical structure and, interestingly, has been observed *in vitro* to bind to cellular RNA, even in absence of an active viral infection, suggesting it does not specifically distinguish between viral and non-viral EBOV RNA[20].

VP35 is one of the most polyvalent proteins encoded by EBOV. As mentioned above, VP35 interacts with NP as a nonenzymatic component of the RNP complex, essential for viral RNA synthesis[21], but also serves as a structural protein due to its role, along with NP and VP24, in transport of the viral nucleocapsid through the cytoplasm[22]. Most importantly, it is critical for overcoming the immune response of a target host. It was demonstrated previously that VP35 could inhibit interferon (IFN) alpha and beta (IFN-α/β) production, as well as activation of interferon regulatory factor (IRF) 3[23,24]. VP35 was also identified as being able to prevent dendritic cell (DC) maturation[25–28].

VP40 serves a predominantly structural role as the matrix protein of EBOV. It interacts not only with cellular factors, but also with the cellular membrane to facilitate assembly and budding of newly formed virions[29,30]. VP40 was shown to initially form dimers, which interact with each other at the cellular membrane via their C-terminus domains (CTD), and eventually oligomerize as hexamers through a twisting motion hypothesized to generate a force sufficient to push through the cellular membrane. These hexamers then assemble as elongated filaments, characteristic of EBOV particles. Structurally speaking, one last function of VP40 that has been described is that an octamer, ring-like structure with RNA-binding properties is thought to play a crucial role in regulation of viral transcription. This octamer, once bound to RNA, localizes perinuclearly and current data, although limited, suggest this event to be crucial for initiation of viral transcription following infection[31]. Finally, recent work has shown that VP40 is capable of inducing bystander apoptosis of lymphocytes, when packaged into exosomes, although the exact mechanism remains to be thoroughly characterized. Current data show that VP40 may do so by regulating the RNA interference (RNAi) machinery, such as Dicer, Ago 1, and Drosha, which in turn promotes induction of apoptosis[32,33].

Of all the EBOV genes, *GP* is by far the most unique. As mentioned previously, *GP* encodes three different proteins, namely $GP_{1,2}$, the full length 676-residue surface glycoprotein; pre-sGP, the 364-residue pre-soluble glycoprotein; and ssGP, the 298-residue small soluble glycoprotein. Of note, it has been established that the transcripts for these proteins are produced *in vitro* at a ratio of 24:71:5, respectively, making sGP the main resulting product of *GP*. The most interesting feature of these proteins, in this context, is most likely the method in which these different glycoproteins are generated. Indeed, $GP_{1,2}$ is generated following a stuttering or slippage of the viral polymerase over an editing site, which contains seven template uridines. This slippage, termed transcriptional editing, causes the addition of an eighth adenosine in the transcript that overrides the premature end of the transcribed messenger RNA (mRNA), allowing the polymerase to pursue its journey and fuse the two separate open reading frames (ORFs), which constitutes $GP_{1,2}$, the sole surface glycoprotein of EBOV which is responsible for determining its tropism[34,35]. In the absence of that stuttering, viral transcription results in production of pre-sGP, which is processed by furin, and homodimerizes in a parallel orientation[36]. However, the roles this protein might play in pathogenesis remain largely undefined[37,38]. Indeed, a structural role for sGP has been described, through substitution of GP_1 to form a functional glycoprotein[39], but it may also serve as a virulence factor due to its elevated production *in vivo*, but not *in vitro*[40]. Finally, sGP was also described as being able to restore endothelial barrier function, but can also act as a decoy antigen[41,42]. Regarding ssGP, a definite function of this protein during infection has yet to be determined. Given its similitude to sGP, it has been hypothesized that both proteins could have a similar role, but no inflammatory functions that sGP possesses, or an effect on endothelial barrier restoration, has been identified yet[35].

As mentioned previously, VP30 is a key member of the RNP complex and plays a crucial role in activating viral transcription. To do so, it must initially undergo hexamerization, which allows RNA binding (of note, the phosphorylated state of VP30 was found to be unable to bind to RNA). Subsequently, VP30 can bind to VP35 in a RNA-dependent manner and exert its function of transcription activation[43]. To regulate this process, multiple factors interact with VP30. First, NP was shown to actively bind to VP30 in NP inclusion bodies[44], and that active phosphorylation and dephosphorylation of VP30 occurred in those bodies. Recent experiments have shown that NP negatively regulates phosphorylation of VP30[45], and that interaction of NP with VP30 is important for recognition of a stem-loop in the viral untranslated region (UTR)[46]. However, additional work is required to assess the role of this recognition in viral transcription initiation. Second, experiments using affinity tag-purification mass spectrometry revealed that the retinoblastoma-binding protein 6 (RBBP6), a host ubiquitin ligase, could bind to VP30 using the same region used by NP, negatively impacting viral transcription and EBOV replication overall[47]. Finally, others have shown that the protein phosphatase 1 (PP1)[48], as well as the protein phosphatase 2A-B56 domain (PP2A-B56), which are recruited through a specific LxxIxE motif on NP[49], are capable of dephosphorylating VP30, which in turn allows for viral transcription.

The second to last protein encoded by EBOV is VP24. As discussed above, this protein is essential for nucleocapsid assembly and transport, as well as genome packaging, in which it has been suggested that VP24 acts by condensing the RNP, thereby preventing polymerase activity[22,50,51]. However, like many other viral proteins, there is a wide range of functions that have been attributed to it. Most notably, VP24 has been found to bind to karyopherin alpha (KPNA), a transporter responsible for translocating the tyrosine-phosphorylated signal transducer and activator of transcription 1 (STAT1) to the nucleus, where it would normally act as a transcription factor for interferon-stimulated genes[52]. Additional work has even shown that VP24 can directly interact with STAT1, indicating that it can antagonize at least 2 separate pathways involved in interferon signalling[53]. Similarly, VP24 was also shown to prevent IFN-β-mediated phosphorylation of the p38 mitogen-activated protein (MAP) kinase, which is essential for activation of various branches of the immune system, including innate, T, and B cells[54,55].

Finally, despite being the largest protein produced by EBOV, its polymerase (L) is most likely the least studied protein of this virus, due in part to the lack of suitable reagents such as good specific antibodies. It is a RNA-dependent RNA polymerase, which requires the presence of Mg^{2+} as a cofactor, but was not found to be active on its own; at the minimum VP35 was required[56]. Similarly, others have identified the catalytic site of the polymerase to contain a GDNQ-motif, which is required for both transcription and viral genome replication[57].

Viral replication cycle

Attachment and entry

EBOV replicates within the cytoplasm of a multitude of target host cells, such as monocytes and macrophages, dendritic cells, hepatocytes, fibroblasts, and endothelial cells (Figure 8: Ebola virus genome structure and life cycle.

Figure 9: Detection of Ebola virus infection in nonfatal versus fatal casesFigure 10). Therefore, attachment, which is mostly mediated by $GP_{1,2}$, relies on various host factors such as lectins (mannose-binding, DC-Specific Intercellular adhesion molecule-3-Grabbing Non-integrin [DC-SIGN], Liver/lymph node-specific Intercellular adhesion molecule-3-Grabbing Non-Integrin [L-SIGN], human macrophage galactose- and *N*-acetylgalactosamine-specific C-type lectin), some members of the Tyro3 receptor tyrosine kinase (Axl, Dtk, and Mer), folate receptor-α, β1 integrins, as well as the T-cell immunoglobulin and mucin domain 1 (TIM-1), a phosphatidylserine (PS) receptor[58–65]. Notably, none of these factors are essential in relevant cell types, suggesting that other mechanisms are involved for entry. To this effect, regarding TIM-1, entry was shown to be dependent on the PS present in the envelope of the virus, rather than $GP_{1,2}$. Indeed, apoptotic cells such as monocytes and macrophages are known to use their PS receptor to clear apoptotic debris. However, viral envelopes such as that of EBOV can acquire PS following budding. This suggests that EBOV, at least in part, uses a phenomenon named apoptotic mimicry to enter cells such as phagocytes through phosphatidylserine receptors[66]. Interestingly, others have shown that both GP and VP40 colocalize with lipid rafts and associate with virus entry and release, suggesting the importance of these areas of the cell membrane for pathogenesis[67].

Following attachment, the virus is taken up into the cell by macropinocytosis, and macropinosomes further mature into endosomes[68,69], where the acidic content is a favorable environment for host cathepsins B and L to convert the surface $GP_{1,2}$ into a fusion-active, cleaved GP_{CL}[70]. This new form of the surface glycoprotein can now interact with the Niemann-Pick C1 (NPC1) receptor, triggering the fusion of the endosome and viral membranes[71], and the release of the nucleocapsid into the cytoplasm.

Transcription, replication and protein production

Although it remains to be clarified, it is hypothesized that the subsequent release of VP24 from the RNP would lead to a relaxation of the nucleocapsid, therefore enabling transcription and replication of the genome[51]. As stated above, transcription of genomic RNA occurs in the cytoplasm through the RNP complex composed of NP, VP35, VP30, and L[72]. The newly synthesized proteins, especially NP, also leads to the formation of inclusion

bodies, dynamic aggregates of proteins previously thought to have no function in viral replication, but later found to be the location in which genome replication actually takes place[73]. In regard to transcription, it has also been shown that VP30 exists within an infected cell mostly in its dephosphorylated state, a requirement for activation of transcription. Given that phosphorylated VP30 was found to associate with NP, it has been shown that NP can also recruit the host PP2A-B56 phosphatase, leading to dephosphorylation of VP30 and activation of viral transcription. The host cell PP1 was also identified as capable of dephosphorylating VP30[45,48,49].

Assembly and budding

Similar to the unpacking that takes place following infection of the cell, available data suggest that VP24 is responsible for tightly packaging the newly synthesized RNP complex, meaning that replication and transcription cannot proceed further[50]. These newly formed structures can then be transported to the cell surface using a mechanism that was shown to be actin-dependent[74]. Recently, it was also shown that NP, through its N-terminus, recruits VP40 inside inclusion bodies, which induces a conformational change within the C-terminus of NP, exposing its hydrophobic core and allowing its inclusion into viral particles. This interaction was also found to prevent NP from encapsidating viral RNA, switching the overall viral state from RNA synthesis to packaging[75]. VP40 has been shown to interact with various cell components including actin; the coat protein complex II (COPII), which plays a role in endoplasmic reticulum (ER)-to-Golgi transport of vesicles; the IQ Motif Containing GTPase Activating Protein 1 (IQGAP1), which is normally involved in formation of filopodia and actin cytoskeletal remodeling during cell migration; Rab11, which is involved in the endocytic recycling pathway and actin remodeling, and microtubules[76–80]. As for GP, it is processed from the endoplasmic reticulum to the Golgi apparatus, where it is modified with *O*-linked and *N*-linked glycans[81] and is also cleaved by furin[82]. Interestingly, unlike other viruses, cleavage of the precursor glycoprotein by furin into the final GP_1 and GP_2 forms was shown to not be required as viral mutants lacking the cleavage site, or viruses produced in cell lines lacking furin, were found to be equally capable of replicating[83–85]. Assembly at the membrane is mediated by VP40 [86], through interactions with numerous proteins from the endosomal sorting complex required for transport (ESCRT) pathway, as well as ubiquitin ligases, such as Tsg101, Vps-4, Nedd4, and the E3 ubiquitin ligase Itch, which allows dimerization of VP40 at the inner membrane[87–90]. Overall, VP40 appears to be the key viral protein involved in orchestrating assembly. Once all the components have successfully assembled at the membrane, infectious virus can be released.

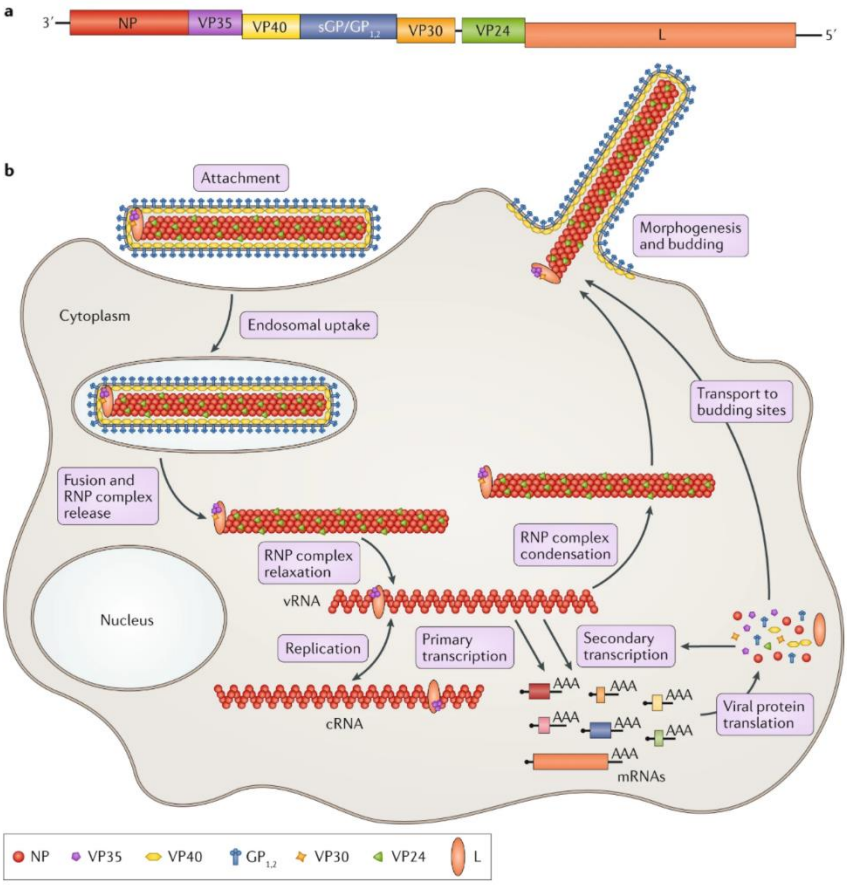

Figure 8: Ebola virus genome structure and life cycle.

Clinical aspects of Ebola virus disease

Due to the increased frequency of outbreaks, our understanding of Ebola virus disease (EVD) has also significantly increased. Multiple phases of EVD have now been characterized, and to the eyes of an unsuspecting clinician, it is easy to overlook EVD as a possible cause, given how non-specific the symptoms of the earlier phases are. Although the exact moment an individual becomes infected is difficult to pinpoint in an outbreak setting, available clinical data indicate that the mean incubation period of the virus, regardless of the route of transmission, is 6.22 ± 1.57 days[91].

This incubation period is followed by the early phase of EVD, which is characterized by a non-specific febrile illness, with patients exhibiting symptoms such as fever, fatigue, myalgia, headache, and anorexia[92]. This phase usually lasts between 1 and 3 days, during which the virus migrates through monocytes and macrophages to regional lymph nodes and further disseminates throughout the organism, particularly the liver and spleen. It then

progresses over next 7 days to a gastrointestinal phase, which is characterized by abdominal pain, nausea, vomiting, and diarrhea. As the disease progresses, the patient either moves towards the terminal phase of the disease, where the majority of deaths occur 7 to 12 days post-onset of symptoms, or towards recovery[93]. The terminal phase of EVD is characterized by multiple organ failure and hypovolemic shock, including renal failure which manifests through oliguria or anuria, respiratory failure, cardiac dysfunction such as myocarditis and pericarditis, and although major signs are rare, neurological manifestations such as confusion, seizures, or encephalopathy have also been observed[94–96]. Of note, the use of the previous name for EVD, *i.e.* Ebola hemorrhagic fever (or EHF), is not recommended anymore, as not all patients exhibit fever or bleeding-associated symptoms[92,97].

Overview of the immune system

The immune system is the main actor when it comes to fending off undesired invaders within the body, whether these are bacteria, viruses, fungi, helminths, or protozoa. In humans, a distinction is made between the two main branches of that system: a somewhat unspecific but rapid innate immunity, as well as a specific but slower adaptive immune response. Both branches have been shown to closely interact, and their ability to discriminate between what is, and what is not, dangerous is critical to prevent the immune system from turning again its host.

Innate immunity

Innate immunity constitutes the first line of defense following entry of a foreign object inside the body, which is activated once protective physical barriers such as the epithelium and mucus layers have been breached by a pathogen. On top of physical defenses, the arsenal of the innate immune system also includes various small molecules that are either passively circulating, such as complement-associated proteins, but that can also be secreted by immune cells such as cytokines, chemokines, enzymes, and reactive free radical species. Finally, the innate system also comprises cytoplasmic and membrane-bound proteins within dendritic cells and macrophages, but also within cells such as fibroblasts and epithelial cells. These proteins recognize pathogen-associated molecular patterns (PAMPs), leading to a downstream activation of immune cells which can further resolve the issue[98]. Following intrusion by a pathogen, the type of molecule(s) activated will depend on the pathogenesis of that intruder, as molecules responsible for identification of PAMPs can be found at various strategic locations within a given cell. These molecules either belong to the Toll-like receptor (TLR) family, which are membrane-associated either at the cell surface or within the membranes of endosomes and lysosomes, while other members belong to a family of DExD/H box RNA helicases such as the retinoic acid-inducible gene I (RIG-I), which can be found in the cytoplasm. These molecules can detect a wide range of molecular patterns, including but not limited to lipopolysaccharides, lipoproteins, peptidoglycans, single- or double-stranded RNA, as well as viral DNA rich in unmethylated CpG-DNA motifs[99]. The subsequent activation of proteins that

recognize PAMPs initiates a cascade of events which eventually leads to the release of inflammatory cytokines and type I interferons, indicating to neutrophils and macrophages that the cell might need to be destroyed as it has been invaded by a pathogen. Neutrophils and macrophages execute this action through the release of various enzymes and reactive free radical species, followed by phagocytosis of the debris. Through this heightened antiviral state, interferon can also act to stimulate natural killer (NK) cells, amplify the activation of DCs, and induce adaptive immunity[100]. DCs then have the responsibility of migrating to the lymph nodes, where training of the adaptive branch of the immune system takes place, so that other immune cells can develop a pathogen-specific response[101].

Adaptive immunity

While innate immunity is designed to recognize general patterns associated with a pathogen, the adaptive immune response is designed to be specifically targeted against the antigen(s) which triggered the immune response in the first place. Unlike innate immunity, the adaptive response also has the ability of inducing a long-term memory, which would lead to faster and better responses following a second encounter of the same pathogen, the guiding principle behind vaccination. Although the actors of the adaptive immune responses are numerous, two main cell types are responsible for mounting an effective antiviral response: T cells and B cells.

T cells can be defined by the expression of the T cell receptor (TCR) at their cell surface. This protein is responsible for recognizing a processed, foreign antigen at the surface of antigen-presenting cells such as DCs, through their association with class I and class II major histocompatibility complex (MHC) molecules. Specifically, class I MHC molecules are responsible for the presentation of peptides generated within a cell, while class II MHC molecules display peptides that have been taken up by the cell from the environment and processed proteolytically[102]. There are two major subsets of T cells, $CD4^+$ and $CD8^+$. $CD4^+$ T cells play a role in regulating cellular and humoral responses, and can be further subdivided into two main populations with distinct cytokine production and roles, namely T_H1 and T_H2[103]. The T_H1 cell subset mainly produces IFN-γ and interleukin (IL) 2, which mediates more of the cellular immunity, including the activation of mononuclear phagocytes, as well as the activation of NK and $CD8^+$ cells. In contrast, T_H2 cells are focused towards the production of IL-4, IL-5, IL-10, and IL-13, cytokines associated with humoral immunity and antibody production[104]. As for $CD8^+$ T cells, and in the context of a viral infection, their main function is to eliminate infected cell via granules they secrete following contact with the target cell. These granules contain granzymes and perforins, proteins capable of inducing apoptosis of the target cell, therefore, effectively putting a halt to virus production.

B cells are the main actors of humoral immunity. They initially develop in the bone marrow independently of a direct contact with a foreign antigen, and upon exit, the immature B cell can be recognized by its expression at its surface of two immunoglobulin (Ig) isotypes, IgD and IgM. Next, activation of B cells can occur under two

distinct mechanisms, either in a T cell-independent, or T cell-dependent manner. T cell-independent activation of B cells occurs for only a limited type of antigens, specifically polymeric ones such as bacterial lipopolysaccharides. This method of activation does not require T-cell costimulatory proteins, but usually does not lead to somatic mutations in B cells, which increases affinity of B cells for their antigens. This is the reason why development of efficacious vaccines against surface molecules of pathogens such as bacteria does not lead to efficient memory responses[102]. In contrast, T cell-dependent activation of B cells will induce isotype switching to produce IgG, IgA, or IgE, which confers different properties to antibodies without affecting their specificity to the antigen, or somatic hypermutations in order to increase affinity to the antigen of interest to the antibody. This T cell-dependent activation is mediated by the interaction of the B cell CD40 protein with the CD40 ligand present on T cells.

Immunopathology and immune evasion of EBOV

Early targets of infection by EBOV have been identified as myeloid dendritic cells (mDCs), as well as monocytes and macrophages[105]. Current data supports the idea that viral replication in these cells is crucial for pathogenesis as hijacking of the cellular machinery leads to disruption of basic cellular functions such as antigen presentation, and induces an immunosuppressive state of infected DCs, therefore preventing early detection of the virus so it can freely replicate and disseminate to the lymph nodes[106]. In contrast, EBOV infection of macrophages leads to their activation, as shown by their tendency to form clumps and the release of proinflammatory cytokines such as tumor necrosis factor alpha (TNF-α) and IL-1β. Clumping of monocytes in smaller blood vessel could drastically affect blood flow, and even lead to the activation of coagulation factors, which have all been described previously[107]. Interestingly, the activated state of monocytes also leads to an increased expression of multiple cell adhesion molecules, which has been hypothesized to contribute to the spread of infected cells from the bloodstream into organs, potentially providing an explanation for the wide tropism of this virus.

As stated above, interferon responses are critical for suppressing viral infections. It was also discussed that the mouse model was not susceptible to infection by wild-type EBOV. Interestingly, subsequent work with IFNAR$^{-/-}$ mice has shown that this model is susceptible to infection by WT-EBOV[108], and that MA-EBOV contains key mutations in NP and VP24 that allow this mutated virus to efficiently counter interferon-induced responses[109]. This highlights the key role played by viral proteins in suppressing the interferon response, so that EBOV can replicate unchecked. Indeed, further work revealed that VP24 is able to bind KPNA proteins, which are usually responsible for mediating nuclear accumulation of STAT1 complexes, which mediates the activation of many interferon-stimulated genes[52,110]. Another key protein for EBOV is VP35. Indeed, the ability to bind to double-stranded RNA prevents the recognition of the latter by RIG-I and melanoma differentiation-associated protein 5 (MDA5), two cellular sensors of viral infection[23,111]. VP35 was also identified as a binding partner of the protein kinase R (PKR) activator (PACT), a protein capable of binding double-stranded RNA which subsequently

activates RIG-I[24]. Additionally, VP35 was found to associate with IRF3 and IRF7, recruiting proteins such as the protein inhibitor of activated STAT1 (PIAS1), where PIAS1 was shown to be responsible for SUMOylation of IRF7, effectively preventing it from exhibiting its normal IFNβ promoter activity[112]. VP35 was also shown to act as a decoy for the inhibitor of nuclear factor kappa-B kinase (IKKε) and the TANK-binding kinase 1 (TBK-1), two kinases which usually activate IRF3 and IRF7[113]. Finally, although the mechanism has yet to be fully uncovered, VP35 was shown to prevent autophosphorylation of PKR, which in turn usually phosphorylates the eukaryotic initiation factor 2 alpha (eIF-2α), a regulator of the initiation phase of mRNA translation[114,115].

Given the reduced number of viral proteins encoded by EBOV, it is not surprising that many of them serve multiple purposes, from structural roles to immune evasion. This is the case for the EBOV glycoprotein; although it facilitates entry into a target cell, it was later found to also play a major role in facilitating viral budding. Indeed, tetherin is a typical antiviral host factor which is induced by interferon. Due to its structure, it is capable of binding both the cell and viral membranes, therefore preventing the release of newly formed virions, including EBOV, from an infected cell. Therefore, the Ebola virus evolved tools to counteract the effects of tetherin, although the exact mechanism through which GP does so has yet to be fully elucidated. However, current data report that for the antagonism of tetherin by EBOV GP, both the receptor-binding domain and *N*-glycosylation of GP had to be intact[116,117]. Early work from 1998 also reported that during infection, $GP_{1,2}$ could be found at the surface of virosomes, small vesicles which are produced from GP-expressing cells, but a clear role for it could not be identified at the time[118]. Subsequently, Nehls and colleagues showed that these virosomes, which can be trapped at the cell surface by tetherin, could act as a decoy for neutralizing antibodies. Furthermore, these virosomes were shown to also possess immunomodulatory functions as treatment of macrophages with GP-containing virosomes led to reduced cytokine expression, namely of the C-C motif chemokine ligand (CCL) 2, CCL5, and TNF-α, which usually contribute to chemoattraction of other immune cells and activation of macrophages[119].

Finally, one key feature of EBOV pathogenesis is the observed lymphocyte apoptosis within lymphoid tissues of NHPs[120]. Similarly, studies following the 1996 outbreaks in Gabon have shown that in fatal human cases, levels of CD3, CD8, and TCR mRNA would drastically diminish a few days before death, including downregulation of the anti-apoptotic B-cell lymphoma 2 (BCL-2) protein[121]. Whether that reduction in circulating T cells was due to actual apoptosis, or extravasation of the cells to infected tissues could not be clearly defined. However, while NK cells have been shown to accumulate in the kidneys, lungs, and livers of infected mice following MA-EBOV challenge, the same could not be said for T cells, as their levels in those particular tissues were found to be significantly reduced[122]. Notably, T cells are not susceptible to infection by EBOV, suggesting a bystander effect must be at play. Recent work in a mouse model of EBOV infection revealed that animals that had been depleted of NK cells exhibited higher levels of hepatic T cells, when compared to animals with intact NK cells. This

suggests a detrimental role, whether direct or indirect, of NK cells towards T cell populations in the context of EBOV infection, at least in a mouse model[122].

Ecology

Current evidence suggests that EVD is a typical zoonosis, *i.e.* an infectious disease that can be transmitted between animals and humans[10]. Indeed, many outbreaks have been associated with the handling of gorilla or chimpanzee carcasses, but these are considered dead-end hosts given that they succumb to infection[123]. The reservoir(s) for EBOV remains elusive to this day. In an attempt to elucidate this unknown aspect of the disease, an early study, conducted under laboratory conditions, experimentally infected 24 species of plants and 19 species of vertebrates and invertebrates. The authors reported that one species of fruit bats, *Epomophorus walhbergi*, as well as two species of insectivorous bats, *Tadarida condylura* and *Tadarida pumila*, could support EBOV replication without succumbing to the disease or even exhibiting any symptoms[124]. A subsequent study, using samples collected between 1979-1980 following the 1976 outbreaks in the Democratic Republic of the Congo (DRC) and southern Sudan, examined 1664 animals, which covered 117 different species of primates, bats, squirrels, birds, and reptiles, for the presence of antibodies or virus, but to no avail[125]. Another field study that followed the 1995 epidemic in DRC used similar methods to detect specific antibodies and isolate EBOV in 3066 vertebrates, spanning 151 species of mammals, birds, reptiles and amphibians[126]. Unfortunately, all tests proved to be negative for the presence of EBOV. It was not until 2005 that another trapping expedition was able to detect EBOV-specific IgG, as well as nucleotide sequences of EBOV, in the liver and spleen of three fruit bat species (*Hypsignathus monstrosus*, *Epomops franqueti* and *Myonycteris torquata*) in Gabon and Republic of the Congo[127]. Multiple studies have since confirmed these results in Gabon, Ghana and Bangladesh, and have found serological evidence of EBOV or RESTV in multiple bat species including *Hypsignathus monstrosus, Epomops franqueti*, *Epomophorus gambianus, Nanonycteris veldkampii*, *Myonycteris torquata, Micropteropus pusillus, Mops condylurus, Eidolon helvum, Rousettus leschenaultii* and *Rousettus aegyptiacus*[128–131]. EBOV-specific antibodies have also been observed in pigs from the Philippines, China and Sierra Leone, adding to the pool of potential animal reservoirs[132–134]. Despite these findings, no virus has ever been successfully isolated from wild, captured animals. This focus on bats, regarding the animal reservoir for EBOV, stems from the fact that the *Rousettus aegyptiacus* has been identified as the reservoir for one of its close cousins, MARV[135,136]. Bats are also an excellent candidate for harboring viruses, as current evidence shows high levels of immune tolerance in these animals[137,138]. Interestingly, this tolerance has been hypothesized to be linked, from an evolutionary perspective, to their ability to fly. Indeed, current evidence suggests that flight, a highly demanding activity metabolically speaking, would lead to elevated levels of oxygen free radicals, inducing increased deoxyribonucleic acid (DNA) damage. Given that from a metabolic standpoint generating an immune response

is also demanding, it could be that selective pressure favored bats with lower inflammation responses, creating an ideal reservoir for multiple viruses to replicate unchecked[139].

Epidemiology

The first ever reported outbreak of EVD occurred in 1976 in DRC, formerly known as Zaire, and was caused by EBOV. Due to the unknown nature of the etiological agent at the time and poor infection control and prevention (ICP) measures, this outbreak reached 318 cases, which remains to this day the third largest EBOV outbreak and one of the most lethal with a case fatality rate (CFR) of 88%[140]. Since then, over 20 additional outbreaks have been caused by EBOV, excluding two fatal laboratory incidents in Russia and exported individual cases from the 2013-2016 West African outbreak, making EBOV the most frequent *Ebolavirus* member to cause outbreaks[141]. Overlapping with the 1976 EBOV outbreak in DRC, another viral hemorrhagic fever was evolving in nearby Sudan, now known as South Sudan. Another astonishing 284 cases were reported by the end of the outbreak, with a 53% CFR. The etiological agent was identified as a close relative of *Zaire ebolavirus*, but it eventually necessitated the creation of a new species due to its genetic distance to EBOV. This new species is now referred to as *Sudan ebolavirus*, with the only representative being SUDV. Subsequent to this first epidemic, six additional outbreaks were caused by SUDV, excluding a non-fatal laboratory incident in England. It was not until over a decade later, in 1989, that a new species was identified in the Philippines, but this time the only deaths or even signs of disease were noted in cynomolgus macaques and not humans. Indeed, this new species identified as *Reston ebolavirus*, does not seem to be able to cause a symptomatic disease in humans. Three animal caretakers, however, had detectable antibodies against the virus. This pattern repeated itself on five different occasions in the United States of America, Italy, and the Philippines. Primates and pigs were identified as naturally infected by RESTV, and animal caretakers or pig farmers were screened as seropositive for antibodies against the virus but did not develop any symptoms. Then, in 1994, a scientist performing an autopsy on a deceased non-human primate became ill with symptoms resembling those caused by EBOV or SUDV, days after the autopsy. Initial serological characterization of this strain found it to be related, but different, to EBOV. Genomic analysis later revealed that this new virus was indeed a new species, *Taï Forest ebolavirus*. To this day, this remains the only reported case of human infection by TAFV. Finally, in 2007, a disease outbreak of unknown etiology was reported from the Bundibugyo district in Uganda. Samples were sent to the Centers for Disease Control and Prevention (CDC) in Atlanta, Georgia, and were confirmed following sequencing as BDBV, a novel species of *Ebolavirus*. In total, this outbreak caused by this newly identified species infected 131 individuals, with a reported CFR of 32%, and so far, only one other epidemic caused by BDBV has been reported. Overall, when all outbreaks are accounted for, the CFR for EBOV was calculated to be 43.92±0.7%, while for SUDV and BDBV, their CFR are 53.72±4.456%, and 33.65±8.38%, respectively[142]. Interestingly, over the years, an apparent decline in the CFR for EBOV can be observed, as it has not reached high CFRs in recent years.

Reasons for this may be numerous, and not mutually exclusive. In early outbreaks, one main mode of transmission was through needle re-use, which may lead to higher mortality given how direct this route of infection is. Other factors such as improvement in health care and behavior, which may affect the mode of transmission, may also explain why an apparent reduction in the CFR of EBOV is observed, A summary of previous EBOV, SUDV, BDBV, and TAFV outbreaks is available below (Table 1).

Table 1: Documented outbreaks of Ebola virus disease, sorted by year of occurrence.

Year	Species	Country	Cases	Deaths	CFR (%)
1976	*Zaire ebolavirus*[140]	DRC[a]	318	280	88
	Sudan ebolavirus[143]	Sudan	284	151	53
	Sudan ebolavirus[144]	England	1	0	0
1977	*Zaire ebolavirus*[145]	DRC	1	1	100
1979	*Sudan ebolavirus*[146]	Sudan	34	22	65
1989	*Reston ebolavirus*[147]	Philippines	3	0	0
	Reston ebolavirus[148,149]	USA[b]	4	0	0
1992	*Reston ebolavirus*[150]	Italy	0	0	0
1994	*Taï Forest ebolavirus*[151]	Côte d'Ivoire	1	0	0
	Zaire ebolavirus[152]	Gabon	52	31	60
1995	*Zaire ebolavirus*[153]	DRC	315	254	81
1996	*Zaire ebolavirus*[154]	Russia	1	1	100
	Reston ebolavirus[155]	Philippines	0	0	0
	Reston ebolavirus[156]	USA	0	0	0
	Zaire ebolavirus[157]	South Africa	2	1	50
	Zaire ebolavirus[152]	Gabon	60	45	75
	Zaire ebolavirus[152]	Gabon	37	21	57
2000	*Sudan ebolavirus*[158]	Uganda	425	224	53
2001	*Zaire ebolavirus*[159]	Republic of the Congo	59	44	75
	Zaire ebolavirus[159]	Gabon	65	53	81
2003	*Zaire ebolavirus*[160]	Republic of the Congo	143	128	89
	Zaire ebolavirus[161]	Republic of the Congo	35	29	83
2004	*Zaire ebolavirus*[162]	Russia	1	1	100
	Sudan ebolavirus[163]	Sudan	17	7	41
2005	*Zaire ebolavirus*[164]	Republic of the Congo	12	10	83
2007	*Bundibugyo ebolavirus*[165]	Uganda	131	42	32

	Zaire ebolavirus[166]	DRC	264	187	71
2008	*Zaire ebolavirus*[167]	DRC	32	15	47
	Reston ebolavirus[133,168]	Philippines	6	0	0
2011	*Sudan ebolavirus*[169]	Uganda	1	1	100
2012	*Sudan ebolavirus*[170]	Uganda	6	3	50
	Bundibugyo ebolavirus[170]	DRC	38	13	34
	Sudan ebolavirus[170]	Uganda	11	4	36
2014	*Zaire ebolavirus*[171]	DRC	69	49	71
	Zaire ebolavirus[172]	Guinea	14124	3956	28
	Zaire ebolavirus[173]	Sierra Leone	10675	4809	45
	Zaire ebolavirus[174,175]	Liberia	3811	2543	67
	Zaire ebolavirus[176]	Italy	1	0	0
	Zaire ebolavirus[177]	Mali	8	6	75
	Zaire ebolavirus[178]	Nigeria	20	8	40
	Zaire ebolavirus[179]	Senegal	1	0	0
	Zaire ebolavirus[180]	Spain	1	0	0
	Zaire ebolavirus[181]	USA	4	1	25
2017	*Zaire ebolavirus*[182]	DRC	8	4	50
2018	*Zaire ebolavirus*[183]	DRC	54	33	61
	Zaire ebolavirus[184]	DRC	3470	2287	66
2020	*Zaire ebolavirus*[185]	DRC	130	55	42
2021	*Zaire ebolavirus*[186]	Guinea	23	12	52
	Zaire ebolavirus[187]	DRC	12	6	50

[a] Democratic Republic of the Congo

[b] United States of America

Infection prevention and control

Although the infectious dose of EBOV for humans is unknown, experiments in non-human primates have shown that when aerosolized, only 1 to 10 organisms are required to produce an infection[188]. However, it is important to note that this is not the primary route of infection, as EBOV is spread through direct contact with infected

bodily fluids, which is discussed below in greater details. Given the highly contagious nature of the virus, there are multiple approaches that can be taken to limit the spread of an outbreak[189].

The first approach is the *medical care of patients*; when individuals have been confirmed positive for EVD, their care and isolation from the community will ensure that they cannot infect additional individuals. Although second on the list, activities related to *community engagement and health promotion* are likely the most critical aspect of outbreak response. Indeed, having the community on your side and integrating them fully in outbreak management, ensuring that they understand why foreigners are setting up makeshift hospitals in their towns and villages, what the disease is and how to prevent community spread, ensuring that rumors and misinformation do not spread out of control, and that infected individuals are not being hidden from the healthcare system, are all critical to successfully control an outbreak. Touching on the last point, *surveillance* is essential for finding new cases and chains of transmission. This surveillance relies on setting up reliable means of communication between local actors, such as traditional healers, those in charge of existing health infrastructures, as well as community leaders, and the relevant authorities in charge of outbreak response. This also includes reports of suspicious deaths from hospitals and cemeteries, which could allow the identification of ongoing chains of transmission, assuming these deceased individuals had contact with someone who was not wearing appropriate personal protective equipment (PPE). Similarly, active *contact tracing* is another fundamental aspect of case identification. Once a patient is admitted to an Ebola management center (EMC), it is important to initiate a discussion with him or her about recent contacts they might have had with members of the community, or if they took part in unsafe funeral rites, for example. This might allow epidemiologists and community agents to quickly identify chains of transmission before they get out of control.

Next, there is *environmental decontamination*, which includes that safe and dignified burials should be organized. Indeed, infectious EBOV has been shown to survive for extensive periods of time on soiled surfaces, (as long as 365 hours on stainless steel[190]) and therefore surface decontamination, as well as laundry of soiled linens and clothes, should be performed in order to prevent further contamination. As for burials, they have been shown to represent a risk factor as funeral rites often involve washing the body of the deceased, presenting a direct risk of handling bodily fluids which almost certainly contain infectious virus[191]. One additional aspect of outbreak response that should be considered is *access to healthcare facilities*, which are unrelated to the EVD outbreak. As stated above, the initial clinical phase of EVD is fairly unspecific, therefore it can easily be mistaken for other prevalent diseases in Africa, such as malaria. This reflects the high value of having laboratory capacity, which is discussed further below. However, once an individual presents at an EMC and is found to be suffering from a disease that is unrelated to EVD, it is important to refer this patient to a separate health facility as the risk of exposure to EVD is higher at an EMC, where actual patients with confirmed EVD are being treated. The latest tool in the arsenal of outbreak responders is *vaccination*. Indeed, the recent approval of two vaccine strategies

against EBOV has allowed responders to better control chains of transmission by vaccinating healthcare workers, as well as contacts and contacts-of-contacts, in order to prevent further spread of the disease within communities. Of note, the approved vaccines are only expected to be effective against EBOV specifically, not the other species of ebolaviruses.

Diagnosis methods in the laboratory

Given that the clinical presentation of EVD is fairly non-specific, and that few physicians have experience with this disease, EVD can easily be mistaken for other, more prevalent diseases in Africa. Coupled to the fast progression of the disease in a community if it goes unchecked, it is of paramount importance that accurate and rapid identification of the virus is made, as soon as EVD is suspected.

Indirect fluorescent antibody assay

Following identification of the virus in 1976, the initial tools available for laboratory confirmation of the virus were limited, especially in an outbreak setting. While electron microscopy (EM) was available in modern laboratories, it was not practical for field confirmation of cases. Therefore, during the earlier days of outbreak response, the technique of choice relied on the measurement of indirect fluorescent antibody (IFA) titers. This technique, although quite simple to execute in the field since the equipment required is essentially limited to a fluorescence microscope and a dark room, was shown to be able to detect the presence of antibodies against EBOV as quickly as EM following infection. However, it is certainly not as sensitive as current techniques. Furthermore, the IFA assay was used to detect the antibodies of infected individuals against EBOV, hence laboratory confirmation of cases was done retrospectively on survivors, and it could not identify active infections or confirm community deaths[192]. The major limiting factor to this technique remains that access to fixed- and EBOV-infected cells is required as a critical reagent for the assay, which can only be prepared inside a BSL-4 laboratory. Despite these challenges, the technique was successfully used in outbreak settings, such as the 1976 outbreak in Yambuku[140].

Enzyme-linked immunosorbent assay

Similar to IFA, an enzyme-linked immunosorbent assay (ELISA) allows the detection of antibodies such as IgM and IgG, which develop following exposure to the virus or a vaccine[193]. Given that the body first needs to develop an immune response for these antibodies to be detectable, the technique is not useful for detection of active cases which may very well be in the early phase of the disease and that are yet to mount a proper immune response (Figure 11: Detection of Ebola virus infection in nonfatal versus fatal cases

 Indeed, current data suggest that IgM can be

detected starting 2 to 11 days following onset of symptoms, with persistence of these antibodies being observed until about 30 days, while they typically have disappeared 80 days following onset[194]. In contrast, IgG are usually first detectable around day 7 post-onset of symptoms and can last for years. This means that now more than ever, a detailed medical history of assayed individuals is crucial for correct interpretation of diagnostic results, as vaccination status may interfere with them. Therefore, ELISAs are mostly used retrospectively, such as during seroprevalence studies, in order to assess whether transmission of the virus occurred in a given area or community. When performed in parallel with outbreak response, useful information can still be gained from these types of investigations, such as where did the virus come from *i.e.,* where was it circulating before the outbreak had been reported to authorities, or where is it currently circulating but we still do not know about yet, as health authorities are often trailing behind the epidemic when it comes to case identification.

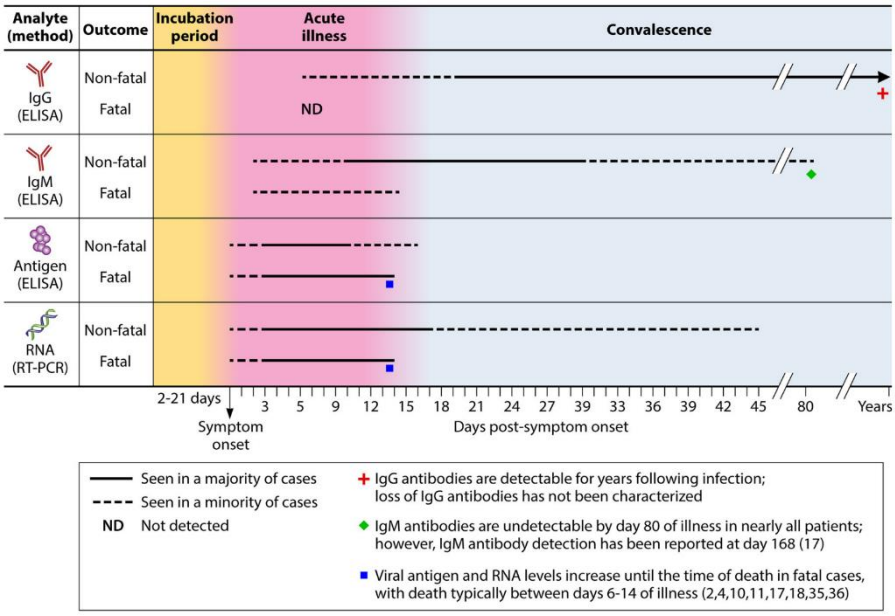

Figure 11: Detection of Ebola virus infection in nonfatal versus fatal cases

Polymerase chain reaction-based methods

The polymerase chain reaction (PCR) revolutionized the field of life sciences, and diagnosis of infectious diseases was no exception. It was not until 1999 that PCR was investigated as a diagnostic tool for EBOV. Early work to assess the potential usefulness of this technique used either non-human primate (NHP) samples from naturally infected animals, *i.e.,* from the outbreaks in NHP colonies in the United States (1989) and the Philippines (1996), or from human serum samples from the 1995 Kikwit outbreak. Both type of samples proved to be an effective substrate for the technique[195]. As such, it was during the following epidemic in 2000 (Gulu,

Uganda) that reverse transcription PCR (RT-PCR) was first used in an outbreak setting[196], although RT-PCR had been evaluated previously in the field on historical samples from Gabon[197]. Notably, in the former study, a direct comparison between ELISA and PCR revealed that EBOV could be detected by PCR 24 to 48h before detection by ELISA, highlighting the sensitivity of this method and its importance in controlling viral transmission within a community. Although PCR-based assays are highly sensitive and specific, they do require expensive and temperature-sensitive reagents, which can be difficult to obtain and conserve properly in resource-poor settings such as rural Africa where uninterrupted electricity can prove challenging. Furthermore, although some simplified PCR kits have been developed, this technique does require laboratory technicians to possess an expertise in molecular biology, as interpretation of the results and controls may not be as obvious as for other techniques. Nonetheless, real-time reverse transcription-PCR remains the gold standard for diagnostic of EVD.

Lateral flow immunochromatographic rapid diagnostic tests

Rapid diagnostic tests (RDTs) were first evaluated in a field setting during the 2014-2016 West African Ebola outbreak, and their principle is similar to those currently used for malaria or the human immunodeficiency virus (HIV), for example[198,199]. A few drops of blood are applied to the test, followed by addition of the supplied solution which allows the viral antigens present in the blood to be captured on fixed immunoglobulins. If the sample does contain the antigen, a visual marker will appear, indicative of positive detection. Overall, they require minimal training, other than biosafety, they require less stringent storage conditions than PCR reagents, and most tests can yield a result within 5 to 15 minutes. For these reasons, they can be useful in scenarios where access to PCR diagnostics can prove challenging, or when the geographical spread of an outbreak does not allow for multiple PCR-based laboratories to be set up where needed. RDTs could also be useful to probe ahead of an outbreak, in order to identify presumptive cases. However, one of the major drawbacks of these tests is their variable sensitivity (84-100%) and specificity (92-98%), therefore a confirmatory PCR should always be performed to ensure accurate diagnosis[200].

Novel methods

Sequencing

Following the substantial investment of both technical and human resources during the 2014 West African outbreak, new tools were brought to the field in order to assess their feasibility and value to frontline healthcare workers. One of these tools came from the laboratory and consists of sequencing platforms capable of providing near real-time genomic data in order to support epidemiological investigations. One of the success stories of this technique comes from work performed during the aforementioned outbreak, in which 1610 genomes sequenced during the outbreak were analyzed, accounting for over 5% of all recorded cases. These genomes were used to understand how and when the virus crossed borders between Sierra Leone, Liberia, and Guinea,

and how administrative, infrastructural, economic, climatic, and demographic factors contributed to the spread of the virus[201]. Similarly, sequencing of human samples has allowed epidemiologists to confirm a suspected case of sexual transmission of EBOV, which had been hypothesized to be plausible based on fragmented data, from a male survivor to his female partner. While this event occurred 199 days following his estimated onset of symptoms, genomic data revealed that the virus present in the sperm of the male individual corresponded to the one sequenced from the blood of the female patient, with only one nucleotide varying between both[202]. Recently, during the 2018 North Kivu outbreak in DRC, sequencing was implemented to provide support to the outbreak response efforts, as well as public health decision making. Genomic data was used to guide vaccine allocation, for which doses were sparse, by detecting superspreading events, so that contacts and contacts-of-contacts were identified quickly. The technique was also used to differentiate between reinfection and relapse of a previous infection[203].

Host transcriptome and viral genome detection

As our understanding of a virus evolves, so should our diagnostic methods. While current techniques mostly rely on detection of viral RNA in the blood, it should be noted that early in the infection, replication of the virus mainly occurs in the spleen and liver, thus delaying our ability to detect the virus in a blood sample. Rapid identification of an infection is paramount in reducing transmission events and increasing effectiveness of therapeutic approaches. Therefore, some researchers have investigated whether it is possible to confirm infection earlier than current methods by coupling the measurement of host RNA transcripts such as those from innate immune response genes, that are upregulated in early stages of EBOV infection, to detection of viral RNA itself. Although preliminary, their results suggest that these host RNAs could indeed be predictive of infection, as work in non-human primates revealed that this technique could correctly identify the etiological agent of infection in a previremic stage from ten EBOV samples, as well as five MARV samples. Validation of the technique on a larger pool of samples, including from humans, remains to be performed. Similarly, further studies aimed at the identification of other potential markers which could enhance the efficacy of this assay warrant further investigation[204].

Animal models of EVD

The low frequency of epidemics and the limited number of individuals infected over the course of such epidemics have for too long hindered our ability to understand key clinical characteristics of EVD. Similarly, because a human challenge model is simply not an option for EVD, evaluation of prophylactic and therapeutic options must be performed in animal models. As such, five different animal models have been developed so far, each with various advantages and disadvantages related to mimicking human disease or technicalities such as cost and availability of reagents. One of these disadvantages common to all rodent models is virus adaptation. These

animals are not naturally susceptible to infection by EBOV, and therefore the virus must be passaged multiple times within a specific species until mutations allowing for viral replication appear and stabilize. This process can take multiple months and is therefore not suitable for timely evaluation of novel isolates, for example in the context of an ongoing outbreak. Furthermore, an adapted virus contains mutations which may not accurately represent the behaviour of its naturally occurring counterpart. A brief overview of some relevant characteristics of current animal models is presented at the end of this section (Table 2: Overview of in vivo model systems

Table 3: Descriptive and bivariable analysis of the patients.Table 4).

Mouse

Mice have been extensively used in biological studies, and the field of filoviruses is no exception. Mice are widely available, and their unit cost is low compared to other animal models. Due to their extensive use in multiple research areas, they are also very well characterized, and reagents to study various parameters are commercially available. However, adult immunocompetent mice are not susceptible to infection by wild-type (WT) EBOV. To this end, EBOV has to be serially passaged in mice livers and spleens through newborn mice, resulting in mouse-adapted EBOV (MA-EBOV)[205]. Interestingly, the same study reported that MA-EBOV was 100% lethal in adult mice when injected intraperitoneally (i.p.), but not subcutaneously (s.c.) or intramuscularly (i.m.). Further characterization later revealed that only eight mutations occurred during passaging, and determinants of virulence were associated with mutations in NP and VP24 that allow for evasion of the interferon response[109]. Others have used resources such as the Collaborative Cross system, a panel of genetically diverse inbred mice which are obtained following systematic cross of eight founder mouse strains. Infection of these mice with MA-EBOV lead to a broad range of phenotypes, from absolute resistance, to lethal disease, to hemorrhagic fever and prolonged coagulation time, suggesting that genetic background determines susceptibility to EVD[206]. Although mice infected with MA-EBOV replicate many features of human EVD, such as high viremia, kidney and liver involvement, and the same target cells, they do not recapitulate fibrin deposition in later stages of the disease, a hallmark of the coagulopathy and hemorrhaging seen in humans[207]. One approach to study WT EBOV in mice involves using immunocompromised animals, such as IFN-α/β receptor (IFNAR) or STAT1 knockout mice[208]. While a similar pathophysiology to immunocompetent mice can be observed, their deficient immune system prevents a thorough understanding of immune correlates of pathogenesis and protection. The use of immunocompromised mice is more expensive than WT mice, but they still allow for rapid evaluation of therapeutic countermeasures against WT EBOV isolates. One final adaptation of these immunocompromised animals is humanized, bone marrow liver thymic mice (hu-BLT). These animals

lack murine macrophages, DC, T, B, and NK cells, but are then engrafted with human cells, where they were shown to exhibit high levels of the human immune cells mentioned above. Infection of these animals with WT-EBOV was shown to result in lethal EVD, where viral loads were high and necropsy of the animals revealed histopathological similarities to the human disease. Interestingly, variability in clinical disease was observed from one human cells donor to the other, an interesting alternative over other mouse models where their genetic background are often homogeneous[209].

Guinea pig

Similar to mice, guinea pigs are not susceptible to infection by WT EBOV. Therefore, adaption of the virus is necessary in order to obtain a guinea pig-adapted EBOV (GA-EBOV). Infection of guinea pigs with this adapted virus does recapitulate human EVD fairly accurately, including high viremia and liver damage, as well as limited coagulopathy, but this model lacks the maculopapular rash and lymphocyte bystander apoptosis observed in humans or more complex animal models[210]. Furthermore, guinea pigs do require enhanced husbandry, have a higher unit cost than mice, and availability of reagents to study immune parameters is limited. The guinea pig is however the only rodent, and smallest animal model, to study transmission of EBOV, facilitating the evaluation of transmission factors such as dose or route of infection[211]. Their relatively small size also allows for experiments to be conducted within a BSL4 laboratory with relatively large numbers of animals, which is a requirement to enable accurate evaluations of statistical significance. Finally, their larger size compared to mice allows for more frequent blood collection, increasing the amount of data that can be generated from the same number of animals.

Syrian golden hamster

The Syrian hamster model is a lesser known and used animal model for the study of EVD. As is the case for other rodent models, this model also requires an adapted virus, although MA-EBOV is lethal when administered i.p. in 6-week-old hamsters at a dose of 10^3 focus forming units (ffu)[212]. Subsequent work has also demonstrated that the natural immunity of hamsters is independent of $CD4^+$ and $CD8^+$ T cells, with the exception of the role that $CD4^+$ cells type play in the development of an antibody response, given that serum transfer from infected animals to CD4-depleted hamsters was protective. Interestingly, hamsters experience a similar disease to mice following challenge, although they additionally exhibit severe coagulopathy, a characteristic not observed in mice and guinea pigs, but a hallmark of EVD in humans and NHPs. Unfortunately, species-specific reagents are still lacking to fully understand biological aspects relating to infection, hence the development of new tools will be paramount in the further use of this model given that it mimics aspects of EVD more accurately than mice. Despite this limitation, hamsters have been successfully used for the study of prophylactics[213] and therapeutics[214] in the context of EVD.

Ferret

The domestic ferret, *Mustela putorius furo*, is the most recently developed animal model for EVD. While the usefulness of the model has been known for a relatively long time in other diseases, mostly respiratory diseases such as influenza, it was only recently characterized as a lethal model following infection with EBOV, SUDV, and BDBV[215–217]. Hallmarks of EVD such as fever, kidney and liver damage, coagulopathy, lymphocyte apoptosis, as well as development of a maculopapular rash, were all noted in ferrets infected with either of these viruses, regardless of whether they had been infected i.n. or i.m. Interestingly, two independent groups have shown that ferrets were not susceptible to infection, *i.e.* an absence of mortality and viremia, by WT MARV or RAVN[218,219]. This indicates that, although closely related, *Ebolavirus* and *Marburgvirus* have very distinct mechanisms of evading the immune response. So far, the ferret model in the context of EVD has been used for multiple types of studies, including the evaluation of prophylactic options such as a trivalent parainfluenza virus-vectored BDBV vaccine[220], therapeutic options such as monoclonal antibodies (mAbs)[221], and evaluation of a novel EBOV isolate through the use of a reverse-genetic system[222]. Furthermore, the publication of a draft genome for the ferret in 2014 has now allowed transcriptomics studies to be conducted, revealing a strong induction of proinflammatory and prothrombic signaling in EBOV-infected ferrets, matching what is observed in NHPs and humans[223,224]. Finally, the ferret has also been used as a novel, small animal model for transmission of EBOV, as discussed further in Chapter 2[225].

Non-human primate

Current rodent models, such as the mouse, hamster and guinea pig, poorly mimic clinical EVD in humans for a number of reasons, and these hosts require adaptation of the virus, a process that usually takes months, making the timely evaluation of a new clinical isolate problematic. Adaptation of the virus also generates mutations, a

Table 2: Overview of in vivo model systems

Characteristic	Standard laboratory mouse	Collaborative Cross (RIX) mouse	Humanized mouse	Guinea pig	Hamster	Ferret	Macaque
Cost	Low	Low	Moderate	Low to moderate	Low to moderate	Moderate	Very high
Availability	High	Low	Low	High	High	High	Low
Coagulation abnormalities	No	Yes (strain dependent)	Yes	No	Yes	Yes	Yes
Virus strain	Adapted (mouse)	Wild-type	Wild-type	Adapted (guinea pig)	Adapted (mouse or hamster)	Wild-type	Wild-type
Predictive power	Low	Unknown	Unknown	Moderate	Unknown	Unknown	High

variable that is not desired in some, if not most, studies since these viruses do not accurately represent their naturally occurring counterparts. The NHP remains the most biologically relevant animal model for pathogenesis studies due to its ability to replicate most human hallmarks of EVD and the fact that it does not require virus adaptation. Rhesus and cynomolgus macaques are the two most commonly used species for research on EBOV, with lethal infection of the latter resulting in death of the animal on average one day earlier than the rhesus macaque. While macaques do recapitulate the course of disease, they are expensive, necessitate additional safety precautions and demand increased ethical considerations, which when taken together, makes the model unsuitable for large-scale experiments.

Prophylactic and therapeutic options

The development of efficacious medical countermeasures relies on our understanding of not only the pathogenesis of the virus, but also on correlates of protection, as they could influence the type of antigen or vaccine platform to be selected. A correlate of protection has been defined as any marker of the immune response that statistically correlates with protection. They can be either mechanistic, meaning they are directly responsible for protection, or non-mechanistic, meaning they are not directly responsible for protection but can nonetheless predict protection through correlation with another immune marker which is mechanistically protective[226]. In regard to EBOV, early studies which looked at passive immunotherapy failed to yield encouraging results; therefore, the role of humoral immunity in protection was downplayed, to the profit of cellular immunity. This notion was reinforced by a vaccine study using a replication-deficient human type 5 adenovirus (AdHu5) vector expressing EBOV GP, which showed that passive transfer of high-titer polyclonal antibodies from vaccinated to non-vaccinated NHPs could only confer protection in 1 out of 4 animals. Follow-up experiments where $CD8^+$ T cells were depleted *in vivo*, without affecting $CD4^+$ T cell or humoral responses, led to abrogation of protection in 4 out of 5 animals[227]. However, this was contradicted by other studies which showed that protection could be achieved by using concentrated, polyclonal IgG antibodies from surviving animals[228], or by using specific monoclonal antibodies[229]. Retrospective analysis of hundreds of mice, guinea pigs, and NHPs which either did or did not succumb to infection, in the context of vaccination studies, also highlighted the importance of B and $CD4^+$ T cells in their survival, namely due to elevated levels of total IgG specific to EBOV GP[230]. Indeed, in the context of vaccination with a vesicular stomatitis virus (VSV) platform expressing the EBOV GP, depletion of CD8+ T cells lead to survival, while depletion of CD4+ T cells prior to vaccination abrogated vaccine protection and antibody production. Interestingly, depletion of CD4+ T cells during challenge did not result in mortality of the animals, suggesting that antibodies play a critical role in protection for this specific vaccine[231]. This highlights the fact that not only the quantity but also the quality of immune responses is important in order to confer protection, but that different correlates of protection might exist for different vaccines.

Vaccines

Multiple platforms have been successfully evaluated over the years regarding the development of an efficacious vaccine against EBOV. These platforms include the vesicular stomatitis virus (VSV)[232], adenovirus[233], a modified vaccinia Ankara platform[234], parainfluenza virus[235], cytomegalovirus[236], Venezuelan equine encephalitis virus[237], lipid-based nanoparticles[238], virus-like particles[239], DNA-based vectors[240], as well as live and inactivated rabies virus[241]. Although the preclinical and clinical progress of each vaccine will not be discussed at length in the context of this thesis, they have been extensively reviewed previously[242].

However, there are two vaccines that do deserve extra attention. The first, Ervebo®, is based on the VSV platform and was the first approved vaccine on the market against EVD. Indeed, it received approval from both the European Medicines Agency (EMA), as well as the American Food and Drug Administration (FDA) in late 2019, 43 years after the initial discovery of the virus. Interestingly, this vaccine was originally developed by scientists in 1997 as a tool to study the functions of the viral glycoprotein of EBOV, not as a medical countermeasure[243]. Indeed, the surface glycoprotein of VSV was genetically replaced with EBOV GP to study cellular tropism. It was not until 2005 that a study reported that NHPs could survive a lethal EBOV challenge following a single-dose immunization of this viral vector, which only expresses the surface glycoprotein of EBOV. The vaccine was later used during the 2014-2016 West African outbreak as part of a ring-vaccination trial, where contacts and contacts-of-contacts of confirmed cases were either immediately vaccinated, or received Ervebo® 10 days after identification of the confirmed case. While none of the 4123 individuals assigned to the immediate vaccination group developed EVD at least 10 days following randomisation into one of the groups, 16 individuals out of the 3528 that were in the delayed vaccination group developed EVD. The authors of the trial therefore concluded a vaccine efficacy of 100% in these conditions[244].

The second vaccine of interest is composed of two different vaccines, namely Zabdeno® and Mvabea®, which both received approval from the EMA in July 2020. The former is a recombinant adenovirus type 26 which encodes for the EBOV GP, while the latter is based on the modified Ankara platform and encodes for the GPs of EBOV, SUDV, and MARV, as well as the NP from TAFV. The two vaccines are administered 8 weeks apart, where Zabdeno® constitutes prime vaccination and Mvabea® is administered as a boost. Although there are currently no available efficacy data in humans, this vaccine regimen was established following clinical trials conducted in Kenya, Uganda, and Tanzania. Indeed, when Zabdeno® was administered as a prime and Mvabea® as a boost, 93% of volunteers developed binding antibodies to EBOV GP at the time of Mvabea® injection after a 4-week interval, while this number reached 100% with an 8-week interval. When both vaccines were administered in the reverse order, seropositivity of volunteers could be as low as 14% following prime vaccination with Mvabea®. Regardless of the order of the vaccines or the interval between both doses, all

individuals were found to be seropositive 21 days following boost—an immune response that decreased after 6 months, but that was detectable in all individuals up to 12 months after vaccination[245,246].

Treatments

The development of therapeutic options for EVD has long been a priority given the high mortality and morbidity rate of the disease. Prior to the 2014-2016 West African outbreak, drug development against EVD followed a somewhat similar pace to that of vaccines. However, given the emergency and scale of the aforementioned outbreak, attempts at drug repurposing skyrocketed and so did potential treatments for EVD. Therefore, similar to the vaccine section of this thesis, details about preclinical and clinical data of every drug developed against EVD cannot be extensively discussed, however, they have recently been extensively reviewed previously[247].

Current therapeutic options against EVD can be divided into two general categories: those directed against the host (indirect-acting), and those directed against the virus (direct-acting). At this time, only direct-acting agents have shown any level of efficacy in NHPs, the gold standard model before any human trial may be contemplated. These direct-acting agents can be further subdivided into two categories: inhibitors of the L polymerase, which act as nucleoside analogs and have all been repurposed from other viral therapies, or mAbs which are directed at the surface glycoprotein and have been specifically designed for EBOV. The efficacy of nucleoside analogs in NHPs has been demonstrated for some cases, although with varying efficacy in clinical trials. Galidesivir (BCX4430), an adenosine ribose analog originally developed against the hepatitis C virus (HCV), has shown 100% protection in NHPs when administered on day 2 post-infection, while it was only 67% protective when administered on day 3. However, this data has yet to be peer-reviewed[248]. In contrast, Remdesivir (GS-5734), another adenosine ribose analog initially discovered in the context of HCV and other RNA viruses, has been shown to be 100% efficacious when administered to NHPs up to 72 hours post-infection, including a reduction of viremia below the detection limit of the assay used[249]. These encouraging results warranted further investigation in a clinical trial, which is discussed below. Favipiravir (T-705), a purine analog initially discovered in the context of Influenza A, had shown promise in mouse models, although poor efficacy was noted in NHPs against EBOV, as shown by only a moderate extension of the time-to-death and reduction of viral load[250]. Ultimately, a clinical trial including 126 individuals during the West African outbreak could not detect any significant clinical value of this drug[251]. Finally, Brincidofovir, a lipid-conjugated deoxycytidine inhibitor originally developed against members of the herpesvirus family and smallpox, was shown to be efficacious *in vitro* against EBOV, and was subsequently used during the West African outbreak under compassionate use. Unfortunately, the trial could only enroll 4 participants before the manufacturer discontinued the use of this drug for EVD, therefore efficacy could not be evaluated thoroughly despite all 4 patients succumbing to EVD. Mouse studies conducted after the fact confirmed a lack of efficacy *in vivo* against EBOV[252].

The second class of molecules evaluated against EVD is antibodies. Preliminary work with antibodies as a treatment was conducted mostly during outbreaks, through the use of convalescent serum from survivors. However, the actual efficacy of treatment could not be accurately determined, as individuals usually received other forms of treatment simultaneously, or the numbers of participants in the study was too low[253]. Similarly, one study conducted during the West African outbreak did not report any significant improvement[254]. Following the hits and misses of hyperimmune serum from animals[255,256] and a highly neutralizing mAb from a human survivor[257], it was shown that purified polyclonal IgG from NHP survivors could protect other primates from infection[228]. Subsequently, cocktails of three mAbs started to be developed and showed efficacy in NHPs, namely ZMAb[229] and MB-003[258]. Notably, a collaboration between the groups responsible for each cocktail resulted in an improved cocktail, ZMapp, that could rescue 100% of infected NHPs even when treatment was initiated 5 days post-infection, an advanced state of disease in this model[259]. Unfortunately for ZMapp, a randomized, controlled trial during the West African outbreak established a posterior probability of ZMapp being superior to the current standard of care at the time to be 91.2%, falling short of the prespecified threshold of 97.5%[260]. Finally, it was not until the second largest recorded outbreak in 2018 that new progress was made for EBOV therapeutics. A clinical trial that took place in DRC sought to evaluate the efficacy of four experimental treatments against each other, namely ZMapp, Remdesivir, the single mAb MAb114, or another cocktail of three mAbs, REGN-EB3[261]. Interestingly, patients assigned to the REGN-EB3 group exhibited a CFR of 33.5%, while those in the MAb114 group exhibited a CFR of 35.1%. In contrast, those assigned to the ZMapp and Remdesivir groups had a reported CFR of approximately 49.7% and 53.1%, respectively. Based on these results, REGN-EB3 became the first FDA-approved therapeutic for EVD in October 2020, under the name Inmazeb™. Shortly after, in December 2020, MAb114 became the second approved treatment for treatment of EVD, under the name Ebanga™. Of note, the three antibodies constituting REGN-EB3 have been isolated from mice immunized with a DNA construct encoding the GP and/or recombinant GP from EBOV-Makona. They were shown to either neutralize EBOV GP pseudotypes, trigger FcγRIIIa, and/or bind to sGP[262]. On the other hand, MAb114 is single monoclonal antibody isolated from a human survivor which targets a highly conserved epitope of the GP receptor binding domain, effectively preventing viral entry into the cytoplasm by blocking the interaction of GP with NPC1[263].

Transmission

Animal-to-human interface

As mentioned above, many outbreaks have been traced back to the handling, hunting, or eating of either gorillas, chimpanzees, or duikers. However, the source of infection was laboratory-confirmed on only three separate occasions, accounting for approximately 10% of outbreaks. For the remaining outbreaks, the original spillover

event could only be speculated over, with speculations ranging from environmental exposure to the hunting or eating of wild animals such as fruit bats, insectivorous bats, non-human primates, antelopes, rodents, elephants, pigs, or other small animals[264]. Of note, not all of these animals were even identified as intermediary hosts for EBOV or shown to support EBOV replication, indicative that further animal studies are needed. However, there are some parameters that can be associated with zoonotic transmission of EBOV. It has been reported previously that a sudden large decline in wild-life populations, such as gorillas, preceded some of the past outbreaks[123,265]. Mathematical models also revealed a strong association between spillover events and high population density. Interestingly, in areas of low population density, increasing vegetation cover would reduce the risks of zoonotic transmission, while as population density from a given area increased, increased vegetation cover was associated with increased risk of zoonotic infection[266]. Studying the transmission of EBOV from the environment into the human population is a challenging endeavour. Indeed, due to the fragilized health care system, often unreliable means of communication, and the remoteness of the epicenter of outbreaks, determining which patient represents the index case can be a challenge on its own; determining where that individual initially contracted the disease is even more complex as authorities may not be notified immediately.

One of the best described examples of this comes from the 2014-2016 West African outbreak. Indeed, the first notification to authorities of mysterious deaths came in early March 2014 from Meliandou, a village near Guéckédou (Guinea), but the index case was traced back to a 2-year old child that had succumbed to a disease consistent with EVD in early December 2013[172], four months prior to the initial notification of the outbreak. Then, in April 2014, a team tasked with investigating the zoonotic origin of the outbreak arrived to Meliandou[267]. Discussions with local authorities, hunters, and women revealed that very few primates lived in the region, hence they were not hunted frequently. The hypothesis of infected bushmeat imported from other regions was also discarded as a hunter who would have brought bushmeat would have likely been among the first victims. However, there were numerous reports of fruit bat migrations through the village, and insectivorous bats were commonly found under the roof of houses, where they were hunted, cooked, and eaten by children. Further investigation identified a nearby hollow tree, in which children used to play, but was unfortunately set on fire by villagers on March 24th, 2014. Villagers described a “rain of bats” as the tree was burning. Analysis of the ashes by the investigative team identified short 16S mitochondrial DNA fragments that could have belonged to *Mops condylurus*, a species previously shown to play a certain role in filoviruses ecology, as denoted by serological infection of EBOV and the identification of viral sequences to BOMV[5,128]. As illustrated by this example, numerous challenges are associated with such retrospective studies. These studies often rely on testimonies from individuals, and delayed collection will inevitably be associated with poor data, as memory may prove unreliable for small but relevant details that may help with the investigation. Finally, the time period between the first casualty and notification of authorities may also affect the environment which could provide valuable clues.

Indeed, carcasses may be disposed of, trees or other structures could be burned, animals could have migrated, and meteorological factors such as heavy rain, wind, and the sun may destroy useful evidence.

Human-to-human interface

It is now well established that in an outbreak setting, transmission of EBOV between humans occurs through contact with infected bodily fluids, where the virus is thought to most commonly enter a susceptible individual through transcutaneous skin lesions, the conjunctiva, as well as the oropharyngeal mucosa. Transmission of the virus from human to human is common during activities for which the appropriate PPE is not worn properly, or at all, such as caring for the sick or during ritual burials, where washing the body by multiple family members is a common practice in Central and Western Africa[268]. This could explain why the proportion of women affected by EVD during a given outbreak can be higher than the proportion of men, given that culturally, women are the ones who often care for the ill within the household[269].

Viral RNA associated with EBOV has been detected in various types of samples such as blood, semen, stool, urine, amniotic and cerebrospinal fluid, aqueous humor, saliva, breast milk, as well as conjunctival, vaginal, and skin swabs[270]. Furthermore, infectious virus has successfully been isolated from blood, urine, saliva, breast milk, semen, and aqueous humor[271]. While the notion that semen could contain EBOV has been around for a long time, it was not until the 2014-2016 West African outbreak that sexual transmission of the virus was observed and confirmed by sequencing of the virus from a previously infected male, to his female partner, months after he had cleared the virus from his blood[202,272]. There are currently no available reports of infectious EBOV having been cultivated from amniotic fluid, however, vertical transmission of the virus from mother to child during pregnancy has been hypothesized given the high rate of neonatal mortality in pregnant women who become infected with EBOV[273,274]. Similarly, there have been reports of infectious EBOV isolated from breastmilk, but a transmission event involving breastfeeding has yet to be reported[275].

Regarding aerosol transmission of the virus, there has been conflicting evidence both from the field and the laboratory. Experimental work with EBOV has shown that this virus is not only able to induce pulmonary lesions, but also to shed via respiratory secretions[276,277]

Knowledge gap

As new filoviruses spill over into the human population, one metric that scientists often use to qualify outbreaks is the CFR associated with the etiological agent of said outbreak. As such, EBOV has often been characterized as the most lethal of the human-affecting ebolaviruses, due to its propensity to reach high CFRs. However, this general idea that EBOV is the deadliest ebolavirus is outdated as it is currently not supported by robust statistical analysis. Indeed, the three most common ebolaviruses behind human epidemics, EBOV, SUDV, and BDBV,

have been characterized by CFRs of 43.92±0.7%, 53.72±4.456%, and 33.65±8.38%, respectively[142]. The reason(s) as to why such variations are observed is currently unknown. These variations could stem from human error and negligence (*e.g.*, a lack of case recognition, surveillance, and readiness of African healthcare systems) or human behavior related to traditional health-seeking customs. Other factors such as genetic variations between distinct communities, nutrition, immune status, and co-infections warrant further investigation.

Therefore, the reason as to why one individual in particular does or does not succumb to EVD is currently unclear. From an immunological perspective, our group has previously demonstrated that following vaccination, antibody levels specific to the surface glycoprotein of EBOV correlate with protection against homologous challenge[230]. In this thesis, the question regarding survival of an individual is being investigated from a viral standpoint, as both the virus and the immune system undeniably compete during infection to generate their respective outcome; the immune system working towards limiting, and eventually eradicating, virus replication, while the virus itself only seeks to replicate unchecked.

Finally, experimental data resulting from lethal challenge of animal models such as non-human primates have consistently showed that peak viremia commonly occurs 6 to 8 days post-infection, or 1 to 2 days preceding death of the animal[276,278]. In parallel, observations from the field during epidemics have revealed that unsafe burials of individuals who succumbed to EVD—meaning that IPC practices were not properly adhered to—represented a significant risk factor for contracting the disease[191]. In the context of this thesis, the role that viral load plays in enabling transmission of the virus from an infected individual to a naïve, susceptible host is also investigated.

Hypothesis

Therefore, the hypothesis for this thesis is: **viral load, as a result of Ebola virus replication, is a predictor of disease severity and transmission.**

Objectives

The role of viral load in disease severity and transmission will be assessed in two different settings: a natural outbreak setting in humans, as well as an experimental setting using both a ferret and a non-human primate model.

1) **To characterize the role of viral load on clinical outcome as a disease severity marker during an outbreak setting in humans.** In collaboration with local authorities and *Médecins Sans Frontières* (MSF), the data obtained at an EMC will be used to assess whether viremia of individuals presenting at the EMC is

associated with outcome, a terminal marker for disease severity. These results are described throughout Chapter 1 of this thesis.

2) **To establish the potential of the ferret as an animal model for transmission of EBOV, as it does not require adaptation of clinical isolates.** Animal models allow for the control of parameters that are nearly impossible to control in a natural outbreak setting such as the exact moment an individual becomes infected. Parameters such as viral shedding from the oral, nasal, and rectal cavities can also be monitored—data that is not routinely collected in a diagnostic setting. Chapter 2 of this thesis builds on previous work with guinea pigs and GA-EBOV by establishing the foundation of a novel small animal model for transmission of WT-EBOV, and by characterizing the effects of direct- and indirect contact on disease transmission.

3) **To characterize the role of viral loads in transmission from non-human primates challenged by various routes of infection, to a susceptible host.** NHPs remain the gold standard animal model for EVD. Results presented in Chapter 3 describe the role that various routes of infection commonly encountered in both natural and laboratory settings, as well as viremia and viral shedding, have on direct transmission of EBOV to a naïve animal.

Chapter 1. Ebola viral load at diagnosis associates with patient outcome and outbreak evolution.

Marc-Antoine de La Vega,[1,2] Grazia Caleo,[3] Jonathan Audet,[1,4] Xiangguo Qiu,[1,4] Robert A. Kozak,[1] James I. Brooks,[5] Steven Kern,[6] Anja Wolz,[7] Armand Sprecher,[8] Jane Greig,[3] Kamalini Lokuge,[9] David K. Kargbo,[10] Brima Kargbo,[10] Antonino Di Caro,[11] Allen Grolla,[1] Darwyn Kobasa,[1] James E. Strong,[1] Giuseppe Ippolito,[11] Michel Van Herp,[7] and Gary P. Kobinger[1,2,4,12]

[1]Special Pathogens Program, National Microbiology Laboratory, Public Health Agency of Canada (PHAC), Winnipeg, Manitoba, Canada. [2]Department of Immunology, University of Manitoba, Winnipeg, Manitoba, Canada. [3]Manson Unit, Médecins Sans Frontières (MSF), London, United Kingdom. [4]Department of Medical Microbiology, University of Manitoba, Winnipeg, Manitoba, Canada. [5]National Laboratory for HIV Genetics, PHAC, Ottawa, Ontario, Canada. [6]Quantitative Sciences, Bill and Melinda Gates Foundation, Seattle, Washington, USA. [7]Medical Department Unit and [8]Operational Centre (Brussels), MSF, Brussels, Belgium. [9]National Centre for Epidemiology and Population Health, Research School of Population Health, Australian National University, Canberra, Australia. [10]Ministry of Health (MoH) and Sanitation, Government of Sierra Leone, Freetown, Sierra Leone. [11]Lazzaro Spallanzani National Institute for Infectious Diseases, Rome, Italy. [12]Department of Pathology and Laboratory Medicine, University of Pennsylvania School of Medicine, Philadelphia, Pennsylvania, USA.

Role of funding source: The PHAC had no role in study design, data collection, or data analysis.
Authorship note: Marc-Antoine de La Vega and Grazia Caleo contributed equally to this work.
Conflict of interest: The authors have declared that no conflict of interest exists.
Submitted: June 8, 2015; **Accepted:** September 28, 2015.
Reference information: J Clin Invest. doi:10.1172/JCI83162

Address correspondence to: Gary P. Kobinger, Special Pathogens Program, National Microbiology Laboratory, PHAC, 1015 Arlington Street, Winnipeg, MB, R3E 3R2 Canada. Phone: 204.784.5923; E-mail: gary.kobinger@phac-aspc.gc.ca.

1.1 Résumé

CONTEXTE. Le virus Ebola (EBOV) est à l'origine d'épidémies de maladie à virus Ebola (MVE) potentiellement mortelles en Afrique. Historiquement, ces épidémies étaient relativement petites et géographiquement limitées; cependant, l'ampleur de l'épidémie qui a débuté en Afrique de l'Ouest en 2014 est sans précédent. Le but de cette étude était de décrire la cinétique virale d'EBOV durant cette épidémie et d'identifier les facteurs qui ont contribué à la progression de cette épidémie. **MÉTHODES.** De juillet à décembre 2014, un laboratoire au Sierra Leone a traité plus de 2,700 échantillons cliniques destinés au diagnostic du virus Ebola par PCR quantitatif (qPCR). La virémie fut mesurée suite à l'admission du patient. L'âge, le sexe, et le temps approximatif de début des symptômes fut aussi enregistré pour chaque patient. Les données ont été analysées en utilisant plusieurs modèles mathématiques afin d'identifier les tendances potentielles d'intérêt. **RÉSULTATS.** L'analyse révèle une différence significative (P = 2.7 x 10^{-77}) entre la virémie à l'admission des survivants (4.02 $\log_{10}$ copies de génome [GEQ]/ml) et les non-survivants (3.18 $\log_{10}$ GEQ/ml). Au niveau de la population, la charge virale des patients était en moyenne plus élevée en juillet, qu'en novembre, et ce même en tenant compte de l'issue des patients et du temps écoulé depuis le début des symptômes. Cette diminution de la charge virale corrèle temporellement avec une augmentation en IgG circulants spécifiques à EBOV parmi les individus suspectés d'avoir été infectés, mais qui ont testés négatifs pour la présence du virus par PCR. **CONCLUSIONS.** Nos résultats indiquent que la charge virale à l'admission est associée avec l'issue d'un individu et la durée d'une épidémie; ainsi, un grand soin se doit d'être apporté lors de la planification d'essais cliniques et des interventions. Des recherches supplémentaires sur l'adaptation du virus et l'impact des facteurs de l'hôte sur la transmission et la pathogénèse d'EBOV sont nécessaires.

1.2 Abstract

BACKGROUND. Ebola virus (EBOV) causes periodic outbreaks of life-threatening EBOV disease in Africa. Historically, these outbreaks have been relatively small and geographically contained; however, the magnitude of the EBOV outbreak that began in 2014 in West Africa has been unprecedented. The aim of this study was to describe the viral kinetics of EBOV during this outbreak and identify factors that contribute to outbreak progression. **METHODS.** From July to December 2014, one laboratory in Sierra Leone processed over 2,700 patient samples for EBOV detection by quantitative PCR (qPCR). Viremia was measured following patient admission. Age, sex, and approximate time of symptom onset were also recorded for each patient. The data was analyzed using various mathematical models to find trends of potential interest. **RESULTS.** The analysis revealed a significant difference (P = 2.7 × 10^{-77}) between the initial viremia of survivors (4.02 $\log_{10}$ genome equivalents [GEQ]/ml) and nonsurvivors (6.18 $\log_{10}$ GEQ/ml). At the population level, patient viral loads were higher on average in July than in November, even when accounting for outcome and time since onset of

symptoms. This decrease in viral loads temporally correlated with an increase in circulating EBOV-specific IgG antibodies among individuals who were suspected of being infected but shown to be negative for the virus by PCR. **CONCLUSIONS.** Our results indicate that initial viremia is associated with outcome of the individual and outbreak duration; therefore, care must be taken in planning clinical trials and interventions. Additional research in virus adaptation and the impacts of host factors on EBOV transmission and pathogenesis is needed.

1.3 Introduction

Ebola virus (EBOV)[1,279] is one of the deadliest pathogens in existence. Infection of a suitable host results in EBOV disease (EVD), which is characterized by the onset of a broad array of flu-like symptoms including fever, myalgia, and a general malaise. Disease progression leads to gastro-intestinal manifestations, multiple-organ failure, and eventual death in up to 90% of cases[10,280]. On March 22, 2014, WHO was notified by the MoH of Guinea that an outbreak of EVD was rapidly unfolding in the south-eastern region of the country, near the borders of Sierra Leone and Liberia[172]. Genomic characterization of the virus identified it as a novel EBOV variant (strain Makona), with notable sequence heterogeneity compared with the 1995 Kikwit reference strain[172,281,282]. Subsequently, Liberia reported its first confirmed case[174], and by the end of May 2014, Sierra Leone was also adding its name to the list of affected countries[173]. Over a year has passed since the beginning of the largest documented Ebola outbreak, and to date (as of August 12, 2015) there have been 27,948 cases (reported and confirmed) and 11,284 deaths. Disconcertingly, Sierra Leone has accounted for almost 50% of the case burden. This study investigated the temporal changes in viral loads among laboratory-confirmed cases that were presented at the Kailahun Ebola Management Centre during a 5-month period of the outbreak and highlighted key factors that may have influenced the progression of the epidemic.

1.4 Methods

1.4.1 Study population.

From July to November 2014, the mobile laboratory operated by the PHAC was deployed to provide diagnostic testing support at an EMC in the Kailahun district of Sierra Leone, managed by MSF. During these 5 months, over 2,700 samples from about 1,200 patients were analyzed. December was excluded from the analysis, as there were only 2 positive cases during this month. Patients were screened on arrival at the EMC and relocated to the relevant areas of the EMC. Patients who tested positive for EBOV were kept at the EMC to receive care until final outcome (death or convalescence), while the ones who were found negative were released. The mobile laboratory staff was evacuated for safety reasons on August 25, 2014; the laboratory was reopened on September 10, 2014.

1.4.2 Procedures.

Samples were received by the onsite laboratory and inactivated using a previously published method[283] inside a flexible film, negative pressure isolator using Rapid Containment Kit (Germfree Laboratories) followed by RNA extraction and purification. qPCR assays targeting the Ebola polymerase (L) and nucleoprotein (NP) genes were used to detect the presence of EBOV using LightCycler 480 RNA Master Hydrolysis reagents (Roche Diagnostics) according to manufacturer's instructions. Primers and probes were as follows: ZEBOV LF (5'-CAGCCAGCAATTTCTTCCAT), ZEBOV LR (5'-TTTC- GGTTGCTGTTTCTGTG), ZEBOV LP1 (FAM-ATCATTGGC/ZEN/ RTACTGGAGGAGCAG-BHQ1), ZEBOV LP2 (FAMTCATTGGCG/ ZEN/TACTGGAGGAGCAGG-BHQ1), ZEBOV NPF (5'-TGCCGAC- GACGAGACGT), ZEBOV NP2 (5'-CGTCCCTGTCCTGTTCTTCAT), and ZEBOV NPP (FAM-AGYCTTCCG/ZEN/CCCTTGGAGTCAGA). Probes were obtained from IDT Labs and contained an internal quencher (/ZEN/), as indicated.

Assays were performed on the LightCycler Nano platform (Roche Diagnostics). Primary testing focused on EBOV diagnosis using cut- off cycle threshold (CT) values for positive, equivocal, and negative of ≤37, 37.1–40, and >40, respectively. The assays detected EBOV at approximately 10 genome equivalents/reaction. Differential diagnostics were also offered for Lassa virus[284] and Plasmodium species[285]. As an internal control for extraction and amplification procedures, MS2 phage was added to each sample as previously described[286] to ensure that the extraction, PCR setup, and run parameters did not change between operators or over time. The data shown was generated from EDTA blood samples collected at the MSF EMC. CT values were converted to GEQ/ml based on the average of 10 replicates of an in-house laboratory standard curve (Supplemental table 1: Coversion between CT values obtained by RT-qPCR and the corresponding viral loads.

Supplemental table 2: Log-unit difference between the end of a given month and July 1st in the linear regressionSupplemental table 3).

IgG ELISA were performed using the Crocodile ELISA miniWork station (5-in-one) (Titertek-Berthold). Polystyrene microtitre plates (Costar, Corning Inc.) were coated with 50 ng/well/100 µl of sucrose purified inactivated EBOV in PBS overnight at 4°C. Sucrose purified inactivated Marburg virus (MARV) was used as a negative control antigen (Ag). Plates were washed with PBS containing 0.1% Tween-20 (washing buffer), then blocked with 200 µl PBS-5% skim milk for 15 minutes at 37°C, before sera diluted in blocking solution (33 µl) was added for 1 hour at 37°C. After washing, 100 µl of detection antibody (Peroxidase-conjugated goat anti-human IgG) (diluted 1:2,000 in blocking solution) was added for 1 hour at 37°C. Subsequently, plates were washed, and 100 µl of substrate (2,2'-azino-bis[3-ethylbenzothiazoline-6-sulphonic acid] [ABTS]; KPL) was added to each well for 20 minutes at 37°C, before reading on a microplate reader at 405 nm. A sample was

positive when the absorbance minus background was higher than the mean plus 4 standard derivations of the serum pool of 20 normal people.

1.4.3 Statistics.

The overall linear regression of viremia over time, *t* tests, and ANOVA were performed using GraphPad Prism version 6.05. For *t* tests, Gaussian distribution was assumed and 2-tailed, unpaired equal variance *t* tests were conducted at a confidence level of 95%. Ordinary 1-way ANOVAs with Tukey's multiple comparisons test (single pooled variance) were conducted at a confidence level of 95%.

In order to assess the difference in viremia over time and between survivors and nonsurvivors, we used a linear model to account for other variables that may have impacted the viral loads. The predictors we explored were: (i) the time (in days) since July 1, 2014; (ii) the time (in days) between the initial sample and onset of symptoms (the onset of symptoms was estimated by the patients and physicians); (iii) the age of the patient; and (iv) the sex of the patient. The significance threshold for including the individual main effects in the model was 0.25, and the significance threshold for keeping a predictor in the full model was 0.1. The linearity of the relationships was verified graphically; the time since July 1, 2014, was the only nonlinear predictor. The differences in CFRs between multiple groups were tested by the χ^2 test followed by the Marascuillo procedure, if the χ^2 test was significant. The data cleaning, preparation, and analysis were performed using Revolution R open (based on R version 3.1.2, with a CRAN snapshot from April 30, 2015; Revolution Analytics). A *P* value less than 0.05 was considered significant.

1.4.4 Study approval.

This work was conducted as part of the international public health response to help with the containment of the outbreak in Sierra Leone, and therefore, informed consent was not obtained from individual patients. Ethics approval was obtained from the Government of Sierra Leone Ethic Review Board in Freetown to use, analyze, and publish controlled, unidentified, anonymous data collected during diagnostic testing. This study met the standards set by the independent MSF Ethics Review Board for retrospective analyses of routinely collected programmatic data[287].

1.5 Results

1.5.1 Characteristics of the study population.

Approximately 1,200 people were tested for EBOV infection at the Kailahun Ebola Management Center (EMC), of which 632 had a complete data set and were included in the analysis. The data set consisted of: age, sex, date of symptom onset, dates of all available sampling, viral load, and patient outcome (deceased or survived).

Individuals without a complete data set were excluded from the analysis. The median age of the study population was 25 years old (mean: 26.9 years old; range: 4 months–75 years old). The population was composed of 319 males and 313 females. Our dataset included 379 survivors and 253 fatalities for an overall case fatality rate (CFR) of 40%. The median time between symptom onset and diagnostic sampling was 7 days, with an interquartile range of 6 days. The characteristics of the cohort studied are summarized in Table 5: Descriptive and bivariable analysis of the patients.

[A]Determined using a 2-tailed unpaired equal variance *t* test for sex and survival. For age and time since onset of symptoms (sampling), the significance was determined using a linear regression of $\log_{10}$ GEQ/ml vs. age in years or $\log_{10}$ GEQ/ml vs. time since onset of symptoms.

Figure 12: Characterization of the viral load levels.Table 6.

Table 5: Descriptive and bivariable analysis of the patients.

[A]Determined using a 2-tailed unpaired equal variance *t* test for sex and survival. For age and time since onset of symptoms (sampling), the significance was determined using a linear regression of $\log_{10}$ GEQ/ml vs. age in years or $\log_{10}$ GEQ/ml vs. time since onset of symptoms.

	Subjects		EBOV viremia on admission (Log_{10} GEQ/ml)		
Feature		**#**	**Mean [95% CI]**	**Difference [95% CI]**	***P* value[A]**
Sex	Male	319	4.87 [4.69, 5.06]	Base	0.8332
	Female	313	4.90 [4.73, 5.07]	0.03 [−0.23, 0.28]	
Age (years)	<5	28	4.55 [3.94, 5.16]	Base	0.0104
	5–14	99	4.72 [4.42, 5.02]	0.17 [−0.72, 1.02]	
	15–40	381	4.79 [4.63, 4.96]	0.24 [−0.57, 1.06]	
	>40	124	5.38 [5.10, 5.66]	0.83 [−0.04, 1.63]	
Sampling	<5 days	172	5.58 [5.35, 5.80]	Base	5.63×10^{-15}
	≥5 days	460	4.63 [4.48, 4.78]	−0.95 [−1.22, −0.67]	
Outcome	Survivors	379	4.02 [3.89, 4.15]	Base	2.70×10^{-77}
	Nonsurvivors	253	6.18 [6.04, 6.32]	2.16 [1.96, 2.36]	
Total		632	4.89 [4.76, 5.02]	–	–

1.5.2 Bivariable analyses.

We initially compared viremia across the different aspects of the population, such as age, sex, and survivorship. Nonsurvivors had a significantly higher viremia on admission (6.18 $\log_{10}$ genome equivalents [GEQ]/ml of blood, 95% CI, 6.04–6.32) compared with survivors (4.02 $\log_{10}$ GEQ/ml of blood, 95% CI, 3.89–4.15) ($P = 2.70 \times 10^{-77}$) (Table 5: Descriptive and bivariable analysis of the patients.

[A]Determined using a 2-tailed unpaired equal variance *t* test for sex and survival. For age and time since onset of symptoms (sampling), the significance was determined using a linear regression of $\log_{10}$ GEQ/ml vs. age in years or $\log_{10}$ GEQ/ml vs. time since onset of symptoms.

Figure 12: Characterization of the viral load levels.Table 6). Age (P = 0.0104) and time between symptom onset and sampling ($P = 5.63 \times 10^{-15}$) were also significantly associated with viremia. There was no difference in initial viremia between the sexes.

1.5.3 Outbreak kinetics.

We first sought to determine if the initial viral loads of patients upon admission to the EMC changed over the course of the outbreak, regardless of outcome. The viral loads of 632 patients who tested positive for EBOV immediately following presentation at the EMC were plotted over the course of the epidemic (Figure 13: Characterization of the viral load levels.

When applicable, the arithmetic mean is shown, and the error bars represent the 95% CI. **(A)** Initial viral loads of the selected 632 patients throughout the outbreak in Kailahun, Sierra Leone. Linear regression is shown in red. (*n* = 632). **(B)** Initial viral loads of patients for the first 2 weeks of July (*n* = 43) and the last 2 weeks of November (*n* = 67). **(C)** Number of days between the reported date of symptom onset and the date of the initial sampling at the EMC on the same data set from **B**. Two-tailed, unpaired t tests. **0.001 < *P* < 0.01.

Figure 14: Correlation between viral load and outcome for the months of July and November.Figure 15A) and fitted to a linear regression. Analysis of this data indicated that the viral loads of patients following arrival at the EMC were lower at the end of the data set in November when compared with July (slope = –0.01051 [95% CI, –0.01336 to –0.007661] log_{10} GEQ/ml per day). The mobile laboratory operated by the PHAC was not active between August 25 and September 9, 2014, (epidemiological weeks 35–37), since the personnel was evacuated for safety reasons, explaining the gap in coverage for this time period (Figure 13: Characterization of the viral load levels.

When applicable, the arithmetic mean is shown, and the error bars represent the 95% CI. **(A)** Initial viral loads of the selected 632 patients throughout the outbreak in Kailahun, Sierra Leone. Linear regression is shown in red. (*n* = 632). **(B)** Initial viral loads of patients for the first 2 weeks of July (*n* = 43) and the last 2 weeks of November (*n* = 67). **(C)** Number of days between the reported date of symptom onset and the date of the initial sampling at the EMC on the same data set from **B**. Two-tailed, unpaired t tests. **0.001 < *P* < 0.01.

Figure 14: Correlation between viral load and outcome for the months of July and November.Figure 15A). However, the same equipment, reagents, and protocols were used before and after the evacuation. Many of the laboratory staff deployed from September to November had also been deployed in July or August. Staff members reported similar performance for internal controls before and after the gap.

A decrease of the mean initial viremia was observed when samples collected at the beginning of this study (first 2 weeks of July, when the EMC was initially opened) were compared with those taken immediately prior to the closing of the facility (final 2 weeks of November). The mean initial viremia for July was 6.168 log_{10} GEQ/ml of blood (95% CI, 5.673–6.662), but had dropped to 5.110 log_{10} GEQ/ml of blood (95% CI, 4.681–5.538) by November (Figure 13: Characterization of the viral load levels.

When applicable, the arithmetic mean is shown, and the error bars represent the 95% CI. **(A)** Initial viral loads of the selected 632 patients throughout the outbreak in Kailahun, Sierra Leone. Linear regression is shown in red. (*n* = 632). **(B)** Initial viral loads of patients for the first 2 weeks of July (*n* = 43) and the last 2 weeks of November (*n* = 67). **(C)** Number of days between the reported date of symptom onset and the date of the initial sampling at the EMC on the same data set from **B**. Two-tailed, unpaired t tests. **0.001 < *P* < 0.01.

Figure 14: Correlation between viral load and outcome for the months of July and November.Figure 15B). An unpaired, 2-tailed t test revealed this difference to be significant (t[108] = 3.184, P = 0.0019). To understand potential factors that may have played a role in the observed decrease in viral loads, we first compared the difference in days between the reported date of disease onset and the date of initial sampling. The analysis revealed that patients in July arrived to the EMC, on average, 6.7 (95% CI, 5.5–8.0) days after the reported onset of symptoms. This average was 7.2 (95% CI, 5.9–8.6) days for November (Figure 13: Characterization of the viral load levels.

When applicable, the arithmetic mean is shown, and the error bars represent the 95% CI. **(A)** Initial viral loads of the selected 632 patients throughout the outbreak in Kailahun, Sierra Leone. Linear regression is shown in red. (*n* = 632). **(B)** Initial viral loads of patients for the first 2 weeks of July (*n* = 43) and the last 2 weeks of November (*n* = 67). **(C)** Number of days between the reported date of symptom onset and the date of the initial sampling at the EMC on the same data set from **B**. Two-tailed, unpaired t tests. **0.001 < *P* < 0.01.

Figure 14: Correlation between viral load and outcome for the months of July and November.Figure 15C). An unpaired, 2-tailed t test indicated this difference to be nonsignificant (t[108] = 0.5220, P = 0.6028). Linear regression analysis revealed that, from July 1 to July 31, there was a nonsignificant 0.22 decrease in log_{10} GEQ/ml of blood [95% CI, –1.25–0.81]. Similarly, a nonsignificant 0.31 log increase in viral loads (95% CI, –0.48–1.10) was observed between July 1 and August 31. However, marked decreases were observed when the analysis spanned from July 1 to September 30 (–2.37 log-units, 95% CI, –2.90 to –1.84), October 31 (–2.08 log-units; 95% CI, –2.56 to –1.61), and November 30 (–1.60 log-units; 95% CI, –2.04 to –1.17) (Supplemental table 4: Log-unit difference between the end of a given month and July 1st in the linear regression

Supplemental table 5: Parameters of the receiver operating characteristic (ROC) analysisSupplemental table 6; supplemental material available online with this article; doi:10.1172/JCI83162DS1).

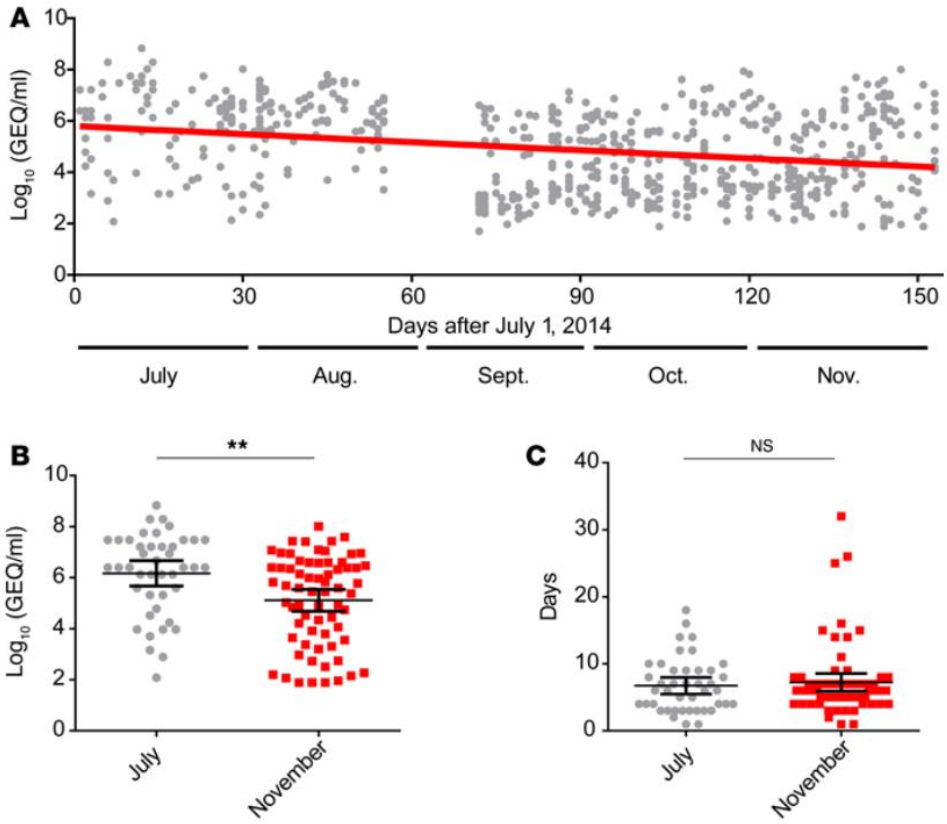

Figure 13: Characterization of the viral load levels.

When applicable, the arithmetic mean is shown, and the error bars represent the 95% CI. **(A)** Initial viral loads of the selected 632 patients throughout the outbreak in Kailahun, Sierra Leone. Linear regression is shown in red. (*n* = 632). **(B)** Initial viral loads of patients for the first 2 weeks of July (*n* = 43) and the last 2 weeks of November (*n* = 67). **(C)** Number of days between the reported date of symptom onset and the date of the initial sampling at the EMC on the same data set from **B**. Two-tailed, unpaired t tests. **0.001 < *P* < 0.01.

1.5.4 Viral load as a predictor of outcome.

We next investigated whether age and viral loads at admission had an impact on patient outcome that changed during the outbreak. To this end, we categorized the same 632 patients by viral load and calculated the CFRs for each group (Supplemental figure 3: Correlation between viral load and outcome for the entire data collection period.

(n=632) The case fatality rate (CFR, %) and the case survival rate (CSR, %) are stacked, divided by viral clusters of high (>6.94), intermediate (4.24-6.94) and low (<4.24) viremia and sub-divided by age groups (Below 5, between 5 and 14, between 15-40 and above 40 years old) for the whole outbreak in Kailahun, Sierra Leone, from July to November. Survivors are shown in blue and non-survivors are shown in red.). Viremia was arbitrarily classified as low, intermediate, or high (<4.24, 4.24–6.94, and >6.94 GEQ/ml, respectively, corresponding to Ct values of >30, 20–30, and <20). Only samples from July (Figure 16: Correlation between viral load and outcome for the months of July and November.

The CFR (%) and the case survival rate (CSR, %) are stacked, divided by viral clusters of low (<4.24), intermediate (4.24–6.94) and high (>6.24) viremia and subdivided by age groups (below 5, between 5 and 14, between 15 and 40, and above 40 years old). ***(A and B)*** *Months of July (n = 93)* ***(A)*** *and November (n = 165)* ***(B)*** *are represented. Survivors are shown in blue and nonsurvivors are shown in red.* ***(C)*** *Sensitivity and 1 minus specificity (ROC curves) are shown at various threshold values of viral loads for each month of the outbreak in Kailahun. (July: green, n = 47; August: yellow, n = 81; September: red, n = 134; October: orange, n = 159; November: blue, n = 164).A) and November (Figure 16: Correlation between viral load and outcome for the months of July and November.*

The CFR (%) and the case survival rate (CSR, %) are stacked, divided by viral clusters of low (<4.24), intermediate (4.24–6.94) and high (>6.24) viremia and subdivided by age groups (below 5, between 5 and 14, between 15 and 40, and above 40 years old). **(A and B)** Months of July (*n* = 93) **(A)** and November (*n* = 165) **(B)** are represented. Survivors are shown in blue and nonsurvivors are shown in red. **(C)** Sensitivity and 1 minus specificity (ROC curves) are shown at various threshold values of viral loads for each month of the outbreak in Kailahun. (July: green, *n* = 47; August: yellow, *n* = 81; September: red, *n* = 134; October: orange, *n* = 159; November: blue, *n* = 164).B) were investigated in order to evaluate differences observed in patients between the beginning and the end of data collection.

The analysis revealed that the CFR for July was significantly higher (52.7%, Figure 16: Correlation between viral load and outcome for the months of July and November.

*The CFR (%) and the case survival rate (CSR, %) are stacked, divided by viral clusters of low (<4.24), intermediate (4.24–6.94) and high (>6.24) viremia and subdivided by age groups (below 5, between 5 and 14, between 15 and 40, and above 40 years old). **(A and B)** Months of July (n = 93) **(A)** and November (n = 165) **(B)** are represented. Survivors are shown in blue and nonsurvivors are shown in red. **(C)** Sensitivity and 1 minus specificity (ROC curves) are shown at various threshold values of viral loads for each month of the outbreak in Kailahun. (July: green, n = 47; August: yellow, n = 81; September: red, n = 134; October: orange, n = 159; November: blue, n = 164).A), than for November (30.9%, Figure 16: Correlation between viral load and outcome for the months of July and November.*

*The CFR (%) and the case survival rate (CSR, %) are stacked, divided by viral clusters of low (<4.24), intermediate (4.24–6.94) and high (>6.24) viremia and subdivided by age groups (below 5, between 5 and 14, between 15 and 40, and above 40 years old). **(A and B)** Months of July (n = 93) **(A)** and November (n = 165) **(B)** are represented. Survivors are shown in blue and nonsurvivors are shown in red. **(C)** Sensitivity and 1 minus specificity (ROC curves) are shown at various threshold values of viral loads for each month of the outbreak in Kailahun. (July: green, n = 47; August: yellow, n = 81; September: red, n = 134; October: orange, n = 159; November: blue, n = 164).B) ($\chi^2[1] = 22.862$, $P = 1.7 \times 10^{-6}$). However, the differences in CFR for each viral load cluster were not significantly different between July and November 2014 (high viral load: $\chi^2[2] = 0.715$, $P = 0.699$; medium viral load: $\chi^2[2] = 4.518$, $P = 0.104$; low viral load $\chi^2[2] = 2.650$, $P = 0.266$). This is known as Simpson's paradox: the difference in the overall rates is a result of the fact that the low and intermediate viral loads are overrepresented in November (Supplemental figure 4: Proportion of cases for the months of July and November*

The proportion of cases for July (Green) and November (Purple) is shown based on viremia. Dashed lines represent the viral clusters defined in the text (<4.24, 4.24-6.94, >6.94)). However, the CFRs by viral load clusters were significantly different from each other within each month (July: $\chi^2[2] = 49.432$, $P = 1.8 \times 10^{-11}$; November: $\chi^2[2] = 115.67$, $P \leq 2.2 \times 10^{-16}$), indicating that patients with different levels of viremia died at differing rates. The Marascuillo procedure for comparing multiple proportions showed that all 3 levels of viremia had statistically different fatality rates for both July and November. The analysis revealed that viral loads above 6.94 $\log_{10}$ GEQ/ml of blood on admission led to fatal outcomes in 89.1% of cases (95% CI, 81.3– 96.9). In contrast, viral loads lower than 4.24 $\log_{10}$ GEQ/ml of blood on admission were associated with death in 7.4% of cases (95% CI, 5.8–9) (Supplemental figure 3: Correlation between viral load and outcome for the entire data collection period.

(n=632) The case fatality rate (CFR, %) and the case survival rate (CSR, %) are stacked, divided by viral clusters of high (>6.94), intermediate (4.24-6.94) and low (<4.24) viremia and sub-divided by age groups (Below 5, between 5 and 14, between 15-40 and above 40 years old) for the whole outbreak in Kailahun, Sierra Leone, from July to November. Survivors are shown in blue and non-survivors are shown in red.). Similarly, there was a difference in outcomes between patients with high and intermediate viremia, and between intermediate and low viremia, with the higher viremia linked to a higher fatality rate.

To identify the optimal threshold of viremia, which would be predictive of nonsurvival for each month (Figure 16: Correlation between viral load and outcome for the months of July and November.

*The CFR (%) and the case survival rate (CSR, %) are stacked, divided by viral clusters of low (<4.24), intermediate (4.24–6.94) and high (>6.24) viremia and subdivided by age groups (below 5, between 5 and 14, between 15 and 40, and above 40 years old). **(A and B)** Months of July (n = 93) **(A)** and November (n = 165) **(B)** are represented. Survivors are shown in blue and nonsurvivors are shown in red. **(C)** Sensitivity and 1 minus specificity (ROC curves) are shown at various threshold values of viral loads for each month of the outbreak in Kailahun. (July: green, n = 47; August: yellow, n = 81; September: red, n = 134; October: orange, n = 159; November: blue, n = 164).C), a receiver operating characteristic analysis (ROC analysis) was performed. Three important summary values of ROC analysis are the sensitivity, the specificity, and the positive predictive value (PPV). The sensitivity represents the fraction of true positives out of the condition positives (true positives plus false negatives), the specificity refers to the fraction of true negatives out of*

the condition negatives (true negatives plus false positives), and the PPV represents the fraction of true positives out of the test positives (true positives plus false positives). The optimal viral load threshold that was predictive of nonsurvival for the month of July was 5.860 log_{10} GEQ/ml of blood (sensitivity: 0.694 [95% CI, 0.554–0.805]; specificity: 0.864 [95% CI, 0.751–0.932]; PPV: 0.810 [95% CI, 0.690–0.930]) (Supplemental table 7: Parameters of the receiver operating characteristic (ROC) analysis

Supplemental table 8: Parameters of the Tukey's multiple comparison testSupplemental table 9). For November, the threshold value was 4.672 log_{10} GEQ/ml of blood (sensitivity: 0.752 [95% CI, 0.670–0.818]; specificity: 0.910 [95% CI, 0.814–0.961]; PPV: 0.942 [95% CI, 0.897–0.987]) (Supplemental table 7: Parameters of the receiver operating characteristic (ROC) analysis

Supplemental table 8: Parameters of the Tukey's multiple comparison testSupplemental table 9). This later threshold could appropriately identify 75.2% of individuals who died and 91% of the individuals who survived. Out of the individuals predicted not to survive, 94.2% died.

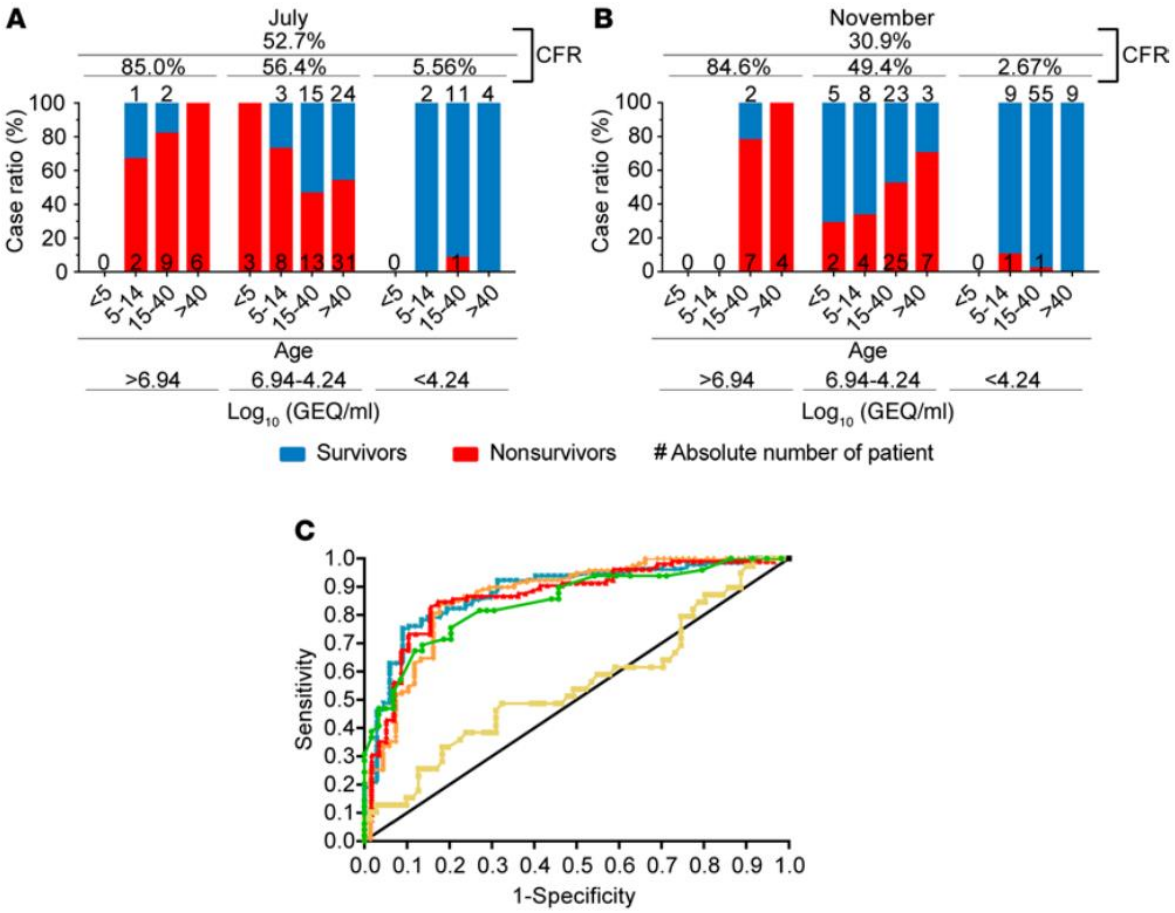

Figure 16: Correlation between viral load and outcome for the months of July and November.

The CFR (%) and the case survival rate (CSR, %) are stacked, divided by viral clusters of low (<4.24), intermediate (4.24–6.94) and high (>6.24) viremia and subdivided by age groups (below 5, between 5 and 14, between 15 and 40, and above 40 years old). **(A and B)** Months of July (*n* = 93) **(A)** and November (*n* = 165) **(B)** are represented. Survivors are shown in blue and nonsurvivors are shown in red. **(C)** Sensitivity and 1 minus specificity (ROC curves) are shown at various threshold values of viral loads for each month of the outbreak in Kailahun. (July: green, *n* = 47; August: yellow, *n* = 81; September: red, *n* = 134; October: orange, *n* = 159; November: blue, *n* = 164).

1.5.5 Effect of age on mortality.

Mortality rates were compared between age groups using the χ^2 test ($\chi^2[3] = 18.888$, $P = 0.00029$), followed by the Marascuillo procedure for comparing multiple proportions. It was observed that there was a marked difference in mortality between the 5- to 14-year-olds and the >40-year-olds, as well as between the 15- to 40-year-olds and the >40-year-olds.

1.5.6 Individual patient viral kinetics and survival.

Patients who presented to the EMC and initially tested positive for EBOV were kept under observation and sampled to monitor disease progression and convalescence according to uneven clinical management requirements. To assess if the viral load kinetics of individual patients correlated with survival, we plotted the

viremia of survivors and nonsurvivors over the course of disease for each month (Figure 17: Viral kinetics of individual patients throughout the outbreak.

The viremia of individual patients was graphically represented by number of days after onset of symptoms. **(A–E)** Patients were divided by months of the outbreak in Kailahun, Sierra Leone, in July (*n* = 10) **(A)**, August (*n* = 8) **(B)**, September (*n* = 8) **(C)**, October (*n* = 4) **(D)**, and November (*n* = 10) **(E)**. Each symbol for a given panel represents a single patient. Survivors are shown in blue, and nonsurvivors are shown in red.

Figure 18: Linear model of the viremia.Figure 19, A–E). It should be noted that nonsurvivors often have very few time points due to sudden mortality, thereby limiting this analysis[196]. Therefore, survivors who had ≥5 samples and nonsurvivors with ≥2 samples were used in our analysis, for a total of 40 patients. The various viral profiles did not reveal meaningful trends that would allow for outcome prediction on an individual-patient basis. This result is consistent with data previously reported regarding the Sudan virus (SUDV) outbreak in Gulu, Uganda [196]. During that outbreak, it was determined that, while viremia in survivors was often found to start high and decrease over time, viremia in non- survivors varied considerably. Interestingly, the second measurement of viremia of patients who experienced a fatal outcome was lower than the first measurement in 4 of the 10 cases versus for 21 of 26 survivors — a significant difference ($\chi^2[1] = 8.47$, $P = 0.0036$).

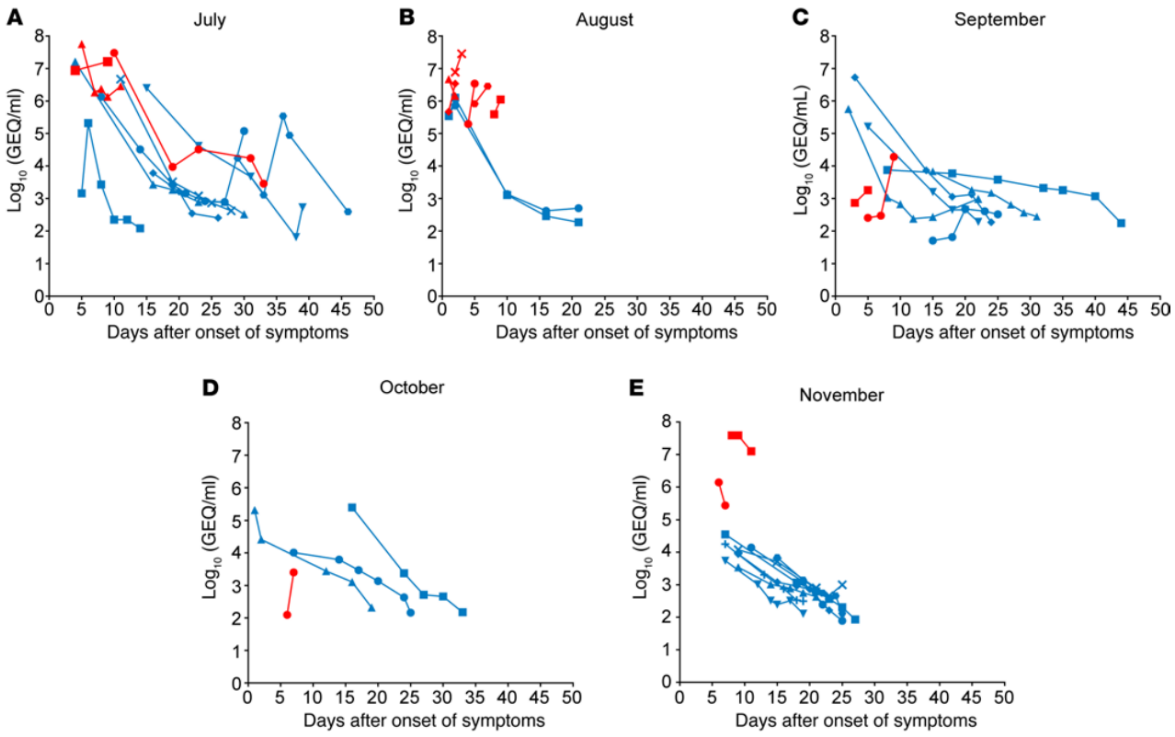

Figure 17: Viral kinetics of individual patients throughout the outbreak.

The viremia of individual patients was graphically represented by number of days after onset of symptoms. **(A–E)** Patients were divided by months of the outbreak in Kailahun, Sierra Leone, in July (*n* = 10) **(A)**, August (*n* = 8) **(B)**, September (*n* = 8) **(C)**, October (*n* = 4) **(D)**, and November (*n* = 10) **(E)**. Each symbol for a given panel represents a single patient. Survivors are shown in blue, and nonsurvivors are shown in red.

1.5.7 Change in initial viral load over time.

To further examine the relationship between the viral load and outbreak progression, as well as viral load and mortality, a linear model was developed (Figure 20: Linear model of the viremia.

Estimating the difference between survivors and nonsurvivors, as well as the effect of outbreak duration on initial viremia. (n = 632). ***(A)*** *Regression coefficients for the Makona outbreak; point estimates and 95% CI. Upper panel: All coefficients. Lower panel: Excludes from the graphical representation the outcome to show the smaller coefficients.* ***(B)*** *Effect of outbreak duration for survivors and nonsurvivors. (Showing best line and 95% CI).* ***(C)*** *Effect of time since onset of symptoms at sampling time for survivors and nonsurvivors (showing best line and 95% CI).A; see Annex I in the supplemental material). This model allowed to account for any effect that the time since onset of symptoms may have had on viremia. Two additional potential predictors (sex and age) were also included in the model and were found to be unrelated to viremia in this dataset, once other predictors were accounted for (see Annex I in the supplemental material). The effect of time since the beginning of the outbreak was found to be more accurately modeled as a quadratic relationship, suggesting that the viral loads were actually increasing toward the end of the data-collection period (Figure 20: Linear model of the viremia.*

Estimating the difference between survivors and nonsurvivors, as well as the effect of outbreak duration on initial viremia. (n = 632). ***(A)*** *Regression coefficients for the Makona outbreak; point estimates and 95% CI. Upper panel: All coefficients. Lower panel: Excludes from the graphical representation the outcome to show the smaller coefficients.* ***(B)*** *Effect of outbreak duration for survivors and nonsurvivors. (Showing best line and 95% CI).* ***(C)*** *Effect of time since onset of symptoms at sampling time for survivors and nonsurvivors (showing best line and 95% CI).B). However, there is still a negative linear component to the regression, which explains*

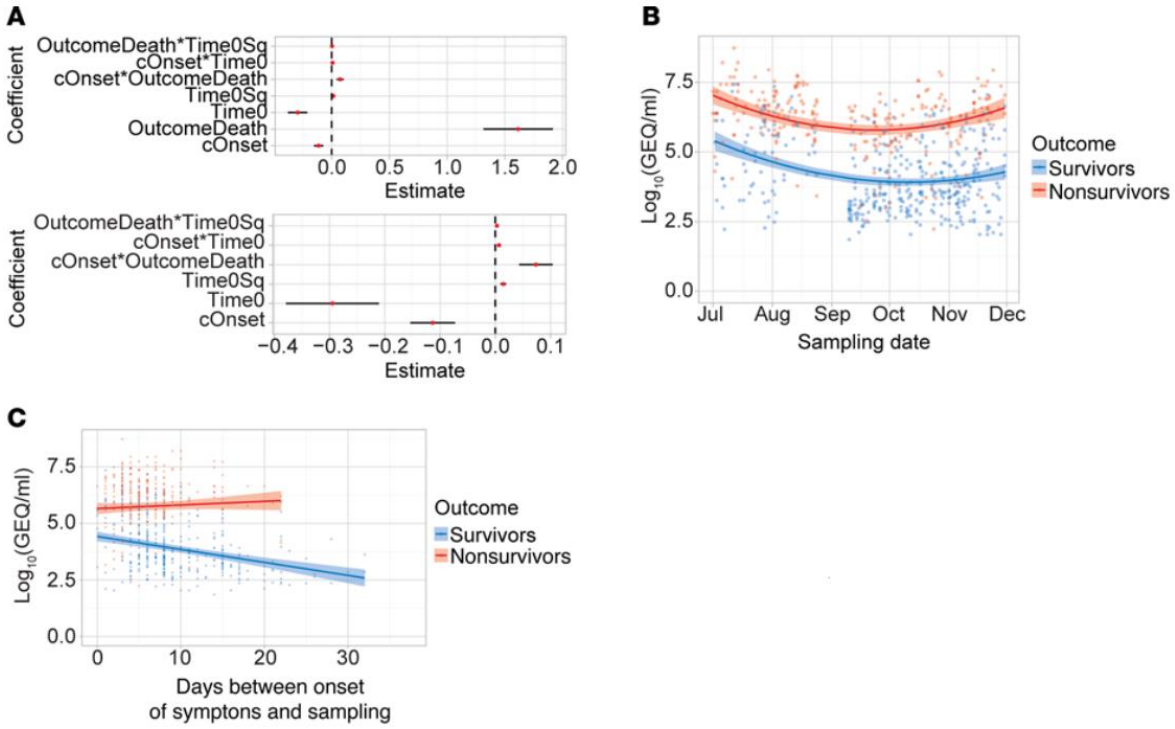

Figure 20: Linear model of the viremia.

Estimating the difference between survivors and nonsurvivors, as well as the effect of outbreak duration on initial viremia. (*n* = 632). **(A)** Regression coefficients for the Makona outbreak; point estimates and 95% CI. Upper panel: All coefficients. Lower panel: Excludes from the graphical representation the outcome to show the smaller coefficients. **(B)** Effect of outbreak duration for survivors and nonsurvivors. (Showing best line and 95% CI). **(C)** Effect of time since onset of symptoms at sampling time for survivors and nonsurvivors (showing best line and 95% CI).

why the simple linear regression in Figure 13: Characterization of the viral load levels.

When applicable, the arithmetic mean is shown, and the error bars represent the 95% CI. **(A)** Initial viral loads of the selected 632 patients throughout the outbreak in Kailahun, Sierra Leone. Linear regression is shown in red. (*n* = 632). **(B)** Initial viral loads of patients for the

first 2 weeks of July (*n* = 43) and the last 2 weeks of November (*n* = 67). **(C)** Number of days between the reported date of symptom onset and the date of the initial sampling at the EMC on the same data set from **B**. Two-tailed, unpaired t tests. **0.001 < *P* < 0.01.

Figure 14: Correlation between viral load and outcome for the months of July and November.Figure 15A had a nonzero negative slope. The difference in viral load for survivors was 1.6 log_{10} GEQ/ml of blood lower than nonsurvivors. This difference increases by 0.073 log_{10} GEQ/ml of blood with every day after the onset of symptoms (Figure 20: Linear model of the viremia.

Estimating the difference between survivors and nonsurvivors, as well as the effect of outbreak duration on initial viremia. (*n* = 632). **(A)** Regression coefficients for the Makona outbreak; point estimates and 95% CI. Upper panel: All coefficients. Lower panel: Excludes from the graphical representation the outcome to show the smaller coefficients. **(B)** Effect of outbreak duration for survivors and nonsurvivors. (Showing best line and 95% CI). **(C)** Effect of time since onset of symptoms at sampling time for survivors and nonsurvivors (showing best line and 95% CI).C).

1.5.8 Survival correlates with population immunity.

Initial viral loads of patients were higher in July when compared with November in Kailahun, Sierra Leone (Figure 13: Characterization of the viral load levels.

When applicable, the arithmetic mean is shown, and the error bars represent the 95% CI. **(A)** Initial viral loads of the selected 632 patients throughout the outbreak in Kailahun, Sierra Leone. Linear regression is shown in red. (*n* = 632). **(B)** Initial viral loads of patients for the first 2 weeks of July (*n* = 43) and the last 2 weeks of November (*n* = 67). **(C)** Number of days between the reported date of symptom onset and the date of the initial sampling at the EMC on the same data set from **B**. Two-tailed, unpaired t tests. **0.001 < *P* < 0.01.

Figure 14: Correlation between viral load and outcome for the months of July and November.Figure 15A and Supplemental figure 2: Monthly average viremia

*(n=632) The mean viremia for each month of the outbreak in Kailahun. Error bars represent the 96% confidence interval for each mean. Ordinary one-way ANOVAs with Tukey's multiple comparison test. ****:p<0.0001, *:0.01<p<0.05). Interestingly, the CFRs for each month followed an overall downward trend. The monthly CFRs were 52.7%, 67.4%, 31.8%, 32.9%, and 30.9%, respectively (Figure 21: Evolution of the CFRs and immunity in the population.*

Monthly CFRs (blue triangles) and percentage of the tested population with an immunity to EBOV (purple squares) are overlaid with the initial viremia of the selected 632 patients (gray circles). Linear regression of the viremia is shown in red (n = 632).). A χ^2 test for independence revealed an association between month and CFR (χ^2= 118.37, degrees of freedom = 9, P < 2.2 × 10^{-16}). The significant χ^2 was followed by the Marascuillo procedure to compare multiple proportions, which showed significant differences in CFR between July and the months of September, October, and November, as well as between August and the months of September, October, and November (Supplemental table 10: Parameters of the Tukey's multiple comparison test

ns: not significant, *: 0.01<p<0.05, **:0.001<p<0.01, ****: p<0.0001

33 0.01<p<0.05, **:0.001<p<0.01, ****: p<0.0001

Supplemental table 11: Number of patients tested for IgG levels by ELISA and their titers for the given monthsSupplemental table 12). It was hypothesized that increasing immunity in the population could be one of the contributors to the lower viral loads by reaching a herd immunity threshold as the outbreak progressed. To evaluate this hypothesis, the seroprevalence of EBOV-specific IgG was analyzed. Ninety-four patients who presented at the EMC for diagnostic testing, but who were determined to be negative for EBOV by reverse transcription PCR (RT-PCR) between July and November 2014, were assessed for EBOV-specific IgG. Out of these 94 patients, 46 reported history of contact with a sick person or funeral exposure; 17 reported no exposure to an infected individual or attendance to a funeral; and, for the 31 other individuals, the information was not available. Forty-five of these 94 patients (47.9%) had detectable IgG antibodies against EBOV (Supplemental table 13: Number of patients tested for IgG levels by ELISA and their titers for the given months

Supplemental figure 1: Monthly average viremiaSupplemental table 14).

The analysis indicated that immunity in EBOV-negative patients was increasing, concurrent with decreasing viral loads in infected patients (Figure 21: Evolution of the CFRs and immunity in the population.

Monthly CFRs (blue triangles) and percentage of the tested population with an immunity to EBOV (purple squares) are overlaid with the initial viremia of the selected 632 patients (gray circles). Linear regression of the viremia is shown in red (n = 632).). In July, the EBOV seroprevalence rate was 14.3% (1 patient out of 7; 95% CI, 0%–40.2%), while in September, the rate increased to 55.9% (19 patients out of 34; 95% CI, 44.3%–67.4%). This trend continued through October (12 patients out of 25; 48.0%; 95% CI, 28.4%–67.6%) and November, where 13 patients out of 28 (46.4%; 95% CI, 27.9%–64.9%) were seropositive for EBOV-IgG. Linear regression analysis established that the increase in the monthly immunity was significant ($F_{1,2}$= 20.29, P = 0.0459). Unfortunately, samples from late August 2014 were unavailable for testing, which prevented us from further detailing the crossover in CFR and EBOV seroprevalence.

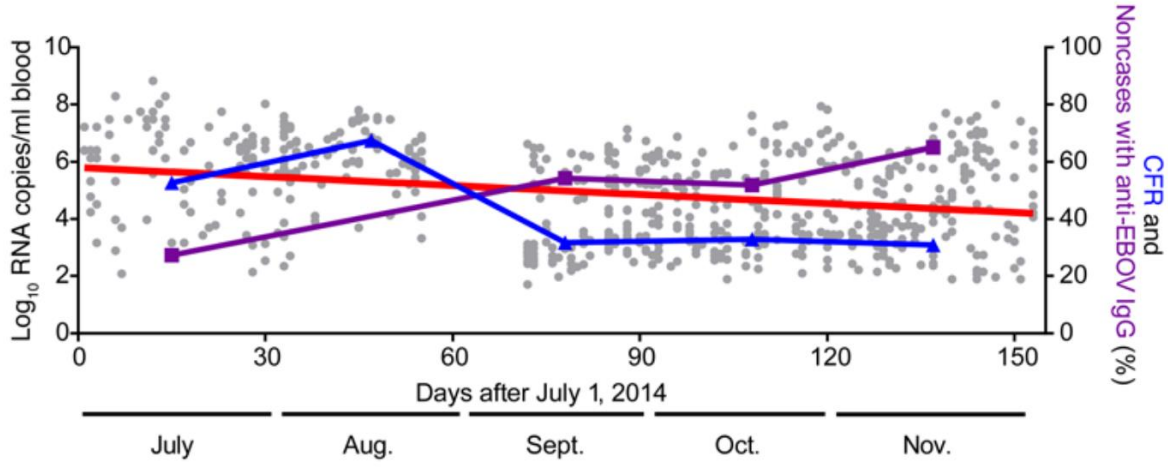

Figure 21: Evolution of the CFRs and immunity in the population.

Monthly CFRs (blue triangles) and percentage of the tested population with an immunity to EBOV (purple squares) are overlaid with the initial viremia of the selected 632 patients (gray circles). Linear regression of the viremia is shown in red (n = 632).

1.6 Discussion

The current findings suggest that the viral load of a patient on arrival to the EMC is statistically predictive of outcome. Individual viral kinetics were only associated with outcome in regards to the second viral load determination in relation to the first one (e.g., nonsurvivors tend to show higher second measurements). Interestingly, 1/3 of the patients who experienced a fatal outcome were not following this trend — a counterintuitive observation, since virus clearance should be associated with survival. Presence of one or many co-morbidities or irreparable tissue damage resulting from virus replication could explain this phenomenon. This is in line with a previous study[196], which showed, in the context of SUDV infections, that predicting an outcome based on an overall viral- load profile was not accurate. However, this could also be explained by an insufficient data set, where many nonsurvivors had few data points available. Therefore, this analysis cannot rule out that individual kinetics could be associated with clinical outcome.

Linear modeling of the initial viremia as a function of (i) the time between onset of symptoms and sampling, (ii) the time since the beginning of data collection, and (iii) the outcome of the patients allowed for the analysis of subtler trends in the viremia. From the start of the outbreak, there was a difference in viremia of about 1.6 log-units (95% CI, 1.3–1.9) between survivors and nonsurvivors, and this difference increased as the outbreak progressed. However, a quadratic component to the relation between viremia and the time since the beginning of data collection also emerged, which suggests that the viremia was not decreasing during the months of October and November. This explains why the decrease in viremia between July 1 and October 31 (or November 30) was lower than the decrease between July 1 and September 30. As expected, the difference in viremia was also increasing with the time since onset of symptoms. These results suggest that, for fatal cases, the time since onset of symptoms had a neutral to positive effect on viremia, whereas, for the survivors, the more time there was between onset of symptoms and sampling, the lower the viremia. Overall, this model supports other analyses in concluding that there was indeed a decrease in initial viremia, even when we account for variation in time since onset of symptoms.

An intriguing finding is the correlation between the observed increase in EBOV-specific antibodies in the population and the decrease in initial viral loads of infected patients. Previous work conducted by the Lassa Diagnostic Laboratory at the Kenema General Hospital (KGH), Sierra Leone, between October 2006 and October 2008 revealed that 19 of the 220 (8.6%) serum samples tested during that period had an antibody response against EBOV[288]. This number seems to be in accordance with another study conducted in rural areas of Gabon, a country that had been affected by 5 outbreaks of EBOV at the time of this serological survey. The Gabonese study, conducted from 2005–2008, established that 667 participants out of 4,349 (15.3%) were seropositive for EBOV-specific IgG[289]. The higher seroprevalence observed in this last study compared with the one in Sierra Leone, despite similar sampling times, could potentially be explained by the higher occurrence of

outbreaks in Gabon, leading to a larger fraction of the population being exposed to EBOV. A second study conducted at the KGH, from June 2011 to March 2014, analyzed a subset of 242 serum samples[290]. Of those samples, between 16 (6.8%) and 53 (22%) were seropositive for IgG against EBOV, depending on the stringency of the cut-off applied to the assay. The findings presented here with an immunity of 14% for the month of July are in accordance with this later study, despite the few data points available in the present analysis in July. Overall, these serological surveys demonstrate that EBOV-specific IgG can be found in the population outside of an epidemic context, but also in regions where an EBOV outbreak has never been documented. It should be noted that genomic analysis had postulated that the currently circulating strain may have diverged and been introduced to West Africa in 2004[281]. Thus, it is tempting to speculate that occasional exposure to this virus, which would generate a low level of population immunity, may have occurred prior to the current outbreak. A study published in 2000 suggested that asymptomatic, replicative Ebola infection can occur in humans and that a fraction of those individuals can develop an antibody response[291]. Similar to the serosurveys mentioned above, the one conducted in the current study could only use a small number of samples relative to the number of patients used for viremia assessment. In addition, as in previous studies, it is important to mention that the results were generated from patients reporting at a clinic with symptoms (in the present case at the EMC) and not from a random sample of the community. In this case, specifically, the patients were sick but EBOV-negative by quantitative PCR (qPCR), which may have introduced a bias and not necessarily represent the immune status of the general population. Therefore, although interesting, interpretation from these observations should be taken with caution until data from an extended number of samples are available.

Overall, the present data suggest a significant decrease in the viral loads over time in patients in their initial screen for EBOV upon arrival to the EMC in Kailahun, Sierra Leone. Hypotheses to explain this decrease are numerous and not mutually exclusive. As the outbreak progressed and more cases arose, the awareness of the disease among the population could have increased, and in the event that one family member fell ill, every household member could seek early medical care or actively reduce their exposure by limiting their contacts with sick individuals. However, the fact that there is no statistically significant difference in time between onset of symptoms and initial diagnostic sampling suggests that faster reporting to the EMC is not supported by the current data.

It also remains possible that the decrease is due to a detection bias. As the outbreak progressed, a growing spectrum of cases were identified and tested, whereas early in the outbreak, it is possible that more of the severe cases (with expected higher viremia) were detected and tested. Anecdotally, however, many individuals are still refusing to acknowledge the disease and prefer not to report to an EMC. Even now, over a year after the outbreak was officially declared, many security incidents are still being reported, indicating that there is still a lack of trust in certain populations toward healthcare facilities and outbreak responders. Another possibility is the existence

of patients with atypical infections, who do not show traditional symptoms of EVD, such as subclinical infections. The individuals would be far more mobile than patients with a more typical infection. As such, individuals with an atypical infection could spread the virus ahead of the wave of severe infections and increase the levels of immunity in the population. Once the level of immunity reaches a critical threshold, fatality rates and viremia would go down, as observed in the present study.

It is fair to assume that, as the outbreak progresses through time, it is also progressing in geographical distribution. As the outbreak moved away from the epicenter, where the EMC was located, it is possible that severely afflicted patients were unable to complete or even undertake the journey to the EMC, thereby filtering out the patients with the highest viremia. However, given that highly viremic patients tend to be very contagious, a large flare-up would have been expected, which did not occur. Future work will need to assess the impact of this parameter, among others, on outbreak progression. Finally, another hypothesis to consider is genetic variation of the virus. As described recently[292], isolates collected in Kailahun from July to November 2014 were shown to have become more phylogenetically and genetically diverse, resulting in the emergence of a multitude of novel lineages. Even though this diversification has not been linked to any phenotype of the virus[293], it could be the result of an adaptation of EBOV to its host, resulting in slower replication and a lower viremia.

Overall, the current study offers a detailed view on viral loads in relation to epidemiological data from a highly active site of EBOV transmission and spread. These data could inform the development of vaccine, therapeutics, and importantly, the design of optimal clinical trials by associating promising clinical modalities in a way to better benefit a subgroup of individuals with the highest predicted CFR.

1.7 Author contributions

MADLV, GC, JA, AS, and GPK designed the research study. GC, XQ, JIB, JG, KL, DKK, BK, AG, DK, JES, and GPK acquired the data. MADLV, JA, and SK analyzed the data. MADLV, JA, and GPK wrote the manuscript. MADLV, GC, JA, RAK, AW, AS, ADC, GI, MVH, and GPK edited the manuscript.

1.8 Acknowledgements

The authors thank the government of Sierra Leone for their collaboration, MSF for their deployment and field assistance, and everyone who was deployed and helped, even remotely, in generating the data used in this article. This work was supported by the PHAC. M.A. de La Vega is the recipient of a Master Research Award from the Canadian Institute for Health Research (CIHR).

1.9 Supplemental material

Supplemental table 1: Coversion between CT values obtained by RT-qPCR and the corresponding viral loads.

CT	Corresponding Viral load	
	GEQ/mL	Log10(GEQ/mL)
15	1,95E+08	8,29
18	3,02E+07	7,48
20	8,71E+06	6,94
22	2,51E+06	6,40
25	3,89E+05	5,59
30	1,74E+04	4,24
35	7,76E+02	2,89

Supplemental table 4: Log-unit difference between the end of a given month and July 1st in the linear regression

Month	Log RNA copies/mL of blood July 1st	Log RNA copies/mL of blood End of the month	Log difference [95% CI]
July	5,95	5,72	-0,22 [-1,25; 0,81]
August	5,77	6,08	0,31 [-0,48; 1,10]
September	6,50	4,13	-2,37 [-2,90; -1,84]
October	6,15	4,06	-2,09 [-2,56; -1,61]
November	5,80	4,20	-1,60 [-2,04; -1,17]

Supplemental table 7: Parameters of the receiver operating characteristic (ROC) analysis

Month	Threshold value Log_{10} (GEQ/mL of blood)	Sensitivity [95% CI]	Specificity [95% CI]	Positive Predictive Value (PPV)	Negative Predictive Value (NPV)	Area Under the Curve (AUC) [95% CI]
July	5,860	0,694 [0,554; 0,805]	0,864 [0,751; 0,932]	0,810	0,773	0,846 [0,779; 0,914]
August	5,941	0,487 [0,339; 0,638]	0,676 [0,560; 0,773]	0,452	0,706	0,553 [0,438; 0,668]
September	4,793	0,848 [0,765; 0,905]	0,828 [0,708; 0,905]	0,899	0,750	0,867 [0,809; 0,925]
October	4,942	0,840 [0,763; 0,896]	0,824 [0,714; 0,897]	0,893	0,747	0,865 [0,809; 0,922]
November	4,672	0,752 [0,670; 0,818]	0,910 [0,814; 0,961]	0,942	0,656	0,880 [0,830; 0,930]

Supplemental table 10: Parameters of the Tukey's multiple comparison test

ns: not significant, *: 0.01<p<0.05, **:0.001<p<0.01, ****: p<0.0001

Tukey's multiple comparisons test	Mean 1	Mean 2	Mean Diff.	95% CI of diff.	Significant?	Summary
July vs. Aug	0,5269	0,6739	-0,147	[-0,3373; 0,04323]	No	ns
July vs. Sept	0,5269	0,3175	0,209	[0,03253; 0,3863]	Yes	*
July vs. Oct	0,5269	0,327	0,200	[0,03093; 0,3688]	Yes	*
July vs. Nov	0,5269	0,3091	0,218	[0,05002; 0,3856]	Yes	**
Aug vs. Sept	0,6739	0,3175	0,357	[0,1790; 0,5339]	Yes	****
Aug vs. Oct	0,6739	0,327	0,347	[0,1774; 0,5164]	Yes	****
Aug vs. Nov	0,6739	0,3091	0,365	[0,1965; 0,5332]	Yes	****
Sept vs. Oct	0,3175	0,327	-0,010	[-0,1639; 0,1447]	No	ns
Sept vs. Nov	0,3175	0,3091	0,008	[-0,1447; 0,1615]	No	ns
Oct vs. Nov	0,327	0,3091	0,018	[-0,1258; 0,1617]	No	ns

Supplemental table 13: Number of patients tested for IgG levels by ELISA and their titers for the given months

Titer	July	September	October	November	Total
0	6	15	13	15	49
100	1	11	2	6	20
400	0	3	0	4	7
1600	0	4	7	2	13
6400	0	1	3	1	5
Total	7	34	25	28	94

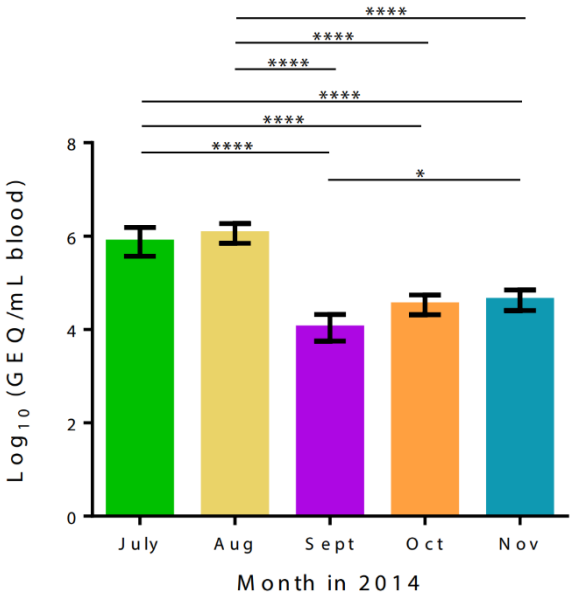

Supplemental figure 2: Monthly average viremia

(n=632) The mean viremia for each month of the outbreak in Kailahun. Error bars represent the 96% confidence interval for each mean. Ordinary one-way ANOVAs with Tukey's multiple comparison test. ****:p<0.0001, *:0.01<p<0.05

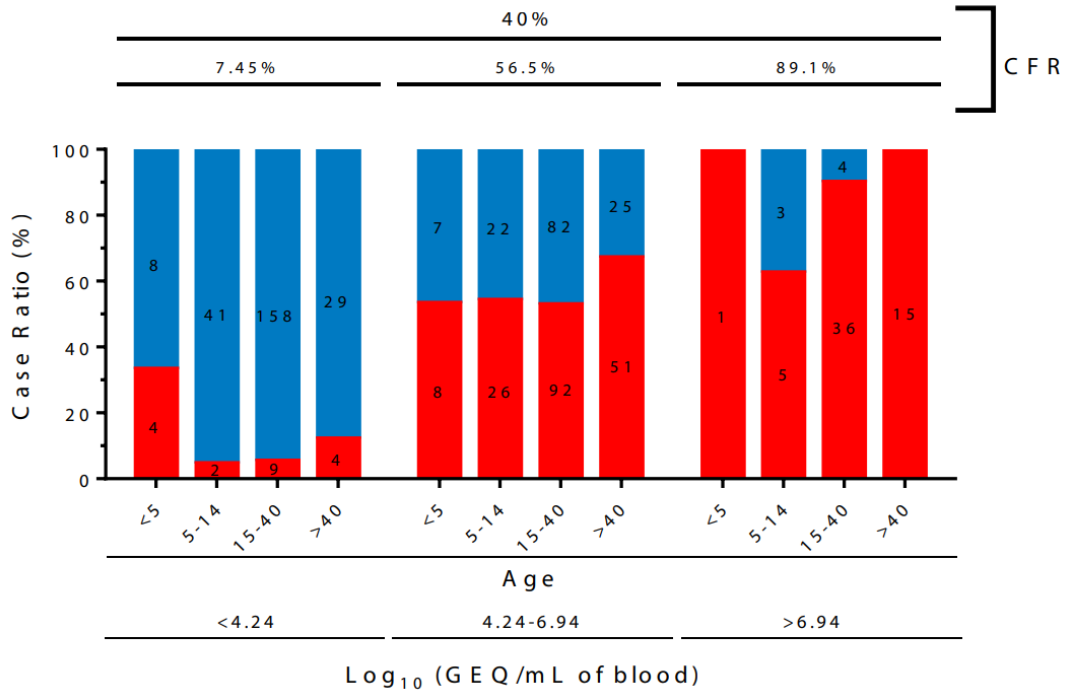

Supplemental figure 3: Correlation between viral load and outcome for the entire data collection period.

(n=632) The case fatality rate (CFR, %) and the case survival rate (CSR, %) are stacked, divided by viral clusters of high (>6.94), intermediate (4.24-6.94) and low (<4.24) viremia and sub-divided by age groups (Below 5, between 5 and 14, between 15-40 and above 40 years old) for the whole outbreak in Kailahun, Sierra Leone, from July to November. Survivors are shown in blue and non-survivors are shown in red.

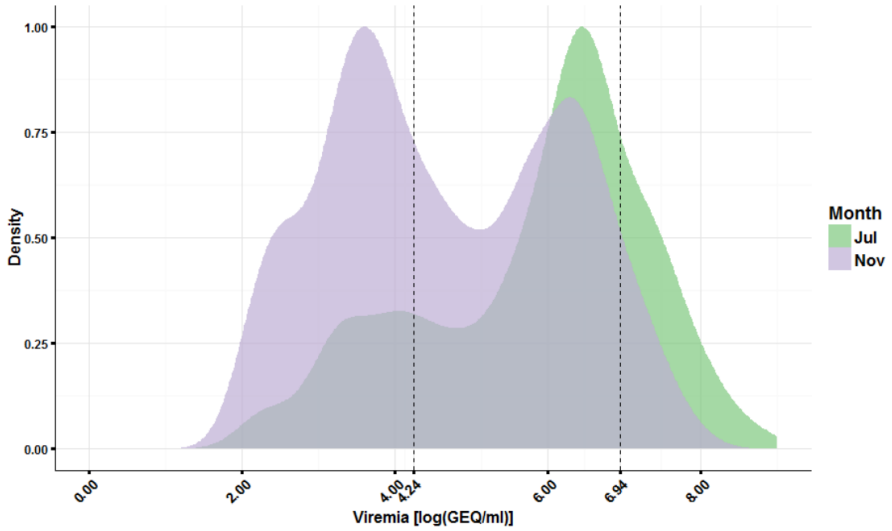

Supplemental figure 4: Proportion of cases for the months of July and November

The proportion of cases for July (Green) and November (Purple) is shown based on viremia. Dashed lines represent the viral clusters defined in the text (<4.24, 4.24-6.94, >6.94)

1.9 References

1. Kuhn, J. H. et al., 2014a: Filovirus RefSeq entries: evaluation and selection of filovirus type variants, type sequences, and names. *Viruses*., **6**, 3663–3682.

10. Feldmann, H. et al., 2011: Ebola haemorrhagic fever. *The Lancet*., **377**, 849–862.

172. Baize, S. et al., 2014: Emergence of Zaire Ebola Virus Disease in Guinea - Preliminary Report. *The New England Journal of Medicine*., **371**, 1418–1425.

173. World Health Organization (WHO), 2014: Ebola virus disease, West Africa – update (May 24th, 2014). *Disease Outbreak News*.

174. World Health Organization (WHO), 2014: Ebola virus disease in Liberia (March 30th, 2014). *Disease Outbreak News*.

196. Towner, J. S. et al., 2004: Rapid Diagnosis of Ebola Hemorrhagic Fever by Reverse Transcription-PCR in an Outbreak Setting and Assessment of Patient Viral Load as a Predictor of Outcome. *Journal of Virology*., **78**, 4330–4341.

279. Kuhn, J. H. et al., 2010: Clarification and guidance on the proper usage of virus and virus species names. *Archives of Virology*., **155**, 445–453.

280. Ansari, A. A., 2014: Clinical features and pathobiology of Ebolavirus infection. *Journal of autoimmunity*., **55**, 1–9.

281. Gire, S. K. et al., 2014: Genomic surveillance elucidates Ebola virus origin and transmission during the 2014 outbreak. *Science*., **345**, 1369–1372.

282. Dudas, G. et al., 2014: Phylogenetic Analysis of Guinea 2014 EBOV Ebolavirus Outbreak. *PLoS currents*., **6**, 1–11.

283. Grolla, A. et al., 2012: Enhanced detection of Rift Valley fever virus using molecular assays on whole blood samples. *Journal of Clinical Virology*., **54**, 313–317.

284. Demby, A. H. et al., 1994: Early diagnosis of Lassa fever by reverse transcription-PCR. *Journal of Clinical Microbiology*., **32**, 2898–2903.

285. Lee, M.-A et al., 2002: Real-Time Fluorescence-Based PCR for Detection of Malaria Parasites Real-Time Fluorescence-Based PCR for Detection of Malaria Parasites. *Journal of Clinical Microbiology*., **40**, 4343–4345.

286. Dreier, J. et al., 2005: Use of bacteriophage MS2 as an internal control in viral reverse transcription-PCR assays. *Journal of Clinical Microbiology*., **43**, 4551–4557.

287. Médecins Sans Frontières, 2013: *Standard Operating Procedures, MSF Ethics Review Board*.

288. Schoepp, R. J. et al., 2014: Undiagnosed acute viral febrile illnesses, Sierra Leone. *Emerging infectious diseases*., **20**, 1176–1182.

289. Becquart, P. et al., 2010: High prevalence of both humoral and cellular immunity to Zaire ebolavirus among rural populations in Gabon. *PLoS ONE*., **5**, 1–9.

290. Boisen, M. L. et al., 2015: Multiple Circulating Infections Can Mimic the Early Stages of Viral Hemorrhagic Fevers and Possible Human Exposure to Filoviruses in Sierra Leone Prior to the 2014 Outbreak. *Viral Immunology*., **28**, 19–31.

291. Leroy, E. M. et al., 2000: Human asymptomatic Ebola infection and strong inflammatory response. *The Lancet*., **355**, 2210–2215.

292. Tong, Y. G. et al., 2015: Genetic diversity and evolutionary dynamics of Ebola virus in Sierra Leone. *Nature*., **524**, 93–96

293. Olabode, A. S. et al., 2015: Ebolavirus is evolving but not changing: No evidence for functional change in EBOV from 1976 to the 2014 outbreak. *Virology*., **482**, 202–207.

Chapter 2. Modeling Ebola virus transmission using ferrets.

Marc-Antoine de La Vega,[a] Geoff Soule,[b] Kaylie N. Tran,[b] Kevin Tierney,[b] Shihua He,[b] Gary Wong,[a,d] Xiangguo Qiu,[b,c] Gary P. Kobinger[a,c,e]

[a]*Département de microbiologie-infectiologie et d'immunologie, Université Laval, Quebec City, Quebec, Canada.* [b]*Special Pathogens Program, National Microbiology Laboratory, Public Health Agency of Canada, Winnipeg, Manitoba, Canada.* [c]*Department of Medical Microbiology, University of Manitoba, Winnipeg, Manitoba, Canada.* [d]*Guangdong Key Laboratory for Diagnosis and Treatment of Emerging Infectious Diseases, Shenzhen Key Laboratory of Pathogen and Immunity, Shenzhen Third People's Hospital, Shenzhen, China.* [e]*Department of Pathology and Laboratory Medicine, University of Pennsylvania School of Medicine, Philadelphia, Pennsylvania, USA*

Received: 6 June 2018
Accepted: 8 October 2018
Published: 31 October 2018

Citation: de La Vega M-A, Soule G, Tran KN, Tierney K, He S, Wong G, Qiu X, Kobinger GP. 2018. Modeling Ebola virus transmission using ferrets. mSphere 3:e00309-18. https://doi.org/ 10.1128/mSphere.00309-18.

Editor: W. Paul Duprex, Boston University School of Medicine

Address correspondence to Gary P. Kobinger, gary.kobinger@crchudequebec.ulaval.ca

Keywords: animal models, Ebola virus, ferret, filovirus, transmission

2.1 Résumé

Le virus Ebola (EBOV) est responsable d'épidémies sporadiques en Afrique Centrale depuis 1976 et possède la capacité de causer des perturbations sociales et une panique généralisée au cœur d'une communauté, tel qu'illustré par l'épidémie de 2013-2016 en Afrique de l'Ouest. La transmission d'EBOV s'effectue est décrite comme possible via un contact avec des liquides corporels infectés, supportés par des données indiquant que du virus infectieux peut être cultivé à partir de sang, de sperme, de salive, d'urine et de lait maternel infecté. Les paramètres influençant la transmission d'EBOV sont, par contre, largement indéfinis en partie dut au manque d'un modèle animal établi permettant l'étude des mécanismes de transmission de l'agent pathogène. Ici, nous avons étudié la transmission d'EBOV chez des furets domestiques mâles et femelles. Suite à une infection intranasale, un animal infecté était placé en contact direct avec un furet naïf et en contact avec un second furet (séparé de l'animal infecté par un double grillage métallique) qui servait d'animal contact-indirect. Tous les animaux infectés, les animaux contacts-directs mâles, ainsi qu'un animal contact-indirect mâle ont développé la maladie à virus Ebola et y ont succombés. Les animaux restants n'étaient pas virémiques et sont demeurés asymptomatiques, mais ont développé des IgM et/ou des IgG spécifiques contre la glycoprotéine de surface d'EBOV – indiquant une transmission virale. La transmission d'EBOV par contact indirect était fréquemment observée dans ce modèle mais a résulté en une maladie moins sévère, contrairement à la transmission directe. Curieusement, ces observations sont cohérentes avec la détection d'anticorps spécifiques chez des individus vivant dans des zones où EBOV est endémique.

2.2 Abstract

Ebola virus (EBOV) has been responsible for sporadic outbreaks in Central Africa since 1976 and has the potential of causing social disruption and public panic as illustrated by the 2013–2016 epidemic in West Africa. Transmission of EBOV has been described to occur via contact with infected bodily fluids, supported by data indicating that infectious EBOV could be cultured from blood, semen, saliva, urine, and breast milk. Parameters influencing transmission of EBOV are, however, largely undefined in part due to the lack of an established animal model to study mechanisms of pathogen spread. Here, we investigated EBOV transmissibility in male and female ferrets. After intranasal challenge, an infected animal was placed in direct contact with a naive ferret and in contact with another naive ferret (separated from the infected animal by a metal mesh) that served as the indirect-contact animal. All challenged animals, male direct contacts, and one male indirect contact developed disease and died. The remaining animals were not viremic and remained asymptomatic but developed EBOV-glycoprotein IgM and/or IgG specific antibodies—indicative of virus transmission. EBOV transmission via indirect contact was frequently observed in this model but resulted in less-severe disease compared to direct contact.

Interestingly, these observations are consistent with the detection of specific antibodies in humans living in areas of EBOV endemicity.

2.3 Importance

Our knowledge regarding transmission of EBOV between individuals is vague and is mostly limited to spreading via direct contact with infectious bodily fluids. Studying transmission parameters such as dose and route of infection is nearly impossible in naturally acquired cases—hence the requirement for a laboratory animal model. Here, we show as a proof of concept that ferrets can be used to study EBOV transmission. We also show that transmission in the absence of direct contact is frequent, as all animals with indirect contact with the infected ferrets had detectable antibodies to the virus, and one succumbed to infection. Our report provides a new small-animal model for studying EBOV transmission that does not require adaptation of the virus, providing insight into virus transmission among humans during epidemics.

2.4 Introduction

In March 2014, an Ebola virus (EBOV) disease (EVD) outbreak was declared in Guéckédou, Guinea, and rapidly spread to Sierra Leone and Liberia[172]. As of 27 March 2016, 28,646 cases of EVD were reported, with 11,323 deaths in 10 countries, making it the biggest and most widespread EVD epidemic to date. According to the World Health Organization, many factors played substantial roles in virus propagation, one of which was that West African EBOV isolates may possess clinical and epidemiological features that differ from those of previous strains[294]. Extensive pathogenicity studies have been conducted with Central African isolates of EBOV, while West African EBOV isolates (EBOV-Makona) were also investigated in nonhuman primates (NHPs). A previous pathogenicity study found that EBOV-Makona, isolate C07, caused delayed disease progression in cynomolgus macaques compared to the reference EBOV-Mayinga isolate (collected from the 1976 outbreak in Central Africa), suggesting decreased virulence of this isolate[295]. In contrast, another study in rhesus macaques showed that EBOV- Makona, isolate C05, could replicate to higher titers than C07 and the reference EBOV-Kikwit strain (isolated from the 1995 outbreak in Central Africa). Monkeys infected by EBOV-Makona-C05 or EBOV-Makona-C07 also experienced more-severe organ damage and shed on average 2-fold to 16-fold more virus via the oral, nasal, and rectal routes, suggesting that animals infected with these West African isolates were more infectious[276].

It is well accepted that human-to-human transmission of EBOV in outbreaks occurs through direct contact with infected bodily fluids[270,271]; however, there have been few studies on EBOV transmission in animal models. A better understanding of all the potential modes of EBOV transmission is important for protecting the general population and clinical personnel against infection. Transmission of EBOV-Mayinga from infected to naive

rhesus macaques in the absence of direct contact has been previously described[296], but similar conditions involving EBOV-Kikwit and cynomolgus macaques did not result in transmission[297]. Pig-to-pig[298] and pig-to-NHP[299] transmissions have been described for EBOV-Kikwit, and a guinea pig model of EBOV transmission was established using guinea pig-adapted EBOV-Mayinga, the first rodent model for transmission studies[211].

2.5 Materials and Methods

2.5.1 Ethics statement.

The experiments described in this study were carried out at the National Microbiology Laboratory (NML) as described in Animal Use Document H-15-029 and were approved by the Animal Care Committee located at the Canadian Science Center for Human and Animal Health, in accordance with the guidelines provided by the Canadian Council on Animal Care. All infectious work was performed inside the biosafety level 4 (BSL4) laboratory at the NML at the Public Health Agency of Canada.

2.5.2 Animals and challenge.

Eighteen 3-month-old ferrets were purchased from Marshall BioResources. The animals weighed between 600 and 900 g on reception, and there were nine males and nine females. The animals were challenged 8 days after reception with passage 1 of Ebola virus/H. sapiens-wt-GIN/ 2014/Makona-C05 (GenBank accession no. KT013254) (order *Mononegavirales*, family *Filoviridae*, species *Zaire ebolavirus*). Infection of the animals was performed via the intranasal (i.n.) route, with a targeted dose of 1,000 times the median tissue culture infectious dose ($TCID_{50}$) (backtitered to 464 $TCID_{50}$ per ferret) diluted in a 0.5-ml total volume (0.25 ml per nostril).

2.5.3 Study design.

Males and females were divided into three aged-matched groups of three same-sex animals, and each group was placed inside a separate unit of the ferret isolator (Allentown Inc., PA, USA). Each unit was divided in half by two metal meshes 2.5 cm apart, which possess 36-mm^2 holes, preventing direct contact between animals on the two sides of the unit. The airflow in this type of isolator is directed from the outside to the inside and was set at approximately 35 cubic feet per min. The challenged animal (C) and its direct-contact cage mate (D) were placed in the outside half of the cage, while the animal that was in the indirect-contact group (I) was placed in the inside half of the cage. Immediately following challenge, the six infected animals were given time to partially recover from anesthesia, the outer side of each animal's nose was wiped, and the animals were placed back into the cage with the corresponding contact animal. All animals were monitored for survival, weight loss, temperature, and clinical symptoms (see Supplemental table 21: Ferret humane endpoint scoring chart

Figure 31: Humoral response of challenged and contact NHPs challenged in the context of aerosol delivery of EBOV-MakonaSupplemental table 22 in the supplemental material). Animals were sampled for blood, and oral and rectal swabs as well as nasal washes were collected on days 3, 5, 7, 9, 12, 19, and 26 (end of experiment) to assess levels of viremia and virus shedding and to perform blood biochemistry and complete blood count characterization. Environmental sampling was also conducted over a 10-cm^2 surface on the front and back of the metal mesh on the side closest to the indirect-contact animal, as well as on the air exhaust located on the side facing the indirect-contact animal.

2.5.4 Serum biochemistry and complete blood count characterization.

Analysis of serum biochemistry was performed using a VetScan VS2 analyzer along with the Comprehensive Diagnostic Profile disk (Abaxis Veterinary Diagnostics), per manufacturer instructions. Analysis of complete blood counts was performed using a VetScan HM5 hematology system (Abaxis Veterinary Diagnostics), per manufacturer instructions.

2.5.5 EBOV quantification by RT-PCR

Oral, rectal, and environmental swabs, as well as nasal washes, were collected in 1 ml of Dulbecco's modified Eagle's medium (DMEM), and RNA was extracted from 140 µl of this solution within hours of collection. For titers measured by RT-qPCR, total RNA was extracted from whole blood or DMEM from swab samples with a QIAamp viral RNA minikit (Qiagen). EBOV was detected with a LightCycler 480 RNA Master Hydrolysis Probes (Roche) kit, with the RNA polymerase (nucleotides 16472 to 16538; accession no. AF086833) as the target gene. The reaction conditions were as follows: 63°C for 3 min, 95°C for 30 s, and cycling of 95°C for 15 s and 60°C for 30 s for 45 cycles on an ABI StepOnePlus system. The sequences of the primers used were as follows: for EBOVLF2, CAGCCAGCAATTTCTTCCAT; for EBOVLR2, TTTCGGTTGCTGTTTCTGTG; and for EBOVLP2FAM, 6-carboxyfluorescein (FAM)-ATCATTGGCGTACTGGAGGAGCAG-black hole quencher 1 (BHQ1). GEQ data were determined using the formula $y = (1{,}000 \times t \times n)/(b \times r)$, where *t* represents the number of copies in the qPCR reaction (calculated from a standard curve using a plasmid containing the L gene of EBOV), *n* represents the elution volume of the RNA extraction, *b* represents the volume of blood from which the RNA was extracted, and *r* represents the volume of RNA used in the qPCR reaction.

2.5.6 ELISA.

Enzyme-linked immunosorbent assays (ELISAs) for analysis of Ebola virus glycoprotein (EBOV GP)-specific IgM and IgG were performed using recombinant EbolaGPΔTM (IBT Bioservices catalog no. 0501-025) as the antigen. Briefly, 96-well half-well plates were coated with 30 µl of protein at a concentration of 1µg/ml, left at 4°C overnight, and then blocked for 1 h at 37°C with phosphate-buffered saline (PBS)–5% skim milk the

following morning. Plates were then washed 3 times with 0.1% PBS–Tween, and the serum dilutions were applied to the plates and incubated at 37°C for 1 h followed by washing 3 times with 0.1% PBS–Tween. Goat anti-human IgG-horseradish peroxidase (IgG-HRP) (KPL catalog no. 074-1006) was added for 1 h at 37°C at a 1:1,500 dilution. The plates were read using ABTS [2,2'-azinobis(3-ethylbenzthiazolinesulfonic acid)] peroxidase substrate (Thermo Fisher catalog no. 37615), which was applied at 50 µl per well, and left for 30 min before reading. Each sample was assayed in duplicate. A titer was considered to represent a positive result if the average value was 7.733 standard deviations above background.

2.5.7 Statistics.

Survival was evaluated using the log rank (Mantel-Cox) test, and time to death was evaluated using the two-tailed, unpaired *t* test with Welch's correction. Differences between average values of viral loads were evaluated by one-way ANOVA with Tukey's multiple-comparison test, with single pooled variance. Results were considered significant if the *P* value was <0.05, and all analyses were conducted in GraphPad Prism 7.02.

2.5.8 Data availability

The data sets generated during the course of the current study are available from the corresponding author on request.

2.6 Results

Recent pathogenesis studies in domestic ferrets with EBOV, as well as other filoviruses, showed that ill animals shed high amounts of live virus[215–217]. Here, we demonstrated the potential for using domesticated ferrets to study direct and indirect EBOV transmission with EBOV-Makona, isolate C05. In this study, animals were caged such that transmission via direct and indirect contact could be investigated simultaneously. The direct-contact animal was placed on one side of the cage along with the challenged animal, while the indirect-contact animal was placed downstream (of the airflow) of the first two animals, separated from them by a mesh preventing physical contact between the animals on the two sides of the mesh (Figure 22: Experimental setting of the transmission study.

Challenged animals were placed on the outer half of the divided units along with a nonchallenged, direct-contact animal. Indirect-contact animals were placed in the inner half of the units. Directional airflow is illustrated by arrows, where clean air was introduced in the caging system from the outer half of the unit, passed through each cage, and evacuated through the middle section of the system. Challenged animals are represented by red biohazard symbols, while black biohazard symbols represent nonchallenged animals. Male ferrets were located on the left, and female ferrets were on the right.). Challenged male (CM1 to CM3) and female (CF1 to CF3) ferrets were infected intranasally (i.n.) with 1,000× the 50% tissue culture infective dose ($TCID_{50}$) of EBOV-Makona to mimic mucosal exposure. All challenged males and females succumbed to infection, with mean times to death of 5.7 (standard deviation [SD], 0.6 days; range, 5.0 to 6.0 days) and 6.0 days, respectively. This difference was not statistically significant (two-tailed t test with Welch's correction; $t = 1$, $df = 2$). All direct-contact males (DM1 to DM3) showed disease symptoms and died with a mean time to death of 10.3 days (SD, 0.6; range, 10 to 11 days), whereas all direct-contact females (DF1 to DF3) survived. One indirect- contact male animal (IM3) was found dead on day 19, whereas the other indirect- contact animals (IM1 and IM2) survived. All females in the indirect-contact group (IF1 to IF3) survived (Figure 23: Survival and clinical parameters of challenged and contact ferrets.

Clinical parameters of male and female ferrets challenged or not with EBOV-Makona-C05 are presented. (a) Survival. (b) Temperature. (c) Clinical score. (d) Body weight percent change. Key: C, challenged animal; D, direct-contact animal; I, indirect-contact animal; M, male (left column); F, female (right column); *, animal was found dead and could not be scored.

Figure 24: Viral loads and shedding from all animals.Figure 25a). The surviving animals did not exhibit any EVD-associated symptoms at any point throughout the experiment, unlike the animals that succumbed (Figure 23: Survival and clinical parameters of challenged and contact ferrets.

Clinical parameters of male and female ferrets challenged or not with EBOV-Makona-C05 are presented. (a) Survival. (b) Temperature. (c) Clinical score. (d) Body weight percent change. Key: C, challenged animal; D, direct-contact animal; I, indirect-contact animal; M, male (left column); F, female (right column); *, animal was found dead and could not be scored.

Figure 24: Viral loads and shedding from all animals.Figure 25b). The animals in the latter category typically had a spike in body temperature the day before death (Figure 23: Survival and clinical parameters of challenged and contact ferrets.

Clinical parameters of male and female ferrets challenged or not with EBOV-Makona-C05 are presented. (a) Survival. (b) Temperature. (c) Clinical score. (d) Body weight percent change. Key: C, challenged animal; D, direct-contact animal; I, indirect-contact animal; M, male (left column); F, female (right column); *, animal was found dead and could not be scored.

Figure 24: Viral loads and shedding from all animals.Figure 25c) and experienced mild to moderate weight loss (Figure 23: Survival and clinical parameters of challenged and contact ferrets.

Clinical parameters of male and female ferrets challenged or not with EBOV-Makona-C05 are presented. (a) Survival. (b) Temperature. (c) Clinical score. (d) Body weight percent change. Key: C, challenged animal; D, direct-contact animal; I, indirect-contact animal; M, male (left column); F, female (right column); *, animal was found dead and could not be scored.

Figure 24: Viral loads and shedding from all animals.Figure 25d). While all challenged animals died, male ferrets exhibited more-severe EVD symptoms, such as a petechial rash and fever (see Supplemental table 18: Clinical parameters of male ferrets

Hypothermia was defined as below 35°C. Fever was defined as 1.0°C higher than baseline. Mild rash was defined as focal areas of petechiae covering <10% of the skin, moderate rash as areas of petechiae covering 10 to 40% of the skin and severe rash as areas of petechiae and/or ecchymosis covering >40% of the skin. Leukocytopenia and thrombocytopenia were defined as a >30% decrease in numbers of white blood cells and platelets, respectively. Leukocytosis and thrombocytosis were defined as a twofold or greater increase in numbers of white blood cells and platelets over baseline, where white blood cell count >11 x 10^3. ↑, two- to threefold increase; ↑↑, four- to fivefold increase; ↑↑↑, greater than fivefold increase; ↓, two- to threefold decrease; ↓↓, four- to fivefold decrease; ↓↓↓, greater than fivefold decrease. AMY, amylase; ALP, alkaline phosphatase; ALT, alanine aminotransferase; TBIL, total bilirubin; BUN, blood urea nitrogen; CRE, creatinine; K+, potassium; GLOB, globulin.

Supplemental table 19: Ferret humane endpoint scoring chartSupplemental table to Supplemental table 21: Ferret humane endpoint scoring chart

Figure 31: Humoral response of challenged and contact NHPs challenged in the context of aerosol delivery of EBOV-MakonaSupplemental table 22 in the supplemental material). Of note, rectal temperatures were taken solely on sampling days in order to minimize stress to the animals; therefore, days with fever could have been missed. Changes in blood biochemistry and complete

blood counts after infection in male and female animals were comparable (see Supplemental figure 6: Complete blood counts and biochemical parameters of challenged and contact male ferrets

*Complete blood counts and biological parameters of male ferrets challenged or not with EBOV-Makona-C05. **a**, white blood cells count; **b**, lymphocytes count; **c**, lymphocytes percentage; **d**, platelets count; **e**, neutrophils count; **f**, neutrophils percentage; **g**, alkaline phosphatase; **h**, alanine aminotransferase; **i**, blood urea nitrogen; **j**, creatinine; **k**, glucose. Legend: C: Challenged animal; D: Direct contact animal; I: Indirect contact animal; M: Male. and Supplemental figure 7: Complete blood counts and biochemical parameters of challenged and contact female ferrets*

Complete blood counts and biological parameters of female ferrets challenged or not with EBOV-Makona-C05. **a**, white blood cells count; **b**, lymphocytes count; **c**, lymphocytes percentage; **d**, platelets count; **e**, neutrophils count; **f**, neutrophils percentage; **g**, alkaline phosphatase; **h**, alanine aminotransferase; **i**, blood urea nitrogen; **j**, creatinine; **k**, glucose. Legend: C: Challenged animal; D: Direct contact animal; I: Indirect contact animal; F: Female. in the supplemental material).

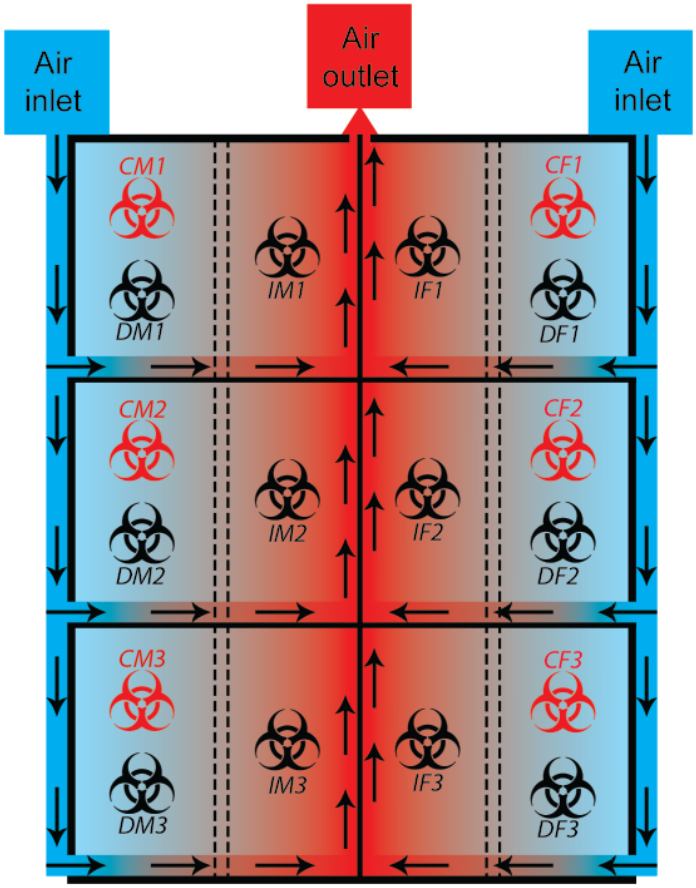

Figure 22: Experimental setting of the transmission study.

Challenged animals were placed on the outer half of the divided units along with a nonchallenged, direct-contact animal. Indirect-contact animals were placed in the inner half of the units. Directional airflow is illustrated by arrows, where clean air was introduced in the caging system from the outer half of the unit, passed through each cage, and evacuated through the middle section of the system. Challenged animals are represented by red biohazard symbols, while black biohazard symbols represent nonchallenged animals. Male ferrets were located on the left, and female ferrets were on the right.

All challenged animals succumbed to infection within a time period consistent with past reports of EVD in ferrets, which has been described to be 5 to 6 days[215–217]. Among the direct-contact and indirect-contact animals, DM1, DM2, and DM3 succumbed to infection 4 to 6 days after CM1, CM2, and CM3 died, suggesting that transmission

likely occurred when the challenged ferrets had advanced or terminal EVD. This is consistent with current knowledge, as viral loads are usually highest at the time of death, suggesting that severely ill animals are the most infectious[109,215,295,300]. Ferret IM3 died 9 days after DM3 succumbed to infection, suggesting that IM3 might have acquired the infection during DM3's late stage of disease but might also have been infected by infectious fomites from CM3 or DM3. While direct physical contact was not possible between animals separated by the mesh, small particles might have passed through the holes to infect indirect-contact animals. This is consistent with findings from a previous study using a similar experimental setup showing that fomites, such as soiled bedding, were important for promoting EBOV transmission in guinea pigs[211].

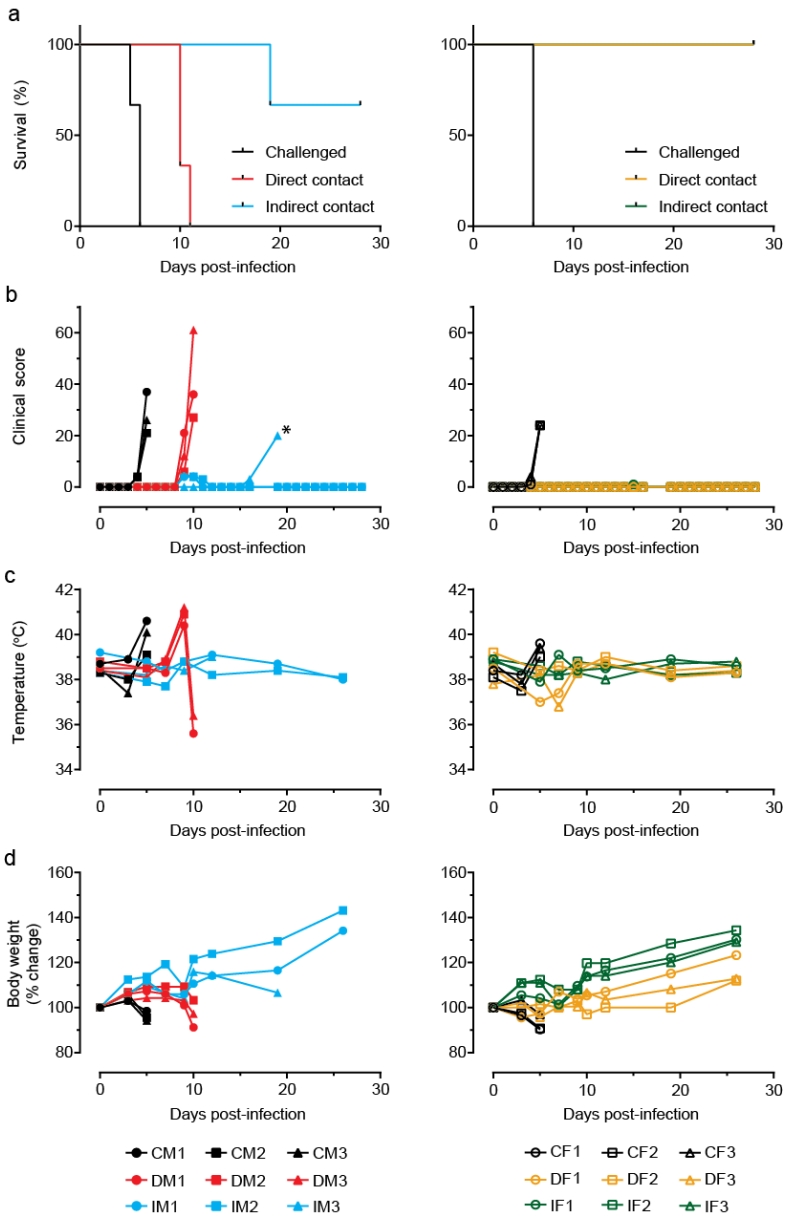

Figure 23: Survival and clinical parameters of challenged and contact ferrets.

Clinical parameters of male and female ferrets challenged or not with EBOV-Makona-C05 are presented. (a) Survival. (b) Temperature. (c) Clinical score. (d) Body weight percent change. Key: C, challenged animal; D, direct-contact animal; I, indirect-contact animal; M, male (left column); F, female (right column); *, animal was found dead and could not be scored.

As infection progressed, animals were evaluated for viremia and virus shedding through the oral, nasal, and rectal mucosae. The average peak viremia levels were 1.79E9 genome equivalent copies (GEQ)/ml and 8.4E8 GEQ/ml for CM1 to CM3 and CF1 to CF3, respectively. The difference was not found to be statistically different [one-way analysis of variance (ANOVA); $F(3,6) = 0.4677$]. DM1 to DM3 had a mean peak viremia level of 3.2E11 GEQ/ml, while IM3 did not have an available sample since it was found dead (Figure 26: Viral loads and shedding from all animals.

Viral loads are measured by RT-qPCR in the blood of male and female ferrets (a), oral swabs (b), nasal washes (c), and rectal swabs (d). Key: C, challenged animal; D, direct-contact animal; I, indirect-contact animal; M, male (left column); F, female (right column). Note that a blood sample was not available from animal IM3 on day 19 as it was found dead.

Figure 27: Humoral response of challenged and contact ferrets.Figure 28a). However, EBOV titers from postmortem oral, nasal, and rectal swabs for IM3 were 7.1E5, 6.4E6, and 3.7E8 GEQ/ml, respectively. The average peak levels of oral, nasal, and rectal shedding for CM1 to CM3 were 1.6E7 GEQ/ml, 9.0E5 GEQ/ml, and 4.0E7 GEQ/ml, respectively. Similarly, CF1 to CF3 exhibited average peak levels of oral, nasal, and rectal shedding of 1.4E7 GEQ/ml, 1.3E6 GEQ/ml, and 7.2E7 GEQ/ml, respectively (Figure 26: Viral loads and shedding from all animals.

Viral loads are measured by RT-qPCR in the blood of male and female ferrets (a), oral swabs (b), nasal washes (c), and rectal swabs (d). Key: C, challenged animal; D, direct-contact animal; I, indirect-contact animal; M, male (left column); F, female (right column). Note that a blood sample was not available from animal IM3 on day 19 as it was found dead.

Figure 27: Humoral response of challenged and contact ferrets.Figure 28b to d). Environmental swabs on the front and back of the metal mesh and the air exhaust on the side of the indirect-contact animals were negative for EBOV by reverse transcription real-time quantitative PCR (RT-qPCR), with the exception of the air exhaust by IM2 on day 7, which was positive for EBOV at 2.3E3 GEQ/ml. These results indicate that low levels of EBOV can be detected in the surroundings of indirect-contact animals, supporting the hypothesis that IM3 was most likely infected by fomites.

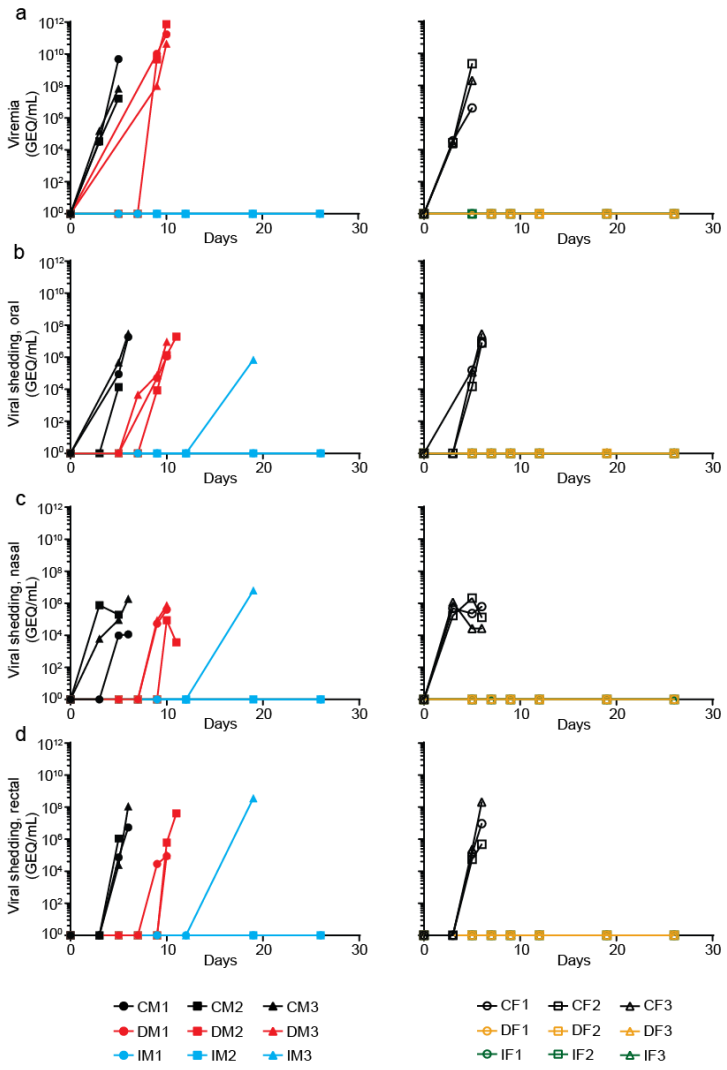

Figure 26: Viral loads and shedding from all animals.

Viral loads are measured by RT-qPCR in the blood of male and female ferrets (a), oral swabs (b), nasal washes (c), and rectal swabs (d). Key: C, challenged animal; D, direct-contact animal; I, indirect-contact animal; M, male (left column); F, female (right column). Note that a blood sample was not available from animal IM3 on day 19 as it was found dead.

All animals were assessed for the presence of EBOV glycoprotein-specific immunoglobulin M (IgM) and immunoglobulin G (IgG) antibodies at the time of euthanasia. DM1 (day 10) and DF3 (day 26) had IgM antibody levels below the limit of detection of the assay, while all other animals were seropositive by the end of the experiment (Figure 29: Humoral response of challenged and contact ferrets.

Data represent endpoint titers of IgM (a and b) and IgG (c and d) antibodies against the glycoprotein of EBOV in the serum of challenged and contact ferrets at euthanasia. C, challenged animal; D, direct-contact animal; I, indirect-contact animal; M, male (left column); F, female (right column).

Supplemental figure 5: Complete blood counts and biochemical parameters of challenged and contact male ferretsFigure 30a and b). All animals were seropositive for IgG except for CM1 (day 5) and CF2 and CF3 (day 5) (Figure 29: Humoral response of challenged and contact ferrets.

Data represent endpoint titers of IgM (a and b) and IgG (c and d) antibodies against the glycoprotein of EBOV in the serum of challenged and contact ferrets at euthanasia. C, challenged animal; D, direct-contact animal; I, indirect-contact animal; M, male (left column); F, female (right column).

Supplemental figure 5: Complete blood counts and biochemical parameters of challenged and contact male ferretsFigure 30c and d). Therefore, all animals were seropositive for either one or both antibody isotypes at the end of the experiment. These results suggest that EBOV transmission via indirect contact is less efficient than direct contact in inducing EVD. As such, only 1 of 6 indirect-contact ferrets received an exposure dose of live virus sufficiently high to result in EVD (Supplemental table 15: Clinical parameters of female ferrets

Hypothermia was defined as below 35°C. Fever was defined as 1.0°C higher than baseline. Mild rash was defined as focal areas of petechiae covering <10% of the skin, moderate rash as areas of petechiae covering 10 to 40% of the skin and severe rash as areas of petechiae and/or ecchymosis covering >40% of the skin. Leukocytopenia and thrombocytopenia were defined as a >30% decrease in numbers of white blood cells and platelets, respectively. Leukocytosis and thrombocytosis were defined as a twofold or greater increase in numbers of white blood cells and platelets over baseline, where white blood cell count >11 x 10^3. ↑, two- to threefold increase; ↑↑, four- to fivefold increase; ↑↑↑, greater than fivefold increase; ↓, two- to threefold decrease; ↓↓, four- to fivefold decrease; ↓↓↓, greater than fivefold decrease. AMY, amylase; ALP, alkaline phosphatase; ALT, alanine aminotransferase; TBIL, total bilirubin; BUN, blood urea nitrogen; CRE, creatinine; K+, potassium; GLOB, globulin.

Supplemental table 16: Clinical parameters of male ferretsSupplemental table 17 and Supplemental table 18: Clinical parameters of male ferrets

Hypothermia was defined as below 35°C. Fever was defined as 1.0°C higher than baseline. Mild rash was defined as focal areas of petechiae covering <10% of the skin, moderate rash as areas of petechiae covering 10 to 40% of the skin and severe rash as areas of petechiae and/or ecchymosis covering >40% of the skin. Leukocytopenia and thrombocytopenia were defined as a >30% decrease in numbers of white blood cells and platelets, respectively. Leukocytosis and thrombocytosis were defined as a twofold or greater increase in numbers of white blood cells and platelets over baseline, where white blood cell count >11 x 10^3. ↑, two- to threefold increase; ↑↑, four- to fivefold increase; ↑↑↑, greater than fivefold increase; ↓, two- to threefold decrease; ↓↓, four- to fivefold decrease; ↓↓↓, greater than fivefold decrease. AMY, amylase; ALP, alkaline phosphatase; ALT, alanine aminotransferase; TBIL, total bilirubin; BUN, blood urea nitrogen; CRE, creatinine; K+, potassium; GLOB, globulin.

Supplemental table 19: Ferret humane endpoint scoring chartSupplemental table) despite the finding that exposure to EBOV via indirect contact was frequent, demonstrated by seroconversion of all ferrets.

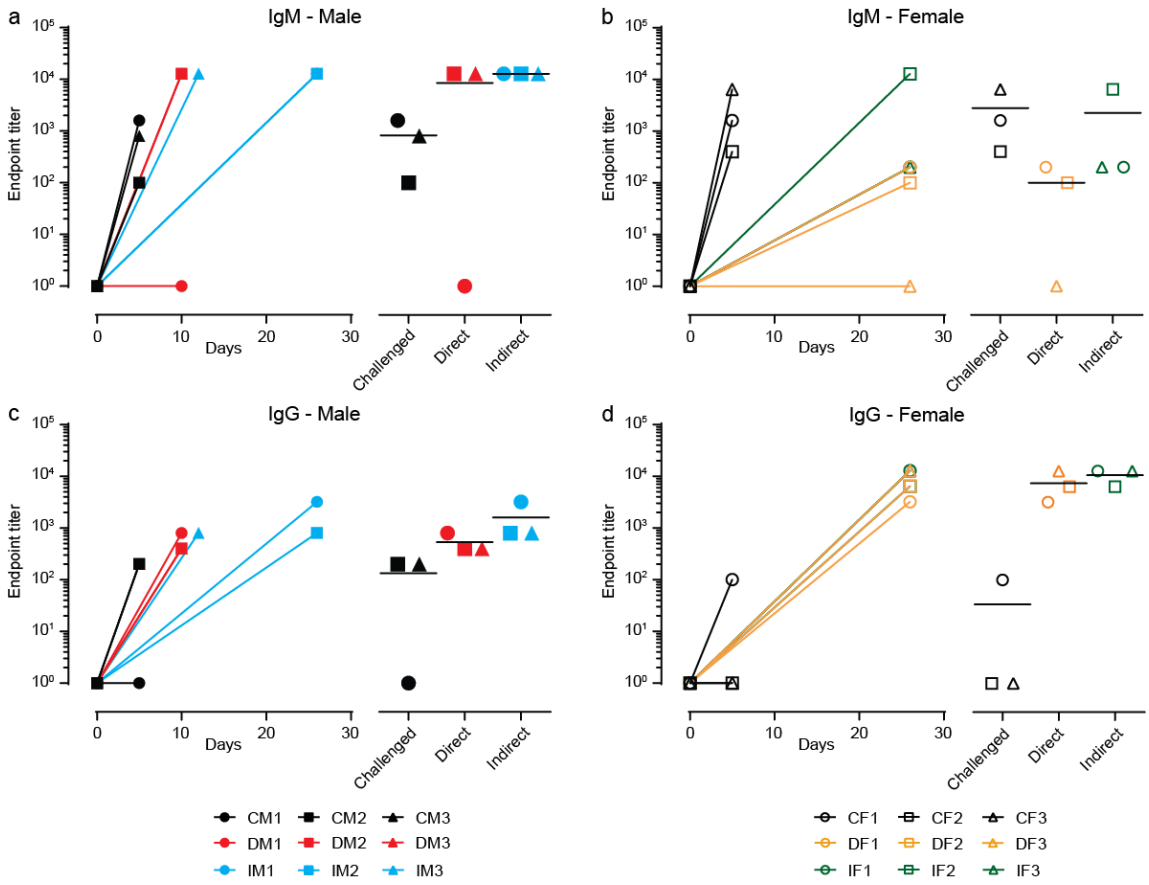

Figure 29: Humoral response of challenged and contact ferrets.

Data represent endpoint titers of IgM (a and b) and IgG (c and d) antibodies against the glycoprotein of EBOV in the serum of challenged and contact ferrets at euthanasia. C, challenged animal; D, direct-contact animal; I, indirect-contact animal; M, male (left column); F, female (right column).

2.7 Discussion

Multiple serosurveys conducted in countries where outbreaks have previously occurred have resulted in reports of higher seroprevalence for EBOV-specific antibodies in human populations residing in forested areas[289,301,302]. A meta-analysis of 51 published seroprevalence studies compared the levels of specific antibodies between asymptomatic participants living with a household or known case contact in an area of EBOV endemicity, living in areas of endemicity but without case contact, or living in areas without known cases of EVD. The analysis showed an estimated seroprevalence of 3.3% in asymptomatic individuals with a household or known case contact. For the other two groups, measured seroprevalence levels were between 0.9% and 17% and between 0% and 24%, respectively, representing a wide range due to the highly heterogeneous nature of the populations, which prevents making an accurate summary estimate[303]. Asymptomatic EVD has been described previously in both humans and NHPs[291,304–306], and a critical factor determining whether disease is symptomatic or

asymptomatic may be the exposure dose or the route of infection. Observations in this study are consistent with the presence of specific antibodies to EBOV under conditions of subclinical disease, a phenomenon first reported from serosurveys in humans. Furthermore, recent data in NHPs showed that challenge with a very low dose of EBOV (10 PFU) via the oral route could lead to viral shedding from the nasal route in the absence of clinical pathology[307]. However, the experimental group examined in that study was composed of only two animals and the data should thus be interpreted accordingly, but the issue warrants further investigation. In contrast, a recent study of EBOV infection in ferrets has shown that animals challenged with 0.1 or 1 PFU succumbed to the disease at day 6 or 7 postinfection, indicating that a lower challenge dose does not result in an increased time to death. In the same study, an experimental group of 3 animals was also challenged with 0.01 PFU. While 1 animal succumbed to infection on day 7, the other 2 did not develop any symptoms during the course of the experiment[222]. This would suggest that IM3, which succumbed to infection 9 days following its cage mate, most likely became infected by fomites after DM3 was removed from the environment. Finally, viral kinetics in guinea pigs have shown that live virus could not be detected in the blood or in oral, nasal, and rectal swabs 1 day postinfection and that virus detection was possible only at day 3 postinfection in nasal and rectal swabs[211].

The lack of overt morbidity and mortality in the female direct-contact animals was surprising, especially considering the outcome seen with their male counterparts. Further investigations performed with larger groups of ferrets, beyond the scope of this current work, are needed to fully understand whether gender plays a role in susceptibility to EBOV in this model. No evidence currently exists in humans to support a biological difference in the levels of male and female susceptibility to EBOV. The fact that women were found to be infected by the virus more often at several outbreaks is more likely linked to an occupational hazard, as, culturally, sub-Saharan Africa women carry a larger share of the responsibility for caring for the ill[308]. In the current study, the similarities in shedding between the two sexes and the differences in mortality observed between male and female contact ferrets could have been due to behavioral factors. For example, it is possible that males engaged more in fighting and/or scratching, which would lead to an increased exposure to infected body fluids, such as blood resulting from injuries, hence leading to higher transmission rates.

This is the first reported small-animal model evaluating transmission of a wild-type EBOV-Makona isolate. Understanding the role of infectivity factors such as exposure dose and route of infection involved in EBOV transmission is relevant to public health and outbreak control efforts. These factors also remain a priority in order to update guidelines following an evidence-based process aimed at protecting health care workers, researchers, and the general public from occupational and accidental exposure. It can be seen from this study that both direct contact and indirect contact with severely ill animals can result in EBOV transmission. Moreover, even with indirect exposure being a less likely event, it is an occurrence that can result in fatal EVD under these conditions. The ferret animal model will be valuable in contributing to our understanding of the many parameters that are

associated with the transmission of EBOV. They may also help better define conditions that are specific to subclinical disease, which could lead to important findings and influence the development of more-efficient protective, preventive, and curative measures.

2.8 Acknowledgements

We thank the staff at the animal facility of the NML for their work and support in this study.

This study was partially supported by a grant (IER-143521) from the Canadian Institute of Health Research to G.P.K. and partially supported by the Public Health Agency of Canada. The funders had no role in study design, data collection and interpretation, or the decision to submit the work for publication. We declare that no conflicting interests exist.

M.-A.D.L.V., G.S., K.N.T., K.T., and S.H. performed the experiments. M.-A.D.L.V., G.W., X.Q., and G.P.K. analyzed the data and wrote the manuscript. M.-A.D.L.V., X.Q., and G.P.K. designed the experiments. All of us have read the manuscript, provided comments, and agreed to the submission of its final version.

2.9 Supplemental material

Supplemental material for this article may be found at https://doi.org/10.1128/ mSphere.00309-18.

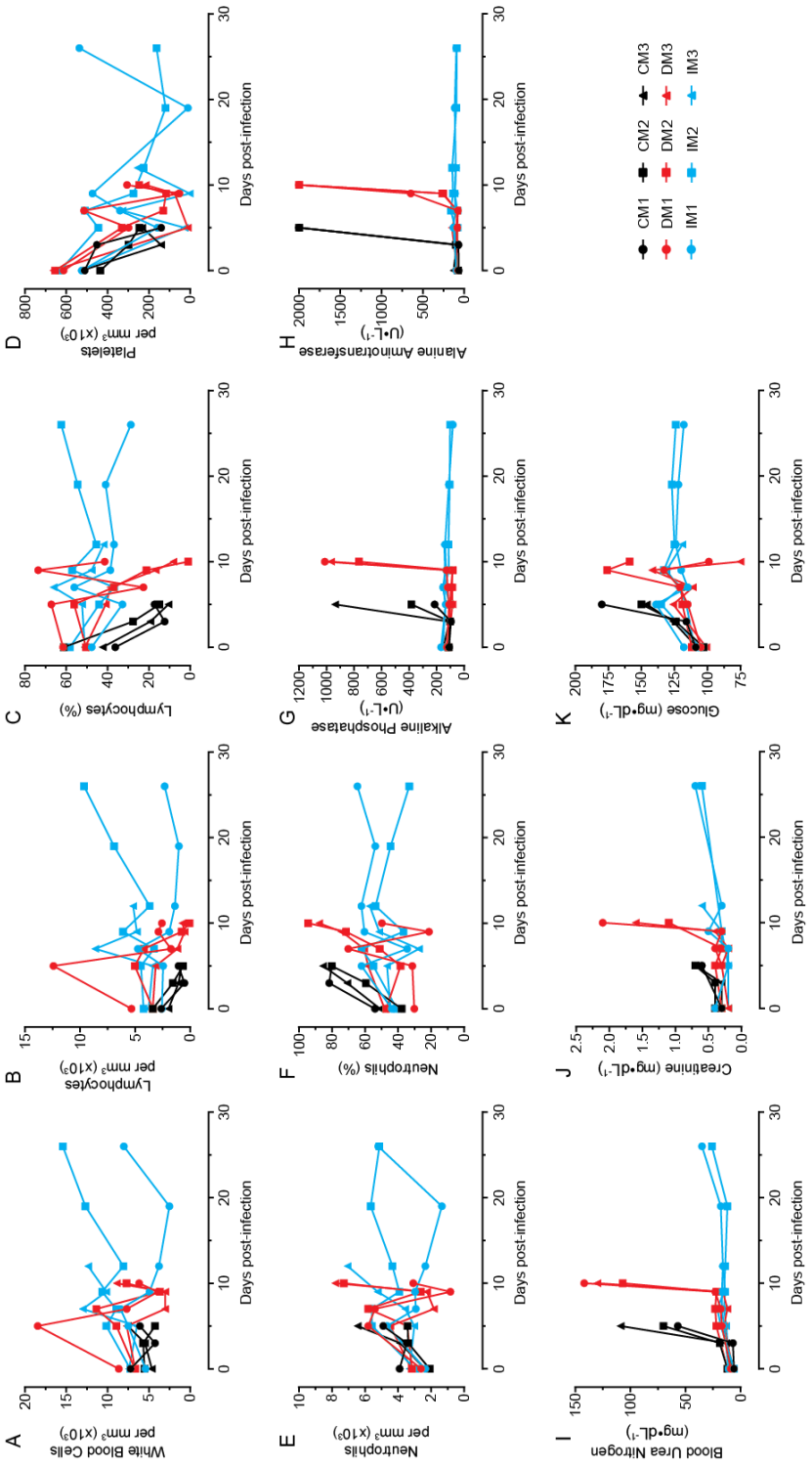

Supplemental figure 6: Complete blood counts and biochemical parameters of challenged and contact male ferrets

Complete blood counts and biological parameters of male ferrets challenged or not with EBOV-Makona-C05. **a**, white blood cells count; **b**, lymphocytes count; **c**, lymphocytes percentage; **d**, platelets count; **e**, neutrophils count; **f**, neutrophils percentage; **g**, alkaline phosphatase; **h**, alanine aminotransferase; **i**, blood urea nitrogen; **j**, creatinine; **k**, glucose. Legend: C: Challenged animal; D: Direct contact animal; I: Indirect contact animal; M: Male.

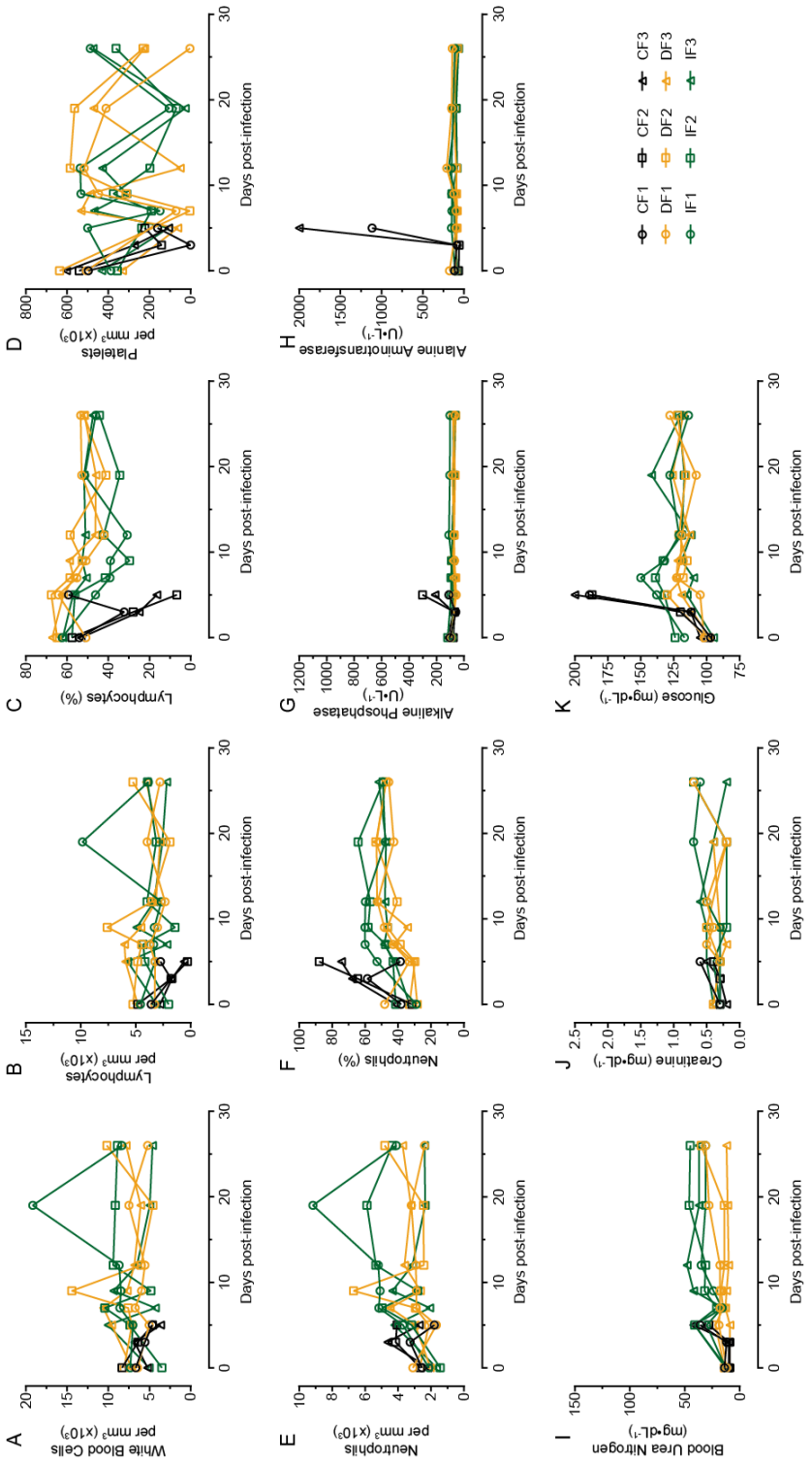

Supplemental figure 7: Complete blood counts and biochemical parameters of challenged and contact female ferrets

Complete blood counts and biological parameters of female ferrets challenged or not with EBOV-Makona-C05. **a**, white blood cells count; **b**, lymphocytes count; **c**, lymphocytes percentage; **d**, platelets count; **e**, neutrophils count; **f**, neutrophils percentage; **g**, alkaline phosphatase; **h**, alanine aminotransferase; **i**, blood urea nitrogen; **j**, creatinine; **k**, glucose. Legend: C: Challenged animal; D: Direct contact animal; I: Indirect contact animal; F: Female.

Supplemental table 15: Clinical parameters of female ferrets

Hypothermia was defined as below 35°C. Fever was defined as 1.0°C higher than baseline. Mild rash was defined as focal areas of petechiae covering <10% of the skin, moderate rash as areas of petechiae covering 10 to 40% of the skin and severe rash as areas of petechiae and/or ecchymosis covering >40% of the skin. Leukocytopenia and thrombocytopenia were defined as a >30% decrease in numbers of white blood cells and platelets, respectively. Leukocytosis and thrombocytosis were defined as a twofold or greater increase in numbers of white blood cells and platelets over baseline, where white blood cell count >11 x 10^3. ↑, two- to threefold increase; ↑↑, four- to fivefold increase; ↑↑↑, greater than fivefold increase; ↓, two- to threefold decrease; ↓↓, four- to fivefold decrease; ↓↓↓, greater than fivefold decrease. AMY, amylase; ALP, alkaline phosphatase; ALT, alanine aminotransferase; TBIL, total bilirubin; BUN, blood urea nitrogen; CRE, creatinine; K+, potassium; GLOB, globulin.

Animal ID	Group	Clinical findings					Outcome
		Body temperature	Rash	White blood cells	Platelets	Biochemistry	
CF1	Challenged	Fever (5 dpi)	Severe (5 dpi)	Leukocytopenia (3 dpi)	Thrombocytopenia (3, 5 dpi)	ALT↑↑↑, TBIL↑, BUN↑, CRE↑, GLOB↑ (5 dpi)	Died, 6 dpi
DF1	Direct contact				Thrombocytopenia (7, 26 dpi)	TBIL↑ (9, 19, 26 dpi), BUN↑ (19, 26 dpi)	Survived
IF1	Indirect Contact			Leukocytopenia (12 dpi)	Thrombocytopenia (7, 19 dpi)	TBIL↑ (12 dpi), BUN↑ (5, 12, 19, 26 dpi), CRE↑ (19, 26 dpi)	Survived
CF2	Challenged			Leukocytopenia (3, 5 dpi)	Thrombocytopenia (3, 5 dpi)	ALP↑, ALT↑↑↑, TBIL↑↑↑, BUN↑, GLOB↑ (5 dpi)	Died, 6 dpi
DF2	Direct contact			Leukocytopenia (12, 19 dpi)	Thrombocytopenia (7, 9, 26 dpi)	BUN↑ (26 dpi), CRE↓ (19 dpi)	Survived
IF2	Indirect Contact				Thrombocytopenia (5, 7, 12, 19 dpi)	TBIL↑ (9, 19 dpi), BUN↑ (5, 9, 12, 19, 26 dpi), CRE↑ (26 dpi)	Survived
CF3	Challenged			Leukocytopenia (3, 5 dpi)	Thrombocytopenia (3, 5 dpi)	ALT↑↑↑, TBIL↑↑↑, BUN↑↑, CRE↑, GLOB↑ (5 dpi)	Died, 6 dpi
DF3	Direct contact			Leukocytopenia (12, 19 dpi)	Thrombocytopenia (5, 12, 26 dpi)		Survived
IF3	Indirect Contact			Leukocytopenia (7, 26 dpi)	Thrombocytopenia (5, 19 dpi)	TBIL↑ (9, 12, 19 dpi), BUN↑ (5, 9, 19, 26 dpi), BUN↑↑ (12 dpi), CRE↓ (26 dpi)	Survived

Supplemental table 18: Clinical parameters of male ferrets

Hypothermia was defined as below 35°C. Fever was defined as 1.0°C higher than baseline. Mild rash was defined as focal areas of petechiae covering <10% of the skin, moderate rash as areas of petechiae covering 10 to 40% of the skin and severe rash as areas of petechiae and/or ecchymosis covering >40% of the skin. Leukocytopenia and thrombocytopenia were defined as a >30% decrease in numbers of white blood cells and platelets, respectively. Leukocytosis and thrombocytosis were defined as a twofold or greater increase in numbers of white blood cells and platelets over baseline, where white blood cell count >11 x 10^3. ↑, two- to threefold increase; ↑↑, four- to fivefold increase; ↑↑↑, greater than fivefold increase; ↓, two- to threefold decrease; ↓↓, four- to fivefold decrease; ↓↓↓, greater than fivefold decrease. AMY, amylase; ALP, alkaline phosphatase; ALT, alanine aminotransferase; TBIL, total bilirubin; BUN, blood urea nitrogen; CRE, creatinine; K+, potassium; GLOB, globulin.

Animal ID	Group	Clinical findings					Outcome
		Body temperature	Rash	White blood cells	Platelets	Biochemistry	
CM1	Challenged	Fever (5 dpi)	Moderate (5 dpi), Severe (6 dpi)	Leukocytopenia (3, 5 dpi)	Thrombocytopenia (5 dpi)	AMY↑ (3 dpi), ALT↑↑↑, TBIL↑↑↑, BUN↑↑↑, CRE↑ (5 dpi)	Died, 6 dpi
DM1	Direct contact	Fever (9 dpi)	Severe (9, 10 dpi)	Leukocytosis (5 dpi), Leukocytopenia (7, 9, 10 dpi)	Thrombocytopenia (5, 9, 10 dpi)	BUN↑, CRE↑ (7 dpi), ALT↑↑↑, TBIL↑, BUN↑ (9 dpi), AMY↑, ALP↑↑↑, ALT↑↑↑, TBIL↑↑↑, BUN↑↑↑, CRE↑↑↑ (10 dpi)	Died, 10 dpi
IM1	Indirect Contact			Leukocytopenia (12, 19 dpi)	Thrombocytopenia (5, 7 dpi)	TBIL↑ (19 dpi), ALP↓, BUN↑ (26 dpi)	Survived
CM2	Challenged		Severe (5 dpi)	Leukocytopenia (3, 5 dpi)	Thrombocytopenia (3, 5 dpi)	ALP↑, ALT↑↑↑, TBIL↑↑↑, BUN↑↑↑, GLOB↑ (5 dpi)	Died, 5 dpi
DM2	Direct contact	Fever (9 dpi)	Severe (10 dpi)	Leukocytopenia (9, 10 dpi)	Thrombocytopenia (5, 7, 9, 10 dpi)	ALT↑, GLOB↑ (9 dpi), ALP↑↑↑, ALT↑↑↑, TBIL↑↑↑, BUN↑↑↑, CRE↑, GLOB↑ (10 dpi)	Died, 11 dpi
IM2	Indirect Contact				Thrombocytopenia (9, 12, 19, 26 dpi)	BUN↑ (5, 7, 9, 12, 19 dpi), ALT↑ (7 dpi), BUN↑↑, CRE↑ (26 dpi)	Survived
CM3	Challenged	Fever (5 dpi)		Leukocytopenia (3, 5 dpi)	Thrombocytopenia (3, 5 dpi)	ALP↑↑↑, ALT↑↑↑, TBIL↑↑↑, BUN↑↑↑, CRE↑ (5 dpi)	Died, 6 dpi
DM3	Direct contact	Fever (9 dpi)	Mild (9 dpi), Severe (10 dpi)	Leukocytopenia (7, 9, 10 dpi)	Thrombocytopenia (5, 9, 10 dpi)	BUN↑ (5 dpi)ALT↑, TBIL↑, BUN↑, CRE↑, GLOB↑ (9 dpi), ALP↑↑↑, ALT↑↑↑, TBIL↑↑↑, BUN↑↑↑, CRE↑↑↑, K^+↑, GLOB↑ (10 dpi)	Died, 10 dpi
IM3	Indirect Contact				Thrombocytopenia (7, 12 dpi)	CRE↑↑↑ (12 dpi)	Died, 19 dpi

Supplemental table 21: Ferret humane endpoint scoring chart

Ferret Humane Endpoint Scoring Chart; **Version 2016-01; Date 2016-11-01**

Prepared for the week of: **Animal ID #:**

Parameter	Degree of parameter	DPI	1	2	3	4	5	6	7
		Possible Score	Score	Score	Score	Score	Score	Score	Score
Posture	Normal	0							
	Decreasing activity, Decreasing normal behaviour, pilo-erection	3							
	Huddled , not moving in cage	5							
Temperature Change	Increase in body temperature above 2°C (n=38.9)	5							
Weight Change	Decrease in body weight of more than 10%	10							
Respiration	Normal	0							
	Increased or Decreased	2							
	Laboured, breathing through mouth	10							
	Cough or sneeze	2							
Feces + Urine	Normal consistency volume / Soft normal stool	0							
	Feces absent or dry / Decreased urine output / Cloudy urine	2							
	Wet pasty / Small very dry stool / dark stool	2							
	Liquid stool / blood in stool or urine No urine > twice	10							
Food + water	Normal eating / drinking	0							
	Mildly decreased E /D 25%	1							
	Moderately decreased E / D 50 %	3							
	Severely decreased E/D 75%	4							
	Seriously decreased - refusing all food, dehydration apparent > 2 days	10							
Recumbent	No symptoms	0							
	Huddled on camera, active when cage opened	3							
	Lies down but moves around	15							
	Lies down and won't move	25							
Attitude	Normal	0							
	Mildly depressed, responds to treats and toys	1							
	Moderately depressed, response requires prodding, loses interest in treats and toys,	3							
	Severely depressed, no interest in treats, does not respond to human presence	10							
Other	Flushed appearance to skin	2							
	Nasal discharge	2							
	Visible Rash	5							
	Cyanosis	5							
	Haemorrhage Subcutaneous	10							
	Haemorrhage Orifices	15							
Total score*		0-64*							
BODY Weight									
SCAN Temp									
Rectal Temp									

** The PI or co-investigator will consult with a veterinarian to make a decision regarding euthanasia when a total score of 25 is reached*

** The control animals will only be allowed to reach a score of 20 before a decision is made regarding euthanasia.*

2.10 References

109. Ebihara, H. et al., 2006: Molecular determinants of Ebola virus virulence in mice. *PLoS Pathogens*., **2**, 0705–0711.

172. Baize, S. et al., 2014: Emergence of Zaire Ebola Virus Disease in Guinea - Preliminary Report. *The New England journal of medicine*., **371**, 1418–1425.

211. Wong, G. et al., 2015a: Ebola virus transmission in guinea pigs. *Journal of virology*., **89**, 1314–1323.

215. Cross, R. W. et al., 2016: The Domestic Ferret (Mustela putorius furo) as a Lethal Infection Model for Three Different Species of Ebolavirus. *Journal of Infectious Diseases*., **214**, 565–569.

216. Kroeker, A. et al., 2017: Characterization of Sudan Ebolavirus infection in ferrets. *Oncotarget*., **8**, 46262–46272.

217. Kozak, R. et al., 2016: Ferrets infected with Bundibugyo virus or Ebola virus recapitulate important aspects of human filoviral disease. *Journal of Virology*., **90**, 9209–9223.

222. Wong, G. et al., 2018b: The Makona Variant of Ebola Virus Is Highly Lethal to Immunocompromised Mice and Immunocompetent Ferrets. *The Journal of Infectious Diseases*., **0**, 1–5.

270. Bausch, D. G. et al., 2007: Assessment of the risk of Ebola virus transmission from bodily fluids and fomites. *The Journal of infectious diseases*., **196**, S142-147.

271. Vetter, P. et al., 2016: Ebola Virus Shedding and Transmission: Review of Current Evidence. Journal of Infectious Diseases., 214, S177–S184.

276. Wong, G. et al., 2016: Pathogenicity Comparison Between the Kikwit and Makona Ebola Virus Variants in Rhesus Macaques. *Journal of Infectious Diseases*., **214**, S281–S289.

289. Becquart, P. et al., 2010: High prevalence of both humoral and cellular immunity to Zaire ebolavirus among rural populations in Gabon. *PLoS ONE*., **5**, 1–9.

291. Leroy, E. M. et al., 2000: Human asymptomatic Ebola infection and strong inflammatory response. *Lancet*., **355**, 2210–2215.

294. World Health Organization (WHO), 2015b: Factors that contributed to undetected spread of the Ebola virus and impeded rapid containment.

295. Marzi, A. et al., 2015: Delayed Disease Progression in Cynomolgus Macaques Infected with Ebola Virus Makona Strain. *Emerg Inf Disease*., **21**, 1777–1783.

296. Jaax, N. K. et al., 1995: Transmission of Ebola virus (Zaire strain) to uninfected control monkeys in a biocontainment laboratory. *The Lancet*., **346**, 1669–1671.

297. Alimonti, J. B. et al., 2014: Evaluation of transmission risks associated with in vivo replication of several high containment pathogens in a biosafety level 4 laboratory. *Scientific reports*., **4**, 1–7.

298. Kobinger, G. P. et al., 2011: Replication, pathogenicity, shedding, and transmission of Zaire ebolavirus in pigs. *The Journal of Infectious Diseases*., **204**, 200–208.

299. Weingartl, H. M. et al., 2012: Transmission of Ebola virus from pigs to non-human primates. *Scientific reports*., **2**, 1–4.

300. Spengler, J. R. et al., 2015: Utility of Oral Swab Sampling for Ebola Virus Detection in Guinea Pig Model, **21**, 1816–1819.

301. Nkoghe, D. et al., 2011b: Risk factors for zaire ebolavirus-specific IgG in rural gabonese populations. *Journal of Infectious Diseases*., **204**, S768–S775.

302. Busico, K. M. et al., 1999: Prevalence of IgG antibodies to Ebola virus in individuals during an Ebola outbreak, Democratic Republic of the Congo, 1995. *The Journal of infectious diseases*., **179**, S102–S107.

303. Bower, H. et al., 2017: A systematic review and meta-analysis of seroprevalence surveys of ebolavirus infection. *Scientific Data*., **4**, 1–9.

304. Zeng, X. et al., 2017: Identification and pathological characterization of persistent asymptomatic Ebola virus infection in rhesus monkeys. *Nature Microbiology*., **2**, 1–11.

305. Akerlund, E. et al., 2015: Shedding of Ebola Virus in an Asymptomatic Pregnant Woman. *The New England journal of medicine*., **372**, 2467–2469.

306. Leroy, E. M. et al., 2001: Early immune responses accompanying human asymptomatic Ebola infections. *Clinical and Experimental Immunology*., **124**, 453–460.

307. Mire, C. E. et al., 2016: Oral and Conjunctival Exposure of Nonhuman Primates to Low Doses of Ebola Makona Virus. *Journal of Infectious Diseases*., **214**, S263–S267.

308. Nkangu, M. N. et al., 2017: The perspective of gender on the Ebola virus using a risk management and population health framework: A scoping review. *Infectious Diseases of Poverty*., **6**, 1–9.

Chapter 3. Role of key infectivity parameters in the transmission of Ebola virus Makona in macaques.

Marc-Antoine de La Vega[1], Gary Wong[2], Haiyan Wei[3], Shihua He[2], Alexander Bello[2], Hugues Fausther-Bovendo[1], Jonathan Audet[2], Kevin Tierney[2], Kaylie Tran[2], Geoff Soule[2], Trina Racine[4], James E. Strong[2], Xiangguo Qiu[2], Gary P. Kobinger[1, 5, *]

*Corresponding author

[1]Département de microbiologie-infectiologie et d'immunologie, Université Laval, Québec, QC, Canada; [2]Special Pathogens Program, National Microbiology Laboratory, Public Health Agency of Canada, Winnipeg, MB, Canada; [3]Institute of Infectious Disease, Henan Center for Disease Control and Prevention, Zhengzhou, Henan, China; [4]Vaccine and Infectious Disease Organization, University of Saskatchewan., Saskatoon, SK, Canada; [5]Department of Pathology and Laboratory Medicine, University of Pennsylvania School of Medicine, Philadelphia, PA, USA

Running title: EBOV transmission in macaques

Keywords: Ebola virus, transmission, rhesus macaque, viral load, route of infection

Word count (Abstract): 150

Word count (Text): 3469

3.1 Résumé

À ce jour, plusieurs caractéristiques associées avec la maladie à virus Ebola (MVE) demeurent partiellement incomprises. Il est reconnu qu'un contact direct avec des fluides corporels infectés représente un facteur de risque pour le développement d'une infection, mais peu d'études ont étudié l'effet de paramètres associés avec la transmission entre individus, tels que la dose de virus nécessaire pour faciliter la transmission ou la voie par laquelle un individu est infecté. Par conséquent, nous avons cherché à caractériser l'impact de la voie d'infection, de la virémie, ainsi que de l'excrétion virale par différentes muqueuses, sur la transmission intra-espèces du virus Ebola dans un modèle de primates non-humains. Dans cette étude, l'infection de primates par l'œsophage ou des aérosols au visage n'a pas mené au développement d'une infection clinique, bien qu'une séroconversion des animaux ait été observée lors de cette dernière expériences. Des études subséquentes où les primates ont été infectés par la voie intramusculaire ou intratrachéale suggèrent que la charge virale détermine la probabilité de transmission à un animal naïf dans un modèle d'infection par voir intramusculaire, et que cette transmission est grandement facilitée dans un modèle intratrachéal d'infection où la transmission d'un animal infecté à un animal contact fut observée de manière consistante.

3.2 Abstract

Many characteristics associated with Ebola virus disease remain to be fully understood. It is known that direct contact with infected bodily fluids is an associated risk factor, but few studies have investigated parameters associated with transmission between individuals, such as the dose of virus required to facilitate spread and route of infection. Therefore, we sought to characterize the impact by route of infection, viremia, and viral shedding through various mucosae, with regards to intraspecies transmission of Ebola virus in a non-human primate model. Here, challenge via the esophagus or aerosol to the face did not result in clinical disease, although seroconversion of both challenged and contact animals was observed in the latter. Subsequent intramuscular or intratracheal challenges suggest that viral loads determine transmission likelihood to naïve animals in an intramuscular-challenge model, which is greatly facilitated in an intratracheal-challenge model where transmission from challenged to direct contact animal was observed consistently.

3.3 Background

Ebola virus (EBOV) has been known within the scientific community since 1976, when it was first isolated from the Yambuku outbreak in the Democratic Republic of Congo (DRC)[140]. However, EBOV recently gained the attention of the general public after the much publicized 2013–2016 West African epidemic, caused by a new viral variant, EBOV-Makona[172,309]. During that timeframe, the DRC was hit by an outbreak of their own in 2016 in Boende[171], and later faced four subsequent outbreaks in the Likati[310] and Bikoro[311] health zones, as well as

the second largest EBOV epidemic ever recorded, in the North Kivu and Ituri provinces between 2018 and 2020. An ongoing outbreak in Guinea was also reported in early February 2021[312]. Although a considerable number of advances have been made regarding specific prophylactic and therapeutic options[313], as well as post-EBOV disease syndrome (PEVDS)[314,315], various aspects of pathogenesis and transmission remain to be defined. For example, the term ”superspreader” was widely used during the West African outbreak and defines contagious individuals that go on to infect a high number of contacts, resulting in multiple secondary infections[316,317]. Although numerous environmental and behavioural factors can partially account for such superspreading events, it has been hypothesized that these individuals can shed higher amounts of virus and/or for an extended period of time, thereby facilitating the infection of naïve susceptible hosts[318]. Whether this is virus-dependent, host-dependent, or both, remains to be clarified. Detection of EBOV viral RNA from humans has been described in blood, saliva, urine, aqueous humour, breast milk, semen, stool, amniotic and cerebrospinal fluid, as well as conjunctival, vaginal and skin swabs, while laboratory culture of these samples only reported the presence of infectious particles in the first six types of samples[271]. Viral shedding has also been characterized in various animal models following EBOV infection including guinea pigs, ferrets, pigs, and non-human primates (NHPs). Shedding was found to increase with disease progression and has been reported from the oral, nasal and rectal cavities in all four models[211,217,276,299]. However, the role of key infectivity parameters, such as dose and route of infection, are not well understood. Of note, a study in guinea pigs has shown that animals infected intranasally (i.n.) with guinea pig-adapted EBOV (GA-EBOV) were more contagious to their naïve counterparts compared to animals that were infected intraperitoneally (i.p.). Indeed, i.n.-infected animals shed GA-EBOV from their nasal cavity earlier than i.p.-infected animals and had a delayed time to death, prolonging the exposure of naïve animals[211]. This suggests that, in this model at least, route of infection and time of exposure are factors that may influence disease progression and viral transmission. However, current small animal models, which include mice, hamsters, and guinea pigs, poorly mimic clinical EVD in humans. These hosts also require infection with a host-adapted variant of EBOV, as wild type viruses do not cause disease. As such, the timely evaluation of a new clinical EBOV isolate can be problematic in rodent models[319]. Adaptation of the virus to the host also generates mutations, a variable that is not desired in some, if not most studies since these viruses do not always accurately represent their naturally occurring counterparts. The NHP remains the most biologically relevant animal model for pathogenesis studies due to its ability to replicate most human hallmarks of EVD and that it does not require virus adaptation. Regarding transmission, the NHP as a gold standard model will complement nicely with published work in ferrets[225] and guinea pigs[211] to give the best possible insight into parameters involved with EBOV spread. Infection of NHPs with EBOV in the laboratory has mostly been performed with an intramuscular (i.m.) injection. Currently, it is controversial whether these i.m.-infected animals are contagious to their naive counterparts without direct contact. Although i.m. infection of rhesus NHPs with EBOV-Mayinga has been reported to have resulted in the infection of naïve rhesus animals in the absence of contact[296], a more

recent study did not observe transmission of EBOV-Kikwit from i.m. inoculated rhesus to cynomolgus macaques[297].

In the current study, we sought to characterize the role of viral load, shedding, and route of infection in the likelihood of intraspecies EBOV transmission, within the context of a rhesus macaque model. A series of independent studies were carried out, in which experimentally challenged animals were inoculated via the intraesophageal, aerosol, i.m., or intratracheal (i.t.) routes, and then placed in direct contact with naïve animals. Viremia and viral shedding were monitored throughout the course of the experiments and transmission events were recorded to characterize virus spread.

3.4 Methods

3.4.1 Ethics statement

The experiments described in this study were carried out at the National Microbiology Laboratory (NML) as described in the Animal use document #H-14-011, and was approved by the Animal Care Committee located at the Canadian Science Center for Human and Animal Health, in accordance with the guidelines provided by the Canadian Council on Animal Care.

3.4.2 Viruses

The viruses used for challenge in NHPs were Ebola virus/H.sapiens-tc/COD/1995/Kikwit-9510621 (EBOV-K; GenBank accession no. AY354458; order Mononegavirales, family Filoviridae, species Zaire ebolavirus) and Ebola virus/H.sapiens-wt-GIN/2014/Makona-C05 (EBOV-C05; GenBank accession no. KT013254; order Mononegavirales, family Filoviridae, species Zaire ebolavirus). Passage 3 from the original stock was used for EBOV-K and passage 1A was used for EBOV-C05.

3.4.3 Animal studies

A total of 30 non-human primates (rhesus macaques; *Macaca mulatta*) were used for the experiments described here. The 12 animals used for the aerosol and the first i.m. challenge experiments were purchased from Primus Bio-Ressources Inc. and were all males weighing between 3.6 and 6.0 kg. The 18 animals used for the intraesophageal, repeat i.m., and i.t. challenge experiments were purchased from PrimGen and were mixed genders, weighing between 3.1 and 4.3 kg. Animals were fed standard monkey chow, fruits, vegetables, and treats ad libitum. NHPs were challenged either intramuscularly (i.m.), intraesophageally, intratracheally (i.t.) or by aerosol with a targeted dose of 1000 × TCID50 of EBOV-Makona. The virus was prepared in Dulbecco's Modified Eagle Medium (DMEM) for all challenges. The animals were then scored daily for observable signs of disease, in addition to changes in food and water consumption. All challenges and sampling were performed

following intramuscular injection of 6–8 mg/kg of ketamine. Blood was taken for serum biochemistry, complete blood counts, and quantification of viremia. Oral, nasal and rectal swabs were taken to quantify levels of virus shedding. Aerosol challenge was performed using an in-house nebulizer inside a biosafety cabinet. Briefly, the nebulizer was attached into one end of a tube about 10 cm in diameter and 30 cm in length, with a breathing mask on the other end. Animals were given 2 mists of 500 µL each at 2.5 min intervals in the presence of continuous oxygen. After 5 min, the face of the animals was wiped down with a towel sprayed with 70% EtOH. Animals challenged i.m. were given 1 injection of 500 µL in each thigh while intraesophageal and i.t. challenges were performed using a tracheal tube. Briefly, the sedated animals were laid on their back, and the tube was inserted about 15 cm in the esophagus using a laryngoscope. The 4 mL virus inoculum was then slowly added in the tube via the use of a syringe.

3.4.4 EBOV titration by $TCID_{50}$ and RT-qPCR

Titration of live EBOV was determined by adding 100 µL of 10-fold serial dilutions of whole blood or swab sample (in Dulbecco's modified Eagle's medium) to VeroE6 cells, with three replicates per dilution. The plates were scored for cytopathic effect at 13 dpi, and titers were calculated with the Reed-Muench method. For titers measured by RT-qPCR, total RNA was extracted from whole blood or DMEM from swab samples with the QIAamp Viral RNA Mini Kit (Qiagen). EBOV was detected with the LightCycler 480 RNA Master Hydrolysis Probes (Roche) kit, with the RNA polymerase (nucleotides 16472 to 16538, AF086833) as the target gene. The reaction conditions were as follows: 63°C for 3 minutes, 95°C for 30 seconds, and cycling of 95°C for 15 seconds, 60°C for 30 seconds for 45 cycles on the ABI StepOnePlus. The lower detection limit for this assay is 86 GEQ/mL. The sequences of primers used were as follows: EBOVLF2 (CAGCCAGCAATTTCTTCCAT), EBOVLR2 (TTTCGGTTGCTGTTTCTGTG), and EBOVLP2FAM (FAM-ATCATTGGCGTACTGGAGGAGCAG-BHQ1).

3.4.5 ELISA

IgM and IgG ELISA to determine pre-existing antibodies against EBOV-G and EBOV-K was performed as described previously[225], using EBOV-GPΔTM (IBT BioServices) as a capture antigen. Each sample was assayed in triplicate. A titer was considered to represent a positive result if the average value was 7.733 standard deviations above background.

3.5 Results

3.5.1 Intraesophageal challenge results in neither disease nor seroconversion.

To investigate virus replication and transmission likelihood after ingestion of EBOV, three NHPs (A1-A3) were experimentally infected intraesophageally with a target dose of 1000 x $TCID_{50}$ of EBOV-Makona. Each of these animals was then co-housed with a naïve animal (A4-A6) immediately after infection in order to assess the transmission potential of the virus. By the end of the experiment, at 28 days post-infection (dpi), none of the infected or contact animals succumbed to infection or developed any clinical signs of disease. Furthermore, none of the animals became viremic or seroconverted, as assessed by the absence of viral loads, and anti-EBOV IgM and IgG antibodies (Supplemental table 23). This suggests that gastric exposure does not facilitate infection with EBOV in macaques.

3.5.2 Facial aerosol exposure with EBOV in NHPs Resulted in Subclinical Infection.

To assess the impact of aerosol exposure to the face on EBOV transmissibility, animals B1, B2, and B3 were challenged via a spray to the face with a target dose of 1000 x $TCID_{50}$ of EBOV-Makona, wiped, pair-housed with a naïve animal (B4, B5, and B6, respectively), and monitored for survival and clinical signs. Surprisingly, challenged animals did not succumb to infection or demonstrate any observable signs of disease (Supplemental figure 8). Viremia was not detected by reverse-transcription quantitative polymerase chain reaction (RT-qPCR), raising the possibility that the aerosolization process to the face may not be efficient for delivering virus to a susceptible host. Interestingly, EBOV-specific IgM and IgG were detected from all animals by 21 dpi. For IgM, all challenge (B1, B2, and B3) and contact animals (B4, B5, and B6) exhibited seropositivity to EBOV-Makona, with endpoint titers peaking between 3 x 10^3 and 1 x 10^5. For IgG, the challenged animal B1 along with contact animals B4 and B6 were shown to be seropositive for EBOV, with endpoint dilution titers ranging from 1 x 10^4 to 3 x 10^5 (Figure 32: Humoral response of challenged and contact NHPs challenged in the context of aerosol delivery of EBOV-Makona

Endpoint titers of IgM **(a)** and IgG **(b)** antibodies against the glycoprotein of EBOV throughout the course of the experiment are shown. *IgM: Immunoglobulin M; IgG: Immunoglobulin G*). These results indicate that an infection with EBOV likely occurred, resulting in antibody seroprevalence, but clinical signs (if any) were subclinical. As such, evaluating transmission was difficult with facial aerosol challenge.

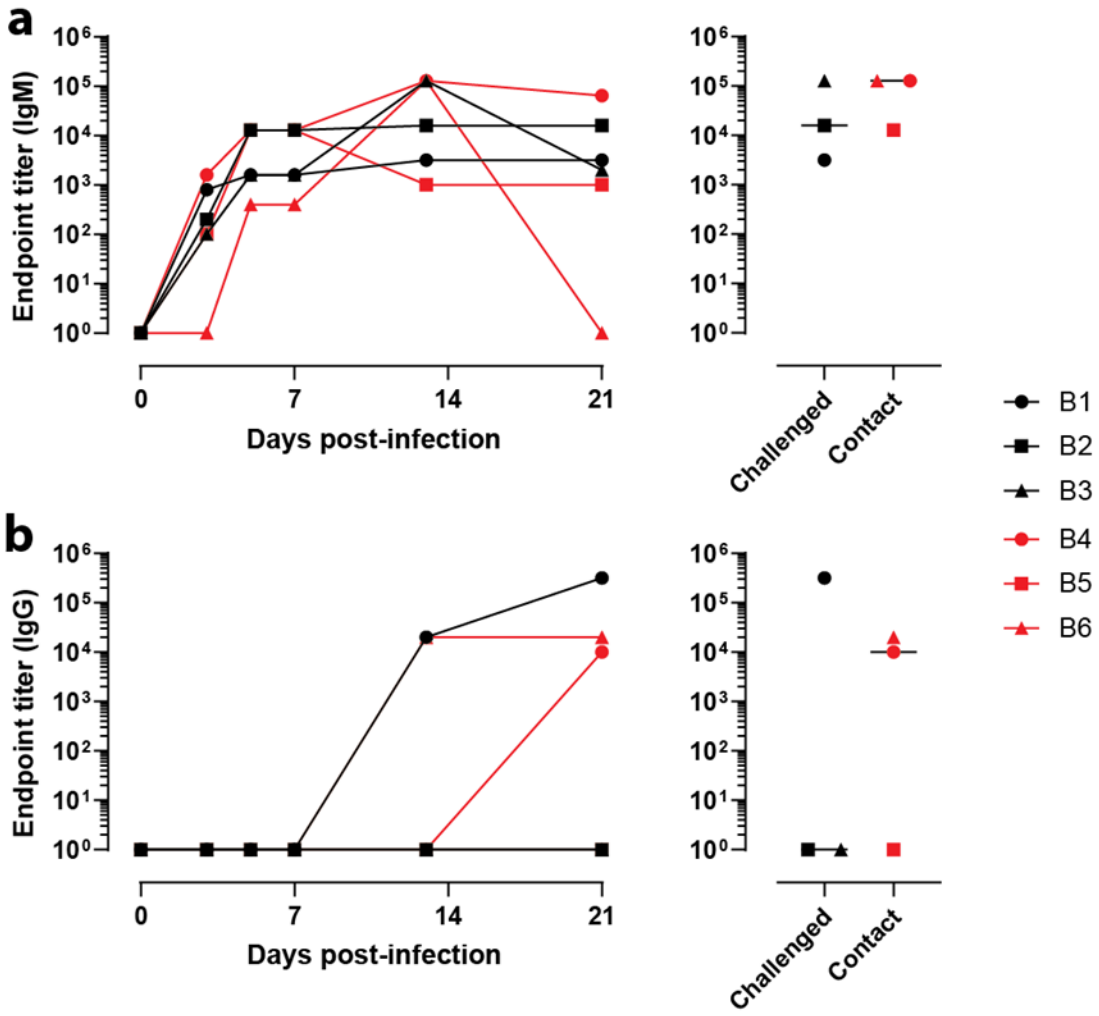

Figure 32: Humoral response of challenged and contact NHPs challenged in the context of aerosol delivery of EBOV-Makona

Endpoint titers of IgM **(a)** and IgG **(b)** antibodies against the glycoprotein of EBOV throughout the course of the experiment are shown. *IgM: Immunoglobulin M; IgG: Immunoglobulin G*

3.5.3 High Viral Loads, but not Pre-Existing Immunity, Impact EBOV Transmission.

The goal of these initial pilot experiments was to evaluate routes of EBOV infection that are more commonly encountered in a natural outbreak setting[142]. However, symptomatic disease could not be easily achieved in these animals and therefore more typical routes known to cause clinical EVD were investigated. To this end, the same animals from the facial aerosol challenge were re-used following approval from the animal care committee, as none of them succumbed to challenge nor presented clinical manifestations. At 21 dpi of the facial aerosol challenge experiment, animals that were in the contact group (B4, B5*, and B6*) were challenged i.m. with a target dose of 1000 x $TCID_{50}$, while animals that were challenged in the previous experiment (B1*, B2*, and B3*) became the direct contact group (Supplemental figure 9). The challenged NHPs all succumbed to infection at 7 or 8 dpi, despite detection*

of pre-existing immunity against EBOV in B4 and B6*, which was developed following mucosal exposure to EBOV (Figure 33: Survival and clinical parameters of challenged and contact NHPs in the context of i.m. delivery of EBOV-Makona in animals exhibiting pre-existing immunity*

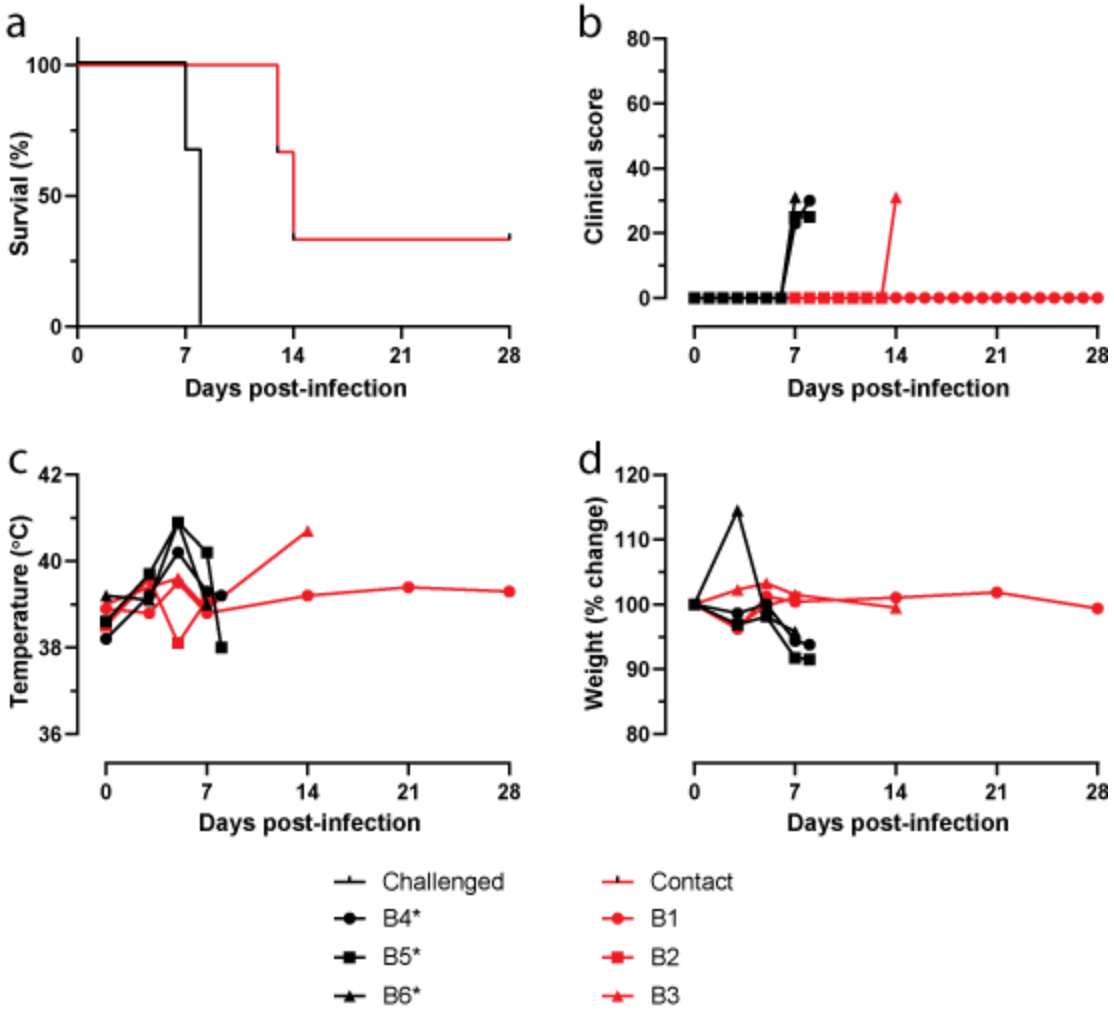

Figure 33: Survival and clinical parameters of challenged and contact NHPs in the context of i.m. delivery of EBOV-Makona in animals exhibiting pre-existing immunity

(a) Survival. **(b)** Clinical score. **(c)** Temperature. **(d)** Body weight percent change.

(a) Survival. **(b)** Clinical score. **(c)** Temperature. **(d)** Body weight percent change.

Figure 34: Viremia and shedding from challenged and contact NHPs in the context of i.m. delivery of EBOV-Makona in animals exhibiting pre-existing immunity.Figure 35).

Regarding contact animals, B2 and B3* both succumbed throughout the course of the experiment, however, B2* did not have detectable viremia at the time of death. Since symptoms in this animal started following anesthesia and were not*

consistent with EVD, the cause of death was attributed to an unknown cause, possibly an adverse event due to the anesthetic procedure. As for B3, it succumbed to EVD on 14 dpi, thus the timeline is consistent with this animal being infected by its terminally-ill cagemate (B6*). Interestingly, B6*, which was the only animal to transmit EBOV to its naïve cagemate, displayed the highest viremia and viral shedding. Indeed, this animal exhibited a peak viremia of >1e8 $TCID_{50}$/mL, which was over the limit of detection of the assay, (2.8e7 GEQ/mL) while the other macaques did not exceed 6.8e7 $TCID_{50}$/mL (7.3e5 GEQ/mL) (Figure 36: Viremia and shedding from challenged and contact NHPs in the context of i.m. delivery of EBOV-Makona in animals exhibiting pre-existing immunity.*

*Viral loads are measured by $TCID_{50}$/mL in **(a)** blood, **(b)** oral swabs, **(c)** nasal swabs, and **(d)** rectal swabs. The blue line represents a sample that was still positive at the upper limit of the assay. $TCID_{50}$: Median Tissue Culture Infectious Dosea, Supplemental figure 10). Viral shedding through the oral, nasal and rectal cavities followed a similar trend, in which the transmitting challenged animal exhibited peak shedding of 0, 1.5e1, and 1.5e1 $TCID_{50}$/mL (7.6e4, 5.7e5 and 8.2e5 GEQ/mL), respectively, whereas non-transmitting challenged animals peaked at an average of 1.6e2, 7.3e0, and 0 $TCID_{50}$/mL (5.2e4, 5.2e4, and 1.8e4 GEQ/mL), respectively (Figure 36: Viremia and shedding from challenged and contact NHPs in the context of i.m. delivery of EBOV-Makona in animals exhibiting pre-existing immunity.*

*Viral loads are measured by $TCID_{50}$/mL in **(a)** blood, **(b)** oral swabs, **(c)** nasal swabs, and **(d)** rectal swabs. The blue line represents a sample that was still positive at the upper limit of the assay. $TCID_{50}$: Median Tissue Culture Infectious Doseb-d, Supplemental figure 10b-d). The contact NHP (B1*) that survived the exposure to its infected cagemate was coincidentally the animal exhibiting the highest levels of pre-existing immunity, as measured by endpoint IgG titers (Figure 32: Humoral response of challenged and contact NHPs challenged in the context of aerosol delivery of EBOV-Makona*

Endpoint titers of IgM **(a)** and IgG **(b)** antibodies against the glycoprotein of EBOV throughout the course of the experiment are shown. *IgM: Immunoglobulin M; IgG: Immunoglobulin G*b). However, due to the low number of animals used and that pre-existing immunity may have interfered with our hypothesis that high viral shedding positively influences viral transmission rates, a repeat experiment was necessary to strengthen any interpretations.

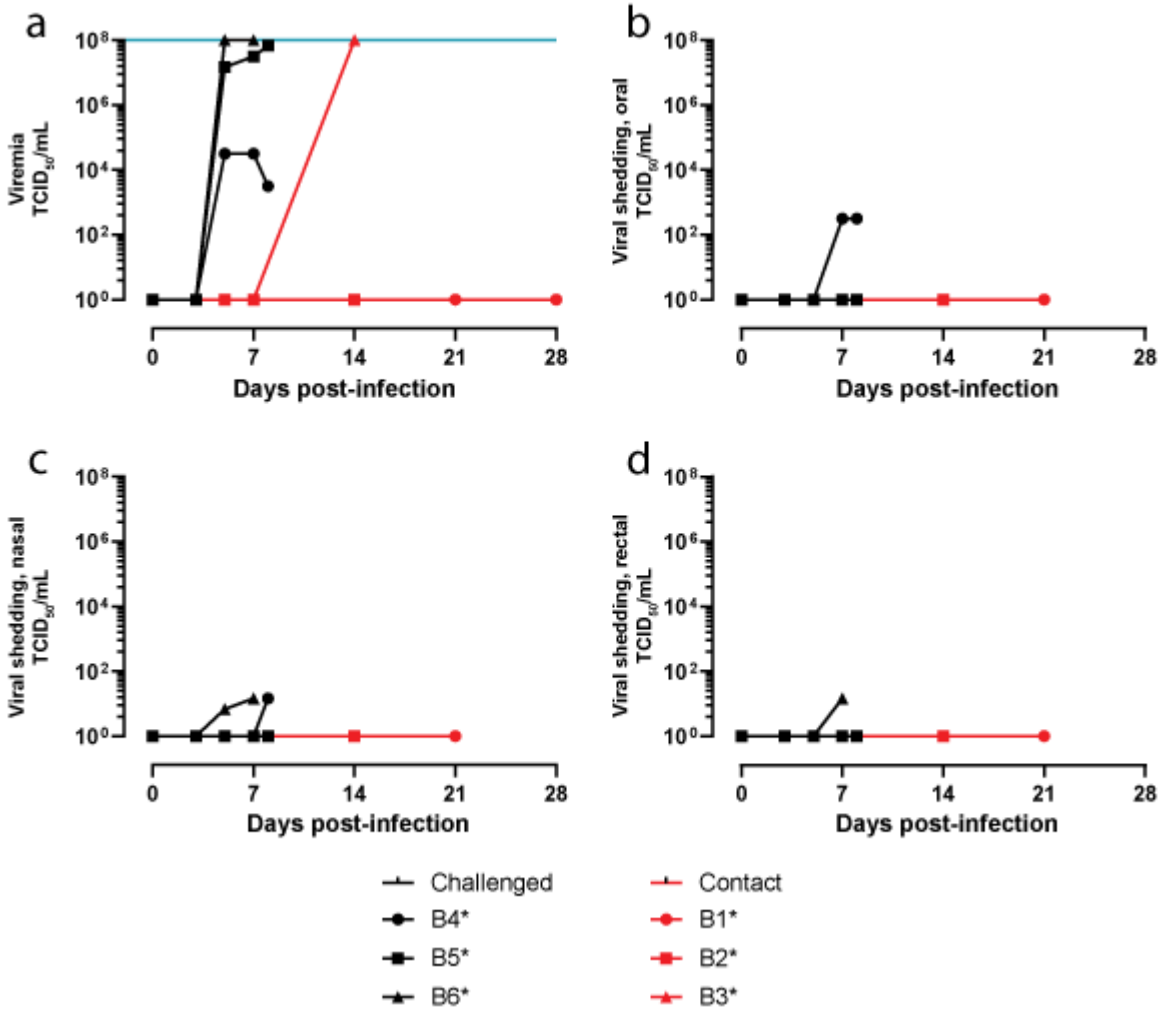

Figure 36: Viremia and shedding from challenged and contact NHPs in the context of i.m. delivery of EBOV-Makona in animals exhibiting pre-existing immunity.

Viral loads are measured by $TCID_{50}$/mL in **(a)** blood, **(b)** oral swabs, **(c)** nasal swabs, and **(d)** rectal swabs. The blue line represents a sample that was still positive at the upper limit of the assay. *$TCID_{50}$: Median Tissue Culture Infectious Dose*

To this end, three additional NHPs (C1, C2 and C3), which had never been exposed to EBOV, were infected i.m. with a target dose of 1000 x $TCID_{50}$ of EBOV-Makona. All animals succumbed to infection on 6, 7, and 8 dpi, respectively. These animals were found to be viremic, shed virus, and displayed clinical symptoms typical of EVD (Supplemental figure 11). Immediately following infection, each challenged animal was paired with a naïve NHP (C4, C5, and C6 respectively), in order to evaluate transmission. All three contact animals not only survived for the whole duration of the experiment, but they also did not become viremic or seroconvert (Supplemental figure 12). The lack of transmission in the absence of pre-existing immunity suggests that high viral loads in the blood from an i.m. exposure do not necessarily lead to transmission. In the previous i.m.-challenge experiment, the transmitting animal reached a peak viremia of >1e8 $TCID_{50}$/mL (2.8e7 GEQ/mL), while peak oral, nasal, and rectal shedding were of 0, 1.5e1, 1.5e1 $TCID_{50}$/mL (7.6e4, 5.7e5 and 8.2e5 GEQ/mL), respectively. In the second experiment, the peak viremia of C1 and C2 was similar to those of NHPs from the first i.m. experiment, >1e8 and 3.16e7 $TCID_{50}$/mL (average of 1.76e7 GEQ/mL) respectively, while C3 failed to reach similar levels (3.16e1 $TCID_{50}$/mL; 6.83e6 GEQ/mL) (Figure 37: Viremia and shedding from challenged and contact NHPs in the context of i.m. delivery of EBOV-Makona in naïve animals.

*Viral loads are measured by $TCID_{50}$/mL in **(a)** blood, **(b)** oral swabs, **(c)** nasal swabs, and **(d)** rectal swabs. The blue line represents a sample that was still positive at the upper limit of the assay. The dotted line represents values obtained for the transmitting animal in the initial i.m. challenge with animals exhibiting pre-existing immunity. $TCID_{50}$: Median Tissue Culture Infectious Dosea, Supplemental*

figure 13a). Furthermore, viral secretions from the oral, nasal and rectal cavities in challenged animals were not nearly as high as those from the previous experiment. Indeed, average peak shedding for challenged NHPs in the second experiment was 1.1e2 $TCID_{50}$/mL (2.4e3 GEQ/mL) for oral, 0 $TCID_{50}$/mL (3.6e3 GEQ/mL) for nasal, and 0 $TCID_{50}$/mL (1.2e3 GEQ/mL) for rectal swabs (Figure 37: Viremia and shedding from challenged and contact NHPs in the context of i.m. delivery of EBOV-Makona in naïve animals.

Viral loads are measured by $TCID_{50}$/mL in **(a)** blood, **(b)** oral swabs, **(c)** nasal swabs, and **(d)** rectal swabs. The blue line represents a sample that was still positive at the upper limit of the assay. The dotted line represents values obtained for the transmitting animal in the initial i.m. challenge with animals exhibiting pre-existing immunity. *$TCID_{50}$: Median Tissue Culture Infectious Dose*b-d, Supplemental figure 13b-d). This suggests that viral loads including from mucosal shedding determine transmission likelihood in an i.m.-challenge model.

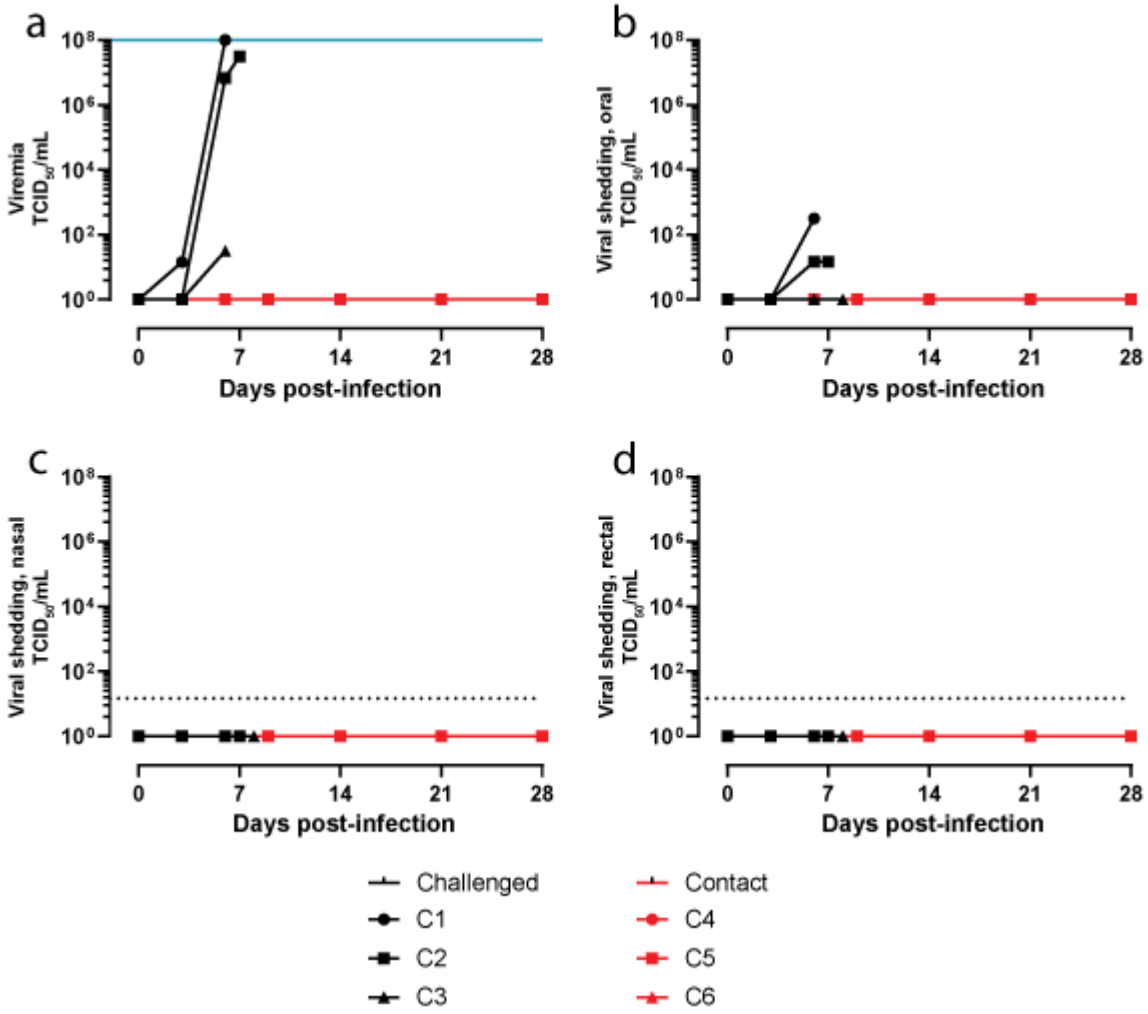

Figure 37: Viremia and shedding from challenged and contact NHPs in the context of i.m. delivery of EBOV-Makona in naïve animals.

Viral loads are measured by $TCID_{50}$/mL in **(a)** blood, **(b)** oral swabs, **(c)** nasal swabs, and **(d)** rectal swabs. The blue line represents a sample that was still positive at the upper limit of the assay. The dotted line represents values obtained for the transmitting animal in the initial i.m. challenge with animals exhibiting pre-existing immunity. *$TCID_{50}$: Median Tissue Culture Infectious Dose*

3.5.4 Intratracheal infection in NHPs leads to efficient transmission of EBOV-Makona.

To investigate lung involvement in the context of transmission, three naïve NHPs (D1, D2, and D3) were infected via the i.t. route with a target dose of 1000 x $TCID_{50}$. Following challenge, these animals were individually co-housed with a naïve NHP (D4, D5, and D6, respectively) to assess transmission. The challenged animals succumbed to infection 7, 8, and 7 dpi, respectively, and all three contact animals also succumbed to infection 16, 14, and 15 dpi, displaying a typical EVD clinical profile (Supplemental figure 14). Viremia in challenged animals at the time of death were all above the 1e8 $TCID_{50}$/mL limit of the assay (1.7e7 GEQ/mL), while peak oral, nasal, and rectal shedding averaged 1.1e3, 2.3E2 and 4.9e2 $TCID_{50}$/mL (6.7e2, 3.1e3, and 3.3e4 GEQ/mL), respectively. Interestingly, viremia from all transmitting animals of the i.t. experiment reached similar levels to that of the transmitting animal from the first i.m. experiment, while shedding was higher regarding the oral (D2), nasal (D3), or rectal (D1) routes (Figure 38, Supplemental figure 15). While PCR data were lower regarding shedding, live virus titration suggest that an i.t. challenge facilitated viral excretion through oral, nasal and rectal mucosae which potentially favored transmission in this context.

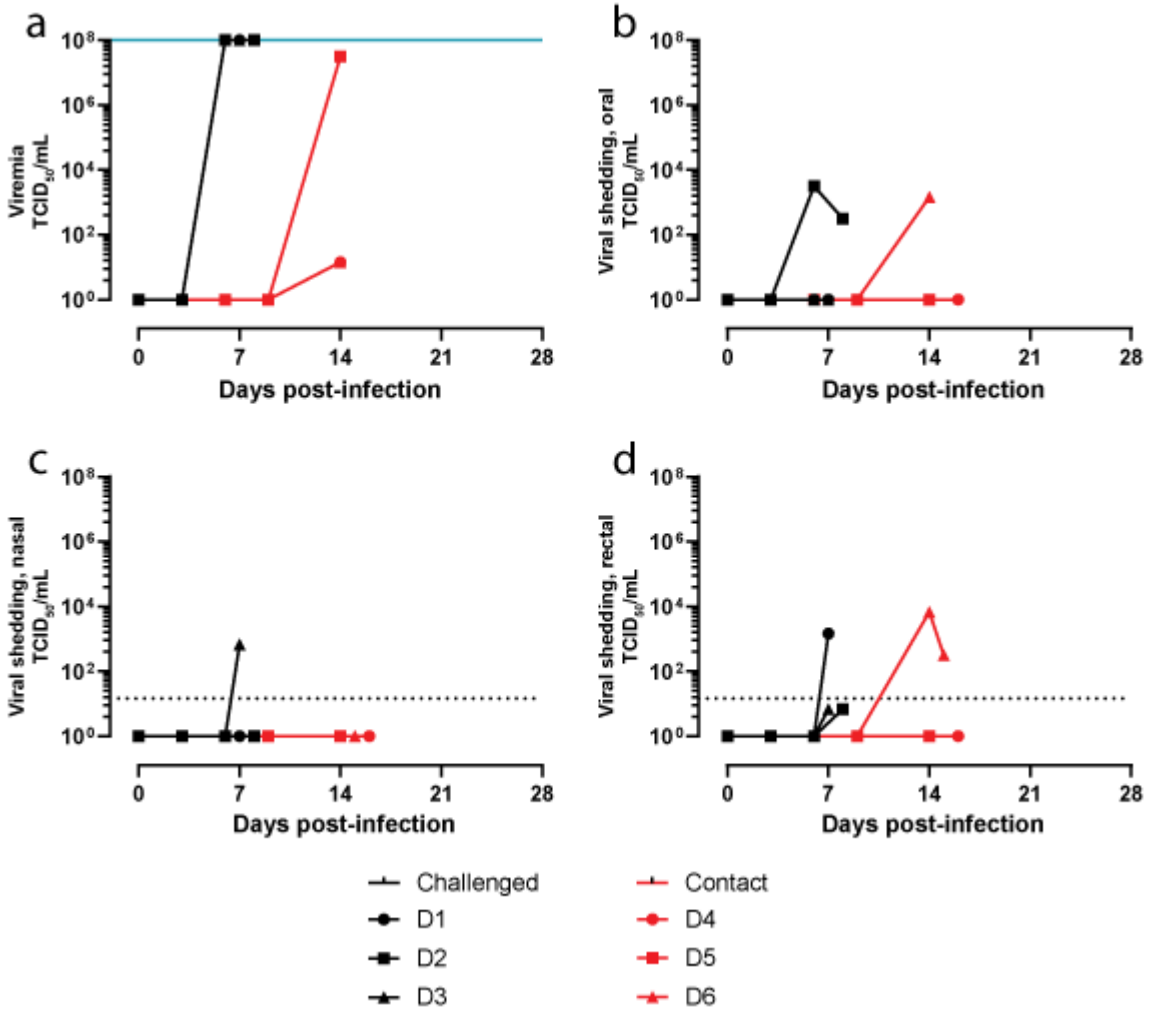

Figure 38: Viremia and shedding from challenged and contact NHPs in the context of i.t. delivery of EBOV-Makona in naïve animals.

Viral loads are measured by $TCID_{50}$/mL in **(a)** blood, **(b)** oral swabs, **(c)** nasal swabs, and **(d)** rectal swabs. The blue line represents a sample that was still positive at the upper limit of the assay. The dotted line represents values obtained for the transmitting animal in the initial i.m. challenge with animals exhibiting pre-existing immunity. *$TCID_{50}$: Median Tissue Culture Infectious Dose*

3.6 Discussion

The widespread and intense transmission seen in the 2013–2016 West African EBOV epidemic has been attributed to societal factors including poverty, close contact between densely populated urban areas, increased travel and community resistance due to fear, misinformation and mistrust of authorities; in addition to organizational factors including the lack of robust healthcare infrastructures and an initial underestimation of the outbreak. However, these factors have also existed to a certain degree in previous instances, and yet past outbreaks have been successfully managed within a comparative short timeframe of several months, with up to hundreds of cases and deaths. During the West African epidemic, health workers directly involved with care of

EBOV patients but without direct contact were oddly found to have also been infected, suggesting that either decontamination procedures were not strictly adhered to, or that certain factors resulted in opportunities for the virus to be transmitted. Here, we sought to better understand the nature of EBOV transmission, which could have impacted and contributed to the large magnitude of the West African EBOV epidemic. During the first few months, when it became obvious that virus spreading was out of control, many raised concerns regarding EBOV transmission resulting from eating or drinking from the same plate or glass as an ill family member. Here, we demonstrate that intraesophageal infection with EBOV is unlikely to result in disease or seroconversion, most likely due to the highly acidic content of the stomach, a chemical property which has been shown to inactivate EBOV[320]. This experiment did not however account for the possibility of viral entry through the buccal cavity, before the virus makes it to the stomach.

Previous work has shown that EBOV-Makona, isolate C05, is more virulent than EBOV-Kikwit in rhesus macaques, as evidenced by the higher viremia following an i.m. challenge. EBOV-Makona also demonstrated a higher affinity for the lungs, as shown by the enhanced lung pathology in some NHPs[276]. A previous study in guinea pigs has also shown that the length of exposure time to EBOV plays a bigger role than the exposure dose during successful EBOV transmission[211]. It will be interesting to investigate in NHPs whether the transmission of EBOV is possible without direct contact between the infected and naïve contact animals.

These results also demonstrate that subclinical infection with EBOV can be achieved with rhesus macaques in the laboratory, and that this phenomenon may be dependent on the route of infection. Indeed, results obtained in the first i.m. study have shown that even the contact animals were seropositive. This means that the infected animals were definitely exposed with live virus and may have shed low levels of virus which infected contact animals. Previous work by our group has shown, in the guinea pig and ferret models, that seroconversion, but not disease, can occur over short distances without direct contact in naïve animals. Interestingly, the high prevalence of asymptomatic infection with EBOV has been previously noted from a large-scale study in Gabon[289]. Of 4349 individuals from 220 randomly selected villages, 15.3% were found to be seropositive to EBOV by IgG ELISA, which raises the possibility that these people were possibly previously exposed to the virus via a route such as to the mucosa, which led to the production of antibodies but without severe clinical disease and death.

The results of this study show that the induced pre-existing antibodies were not always sufficient to protect against EBOV-Makona. Consistent with a past study, non-survivors of EVD demonstrated low levels of EBOV-specific IgG antibodies[230]. This again suggests that the quantity and possibly quality of the antibody response is an important factor in predicting survival from EVD.

The combination of societal, organizational and biological factors is likely to have contributed to the prolonged presence in West Africa. While the exact mechanisms behind virus transmission from infected to contact animals remain to be fully elucidated, the findings from these studies have substantial implications for EBOV outbreaks, as survivors of EVD, whether from fluid replenishment combined with other supportive therapies or an experimental treatment such as mAb114, REGN-EB3, or ZMapp, may still be susceptible to reinfection if the IgG antibody levels are suboptimal. Furthermore, the efficiency of the current vaccine used, rVSV-ZEBOV-GP, would benefit from being evaluated for cross-protection against other EBOV variants. Antibody levels in vaccine recipients need to be checked over time as well to ensure that immunity is sustained against EBOV. The in-depth characterization of EBOV-Makona will allow us to understand the differences between this novel, divergent virus and its phylogenetic cousins, as well as aid in the effective management and termination of future outbreaks.

3.7 Supplemental material

Supplemental table 23: Number of challenged and contact NHPs which tested positive by RT-PCR for Ebola virus in the blood, and by shedding through the oral, nasal and rectal cavities

(Left); number of NHPs which tested positive by ELISA for anti-EBOV IgM and IgG (Right).

	Viral loads				Antibodies	
	Blood	Oral	Nasal	Rectal	IgM	IgG
Challenged	0/3	0/3	0/3	0/3	0/3	0/3
Contact	0/3	0/3	0/3	0/3	0/3	0/3

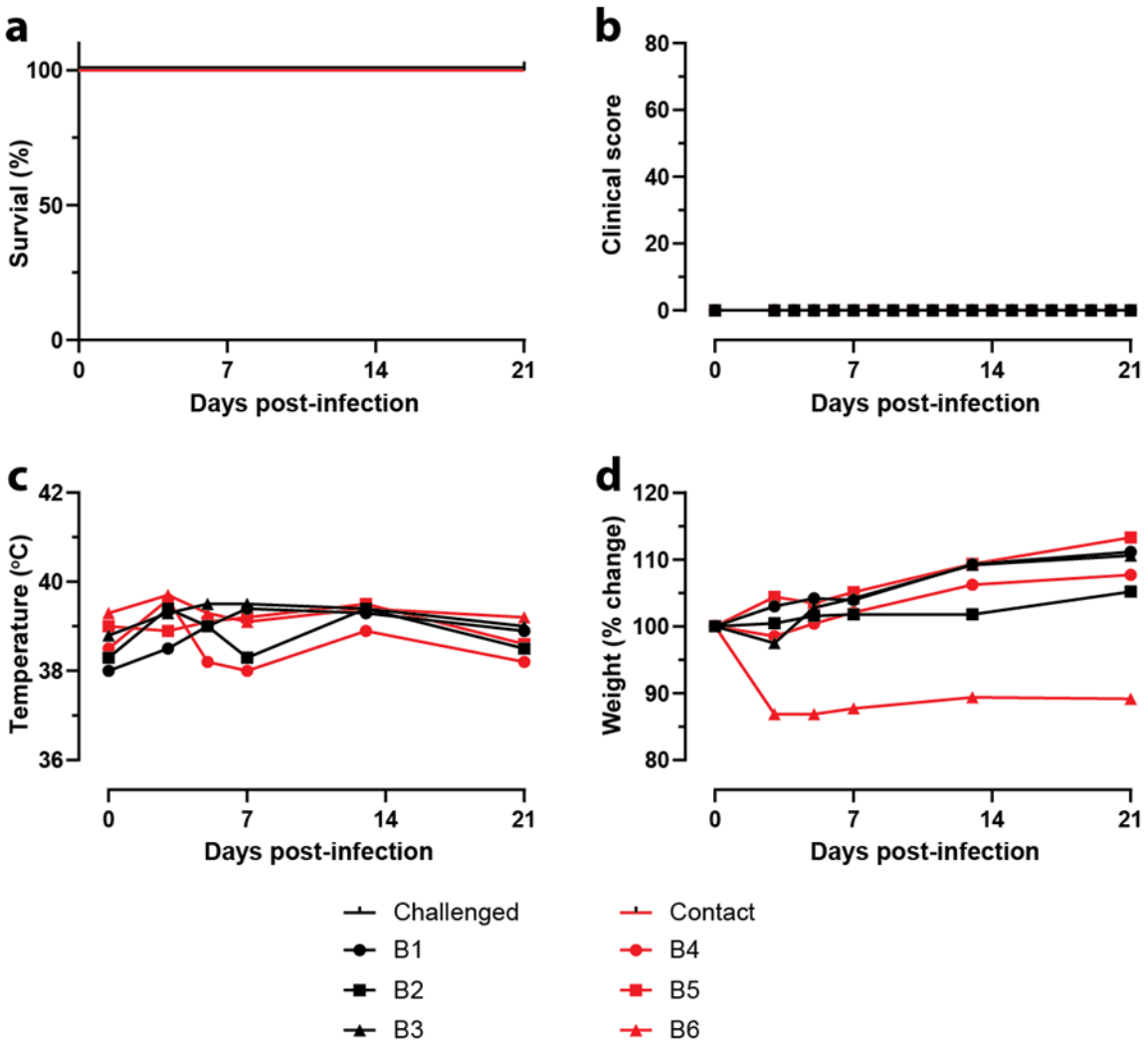

Supplemental figure 8: Survival and clinical parameters of challenged and contact NHPs in the context of aerosol delivery of EBOV-Makona.

(a) Survival. **(b)** Clinical score. **(c)** Temperature. **(d)** Body weight percent change.

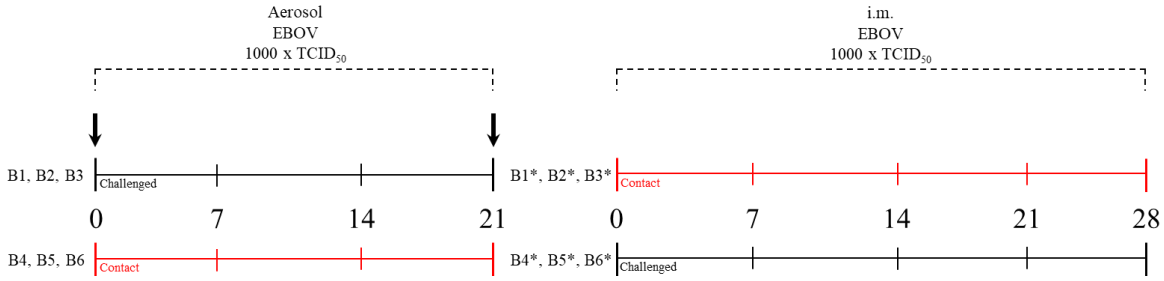

Supplemental figure 9:Timeline of infection for the aerosol and the first i.m. challenge study

Challenged animals from the aerosol experiment were recycled into contacts for the i.m. experiment, and where contact animals from the aerosol experiment were recycled into challenged animals for the i.m. experiment. For clarity purposes, an asterisk was added to the animal identification code when referring to the i.m. experiment.

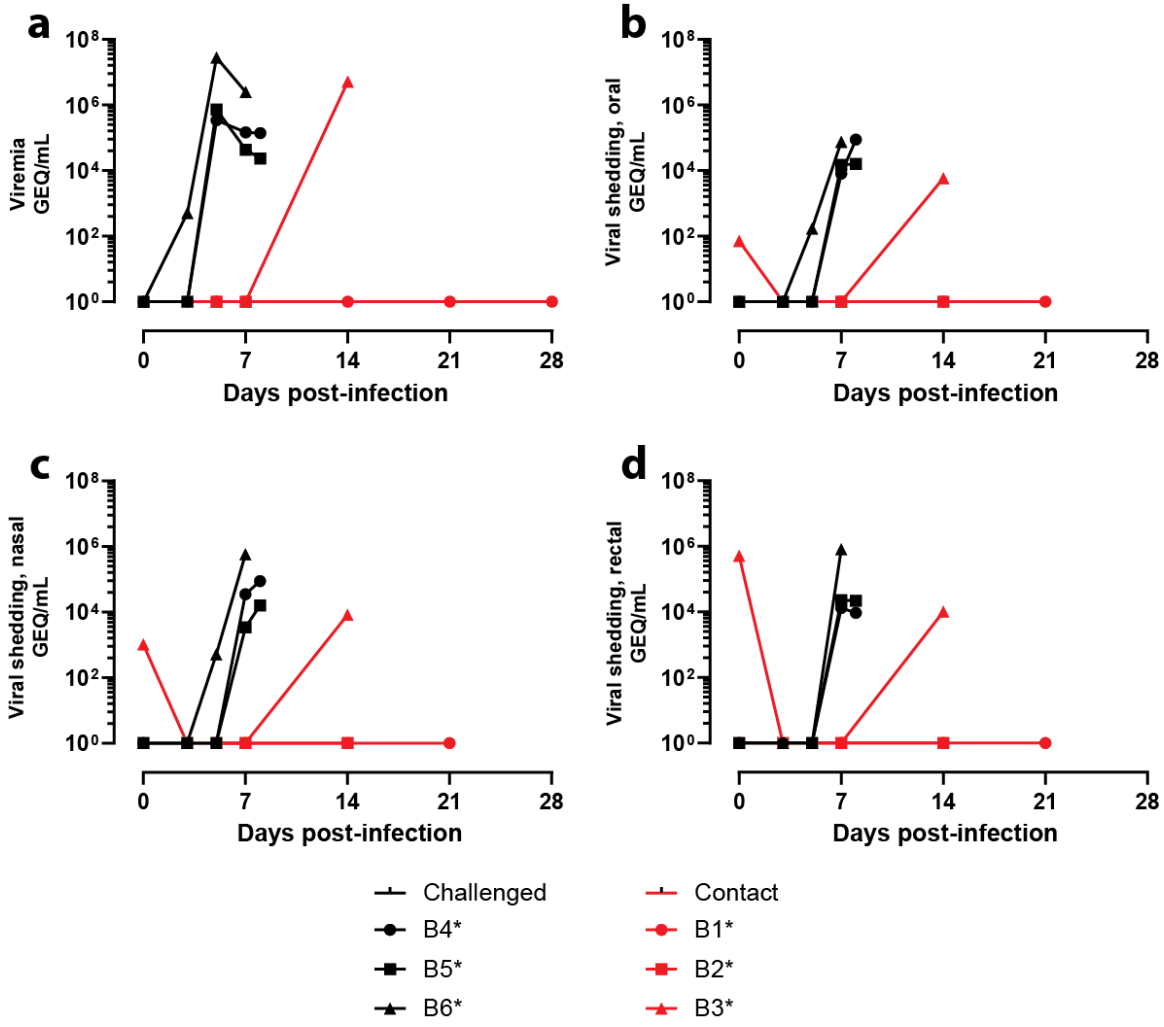

Supplemental figure 10: Viremia and shedding from challenged and contact NHPs in the context of i.m. delivery of EBOV-Makona in animals exhibiting pre-existing immunity.

Viral loads are measured by RT-qPCR in **(a)** blood, **(b)** oral swabs, **(c)** nasal swabs, and **(d)** rectal swabs.

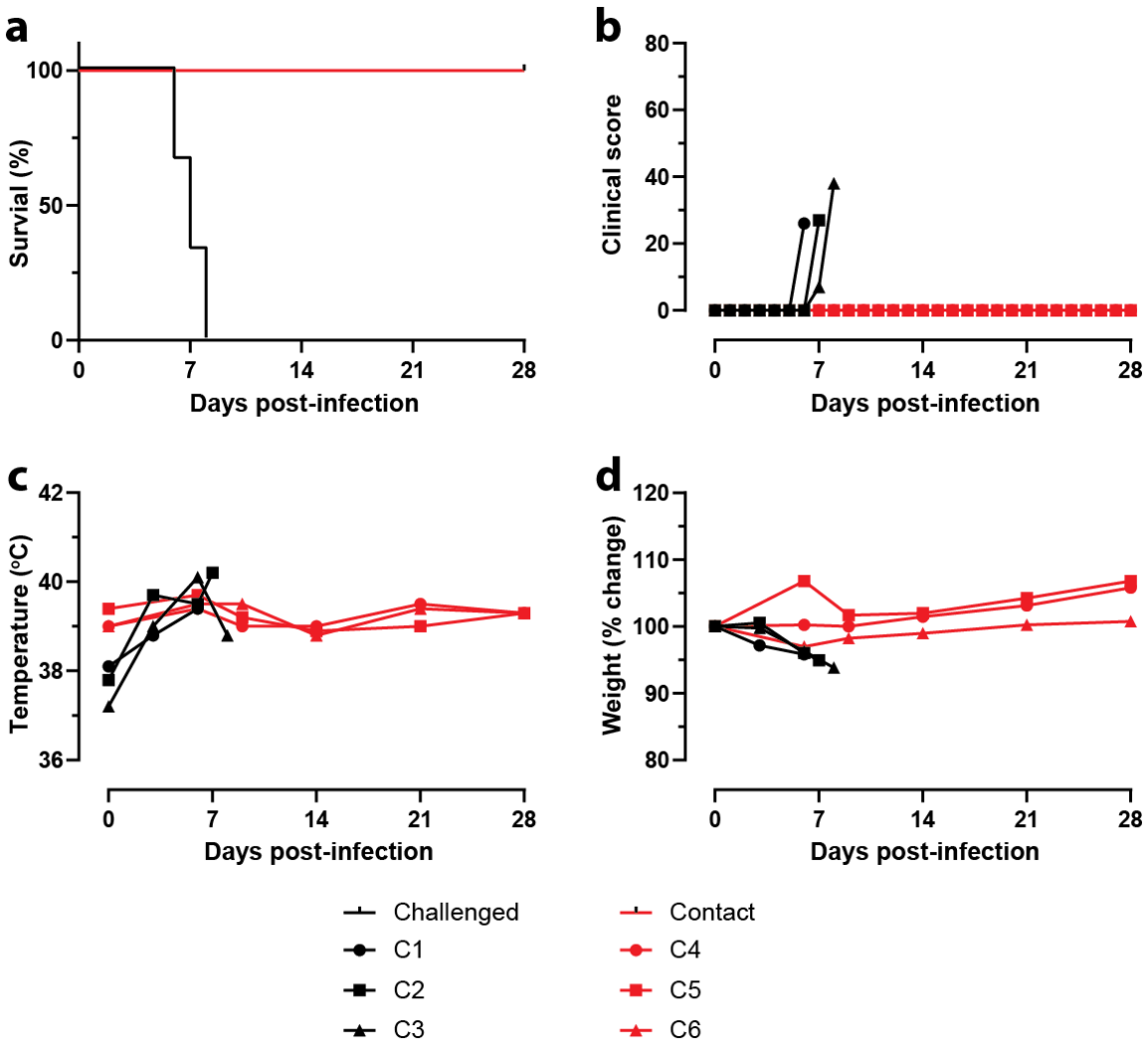

Supplemental figure 11: Survival and clinical parameters of challenged and contact NHPs in the context of i.m. delivery of EBOV-Makona in naïve animals.

(a) Survival. **(b)** Clinical score. **(c)** Temperature. **(d)** Body weight percent change.

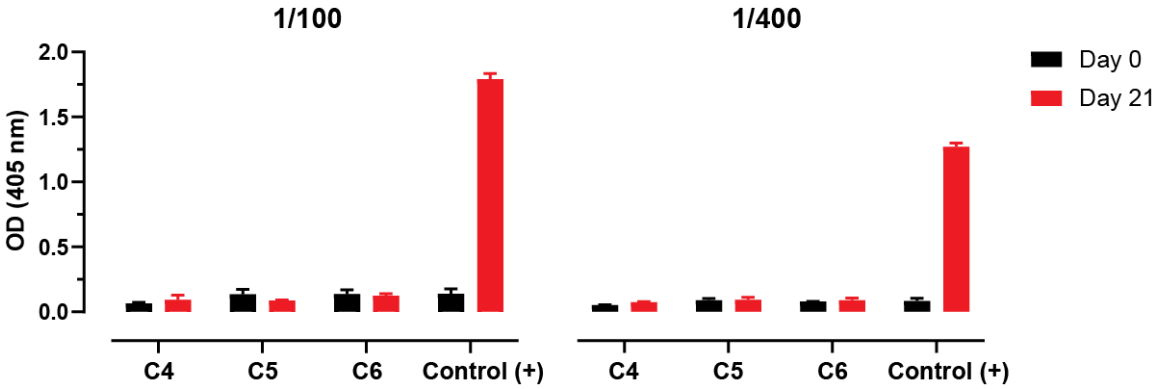

Supplemental figure 12: Humoral response of the three contact NHPs in the context of i.m. delivery of EBOV-Makona to challenged, naïve animals.

Optical density at 405 nm is shown for specific IgG antibodies against the glycoprotein of EBOV at Day 0 (pre-infection) and Day 21 (post-infection). Serum dilutions at 1/100 **(left panel)** and 1/400 **(right panel)** are shown.

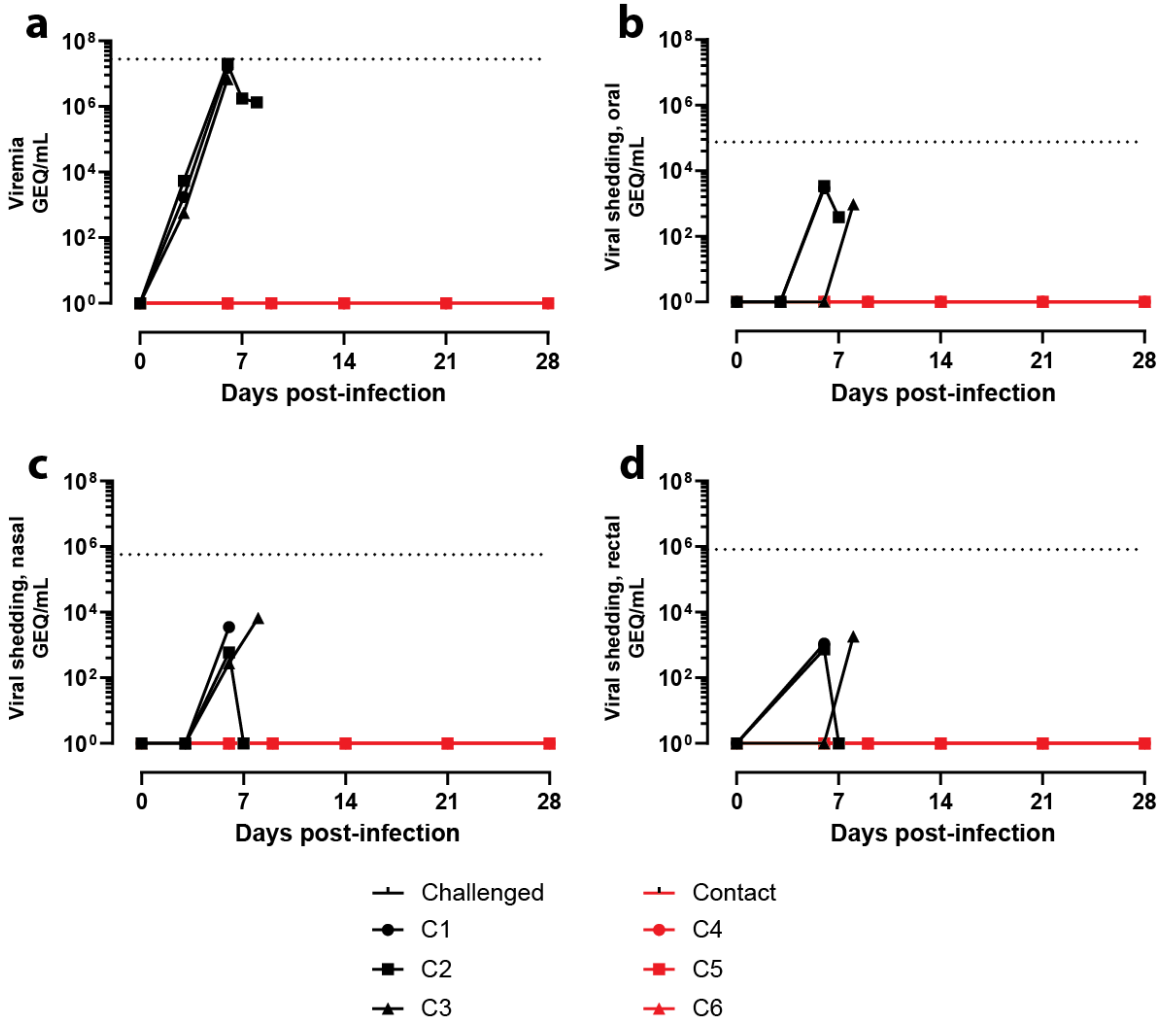

Supplemental figure 13: Viremia and shedding from challenged and contact NHPs in the context of i.m. delivery of EBOV-Makona in naïve animals.

Viral loads are measured by RT-qPCR in (a) blood, (b) oral swabs, (c) nasal swabs, and (d) rectal swabs. The dotted line represents values obtained for the transmitting animal in the initial i.m. challenge with animals exhibiting pre-existing immunity.

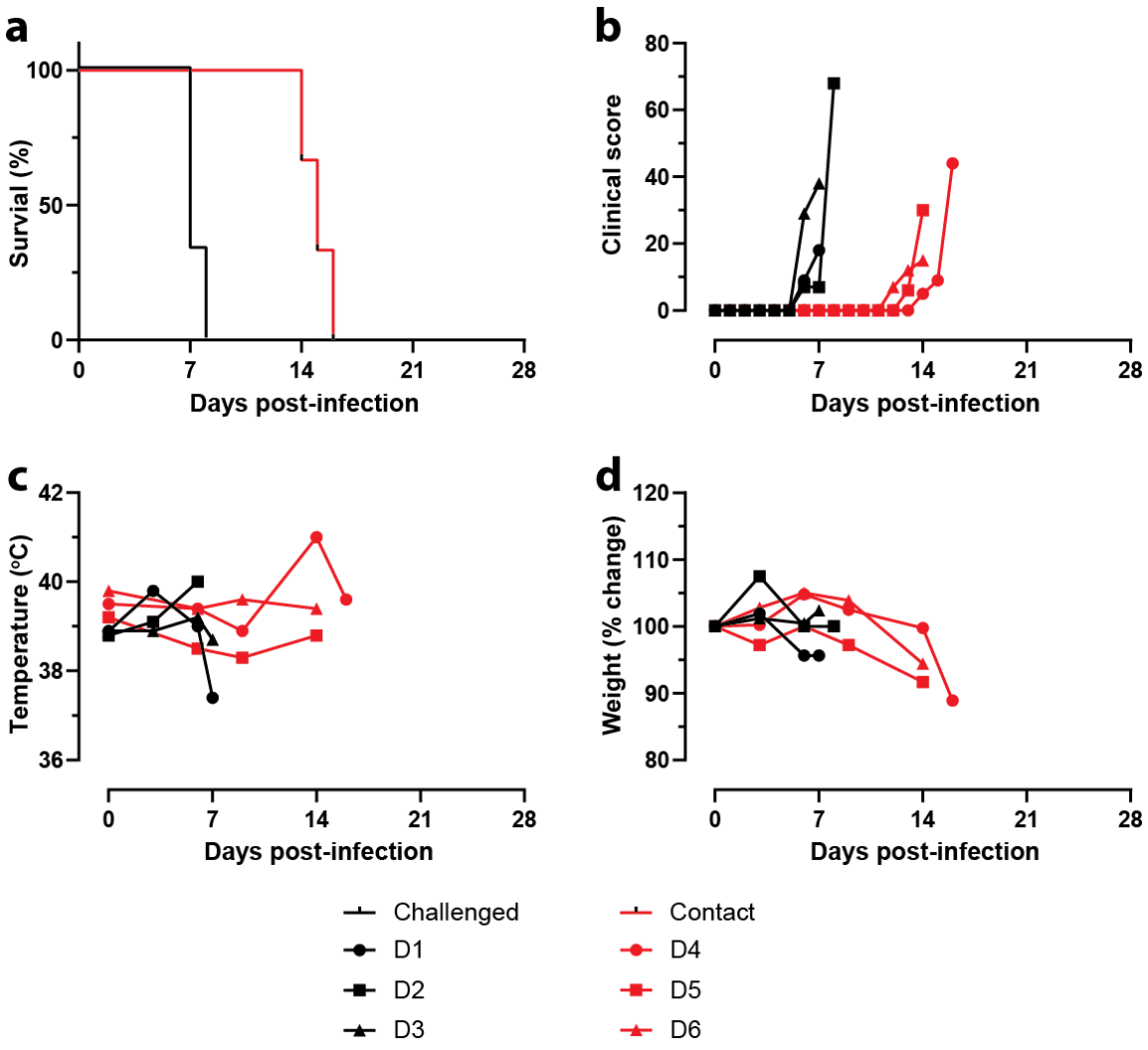

Supplemental figure 14: Survival and clinical parameters of challenged and contact NHPs in the context of i.t. delivery of EBOV-Makona in naïve animals.

(a) Survival. **(b)** Clinical score. **(c)** Temperature. **(d)** Body weight percent change.

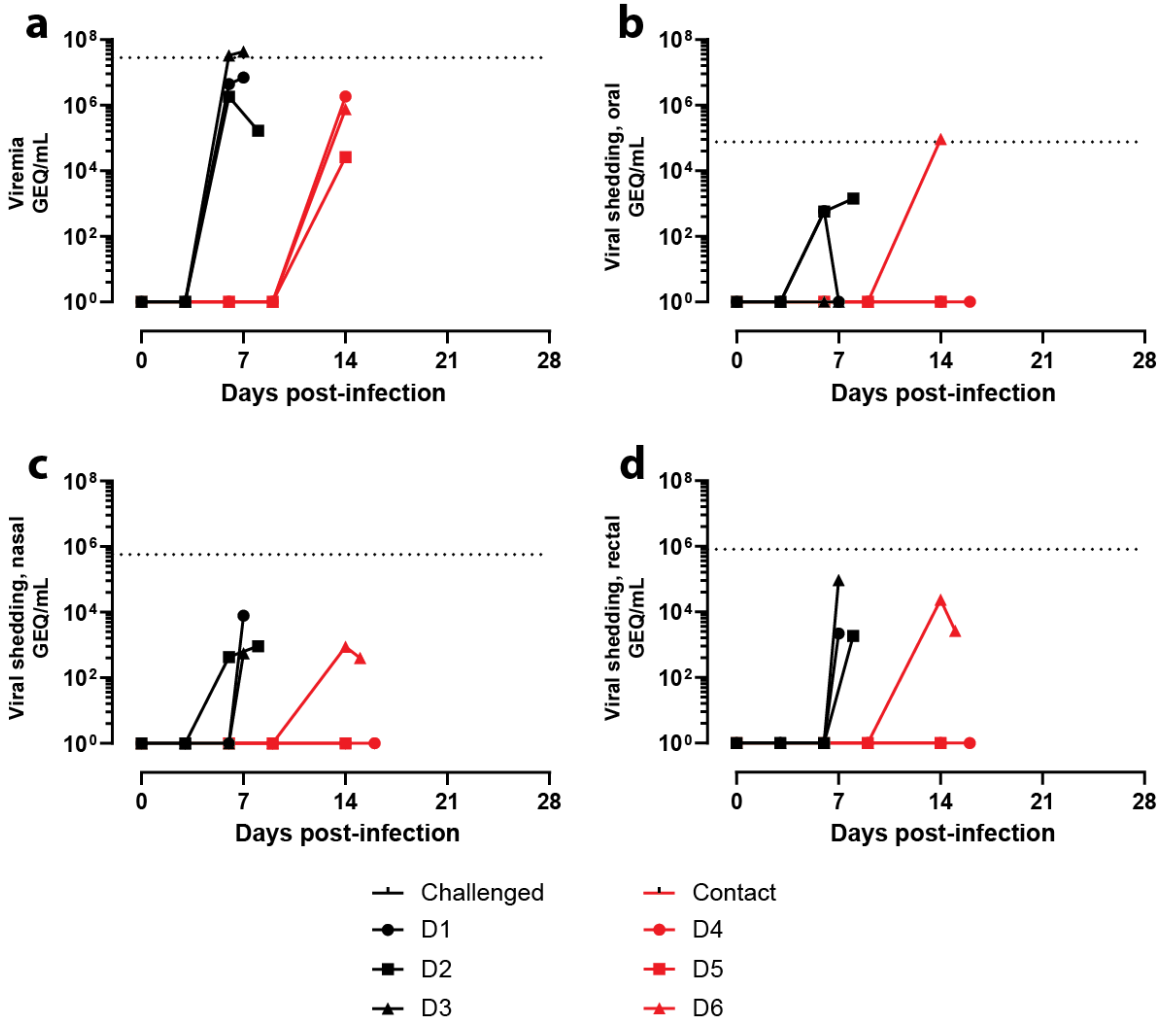

Supplemental figure 15: Viremia and shedding from challenged and contact NHPs in the context of i.m. delivery of EBOV-Makona in naïve animals.

Viral loads are measured by RT-qPCR in **(a)** blood, **(b)** oral swabs, **(c)** nasal swabs, and **(d)** rectal swabs. The dotted line represents values obtained for the transmitting animal in the initial i.m. challenge with animals exhibiting pre-existing immunity.

3.8 References

140. World Health Organization (WHO), 1978a: Ebola heamorrhagic fever in Zaire, 1976. *Bulletin of the World Health Organization*., **56**, 271–293.

171. Maganga, G. D. et al., 2014: Ebola Virus Disease in the Democratic Republic of Congo. *New England Journal of Medicine*., **371**, 2083–2091.

172. Baize, S. et al., 2014: Emergence of Zaire Ebola Virus Disease in Guinea - Preliminary Report. *The New England journal of medicine*., **371**, 1418–1425.

211. Wong, G. et al., 2015a: Ebola virus transmission in guinea pigs. *Journal of virology*., **89**, 1314–1323.

217. Kozak, R. et al., 2016: Ferrets infected with Bundibugyo virus or Ebola virus recapitulate important aspects of human filoviral disease. *Journal of Virology*., **90**, 9209–9223.

225. de La Vega, M.-A et al., 2018: Modeling Ebola Virus Transmission Using Ferrets. *mSphere*., **3**, 309–318.

230. Wong, G. et al., 2012: Immune parameters correlate with protection against ebola virus infection in rodents and nonhuman primates. *Science translational medicine*., **4**, 158ra146.

271. Vetter, P. et al., 2016: Ebola Virus Shedding and Transmission: Review of Current Evidence. *The Journal of Infectious Diseases*., **214**, S177–S184.

276. Wong, G. et al., 2016: Pathogenicity Comparison Between the Kikwit and Makona Ebola Virus Variants in Rhesus Macaques. *Journal of Infectious Diseases*., **214**, S281–S289.

142. Jacob, S. T. et al., 2020: Ebola virus disease. *Nature Reviews Disease Primers*. Springer US, Vol. 6.

289. Becquart, P. et al., 2010: High prevalence of both humoral and cellular immunity to Zaire ebolavirus among rural populations in Gabon. *PLoS ONE*., **5**, 1–9.

296. Jaax, N. K. et al., 1995: Transmission of Ebola virus (Zaire strain) to uninfected control monkeys in a biocontainment laboratory. The Lancet., **346**, 1669–1671.

297. Alimonti, J. B. et al., 2014: Evaluation of transmission risks associated with in vivo replication of several high containment pathogens in a biosafety level 4 laboratory. *Scientific reports*., **4**, 1–7.

299. Weingartl, H. M. et al., 2012: Transmission of Ebola virus from pigs to non-human primates. *Scientific reports*., **2**, 1–4.

309. World Health Organization (WHO). Ebola outbreak 2014-2015. 2018.

310. World Health Organization (WHO), 2017b: Ebola Virus Disease Democratic Republic of Congo: External Situation Report 1. *External Situation Report*., **1**, 1–6.

311. World Health Organization (WHO), 2018d: EBOLA VIRUS DISEASE Democratic Republic of Congo External Situation Report 1. *External Situation Report*., **1**, 1–6.

312. Adepoju, P., 2021: Ebola returns to Guinea and DR Congo. *The Lancet*., **397**, 781.

313. Mendoza, E. J. et al., 2016: Progression of Ebola Therapeutics During the 2014–2015 Outbreak. *Trends in Molecular Medicine*., **22**, 164–173.

314. Scott, J. T. et al., 2016: Post-Ebola Syndrome , Sierra Leone. *Emerging Infectious Diseases*., **22**, 641–646.

315. Carod-Artal, F. J., 2015: Post-Ebolavirus disease syndrome : what do we know ? Expert Review of Anti-infective Therapy., **13**, 1185–1187.

316. Lau, M. S. Y. et al., 2017: Spatial and temporal dynamics of superspreading events in the 2014–2015 West Africa Ebola epidemic. *Proceedings of the National Academy of Sciences*., **114**, 2337–2342.

317. Faye, O. et al., 2015: Chains of transmission and control of ebola virus disease in Conakry, Guniea, in 2014 : an observational study. *Lancet Infectious Diseases*., **15**, 320–326.

318. Wong, G. et al., 2015b: MERS, SARS, and Ebola: The Role of Super-Spreaders in Infectious Disease. *Cell host & microbe*., **18**, 398–401.

319. Nakayama, E. et al., 2013: Animal models for Ebola and Marburg virus infections. *Frontiers in microbiology*., **4**, 267.

320. Mitchell, S. W. et al., 1984: Physicochemical inactivation of Lassa, Ebola, and Marburg viruses and effect on clinical laboratory analyses. *J Clin Microbiol*., **20**, 486–489.

Conclusion

The work presented in this thesis is divided into three main sections. The first section shows that in a natural outbreak setting, the viremia of an individual upon admission at an EMC is statistically predictive of the outcome of this individual, regardless of whether it is death or survival. The second section established a ferret animal model for the study of WT-EBOV transmission, and indicates that transmission in the absence of direct contact with an infected animal is frequent, at least in this model. However, indirect transmission results in a less severe disease, with available evidence suggesting that the contact animals may have been exposed to a lower dose of virus. Finally, the third section of this thesis demonstrates that in non-human primates—the gold standard for the study of Ebola virus disease—viral loads as measured from oral, nasal, and rectal mucosae, but not from blood, are better associated with transmission in an intramuscular challenge, which is greatly facilitated in an intratracheal challenge where transmission was observed consistently. Below, the implications of each chapter will be summarized, study limitations will be further discussed, and their impact on future directions for the field will be further argued.

4.1 Association between viremia at admission and outcome in human patients.

As mentioned previously in this thesis, and until the 2014-2016 West African Ebola outbreak, EBOV had been responsible for localized and sporadic epidemics, where the number of cases never exceeded a few hundred. Therefore, the study of EVD in the context of human infection was problematic; patients were scarce and a period of up to 15 years could separate two different outbreaks. Furthermore, doctors and scientists were not able to benefit from the molecular and diagnostic tools available today. Due to the very nature of the Ebola virus, and the absence of any approved medical countermeasures for over 40 years, working with this virus outside the safety of modern, high containment facilities has been a challenge reserved to a handful of highly trained individuals around the world, including members of our group. Consequently, during the West African Ebola outbreak, our group was involved in assisting various organizations, including the WHO and MSF, with outbreak response in the field, specifically from a diagnostic standpoint. However, experts in EVD and outbreak management knew from very early on in the crisis that this was going to be unlike any outbreak they had seen before. Containing the spread of the virus proved to be more difficult than imagined, and hypotheses as to why this was the case have been numerous. Many behavioural and societal factors were postulated as potential explanations, such as the geographical location of the origin of the outbreak, increased travel and porous borders between Guinea, Sierra Leone, and Liberia, a slow response from the international community, a severe shortage of healthcare workers, weakened health infrastructures, community resistance, and more[294]. However, many of these factors were also present in previous outbreaks to some extent, leading some individuals to

suggest that this genetically distinct isolate could be more virulent and/or transmissible than those previously encountered.

As the first few teams were deployed to operate the diagnostic laboratory at the EMC in Kailahun, Sierra Leone, they began reporting an abnormally high number of individuals with elevated viremia, based on their personal experience with past outbreaks. Anecdotally, laboratory reports from a parallel outbreak close to Boende, DRC, indicated that viremia of patients upon admission were significantly lower than those in Sierra Leone, at least for the first two weeks of July 2014[321]. In order to assess whether this West African isolate was more virulent (from a field perspective as isolates for laboratory experiments were not readily available yet), our team investigated whether any association could be made between viremia of patients and their respective outcome, as an indirect measure of virulence. While this metric of outcome is by no mean an absolute measure of virulence, controlling for other variables such as sex, age, and time between onset of symptoms and admission to the EMC, allowed us to establish an association between viremia at admission and outcome, where individuals with a higher viremia were more likely to succumb to infection.

In order to better assess virulence, other parameters such as symptoms experienced by individuals with high- versus low viremia, as well as the presence or absence of co-morbidities or co-infections, would have allowed for a more accurate representation of the role of viremia in virulence of EBOV human infection–an additional limitation of the study to those already presented in Chapter 1. Similar reports to ours, which included such parameters, were however all directed towards answering questions with a more clinical value, namely predicting EVD severity so that limited resources in the field can be better allocated[322–324]. Therefore, analysis of viremia is rarely evaluated directly against clinical manifestations, but rather against outcome. Nevertheless, one study did specifically assess the relationship between viremia and biomarkers associated with organ damage in human infection by EBOV[325]. Indeed, their results provided strong evidence of an association between viremia and levels of alanine transaminase (ALT), aspartate transaminase (AST), lactate dehydrogenase (LDH), creatine phosphokinase (CPK), activated prothrombin time (aPTT), as well as the international normalized ratio (INR), supporting a role for high viremia in increased liver damage, skeletal muscle tissue damage, as well as coagulation defects.

As mentioned above, multiple hypotheses were proposed in an attempt to explain the uncontrollable nature of the 2014-2016 West African outbreak, one of them being that this isolate could be more transmissible than previous ones. Transmission of a pathogen is a fairly broad concept and depends on a multitude of factors related to the pathogen itself, such as its ability to survive outside a host for prolonged periods of time, its ability to be shed before clinical manifestations are apparent (*i.e.,* asymptomatic shedding), its infectious dose, and its ability to replicate to high levels. Host factors such as co-infections, behaviour (*e.g.*, crowding and cultural practices), genetics, and immune status also need to be accounted for. Finally, environmental factors such as

humidity, temperature, and poor health care are also to be considered for the transmission of certain pathogens[326]. Therefore, although we had already established an association between high viremia and outcome, whether this elevated viremia also associated with transmission remained to be evaluated. Indeed, the term *superspreading* was used abundantly during the West African outbreak, and denotes a single individual that accounts for numerous secondary cases[316,317,327]. Again, although a multitude of behavioural and societal factors can account for superspreading events, we hypothesized that a viral component could also be at play. These *superspreaders* could represent individuals in which bodily fluids contain an increased amount of virus, over those of *non-superspreaders*, thereby facilitating sustained transmission of the virus[276].

Another finding of interest from the results presented in Chapter 1 concerns the detection of EBOV-specific antibodies in individuals who tested negative for EVD. Whether these individuals experienced an asymptomatic or symptomatic infection due to EBOV before presentation to the EMC is unknown. Asymptomatic infections with EBOV have been previously described in two outbreaks from Gabon in 1996[291,306], although convincing data for how frequently this occurs in a given outbreak is still limited. As reviewed by Bower and Glynn, multiple serosurveys have described the presence of EBOV-specific antibodies in individuals that either experienced no symptoms throughout the course of an epidemic, or that reside in countries that never experienced a reported EVD outbreak at all[303]. However, the differences between these serosurveys regarding the type and cut-off values of the assay used, the description of the level of exposure to known cases of EVD, and the availability of data regarding the presence or absence of symptoms in these individuals varied greatly and clear conclusions are hard to draw until standardized protocols are used. The results presented in this thesis as part of Chapter 1 are no exception to these limitations, as clinical manifestations related to EVD of assayed individuals were unclear before presentation at the EMC. Overall, work performed by Leroy *et al.* during the two outbreaks in Gabon suggested that these asymptomatic individuals were infected by EBOV at low dose and over several days, a hypothesis that is nearly impossible to demonstrate in a field setting as these individuals were exposed naturally; the exact dose these individuals were exposed to, through which route they were exposed, and how many times an exposure event that resulted in contact occurred, cannot be guaranteed.

Taken together, the data discussed throughout Chapter 1 indicate that viremia at admission is statistically predictive of outcome in humans, an indirect measure of disease severity. However, determining whether these high viral loads translate into increased transmission was beyond the scope of this first study, hence the necessity of a reliable animal model for transmission of EBOV. Furthermore, the experimental model needed to support the suggestion by Leroy *et al.* that asymptomatic individuals are made possible through low and repeated exposure to EBOV, was evaluated in Chapter 2.

4.2 Establishment of a ferret model for transmission of EBOV, with or without direct contact.

The use of animal models in science is a controversial topic for many. However, it is often necessary for multiple reasons, some of which have already been introduced above. Indeed, scarcity of humans infected with EBOV would considerably slow down our understanding of the disease if we could not rely on laboratory experiments involving animals. Analysis of biochemical and immune parameters associated with the disease can be studied from human samples, but often represents a logistical challenge as outbreaks of EVD usually occur in remote areas of rural Africa, where access to specialized equipment can be challenging. The logistics behind moving samples from an outbreak site to specialized facilities has, however, drastically improved over the years, without compromising the integrity of samples. The nature of outbreak response also does not always allow for answering every valid research question a doctor or scientist might have, as the primary goals remain outbreak control and the care of patients; research protocols, if any, need to be able to insert themselves among the essential activities surrounding outbreak management. For example, samples routinely collected for diagnostic purposes, often venous blood only, might not be sufficient to fully answer specific research questions. As mentioned previously, it is also nearly impossible to study the effect of multiple variables involved in infection such as the viral inoculum and route through which an individual contracts EVD, as the exact context surrounding infection of an individual are usually not known. Finally, the evaluation of medical countermeasures such as prophylactic and therapeutic options cannot ethically be performed on humans due to the high mortality and morbidity incurred by infection with EBOV. Therefore, the development of models that reproduce human infection as accurately as possible is essential to further our understanding of the disease.

The current models available for the study of EBOV transmission are limited to two main animal species, namely the guinea pig and the non-human primate[211,299]. The guinea pig model is the smallest, and only, rodent model that allows for the evaluation of transmission of EBOV. However, this model requires adaptation of the virus, as guinea pigs are not naturally susceptible to infection by clinical isolates. This process of adaptation is slow and can be inconvenient when timely evaluation of pathogenesis and medical countermeasures against a novel and unknown isolate is necessary, as was the case during the West African Ebola outbreak. Additionally, adaption of the virus generates mutations, thereby introducing further biases towards the naturally occurring isolate. On the other hand, non-human primates are susceptible to clinical isolates and accurately models human EVD—two reasons why NHPs are the gold standard for the study of human EVD. However, the cost of NHPs, the ethical considerations, and larger animal size means that fewer animals can be handled at once in high containment facilities. Therefore, an intermediate species that would combine the advantages of both models would greatly facilitate our understanding of transmission.

In Chapter 2, a novel, small animal model for Ebola virus transmission is described. This species, the ferret, has previously been shown to be susceptible to infection by clinical isolates without the need for virus adaptation. Additionally, its smaller size when compared to NHPs should allow for larger-scale experiments in high containment laboratories, although ferrets do still require more space and resources than mice, for example. The caging system used for this experiment allowed for the simultaneous evaluation of direct, and indirect contact transmission; however, it did not have the ability to discriminate between droplet and aerosol transmission. As expected, all male and female challenged animals succumbed to EVD within an average of 6 days, consistent with was has previously been reported for this model[217,328].

Interestingly, while all male, direct contact animals succumbed to infection following transmission from their respective infected cagemate, none of their female counterparts displayed clinical signs of disease, had detectable viremia, or were found to shed virus. Importantly, male direct contact animals succumbed to the disease 10 or 11 days after the beginning of the experiment, suggesting that they were infected by their terminally ill cagemates, based on the known disease progression in this model. This is in accordance with field reports indicating that the unsafe handling of deceased individuals is a risk factor for contracting EVD[191], where more intense or prolonged contact with the corpse has been suggested to be associated with a high CFR[329]. These observations are also consistent with published data indicating that in ferrets infected with either EBOV or SUDV, peak shedding of infectious virus can be detected from various mucosae 1 or 2 days preceding death of the animal[216,217]. As such, we sought to investigate whether viremia or viral shedding from mucosae associates with transmission in this model, as discussed above.

It is important to note that one male indirect contact animal, but again no females, succumbed to EVD 9 days after its direct contact counterpart succumbed to the disease and was removed from the caging system. This could suggest that this male indirect contact was infected with a very low dose of virus that prolonged disease progression and therefore time to death. This hypothesis could be supported by recent data from Brasel *et al.* where a low-dose oral challenge resulted in similar results for 1 out of 4 animals; pair-housed ferrets were challenged orally with a target dose of 1 PFU but one animal from a pair succumbed on day 10 post-infection, rather than day 6 like the remaining ferrets. Whether this was due to the low dose of the challenge, or a delayed transmission event from its cagemate could not be determined, indicating that future studies should focus on single housing in order to prevent ambiguous results[328]. In a similar fashion, a previous study demonstrated that an intramuscular low-dose challenge in ferrets usually does not result in delayed time to death, meaning that there does not seem to be a dose-response to EBOV challenge in this model; either the animal succumbs to EVD or it survives challenge unscathed[222]. Unfortunately, the latter study did not evaluate viral loads of challenged ferrets and although it reported that animals challenged with the lowest dose (0.01 PFU) remained symptom-free, the experiment did not extend past 15 days. Whether animals exhibited a low level of viral

replication, developed an immune response following exposure to these lower doses, or would have succumbed to EVD at a later timepoint like the indirect contact animal described in Chapter 2, is unclear. It is worth mentioning that in humans, who are genetically heterogenous similarly to laboratory ferrets, the incubation period of the virus varies between 2 to 21 days. Therefore, it is possible that the male indirect contact animal from the study described in Chapter 2 required an extended period of time to develop EVD. Another hypothesis regarding the delayed time to death of the male indirect contact could be that this animal was infected through fomites present in the caging system after removal of its cagemates following their euthanasia, as viral RNA was successfully detected in the cage of another male indirect contact. Furthermore, experimental data regarding environmental persistence of EBOV-Makona has shown that a four-log reduction in infectious titers (99.99%) could take up to 365 hours, or about 15 days, on stainless steel, the same material that the caging system was made of[190]. However, detection of both IgM and IgG at day 12 post-infection in our male indirect contact ferret suggest an earlier infection, as well as highlighting the fact that the quality of the immune response is important for protection given that this animal still succumbed to infection.

One hypothesis that would fit the current data would be that this animal was, indeed, infected at an earlier timepoint, possibly at a comparable time as its male direct contact counterpart due to similar humoral responses in both animals, but that viral replication occurred either at levels below the detection limit in blood, or within immunoprivileged sites, ultimately leading to clinical disease and death following a relapse. Indeed, no viral RNA could be detected from this animal at 7-, 9-, and 12 days post-infection. This relapse phenomenon has previously been observed in humans, when a nurse from Scotland who contracted EVD in Sierra Leone during the West African outbreak developed meningitis 9 months after recovery from her initial infection, and infectious EBOV was successfully isolated from her cerebrospinal fluid, but not from blood[330,331]. Unfortunately, whether our male ferret exhibited viral replication within immunoprivileged sites such as testes or the central nervous system was not evaluated. A retrospective study conducted on survivors from Guinea also reported that survivors of an initial infection were five-times more likely of succumbing to complications within the following year, usually attributed to kidney failure although cause of death could not be confirmed for the majority of cases[332]. However, whether these individuals were shedding virus at the time of death, as the presence of viral RNA in nasal washes, oral swabs, and rectal swabs suggest in our ferret, could not be evaluated. However, given the short duration of our study, a true relapse phenomenon like it has been observed in humans, may not accurately represent what happened to our indirect male ferret. The presence of specific antibodies against EBOV does suggest an early infection around days 5 or 6 post-initiation of the experiment, most likely resulting in an asymptomatic infection, where RNAemia was undetectable. Viral replication may have occurred to low levels in either macrophages, monocytes, or DCs, which may have turned systemic around day 14, leading to clinical EVD and death on day 19.

Interestingly, viremia and viral loads as a result of shedding in challenged animals were comparable between males and females, suggesting that additional factors may explain why males, but not females, initiated transmission that led to clinical disease in contact animals. The sexual dimorphism of this animal, which has been reported to display sex-biased health-related issues, may partially account for these differences[333], as it has been described for other diseases in humans [334]. Overall, regarding RNAemia and shedding, peak viral load was observed at the time of euthanasia, which is consistent with what is observed from other animal models and humans. When coupled with the time to death and the known disease progression in this model, at least for male ferrets, transmission events did correlate with these elevated viral loads.

Additionally, behavioural differences between the two sexes such as a potential increase in biting and scratching among males might have led to an increased exposure to infected bodily fluids, a known transmission risk factor for EVD. Finally, a recent report by Francis *et al.* made available on the *bioRxiv* preprint server, shows that in the context of SARS-CoV-2 infection in ferrets, male animals exhibit longer shedding of infectious virus as measured in nasal washes when compared to female animals. This experiment was based on the rationale that demographic analyses across multiple countries indicated that men infected with SARS-CoV-2 suffered from an increased severity of disease and mortality compared to women. The study by Francis and colleagues also reports that female ferrets displayed an earlier antiviral response, as characterized by an upregulation in interferon and antiviral genes, which most likely contributed to the control of viral loads[335]. However, in an independent influenza-challenge study, no apparent clinical differences between male and female ferrets were observed[336]. It is important to note that in the context of human EBOV infection there are no apparent biological differences between males and females; differences, if any, are rather attributed to the nature of exposure as women more often attend to the ill, while men have historically been more often exposed through other activities such as hunting and caring for livestock[308]. Therefore, in the context of Chapter 2, whether female animals developed a stronger and/or faster immune response that could have controlled viral replication and limited transmission of infectious virus in a capacity that could have induced clinical disease in contact animals warrants further investigation. One important limitation of the study presented in Chapter 2 is that, due to time constraints, live virus titration of samples could not be performed, hence the levels of infectious particles shed by the animals could not be evaluated. Given the mucosal nature of the challenge, it will be worth investigating whether Further studies with this model will need to be performed in order to determine whether results obtained by PCR are reflected by live virus titration.

Of note, all six indirect contact animals exhibited IgM and IgG responses by the end of the experiment, despite five of them surviving, exhibiting no symptoms, and where virus could not be detected in their blood at any sampling days. The absence of viral RNA in the blood of asymptomatic individuals was also noted by Leroy *et al.*, although they extended their studies by analyzing circulating white blood cells for the presence of viral RNA,

as monocytes and macrophages are readily infected and support viral replication at the beginning of infection. The use of nested PCR in their study suggested that viral loads were very low, as evidenced by the lack of detectable viral antigens in the blood. They also reported the detection of positive-stranded viral RNA, a clear indication that replication took place as EBOV is a negative-sense RNA virus[291]. Whether indirect contact animals in our study actually supported a low level of viral replication, or were otherwise exposed to non-infectious virus, warrants further investigation.

Taken together, the results presented in Chapter 2 of this thesis established the ferret as novel, small animal model for transmission of Ebola virus. While direct transmission was consistently observed from male challenged to male direct contact animals, these transmission events could not be observed from female challenged to female direct contact animals, despite both sexes exhibiting similar levels of viral RNA in both the blood and various mucosae. However, transmission in males was associated with high RNAemia and shedding from challenged animals, when the disease progression in this model is factored in. Further studies should aim at assessing whether differences exist in the levels of infectious virus truly exist, as this characteristic is essential to initiate an active infection. Additionally, a deeper analysis of immune responses to EBOV infection in both sexes, such as that performed by Francis *et al.* in the context of SARS-CoV-2 infection, could shed light on biological differences during infection in this model. Finally, our study has shown that indirect contact transmission is less efficient than direct contact in inducing EVD, as clinical disease and death occurred in 1 animal out of 6. This is despite the fact that exposure of the indirect contact animal was frequent, as seroconversion of all animals was observed. Further work should focus on assessing if infectious particles were responsible for the development of this humoral response, or if it was due to mere antigenic stimulation from non-infectious particles present in the environment of the animals.

4.3 Impact of the route of infection and viral loads as a result of shedding in a non-human primate model of EBOV transmission

Previous work in guinea pigs has shown that in this model, transmission of EBOV from an infected to a naïve animal was more efficient when the transmitting animal had been infected intranasally, rather than intraperitoneally[211]. Potential explanations as to why that could be include the observation that i.n.-infected animals were found to shed higher amounts of virus within their nasal cavity, when compared to i.p.-infected animals three days after infection. Interestingly, i.p.-infected animals were found to shed similar or higher levels of virus through the oral, nasal, and rectal route at every other single time point until euthanasia of the animals. While the lungs of i.p.-challenged animals displayed little-to-no pathology, those of i.n.-challenged guinea pigs exhibited signs of severe pneumonia and inflammation. Necropsies of animals combined with

immunohistochemistry analysis also revealed the presence of viral antigens in the tracheal epithelium and submucosa of i.n-infected animals, whereas for i.p.-infected guinea pigs, viral antigens were localized to the submucosa only. This suggests that the route of infection may result in differences regarding availability of potentially infectious particles that can be released from an infected animal to a susceptible host.

While data on experimental transmission of Ebola virus in guinea pig and ferret models is limited, available evidence on transmission of this virus in non-human primates is conflicting. Indeed, one report has suggested that infection of a rhesus macaque with EBOV (isolate Mayinga) led to transmission to a naïve animal in the absence of contact, while a more recent study did not observe transmission of EBOV (isolate Kikwit) from infected rhesus to cynomolgus macaques, again in the absence of direct contact[296,297]. Of note, both of these studies were limited to intramuscular challenges. Building on the transmission work performed in guinea pigs and described previously in this thesis, the role of the route of infection was further evaluated in non-human primates, the current animal gold standard for the study of EVD. The role of viremia and viral loads as a result of shedding was also thoroughly defined in the context of transmission.

Community transmission is a huge driver of EBOV transmission during an outbreak, which is especially true at home, where multiple generations of a same family often reside together. As discussed previously, overcrowding and close proximity with a large number of individuals represents an environmental risk factor, which can facilitate the rapid spread of a disease such as EVD. In this context, concerns were raised during the West African Ebola outbreak regarding the risk of infection resulting from eating or drinking from the same plate or glass as a family member who is currently infected with EBOV. As such, we sought to investigate the transmission potential of EBOV following intraesophageal infection. Not only did infected animals fail to transmit the virus, they also failed to develop clinical EVD, become viremic, or seroconvert, suggesting that this route of infection does not facilitate infection by EBOV in macaques. While this is not surprising given the acidic content of the stomach, a chemical property known to inactivate this virus[320], one limitation of that study is that it did not fully model the real-life scenario discussed above as it did not account for viral entry through the buccal cavity. As it is often the case with any Ebola virus-associated studies, oral challenge data in NHPs is scarce, as results from only seven animals are available. The first study assessed whether infection of four rhesus macaques with 158 000 PFUs of EBOV (isolate Mayinga) via the oral route resulted in infection. Surprisingly, lethality in this experiment was not uniform as one animal did survive challenge[337]. More recently, infection of two cynomolgus macaques with 10 PFUs of EBOV (isolate Makona) did not result in clinical illness or viremia, although one animal slightly seroconverted as revealed by the presence of EBOV-specific IgG. Subsequently, infection of an additional animal in the same conditions, but with a dose of 100 PFU, did result in full-blown EVD. The most interesting aspect of this animal is that although symptoms of EVD were first noted on day 7 post-infection, high viremia was detectable by day 5. As discussed above, asymptomatic shedding is a factor we previously

highlighted as playing an important role in person-to-person transmission of a pathogen, but the dogma in the field of filoviruses is that infected individuals are not infectious until they start to show symptoms. However, this study did not mention if oral, nasal, or rectal shedding was present in this animal[307]. It will be interesting to evaluate this route of infection with a larger number of animals, and to assess whether viral loads as a result of shedding make this model suitable for transmission of EBOV to naïve animals. As this route of infection is likely encountered more often than an intramuscular injection in a natural setting, there might be important implications for outbreak control and limiting transmission of the virus at a community level, if this route of infection is confirmed to result in shedding of infectious virus, before symptoms become apparent.

Next, the role of facial aerosol to the face as a potential route of infection for initiating transmission was investigated, in order to mimic droplet exposure. Similar to the intraesophageal challenge above, available evidence suggest that this route may not be suitable for delivering virus to a target host, as none of the exposed animals exhibited clinical signs of disease, became viremic, or succumbed to infection. One important limitation of this study is that at the time of the experiment, the infectious potential of the inoculum used to spray the animals with was not evaluated. Therefore, the possibility that the aerosolization process may have inactivated the virus cannot be ruled out at this time. However, it is worth highlighting that both challenged and contact NHPs seroconverted, as shown by the presence of IgM and/or IgG. Interestingly, the detection of humoral responses occurred at similar timepoints for both experimental groups, as early as day 3 post-infection of challenged animals, suggesting that contact animals were exposed to EBOV around the same time period as the challenged NHPs. Regardless, the inability of this method to induce clinical EVD and generate a replicative infection made the evaluation of transmission difficult.

Therefore, other routes of infection needed to be evaluated. Building on the existing experiments where transmission of EBOV was assessed between non-human primates in the context of intramuscular infection, we sought to further investigate the potential of intramuscular challenge in inducing transmission, but this time as a result of direct contact. Indeed, both existing studies with conflicting results that have been mentioned above reported that animals did not have the possibility of interacting with each other. In the context of the experiments presented in Chapter 3, the decision was made to re-use all six animals from the facial exposure challenge, despite some levels of pre-existing immunity. As previously mentioned, antibody levels against the surface glycoprotein of EBOV were found to correlate with protection[230], but others have revealed the importance of the quality of those antibodies[338]. Given that animals were challenged intramuscularly 21 days following facial exposure, it is expected that their immune responses are not fully mature, and therefore would likely not be protected from a subsequent lethal challenge. In order to maximize the development of clinical EVD and viral replication, the decision was also made to swap the experimental groups, *i.e.,* animals initially challenged by facial exposure became contact animals, and vice-versa.

All challenged animals succumbed to infection within 7 to 8 days, and two of the three contact animals also succumbed during the course of the experiment. However, one of these two contact animals did not show any clinical signs of disease and was not found to be viremic. Its death was attributed to an unknown cause, possibly due to an adverse reaction to anesthesia. The other contact animal that succumbed during the experiment did so on day 14 following its introduction into the same cage as its infected counterpart, a time-to-death that is consistent with infection by its terminally ill cagemate. In order to determine the cause of this transmission event, analysis of viremia and viral loads as a result of shedding was performed. In line with our hypothesis, the terminally ill animal that infected its contact cagemate was the one that exhibited the highest viremia—shedding from the nasal cavity started earlier than for other challenged animals, and it was also the only animal in which shedding was detected from the rectal mucosa. As observed in guinea pigs, the exposure time of a naïve animal to an infected one was an essential factor in determining transmission. Similarly, limited evidence from this intramuscular challenge may suggest that length of exposure to an infected animal is associated with transmission efficiency in non-human primates. Of note, the third contact animal, which did not develop EVD following prolonged contact with its infected cagemate, was also the one exhibiting the highest levels of IgG. Overall, high viremia combined with early viral shedding may positively influence transmission rates in the context of an intramuscular infection. However, given that pre-existing immunity might have interfered with the experiment due to partial control of viral replication, a repeat experiment was performed within the same conditions, but using naïve animals.

While all three newly challenged animals succumbed to EVD 6-, 7-, and 8 days post-infection, none of their respective cagemates were found to become infected, or seroconvert. Interestingly, while two of the animals reached a viremia comparable to the transmitting animal of the previous experiment, shedding of infectious particles was limited to the oral cavity of these two same animals. Therefore, these results suggest that viral loads as a result of shedding, but not viremia, associate better with transmission in an intramuscular challenge model of non-human primates. Indeed, early mucosal shedding from multiple mucosal cavity seems to be important for initiating transmission in an IM model. Finally, building on previous work in guinea pigs infected intranasally that showed elevated transmission when compared to i.p.-infected animals—including the presence of viral antigen in the tracheal epithelium—we sought to evaluate whether intratracheal infection of non-human primates could result in a similar outcome. Interestingly, challenged animals succumbed to clinical EVD 7-, 8-, and 7 days post-infection, while their respective cagemates all succumbed 16-, 14-, and 15 days post-infection, exhibiting all the clinical signs associated with EVD. Analysis of viremia and viral loads as a result of shedding revealed that viremia reached similar levels to animals infected intramuscularly, although each transmitting animal exhibited higher levels of shedding, either via the oral, nasal, or rectal route, supporting the idea that viral loads, as a result of shedding specifically, are a predictor of transmission for Ebola virus. Overall, live virus titration suggests that an intratracheal challenge may have facilitated viral mucosal excretion, thereby facilitating

transmission. Indeed, it is conceivable that this challenge route induced a disease that promoted a more efficient transmission, such as infectious droplets being more easily generated when compared with an IM challenge.

4.4 Concluding remarks and future directions

The combination of published evidence, along with evidence presented throughout this thesis using human, ferret, and non-human primate data, is supportive of the hypothesis that viral load can be used as a predictor of disease severity and transmission. With regard to transmission, we have shown that viral loads as a result of shedding better associate with transmissibility of EBOV than viremia, and that the route of infection induces different transmission patterns. Future work in animal models should now focus on investigating which cell types and organs are specifically targeted in different routes of infections, in order to further our understanding of the underlying differences observed in transmission of EBOV by various infection routes.

Additional work with ferrets would also be required to explain the observed differences between male and female animals. Evaluation of immune activation will be critical in our ability to distinguish whether the discrepancies we observed between sexes were due to biological differences, such as an earlier immune response from females, which would have allowed them to more effectively control viral replication, ultimately preventing transmission of EVD to naïve animals; or whether the differences we observed were merely due to behavioural differences between male and female, where males were more prone to fighting, leading to an increased exposure to infected bodily fluids.

Aerosolization of Ebola virus has been described before, and can result in a lethal infection in animal models[339–341]. Although current evidence does not support a role for aerosol transmission of EBOV in the same way tuberculosis can be spread, this concept has been the subject of debate for years and has been discussed extensively, especially when an outbreak becomes harder to control, or when a genetically distinct isolate is discovered, with fear that novel mutations could confer it airborne-transmission properties[277]. In order to address this question experimentally, and now that the ferret has been established as both a lethal model of infection and transmission, it would be interesting to evaluate transmission within an aerosol transmission chamber, which allows differentiation between droplet and aerosol transmission, and which has been evaluated in the context of influenza infection. Finally, also regarding technological advances, one limitation of most transmission studies is the difficulty of evaluating the presence of fomites in the environment. While environmental sampling has been described previously in the context of outbreak response[342], its usefulness is limited by our ability to collect a sample from where virus is present. Novel techniques that would allow visualization of viruses on surfaces would greatly benefit transmission studies, allowing rapid evaluation of fomites on cage surfaces, for example. Overall, pursuing the evaluation of predictors of disease severity and transmission will be critical to better prioritize the

attribution of limited resources, in order to optimize clinical benefits and ultimately reduce morbidity and mortality associated with EBOV infection.

References

1. Kuhn JH, Andersen KG, Bào Y, et al. Filovirus RefSeq entries: evaluation and selection of filovirus type variants, type sequences, and names. Viruses [Internet] 2014 [cited 2014 Oct 16];6(9):3663–82. Available from: http://www.pubmedcentral.nih.gov/articlerender.fcgi?artid=4189044&tool=pmcentrez&rendertype=abstract

2. Kuhn JH, Bào Y, Bavari S, et al. Virus nomenclature below the species level: a standardized nomenclature for filovirus strains and variants rescued from cDNA. Arch Virol [Internet] 2013 [cited 2014 Jan 10];Available from: http://www.ncbi.nlm.nih.gov/pubmed/24190508

3. Kuhn JH, Andersen KG, Baize S, et al. Nomenclature- and Database-Compatible Names for the Two Ebola Virus Variants that Emerged in Guinea and the Democratic Republic of the Congo in 2014. Viruses [Internet] 2014;6(11):4760–99. Available from: http://www.mdpi.com/1999-4915/6/11/4760/

4. International Committee on Taxonomy of Viruses. Taxonomy [Internet]. EC 50, Washington, DC, July 2018. 2017 [cited 2018 Oct 23];Available from: https://talk.ictvonline.org/taxonomy/

5. Goldstein T, Anthony SJ, Gbakima A, et al. The discovery of Bombali virus adds further support for bats as hosts of ebolaviruses. Nat Microbiol [Internet] 2018;3(10):1084–9. Available from: http://dx.doi.org/10.1038/s41564-018-0227-2

6. Shi M, Lin XD, Chen X, et al. The evolutionary history of vertebrate RNA viruses. Nature 2018;556(7700):197–202.

7. International Committee on Taxonomy of Viruses Filoviridae Study Group. Two (2) new genera each including one (1) novel species in the family Filoviridae (Mononegavirales). ICTV Propos. Taxon. 2018;(September).

8. Yang X-L, Tan CW, Anderson DE, et al. Characterization of a filovirus (Měnglà virus) from Rousettus bats in China. Nat Microbiol [Internet] 2019;1. Available from: http://www.nature.com/articles/s41564-018-0328-y

9. International Committee on Taxonomy of Viruses. ICTV 9th Report (2011) [Internet]. 2011 [cited 2018 Oct 25];Available from: https://talk.ictvonline.org/ictv-reports/ictv_9th_report/negative-sense-rna-viruses-2011/w/negrna_viruses/194/mononegavirales

10. Feldmann H, Geisbert TW. Ebola haemorrhagic fever. Lancet 2011;377(9768):849–62.

11. Beniac DR, Melito PL, DeVarennes SL, et al. The organisation of Ebola virus reveals a capacity for extensive, modular polyploidy. PLoS One 2012;7(1):e29608.

12. Booth TF, Rabb MJ, Beniac DR. How do filovirus filaments bend without breaking? Trends Microbiol [Internet] 2013 [cited 2014 Jan 10];21(11):583–93. Available from: http://www.ncbi.nlm.nih.gov/pubmed/24011860

13. Regnery RL, Johnson KM, Kiley MP. Virion nucleic acid of Ebola virus. J Virol [Internet] 1980;36(2):465–9. Available from: http://www.pubmedcentral.nih.gov/articlerender.fcgi?artid=353663&tool=pmcentrez&rendertype=abstr

act

14. Sanchez A, Kiley MP, Holloway BP, Auperin DD. Sequence analysis of the Ebola virus genome: organization, genetic elements, and comparison with the genome of Marburg virus. Virus Res 1993;29:215–40.

15. Barrette RW, Xu L, Rowland JM, McIntosh MT. Current perspectives on the phylogeny of Filoviridae. Infect Genet Evol [Internet] 2011 [cited 2014 Dec 8];11(7):1514–9. Available from: http://www.ncbi.nlm.nih.gov/pubmed/21742058

16. Mühlberger E. Filovirus replication and transcription. J Plant Dis Prot 2007;2(2):205–15.

17. Sanchez A, Kiley MP, Holloway BP, McCormick JB, Auperin DD. The nucleoprotein gene of ebola virus: Cloning, sequencing, and in vitro expression. Virology 1989;170(1):81–91.

18. Watanabe S, Noda T, Kawaoka Y. Functional Mapping of the Nucleoprotein of Ebola Virus. J Virol 2006;80(8):3743–51.

19. Shi W, Huang Y, Sutton-Smith M, et al. A Filovirus-Unique Region of Ebola Virus Nucleoprotein Confers Aberrant Migration and Mediates Its Incorporation into Virions. J Virol [Internet] 2008;82(13):6190–9. Available from: http://jvi.asm.org/cgi/doi/10.1128/JVI.02731-07

20. Bharat TAM, Noda T, Riches JD, et al. Structural dissection of Ebola virus and its assembly determinants using cryo-electron tomography. Proc Natl Acad Sci [Internet] 2012;109(11):4275–80. Available from: http://www.pnas.org/cgi/doi/10.1073/pnas.1120453109

21. Prins KC, Binning JM, Shabman RS, Leung DW, Amarasinghe GK, Basler CF. Basic Residues within the Ebolavirus VP35 Protein Are Required for Its Viral Polymerase Cofactor Function . J Virol 2010;84(20):10581–91.

22. Takamatsu Y, Kolesnikova L, Becker S. Ebola virus proteins NP, VP35, and VP24 are essential and sufficient to mediate nucleocapsid transport. Proc Natl Acad Sci [Internet] 2018;115(5):1075–80. Available from: http://www.pnas.org/lookup/doi/10.1073/pnas.1712263115

23. Cárdenas WB, Loo Y-M, Gale Jr. M, et al. Ebola Virus VP35 Protein Binds Double-Stranded RNA and Inhibits Alpha / Beta Interferon Production Induced by RIG-I Signaling. J Virol 2006;80(11):5168–78.

24. Luthra P, Ramanan P, Mire CE, et al. Mutual antagonism between the Ebola virus VP35 protein and the RIG-I activator PACT determines infection outcome. Cell Host Microbe 2013;14(1):74–84.

25. Yen B, Mulder LCF, Martinez O, Basler CF. Molecular Basis for Ebolavirus VP35 Suppression of Human Dendritic Cell Maturation. J Virol [Internet] 2014;88(21):12500–10. Available from: http://jvi.asm.org/cgi/doi/10.1128/JVI.02163-14

26. Jin H, Yan Z, Prabhakar BS, et al. The VP35 protein of Ebola virus impairs dendritic cell maturation induced by virus and lipopolysaccharide. J Gen Virol 2010;91:352–61.

27. Lubaki NM, Ilinykh P, Pietzsch C, Tigabu B, Freiberg AN, Koup RA. The Lack of Maturation of Ebola Virus-Infected Dendritic Cells. J Virol 2013;87(13):7471–85.

28. Leung LW, Park M-S, Martinez O, Valmas C, López CB, Basler CF. Ebolavirus VP35 suppresses IFN production from conventional but not plasmacytoid dendritic cells. Immunol Cell Biol 2011;89:792–802.

29. Ruigrok RWH, Schoehn G, Dessen A, et al. Structural Characterization and Membrane Binding Properties of the Matrix Protein VP40 of Ebola Virus. J Mol Biol 2000;300:103–12.

30. Timmins J, Schoehn G, Kohlhaas C, Klenk H-D, Ruigrok RWH, Weissenhorn W. Oligomerization and polymerization of the filovirus matrix protein VP40. Virology 2003;312:359–68.

31. Bornholdt ZA, Noda T, Abelson DM, et al. Structural Rearrangement of Ebola Virus VP40 Begets Multiple Functions in the Virus Life Cycle. Cell 2013;154:763–74.

32. Pleet ML, Mathiesen A, DeMarino C, et al. Ebola VP40 in Exosomes Can Cause Immune Cell Dysfunction. Front Microbiol 2016;7:1–19.

33. Pleet ML, DeMarino C, Lepene B, Aman MJ, Kashanci F. The Role of Exosomal VP40 in Ebola Virus Disease. DNA Cell Biol 2017;36(4):243–8.

34. Sanchez a, Trappier SG, Mahy BW, Peters CJ, Nichol ST. The virion glycoproteins of Ebola viruses are encoded in two reading frames and are expressed through transcriptional editing. Proc Natl Acad Sci U S A 1996;93(8):3602–7.

35. Mehedi M, Falzarano D, Seebach J, et al. A new Ebola virus nonstructural glycoprotein expressed through RNA editing. J Virol [Internet] 2011 [cited 2014 Feb 18];85(11):5406–14. Available from: http://www.pubmedcentral.nih.gov/articlerender.fcgi?artid=3094950&tool=pmcentrez&rendertype=abstract

36. Volchkova VA, Klenk H-D, Volchkov VE. Delta-peptide is the carboxy-terminal cleavage fragment of the nonstructural small glycoprotein sGP of Ebola virus. Virology [Internet] 1999;265(1):164–71. Available from: http://www.ncbi.nlm.nih.gov/pubmed/10603327

37. de La Vega M-A, Wong G, Kobinger GP, Qiu X. The Multiple Roles of sGP in Ebola Pathogenesis. Viral Immunol 2014;28(1):1–7.

38. Zhu W, Banadyga L, Emeterio K, Wong G, Qiu X. The roles of ebola virus soluble glycoprotein in replication, pathogenesis, and countermeasure development. Viruses 2019;11(11).

39. Iwasa A, Shimojima M, Kawaoka Y. sGP serves as a structural protein in Ebola virus infection. J Infect Dis [Internet] 2011 [cited 2014 Mar 31];204 Suppl(Suppl 3):S897-903. Available from: http://www.pubmedcentral.nih.gov/articlerender.fcgi?artid=3218668&tool=pmcentrez&rendertype=abstract

40. Volchkova VA, Dolnik O, Martinez MJ, Reynard O, Volchkov VE. Genomic RNA editing and its impact on Ebola virus adaptation during serial passages in cell culture and infection of guinea pigs. J Infect Dis 2011;204(Suppl 3):S941-6.

41. Wahl-Jensen VM, Afanasieva TA, Seebach J, Ströher U, Feldmann H, Schnittler H-J. Effects of Ebola virus glycoproteins on endothelial cell activation and barrier function. J Virol [Internet] 2005 [cited 2014 Jan 13];79(16):10442–50. Available from: http://jvi.asm.org/content/79/16/10442.short

42. Mohan GS, Li W, Ye L, Compans RW, Yang C. Antigenic subversion: a novel mechanism of host immune evasion by Ebola virus. PLoS Pathog [Internet] 2012 [cited 2013 Sep 16];8(12):e1003065. Available from: http://www.pubmedcentral.nih.gov/articlerender.fcgi?artid=3521666&tool=pmcentrez&rendertype=abstract

43. Biedenkopf N, Schlereth J, Becker S, Hartmann RK. RNA Binding of Ebola Virus VP30 Is Essential for Activating Viral Transcription. J Virol 2016;90(16):7481–96.

44. Kirchdoerfer RN, Moyer CL, Abelson DM, Saphire EO. The Ebola Virus VP30-NP Interaction Is a Regulator of Viral RNA Synthesis. PLoS Pathog 2016;12(10):1–22.

45. Lier C, Becker S, Biedenkopf N. Dynamic phosphorylation of Ebola virus VP30 in NP-induced inclusion bodies. Virology 2017;512:39–47.

46. Xu W, Luthra P, Wu C, et al. Ebola virus VP30 and nucleoprotein interactions modulate viral RNA synthesis. Nat Commun [Internet] 2017;8:1–11. Available from: http://dx.doi.org/10.1038/ncomms15576

47. Batra J, Hultquist JF, Liu D, et al. Protein interaction mapping identifies RBBP6 as a negative regulator of Ebola virus replication. Cell 2018;175(7):1917–30.

48. Ilinykh PA, Tigabu B, Ivanov A, et al. Role of Protein Phosphatase 1 in Dephosphorylation of Ebola Virus VP30 and its Targeting for the Inhibition of Viral Transcription. [Internet]. 2014 [cited 2014 Jul 26]. Available from: http://www.ncbi.nlm.nih.gov/pubmed/24936058

49. Kruse T, Biedenkopf N, Hertz EPT, et al. The Ebola Virus Nucleoprotein Recruits the Host PP2A-B56 Phosphatase to Activate Transcriptional Support Activity of VP30. Mol Cell 2018;69(1):136-145.e6.

50. Banadyga L, Hoenen T, Ambroggio X, Dunham E, Groseth A, Ebihara H. Ebola virus VP24 interacts with NP to facilitate nucleocapsid assembly and genome packaging. Sci Rep [Internet] 2017;7(1):1–14. Available from: http://dx.doi.org/10.1038/s41598-017-08167-8

51. Watt A, Moukambi F, Banadyga L, et al. A novel lifecycle modeling system for Ebola virus shows a genome length-dependent role of VP24 on virus infectivity. J Virol [Internet] 2014 [cited 2014 Jun 30];88(18):10511–24. Available from: http://www.ncbi.nlm.nih.gov/pubmed/24965473

52. Xu W, Edwards MR, Borek DM, et al. Ebola Virus VP24 Targets a Unique NLS Binding Site on Karyopherin Alpha 5 to Selectively Compete with Nuclear Import of Phosphorylated STAT1. Cell Host Microbe 2014;16(2):187–200.

53. Zhang APP, Bornholdt ZA, Liu T, et al. The ebola virus interferon antagonist VP24 directly binds STAT1 and has a novel, pyramidal fold. PLoS Pathog 2012;8(2).

54. Huang G, Shi LZ, Chi H. Regulation of JNK and p38 MAPK in the immune system: Signal integration, propagation and termination. Cytokine [Internet] 2009;48(3):161–9. Available from: https://www.ncbi.nlm.nih.gov/pmc/articles/PMC3624763/pdf/nihms412728.pdf

55. Halfmann P, Neumann G, Kawaoka Y. The Ebolavirus VP24 protein blocks phosphorylation of p38 mitogen-activated protein kinase. J Infect Dis 2011;204(SUPPL. 3):953–6.

56. Tchesnokov EP, Raeisimakiani P, Ngure M, Marchant D, Götte M. Recombinant RNA-Dependent RNA Polymerase Complex of Ebola Virus. Sci Rep 2018;8(1):1–9.

57. Schmidt ML, Hoenen T. Characterization of the catalytic center of the Ebola virus L polymerase. PLoS Negl Trop Dis 2017;11(10):1–14.

58. Alvarez CP, Lasala F, Carrillo J, Muñiz O, Corbí AL, Delgado R. C-Type Lectins DC-SIGN and L-

SIGN Mediate Cellular Entry by Ebola Virus in cis and in trans . J Virol 2002;76(13):6841–4.

59. Takada A, Fujioka K, Tsuiji M, et al. Human Macrophage C-Type Lectin Specific for Galactose and N -Acetylgalactosamine Promotes Filovirus Entry . J Virol 2004;78(6):2943–7.

60. Ji X, Olinger GG, Aris S, Chen Y, Gewurz H, Spear GT. Mannose-binding lectin binds to Ebola and Marburg envelope glycoproteins, resulting in blocking of virus interaction with DC-SIGN and complement-mediated virus neutralization. J Gen Virol 2005;86(9):2535–42.

61. Chan SY, Empig CJ, Welte FJ, et al. Folate receptor-α is a cofactor for cellular entry by Marburg and Ebola viruses. Cell 2001;106(1):117–26.

62. Takada A, Watanabe S, Ito H, Okazaki K, Kida H, Kawaoka Y. Downregulation of beta1 integrins by Ebola virus glycoprotein: implication for virus entry. Virology 2000;278(1):20–6.

63. Shimojima M, Takada A, Ebihara H, et al. Tyro3 Family-Mediated Cell Entry of Ebola and Marburg Viruses. J Virol 2006;80(20):10109–16.

64. Kondratowicz AS, Lennemann NJ, Sinn PL, et al. T-cell immunoglobulin and mucin domain 1 (TIM-1) is a receptor for Zaire ebolavirus and Lake Victoria marburgvirus. Proc Natl Acad Sci U S A 2011;108(20):8426–31.

65. Moller-Tank S, Kondratowicz AS, Davey RA, Rennert PD, Maury W. Role of the Phosphatidylserine Receptor TIM-1 in Enveloped-Virus Entry. J Virol 2013;87(15):8327–41.

66. Acciani M, Lay M, Havranek KE, et al. Ebola Virus Requires Phosphatidylserine Scrambling Activity for Efficient Budding and Optimal Infectivity. J Virol 2021;1–40.

67. Jin C, Che B, Guo Z, et al. Single virus tracking of Ebola virus entry through lipid rafts in living host cells. Biosaf Heal [Internet] 2020;2(1):25–31. Available from: https://doi.org/10.1016/j.bsheal.2019.12.009

68. Nanbo A, Imai M, Watanabe S, et al. Ebolavirus is internalized into host cells via macropinocytosis in a viral glycoprotein-dependent manner. PLoS Pathog 2010;6(9).

69. Aleksandrowicz P, Marzi A, Biedenkopf N, et al. Ebola virus enters host cells by macropinocytosis and clathrin-mediated endocytosis. J Infect Dis 2011;204(SUPPL. 3):957–67.

70. Chandran K, Sullivan NJ, Felbor U, Whelan SP, Cunningham JM. Endosomal Proteolysis of the Ebola Virus Glycoprotein Is Necessary for Infection. Science (80-) 2005;308(5728):1643–5.

71. Carette JE, Raaben M, Wong AC, et al. Ebola virus entry requires the cholesterol transporter Niemann-Pick C1. Nature 2011;477(7364):340–3.

72. Mühlberger E, Weik M, Volchkov VE, Klenk H-D, Becker S. Comparison of the Transcription and Replication Strategies of Marburg Virus and Ebola Virus by Using Artificial Replication Systems. J Virol 1999;73(3):2333–42.

73. Hoenen T, Shabman RS, Groseth A, et al. Inclusion Bodies Are a Site of Ebolavirus Replication. J Virol 2012;86(21):11779–88.

74. Schudt G, Dolnik O, Kolesnikova L, Biedenkopf N, Herwig A, Becker S. Transport of Ebolavirus

Nucleocapsids Is Dependent on Actin Polymerization: Live-Cell Imaging Analysis of Ebolavirus-Infected Cells. J Infect Dis 2015;212(Suppl 2):S160–6.

75. Wu L, Jin D, Wang D, et al. The two-stage interaction of Ebola virus VP40 with nucleoprotein results in a switch from viral RNA synthesis to virion assembly/budding. Protein Cell [Internet] 2020;Available from: https://doi.org/10.1007/s13238-020-00764-0

76. Adu-Gyamfi E, Digman MA, Gratton E, Stahelin R V. Single-particle tracking demonstrates that actin coordinates the movement of the Ebola virus matrix protein. Biophys J [Internet] 2012;103(9):L41–3. Available from: http://dx.doi.org/10.1016/j.bpj.2012.09.026

77. Ruthel G, Demmin GL, Kallstrom G, et al. Association of Ebola Virus Matrix Protein VP40 with Microtubules. J Virol 2005;79(8):4709–19.

78. Lu J, Qu Y, Liu Y, et al. Host IQGAP1 and Ebola Virus VP40 Interactions Facilitate Virus-Like Particle Egress. J Virol 2013;87(13):7777–80.

79. Yamayoshi S, Noda T, Ebihara H, et al. Ebola Virus Matrix VP40 Protein Uses the COPII Transport System for Its Intracellular Transport. Cell Host Microbe 2009;3(3):168–77.

80. Nanbo A, Ohba Y. Budding of Ebola Virus Particles Requires the Rab11-Dependent Endocytic Recycling Pathway. J Infect Dis 2018;218(Suppl 5):S388–96.

81. Feldmann H, Nichol ST, Klenk H-D, Peters CJ, Sanchez A. Characterization of Filoviruses Based on Differences in Structure and Antigenicity of the Virion Glycoprotein. Virology 1994;199:469–73.

82. Volchkov VE, Feldmann H, Volchkova VA, Klenk H-D. Processing of the Ebola virus glycoprotein by the proprotein convertase furin. Proc Natl Acad Sci U S A [Internet] 1998;95(10):5762–7. Available from: http://www.pubmedcentral.nih.gov/articlerender.fcgi?artid=20453&tool=pmcentrez&rendertype=abstract

83. Ito H, Watanabe S, Takada A, Kawaoka Y. Ebola virus glycoprotein: proteolytic processing, acylation, cell tropism, and detection of neutralizing antibodies. J Virol [Internet] 2001 [cited 2014 Mar 18];75(3):1576–80. Available from: http://jvi.asm.org/content/75/3/1576.short

84. Wool-Lewis RJ, Bates P. Endoproteolytic Processing of the Ebola Virus Envelope Glycoprotein: Cleavage Is Not Required for Function. J Virol 1999;73(2):1419–26.

85. Neumann G, Feldmann H, Watanabe S, Lukashevich I. Reverse Genetics Demonstrates that Proteolytic Processing of the Ebola Virus Glycoprotein Is Not Essential for Replication in Cell Culture. J Virol 2002;76(1):406–10.

86. Pavadai E, Gerstman BS, Chapagain PP. A cylindrical assembly model and dynamics of the Ebola virus VP40 structural matrix. Sci Rep [Internet] 2018;8(1):1–11. Available from: http://dx.doi.org/10.1038/s41598-018-28077-7

87. Licata JM, Simpson-Holley M, Wright NT, Han Z, Paragas J, Harty RN. Overlapping motifs (PTAP and PPEY) within the Ebola virus VP40 protein function independently as late budding domains: involvement of host proteins TSG101 and VPS-4. J Virol [Internet] 2003;77(3):1812–9. Available from: http://ovidsp.ovid.com/ovidweb.cgi?T=JS&PAGE=reference&D=emed6&NEWS=N&AN=2003039328

88. Timmins J, Schoehn G, Ricard-Blum S, et al. Ebola virus matrix protein VP40 interaction with human cellular factors Tsg101 and Nedd4. J Mol Biol 2003;326(2):493–502.

89. Han Z, Sagum CA, Bedford MT, Sidhu SS, Sudol M, Harty RN. ITCH E3 Ubiquitin Ligase Interacts with Ebola Virus VP40 To Regulate Budding. J Virol 2016;90(20):9163–71.

90. Harty RN, Brown ME, Wang G, Huibregtse J, Hayes FP. A PPxY motif within the VP40 protein of Ebola virus interacts physically and functionally with a ubiquitin ligase: Implications for filovirus budding. Proc Natl Acad Sci [Internet] 2000;97(25):13871–6. Available from: http://www.pnas.org/cgi/doi/10.1073/pnas.250277297

91. Velásquez GE, Aibana O, Ling EJ, Diakite I, Mooring EQ, Murray MB. Time from Infection to Disease and Infectiousness for Ebola Virus Disease, a Systematic Review. Clin Infect Dis 2015;61(7):1135–40.

92. Lado M, Walker NF, Baker P, et al. Clinical features of patients isolated for suspected Ebola virus disease at Connaught Hospital, Freetown, Sierra Leone: A retrospective cohort study. Lancet Infect Dis [Internet] 2015;15(9):1024–33. Available from: http://dx.doi.org/10.1016/S1473-3099(15)00137-1

93. Chertow DS, Kleine C, Edwards JK, Scaini R, Giuliani R, Sprecher A. Ebola Virus Disease in West Africa - Clinical Manifestations and Management. N Engl J Med 2014;371(22):2054–7.

94. Hunt L, Gupta-Wright A, Simms V, et al. Clinical presentation, biochemical, and haematological parameters and their association with outcome in patients with Ebola virus disease: An observational cohort study. Lancet Infect Dis 2015;15(11):1292–9.

95. De Greslan T, Billhot M, Rousseau C, et al. Ebola Virus-Related Encephalitis. Clin Infect Dis 2016;63(8):1076–8.

96. Sagui E, Janvier F, Baize S, et al. Severe Ebola Virus Infection with Encephalopathy: Evidence for Direct Virus Involvement. Clin Infect Dis 2015;61(10):1627–8.

97. Rojek A, Horby P, Dunning J. Insights from clinical research completed during the west Africa Ebola virus disease epidemic. Lancet Infect Dis [Internet] 2017;17(9):e280–92. Available from: http://dx.doi.org/10.1016/S1473-3099(17)30234-7

98. Chaplin DD. Overview of the immune response. J Allergy Clin Immunol 2010;125(2):S3-23.

99. Kawasaki T, Kawai T. Toll-like receptor signaling pathways. Front Immunol 2014;5(SEP):1–8.

100. Pichlmair A, Reis e Sousa C. Innate Recognition of Viruses. Immunity 2007;27(3):370–83.

101. Malissen B, Tamoutounour S, Henri S. The origins and functions of dendritic cells and macrophages in the skin. Nat Rev Immunol 2014;14(6):417–28.

102. Chaplin DD. Overview of the immune response. J Allergy Clin Immunol [Internet] 2010;125(2):S3–23. Available from: https://linkinghub.elsevier.com/retrieve/pii/S0091674909028371

103. Mosmann TR, Cherwinski H, Bond MW, Giedlin MA, Coffman RL. Two types of murine helper T cell clone. I. Definition according to profiles of lymphokine activities and secreted proteins. J Immunol [Internet] 1986;136(7):2348–57. Available from: http://www.ncbi.nlm.nih.gov/pubmed/2419430

104. Bonilla FA, Oettgen HC. Adaptive immunity. J Allergy Clin Immunol [Internet] 2010;125(2 SUPPL.

2):S33–40. Available from: http://dx.doi.org/10.1016/j.jaci.2009.09.017

105. Geisbert TW, Hensley LE, Larsen T, et al. Pathogenesis of Ebola hemorrhagic fever in cynomolgus macaques: evidence that dendritic cells are early and sustained targets of infection. Am J Pathol [Internet] 2003 [cited 2014 Mar 3];163(6):2347–70. Available from: http://www.pubmedcentral.nih.gov/articlerender.fcgi?artid=1892369&tool=pmcentrez&rendertype=abstract

106. Mahanty S, Hutchinson K, Agarwal S, Mcrae M, Rollin PE, Pulendran B. Cutting Edge: Impairment of Dendritic Cells and Adaptive Immunity by Ebola and Lassa Viruses. J Immunol 2003;170(6):2797–801.

107. Ströher U, West E, Bugany H, Klenk H-D, Schnittler H-J, Feldmann H. Infection and Activation of Monocytes by Marburg and Ebola Viruses. J Virol 2001;75(22):11025–33.

108. Brannan JM, Froude JW, Prugar LI, et al. Interferon α/β Receptor-Deficient Mice as a Model for Ebola Virus Disease. J Infect Dis 2015;212(Suppl 2):S282–94.

109. Ebihara H, Takada A, Kobasa D, et al. Molecular determinants of Ebola virus virulence in mice. PLoS Pathog 2006;2(7):0705–11.

110. Reid SP, Leung LW, Hartman AL, et al. Ebola Virus VP24 Binds Karyopherin α1 and Blocks STAT1 Nuclear Accumulation. J Virol 2006;80(11):5156–67.

111. Yen B, Mulder LC, Martinez O, Basler CF. Molecular Basis for Ebola Virus VP35 Suppression of Human Dendritic Cell Maturation. 2014.

112. Kubota T, Matsuoka M, Chang TH, et al. Virus infection triggers SUMOylation of IRF3 and IRF7, leading to the negative regulation of type I interferon gene expression. J Biol Chem 2008;283(37):25660–70.

113. Prins KC, Cárdenas WB, Basler CF. Ebola Virus Protein VP35 Impairs the Function of Interferon Regulatory Factor-Activating Kinases IKKε and TBK-1. J Virol 2009;83(7):3069–77.

114. Feng Z, Cerveny M, Yan Z, He B. The VP35 Protein of Ebola Virus Inhibits the Antiviral Effect Mediated by Double-Stranded RNA-Dependent Protein Kinase PKR. J Virol 2007;81(1):182–92.

115. Gal-Ben-Ari S, Barrera I, Ehrlich M, Rosenblum K. PKR: A kinase to remember. Front Mol Neurosci 2019;11(January):1–20.

116. Brinkmann C, Nehlmeier I, Walendy-Gnirß K, et al. The Tetherin Antagonism of the Ebola Virus Glycoprotein Requires an Intact Receptor-Binding Domain and Can Be Blocked by GP1-Specific Antibodies. J Virol 2016;90(24):11075–86.

117. Kaletsky RL, Francica JR, Agrawal-Gamse C, Bates P. Tetherin-mediated restriction of filovirus budding is antagonized by the Ebola glycoprotein. Proc Natl Acad Sci U S A 2009;106(8):2886–91.

118. Volchkov VE, Volchkova VA, Slenczka W, Klenk HD, Feldmann H. Release of viral glycoproteins during Ebola virus infection. Virology 1998;245(1):110–9.

119. Nehls J, Businger R, Hoffmann M, et al. Release of Immunomodulatory Ebola Virus Glycoprotein-Containing Microvesicles Is Suppressed by Tetherin in a Species-Specific Manner. Cell Rep 2019;26(7):1841-1853.e6.

120. Geisbert TW, Hensley LE, Gibb TR, Steele KE, Jaax NK, Jahrling PB. Apoptosis induced in vitro and in vivo during infection by Ebola and Marburg viruses. Lab Invest [Internet] 2000;80(2):171–86. Available from: http://www.ncbi.nlm.nih.gov/pubmed/10701687

121. Baize S, Leroy EM, Georges-Courbot M-C, et al. Defective humoral responses and extensive intravascular apoptosis are associated with fatal outcome in Ebola virus-infected patients. Nat Med [Internet] 1999;5(4):423–6. Available from: http://www.ncbi.nlm.nih.gov/pubmed/10202932

122. Fausther-Bovendo H, Qiu X, He S, et al. NK Cells Accumulate in Infected Tissues and Contribute to Pathogenicity of Ebola Virus in Mice. J Virol 2019;93(10):1–12.

123. Leroy EM, Rouquet P, Formenty P, et al. Multiple Ebola Virus Transmission Events and Rapid Decline of Central African Wildlife. Science (80-) 2004;303(5656):387–90.

124. Swanepoel R, Leman PA, Burt FJ, et al. Experimental Inoculation of Plants and Animals with Ebola Virus. Emerg Infect Dis 1996;2(4):321–5.

125. Breman JG, Johnson KM, van der Groen G, et al. A Search for Ebola Virus in Animals in the Democratic Republic of the Congo and Cameroon: Ecologic, Virologic, and Serologic Surveys, 1979–1980. J Infect Dis [Internet] 1999;179(s1):S139–47. Available from: https://academic.oup.com/jid/article-lookup/doi/10.1086/514278

126. Leirs H, Mills JN, Krebs JW, et al. Search for the Ebola virus reservoir in Kikwit, Democratic Republic of the Congo: reflections on a vertebrate collection. J Infect Dis [Internet] 1999;179 Suppl(Suppl 1):S155-63. Available from: http://www.ncbi.nlm.nih.gov/pubmed/9988179

127. Leroy EM, Kumulungui B, Pourrut X, et al. Fruit bats as reservoirs of Ebola virus. Nature 2005;438(7068):575–6.

128. Pourrut X, Souris M, Towner JS, et al. Large serological survey showing cocirculation of Ebola and Marburg viruses in Gabonese bat populations, and a high seroprevalence of both viruses in Rousettus aegyptiacus. BMC Infect Dis 2009;9:159.

129. Olival K, Islam A, Yu M. Ebola virus antibodies in fruit bats, Bangladesh. Emerg Infect Dis 2013;19(2):270–3.

130. Hayman DTS, Emmerich P, Yu M, et al. Long-term survival of an urban fruit bat seropositive for ebola and lagos bat viruses. PLoS One 2010;5(8):2008–10.

131. Hayman DTS, Yu M, Crameri G, et al. Ebola virus antibodies in fruit bats, Ghana, West Africa. Emerg Infect Dis 2012;18(7):1207–9.

132. Pan Y, Zhang W, Cui L, Hua X, Wang M, Zeng Q. Reston virus in domestic pigs in China. Arch Virol 2014;159(5):1129–32.

133. World Health Organization (WHO). Ebola Reston in pigs and humans, Philippines. Wkly Epidemiol Rec 2009;84(7):49–50.

134. Fischer K, Jabaty J, Suluku R, et al. Serological Evidence for the Circulation of Ebolaviruses in Pigs From Sierra Leone. J Infect Dis [Internet] 2018;jiy330:1–7. Available from: http://fdslive.oup.com/www.oup.com/pdf/production_in_progress.pdf

135. Towner JS, Amman BR, Sealy TK, et al. Isolation of genetically diverse Marburg viruses from Egyptian fruit bats. PLoS Pathog 2009;5(7):e1000536.

136. Jones MEB, Schuh AJ, Amman BR, et al. Experimental inoculation of egyptian rousette bats (Rousettus aegyptiacus) with viruses of the ebolavirus and marburgvirus genera. Viruses 2015;7(7):3420–42.

137. Ahn M, Anderson DE, Zhang Q, et al. Dampened NLRP3-mediated inflammation in bats and implications for a special viral reservoir host. Nat Microbiol [Internet] 2019;4(5):789–99. Available from: http://dx.doi.org/10.1038/s41564-019-0371-3

138. Guito JC, Prescott JB, Arnold CE, et al. Asymptomatic Infection of Marburg Virus Reservoir Bats Is Explained by a Strategy of Immunoprotective Disease Tolerance. Curr Biol [Internet] 2021;31(2):257-270.e5. Available from: http://dx.doi.org/10.1016/j.cub.2020.10.015

139. Subudhi S, Rapin N, Misra V. Immune system modulation and viral persistence in bats: Understanding viral spillover. Viruses 2019;11(2).

140. World Health Organization (WHO). Ebola heamorrhagic fever in Zaire, 1976. Bull World Health Organ 1978;56(2):271–93.

141. Centers for Disease Control and Prevention. 40 Years of Ebola Virus Disease around the World. 2019;

142. Jacob ST, Crozier I, Fischer WA, et al. Ebola virus disease [Internet]. Springer US; 2020. Available from: http://dx.doi.org/10.1038/s41572-020-0147-3

143. World Health Organization (WHO). Ebola haemorrhagic fever in Sudan, 1976. 1978.

144. Emond RTD, Evans B, Bowen ETW, Lloyd G. A case of Ebola virus infection. Br Med J 1977;2:541–4.

145. Heymann DL, Weisfeld JS, Webb PA, Johnson KM, Cairns T, Berquist H. Ebola Hemorrhagic Fever : Tandala , Zaire , 1977-1978. J Infect Dis 1980;142(3):1977–8.

146. Baron RC, McCormick JB, Zubeir OA. Ebola virus disease in southern Sudan: hospital dissemination and intrafamilial spread. 1983.

147. Miranda MEG, White ME, Dayrit MM, Hayes CG, Ksiazek TG, Burans JP. Seroepidemiological study of filovirus related to Ebola in the Philippines. Lancet 1991;337:425–6.

148. Jahrling PB, Geisbert TW, Dalgard DW, et al. Preliminary report: isolation of Ebola virus from monkeys imported to USA. Lancet 1990;335:502–5.

149. Center for Disease Control and Prevention. Filovirus infection in animal handlers [Internet]. Morb. Mortal. Wkly. 1990;39(13):221. Available from: https://www.cdc.gov/mmwr/preview/mmwrhtml/00001593.htm

150. World Health Organization (WHO). Viral haemorrhagic fever in imported monkeys. Wkly Epidemiol Rec 1992;24:183.

151. Le Guenno B, Formenty P, Wyers M, Gounon P, Walker F, Boesch C. Isolation and partial characterisation of a new strain of Ebola virus. Lancet 1995;345:1271–4.

152. Georges A-J, Leroy EM, Renaut AA, et al. Ebola hemorrhagic fever outbreaks in Gabon, 1994-1997: epidemiologic and health control issues. J Infect Dis 1999;179 Suppl:S65–75.

153. Khan AS, Tshioko FK, Heymann DL, et al. The Reemergence of Ebola Hemorrhagic Fever, Democratic Republic of the Congo, 1995. J Infect Dis 1999;179:S76–86.

154. Borisevich I V., Markin VA, Firsova I V., Evseev AA, Khamitov RA, Maksimov VA. Hemorrhagic (Marburg, Ebola, Lassa, and Bolivian) fevers: epidemiology, clinical pictures, and treatment. Vopr Virusol - Probl Virol 2006;51(5):8–16.

155. Miranda ME, Ksiazek TG, Retuya TJ, et al. Epidemiology of Ebola (subtype Reston) virus in the Philippines, 1996. J Infect Dis 1999;179 Suppl(Suppl 1):S115–9.

156. Rollin PE, Williams RJW, Bressler DS, et al. Ebola (subtype Reston) virus among quarantined nonhuman primates recently imported from the Philippines to the United States. J Infect Dis 1999;179 Suppl:S108–14.

157. World Health Organization (WHO). Ebola haemorrhagic fever, South Africa. Wkly Epidemiol Rec 1996;71(47):113–20.

158. Okware SI, Omaswa FG, Zaramba S, et al. An outbreak of Ebola in Uganda. Trop Med Int Heal 2002;7(12):1068–75.

159. World Health Organization (WHO). Outbreak(s) of Ebola haemorrhagic fever, Congo and Gabon, October 2001-July 2002. Wkly Epidemiol Rec 2003;26:223–8.

160. Formenty P, Libama F, Epelboin A, et al. Outbreak of Ebola hemorrhagic fever in the Republic of the Congo, 2003: a new strategy? Médecine Trop 2003;63(3):291–5.

161. World Health Organization (WHO). Ebola haemorrhagic fever in the Republic of the Congo - update 6. Dis Outbreak News 2004;

162. Akinfeyeva LA, Aksyonova OI, Vasilyevich I V., et al. A case of Ebola hemorrhagic fever. Infektsionnye Bolezn 2005;3:85–8.

163. World Health Organization (WHO). Outbreak of Ebola haemorrhagic fever in Yambio, south Sudan, April - June 2004. Wkly Epidemiol Rec 2005;(43):369–76.

164. Nkoghe D, Kone ML, Yada A, Leroy EM. A limited outbreak of Ebola haemorrhagic fever in Etoumbi, Republic of Congo, 2005. Trans R Soc Trop Med Hyg 2011;105(8):466–72.

165. MacNeil A, Farnon EC, Morgan OW, et al. Filovirus outbreak detection and surveillance: Lessons from bundibugyo. J Infect Dis 2011;204(Suppl 3):761–7.

166. MakwKaput V. Déclaration fin d'épidémie de FHV à virus Ebola dans les zones de santé de Mweka, Bulape et Luebo, province du Kasai occidental, RD Congo. Memorandum 2007;

167. World Health Organization (WHO). End of Ebola outbreak in the Democratic Republic of the Congo [Internet]. Dis. Outbreak News. 2009 [cited 2019 Jan 22];Available from: https://www.who.int/csr/don/2009_02_17/en/

168. Barrette RW, Metwally SA, Rowland JM, et al. Discovery of swine as a host for the Reston ebolavirus.

Science 2009;325(5937):204–6.

169. MacNeil A, Shoemaker T, Balinandi S, et al. Reemerging Sudan Ebola virus disease in Uganda, 2011. Emerg Infect Dis 2012;18(9):1480–3.

170. Albariño CG, Shoemaker T, Khristova ML, et al. Genomic analysis of filoviruses associated with four viral hemorrhagic fever outbreaks in Uganda and the Democratic Republic of the Congo in 2012. Virology 2013;442(2):97–100.

171. Maganga GD, Kapetshi J, Berthet N, et al. Ebola Virus Disease in the Democratic Republic of Congo. N Engl J Med 2014;371(22):2083–91.

172. Baize S, Pannetier D, Oestereich L, et al. Emergence of Zaire Ebola Virus Disease in Guinea. N Engl J Med 2014;371:1418–25.

173. World Health Organization (WHO). Ebola virus disease, West Africa – update (May 28th, 2014). Dis. Outbreak News. 2014;

174. World Health Organization (WHO). Ebola virus disease in Liberia (March 30th, 2014) [Internet]. Dis. Outbreak News. 2014 [cited 2019 Jan 22];Available from: https://www.who.int/csr/don/2014_03_30_ebola_lbr/en/

175. Cenciarelli O, Pietropaoli S, Malizia A, et al. Ebola virus disease 2013-2014 outbreak in west Africa: an analysis of the epidemic spread and response. Int J Microbiol 2015;2015:769121.

176. World Health Organization (WHO). Ebola virus disease - Italy [Internet]. Dis. Outbreak News. 2015 [cited 2019 Jan 22];Available from: https://www.who.int/csr/don/13-may-2015-ebola/en/

177. World Health Organization (WHO). Ebola virus disease - Mali [Internet]. Dis. Outbreak News. 2014 [cited 2019 Jan 22];Available from: https://www.who.int/csr/don/31-october-2014-ebola/en/

178. World Health Organization (WHO). Ebola virus disease, West Africa - update [Internet]. Dis. Outbreak News. 2014 [cited 2019 Jan 22];Available from: https://www.who.int/csr/don/2014_07_31_ebola/en/

179. World Health Organization (WHO). Ebola virus disease update - Senegal [Internet]. Dis. Outbreak News. 2014 [cited 2019 Jan 22];Available from: https://www.who.int/csr/don/2014_08_30_ebola/en/

180. World Health Organization (WHO). Ebola virus disease - Spain [Internet]. Dis. Outbreak News. 2014 [cited 2019 Jan 22];Available from: https://www.who.int/csr/don/09-october-2014-ebola/en/

181. World Health Organization (WHO). Ebola virus disease - United States of America [Internet]. Dis. Outbreak News. 2014 [cited 2019 Jan 22];Available from: https://www.who.int/csr/don/01-october-2014-ebola/en/

182. World Health Organization (WHO). Ebola virus disease - Democratic Republic of the Congo [Internet]. Dis. Outbreak News. 2017 [cited 2019 Jan 22];Available from: https://www.who.int/csr/don/13-may-2017-ebola-drc/en/

183. World Health Organization (WHO). Ebola virus disease - Democratic Republic of the Congo [Internet]. Dis. Outbreak News. 2018 [cited 2019 Jan 22];Available from: https://www.who.int/csr/don/10-may-2018-ebola-drc/en/

184. World Health Organization (WHO). Ebola virus disease - Democratic Republic of the Congo [Internet]. Dis. Outbreak News. 2018 [cited 2019 Jan 22];Available from: https://www.who.int/csr/don/4-august-2018-ebola-drc/en/

185. World Health Organization. Ebola - Democratic Republic of the Congo [Internet]. [cited 2021 Jun 29];Available from: https://www.who.int/emergencies/disease-outbreak-news/item/2021-DON310

186. World Health Organization. Ebola - Guinea [Internet]. 2021 [cited 2021 Jun 29];Available from: https://www.who.int/emergencies/disease-outbreak-news/item/2021-DON328

187. World Health Organization. Ebola - Democratic Republic of the Congo [Internet]. 2021 [cited 2021 Jun 29];Available from: https://www.who.int/emergencies/disease-outbreak-news/item/2021-DON325

188. Franz DR, Jahrling PB, Friedlander AM, et al. Clinical recognition and management of patients exposed to biological warfare agents. J Am Med Assoc 1997;278(5):399–411.

189. Ministère de la Santé - RDC. Strategic response plan for the Ebola virus disease outbreak in the provinces of North Kivu and Ituri Democratic Republic of the Congo. 2019.

190. Cook BWM, Cutts TA, Nikiforuk AM, et al. Evaluating environmental persistence and disinfection of the Ebola virus Makona variant. Viruses 2015;7(4):1975–86.

191. Tiffany A, Dalziel BD, Kagume Njenge H, et al. Estimating the number of secondary Ebola cases resulting from an unsafe burial and risk factors for transmission during the West Africa Ebola epidemic. PLoS Negl Trop Dis 2017;11(6):1–15.

192. El Mekki AA, Van Der Groen G. A comparison of indirect immunofluorescence and electron microscopy for the diagnosis of some haemorrhagic viruses in cell cultures. J Virol Methods 1981;3(2):61–9.

193. Ksiazek TG, West CP, Rollin PE, Jahrling PB, Peters CJ. ELISA for the Detection of Antibodies to Ebola Viruses. J Infect Dis [Internet] 1999;179(Supplement 1):S192–8. Available from: http://jid.oxfordjournals.org/content/179/Supplement_1/S192.abstract

194. Broadhurst MJ, Brooks TJG, Pollock NR. Diagnosis of ebola virus disease: Past, present, and future. Clin Microbiol Rev 2016;29(4):773–93.

195. Sanchez A, Ksiazek TG, Rollin PE, et al. Detection and molecular characterization of Ebola viruses causing disease in human and nonhuman primates. J Infect Dis 1999;179 Suppl(Suppl 1):S164-9.

196. Towner JS, Rollin PE, Bausch DG, et al. Rapid Diagnosis of Ebola Hemorrhagic Fever by Reverse Transcription-PCR in an Outbreak Setting and Assessment of Patient Viral Load as a Predictor of Outcome. J Virol 2004;78(8):4330–41.

197. Leroy EM, Baize S, Lu CY, et al. Diagnosis of Ebola haemorrhagic fever by RT-PCR in an epidemic setting. J Med Virol 2000;60(4):463–7.

198. Broadhurst MJ, Kelly JD, Miller A, et al. ReEBOV Antigen Rapid Test kit for point-of-care and laboratory-based testing for Ebola virus disease: a field validation study. Lancet 2015;6736(15):1–8.

199. Jean Louis F, Huang JY, Nebie YK, et al. Implementation of broad screening with Ebola rapid diagnostic tests in Forécariah, Guinea. Afr J Lab Med 2017;6(1):1–7.

200. Dhillon RS, Srikrishna D, Kelly JD. Deploying RDTs in the DRC Ebola outbreak. Lancet [Internet] 2018;391(10139):2499–500. Available from: http://dx.doi.org/10.1016/S0140-6736(18)31315-1

201. Dudas G, Carvalho LM, Bedford T, et al. Virus genomes reveal factors that spread and sustained the Ebola epidemic. Nature 2017;544(7650):309–15.

202. Mate SE, Kugelman JR, Nyenswah TG, et al. Molecular Evidence of Sexual Transmission of Ebola Virus. New Englang J Med 2015;373:2448–54.

203. Kinganda-Lusamaki E, Black A, Mukadi DB, et al. Integration of genomic sequencing into the response to the Ebola virus outbreak in Nord Kivu, Democratic Republic of the Congo. Nat Med [Internet] 2021;1–7. Available from: http://dx.doi.org/10.1038/s41591-021-01302-z

204. Speranza E, Caballero I, Honko AN, et al. Previremic Identification of Ebola or Marburg Virus Infection Using Integrated Host-Transcriptome and Viral Genome Detection. 2020;11(3):1–14.

205. Bray M, Davis KJ, Geisbert T, Schmaljohn CS, Huggins J. A Mouse Model for Evaluation of Prophylaxis and Therapy of Ebola Hemorrhagic Fever. J Infect Dis 1998;178:651–61.

206. Rasmussen AL, Okumura A, Ferris MT, et al. Host genetic diversity enables Ebola hemorrhagic fever pathogenesis and resistance. Science (80-) [Internet] 2014 [cited 2014 Nov 29];346(6212):987–91. Available from: http://www.sciencemag.org/content/early/2014/10/29/science.1259595.short

207. Gibb TR, Bray M, Geisbert TW, et al. Pathogenesis of Experimental Ebola Zaire Virus Infection in BALB/c Mice. J Comp Pathol 2001;125:233–42.

208. Bray M. The role of the Type I interferon response in the resistance of mice to filovirus infection. J Gen Virol 2001;82:1365–73.

209. Bird BH, Spengler JR, Chakrabarti AK, et al. Humanized mouse model of Ebola virus disease mimics the immune responses in human disease. J Infect Dis 2015;212(11):703–11.

210. Connolly BM, Steele KE, Davis KJ, et al. Pathogenesis of Experimental Ebola Virus Infection in Guinea Pigs. J Infect Dis 1999;179(Suppl 1):S203–17.

211. Wong G, Qiu X, Richardson JS, et al. Ebola virus transmission in guinea pigs. J Virol 2015;89(2):1314–23.

212. Ebihara H, Zivcec M, Gardner D, et al. A syrian golden hamster model recapitulating ebola hemorrhagic fever. J Infect Dis 2013;207(2):306–18.

213. Tsuda Y, Safronetz D, Brown KS, et al. Protective efficacy of a bivalent recombinant vesicular stomatitis virus vaccine in the Syrian hamster model of lethal Ebola virus infection. J Infect Dis [Internet] 2011;204 Suppl(1):S1090-7. Available from: http://www.pubmedcentral.nih.gov/articlerender.fcgi?artid=3189997&tool=pmcentrez&rendertype=abstract

214. Falzarano D, Safronetz D, Prescott J, Marzi A, Feldmann F, Feldmann H. Lack of protection against ebola virus from chloroquine in mice and hamsters. Emerg Infect Dis 2015;21(6):1065–7.

215. Cross RW, Mire CE, Borisevich V, Geisbert JB, Fenton KA, Geisbert TW. The Domestic Ferret (Mustela putorius furo) as a Lethal Infection Model for Three Different Species of Ebolavirus. J Infect

Dis 2016;214(4):565–9.

216. Kroeker A, He S, de La Vega M, Wong G, Embury-Hyatt C, Qiu X. Characterization of Sudan Ebolavirus infection in ferrets. Oncotarget 2017;8(28):46262–72.

217. Kozak R, He S, Kroeker A, et al. Ferrets infected with Bundibugyo virus or Ebola virus recapitulate important aspects of human filoviral disease. J Virol 2016;90(20):9209–23.

218. Cross RW, Mire CE, Agans KN, Borisevich V, Fenton KA, Geisbert TW. Marburg and Ravn Viruses Fail to Cause Disease in the Domestic Ferret (Mustela putorius furo). J Infect Dis 2018;218(Suppl 5):S448–52.

219. Wong G, Zhang Z, He S, et al. Marburg and Ravn Virus Infections Do Not Cause Observable Disease in Ferrets. J Infect Dis 2018;0(June):1–4.

220. Kimble JB, Malherbe DC, Meyer M, et al. Antibody-Mediated Protective Mechanisms Induced by a Trivalent Parainfluenza Virus-Vectored Ebolavirus Vaccine. J Virol 2019;93(4):1–24.

221. Gilchuk P, Kuzmina N, Ilinykh PA, et al. Multifunctional Pan-ebolavirus Antibody Recognizes a Site of Broad Vulnerability on the Ebolavirus Glycoprotein. Immunity [Internet] 2018;49(2):363-374.e10. Available from: https://doi.org/10.1016/j.immuni.2018.06.018

222. Wong G, Leung A, He S, et al. The Makona Variant of Ebola Virus Is Highly Lethal to Immunocompromised Mice and Immunocompetent Ferrets. J Infect Dis [Internet] 2018;0(July):1–5. Available from: https://academic.oup.com/jid/advance-article/doi/10.1093/infdis/jiy141/5034235

223. Peng X, Alföldi J, Gori K, et al. The draft genome sequence of the ferret (Mustela putorius furo) facilitates study of human respiratory disease. Nat Biotechnol 2014;32(12):1250–5.

224. Cross RW, Speranza E, Borisevich V, et al. Comparative Transcriptomics in Ebola Makona-Infected Ferrets, Nonhuman Primates, and Humans. J Infect Dis 2018;218(Suppl 5):S486–95.

225. de La Vega M-A, Soule G, Tran KN, et al. Modeling Ebola Virus Transmission Using Ferrets. mSphere 2018;3(5):309–18.

226. Plotkin SA, Gilbert PB. Nomenclature for immune correlates of protection after vaccination. Clin Infect Dis 2012;54(11):1615–7.

227. Sullivan NJ, Hensley LE, Asiedu C, et al. CD8 + cellular immunity mediates rAd5 vaccine protection against Ebola virus infection of nonhuman primates. Nat Med [Internet] 2011;17(9):1128–31. Available from: http://dx.doi.org/10.1038/nm.2447

228. Dye JM, Herbert AS. Postexposure antibody prophylaxis protects nonhuman primates from filovirus disease. Proc Natl Acad Sci [Internet] 2012 [cited 2013 Oct 14];109(13):1–6. Available from: http://www.pnas.org/content/109/13/5034.short

229. Qiu X, Audet J, Wong G, et al. Successful treatment of ebola virus-infected cynomolgus macaques with monoclonal antibodies. Sci Transl Med 2012;4(138):138ra81.

230. Wong G, Richardson JS, Pillet S, et al. Immune parameters correlate with protection against ebola virus infection in rodents and nonhuman primates. Sci Transl Med 2012;4(158):158ra146.

231. Marzi A, Engelmann F, Feldmann F, et al. Antibodies are necessary for rVSV/ZEBOV-GP-mediated protection against lethal Ebola virus challenge in nonhuman primates. Proc Natl Acad Sci U S A [Internet] 2013 [cited 2014 Jan 21];110(5):1893–8. Available from: http://www.pubmedcentral.nih.gov/articlerender.fcgi?artid=3562844&tool=pmcentrez&rendertype=abstract

232. Jones SM, Feldmann H, Ströher U, et al. Live attenuated recombinant vaccine protects nonhuman primates against Ebola and Marburg viruses. Nat Med 2005;11(7):786–90.

233. Ledgerwood JE, DeZure AD, Stanley DA, et al. Chimpanzee Adenovirus Vector Ebola Vaccine. N Engl J Med 2017;376:928–38.

234. Domi A, Feldmann F, Basu R, et al. A Single Dose of Modified Vaccinia Ankara expressing Ebola Virus Like Particles Protects Nonhuman Primates from Lethal Ebola Virus Challenge. Sci Rep 2018;8(864):1–9.

235. Lingemann M, Liu X, Surman S, et al. Attenuated Human Parainfluenza Virus GP Administered Intranasally Is Immunogenic in African Green Monkeys. J Virol 2017;91(10):1–19.

236. Tsuda Y, Parkins CJ, Caposio P, et al. A cytomegalovirus-based vaccine provides long-lasting protection against lethal Ebola virus challenge after a single dose. Vaccine 2015;33(19):2261–6.

237. Olinger GG, Bailey MA, Dye JM, et al. Protective Cytotoxic T-Cell Responses Induced by Venezuelan Equine Encephalitis Virus Replicons Expressing Ebola Virus Proteins. J Virol 2005;79(22):14189–96.

238. Bazzill JD, Stronsky SM, Kalinyak LC, et al. Vaccine nanoparticles displaying recombinant Ebola virus glycoprotein for induction of potent antibody and polyfunctional T cell responses. Nanomedicine Nanotechnology, Biol Med [Internet] 2019;1–12. Available from: https://doi.org/10.1016/j.nano.2018.11.005

239. Warfield KL, Swenson DL, Olinger GG, Kalina W V., Aman MJ, Bavari S. Ebola virus-like particle-based vaccine protects nonhuman primates against lethal Ebola virus challenge. J Infect Dis 2007;196(SUPPL. 2).

240. Vanderzanden L, Bray M, Fuller D, et al. DNA vaccines expressing either the GP or NP genes of Ebola virus protect mice from lethal challenge. Virology [Internet] 1998;246(1):134–44. Available from: http://www.ncbi.nlm.nih.gov/pubmed/9657001

241. Blaney JE, Wirblich C, Papaneri AB, et al. Inactivated or Live-Attenuated Bivalent Vaccines That Confer Protection against Rabies and Ebola Viruses. J Virol 2011;85(20):10605–16.

242. Ohimain EI. Recent advances in the development of vaccines for Ebola virus disease. Virus Res [Internet] 2016;211:174–85. Available from: http://dx.doi.org/10.1016/j.virusres.2015.10.021

243. Takada A, Robinson C, Goto H, et al. A system for functional analysis of Ebola virus glycoprotein. Proc Natl Acad Sci 1997;94:14764–9.

244. Henao-Restrepo AM, Longini IM, Egger M, et al. Efficacy and effectiveness of an rVSV-vectored vaccine expressing Ebola surface glycoprotein: interim results from the Guinea ring vaccination cluster-randomised trial. Lancet [Internet] 2015;386(9996):857–66. Available from: http://linkinghub.elsevier.com/retrieve/pii/S0140673615611175

245. Anywaine Z, Whitworth H, Kaleebu P, et al. Safety and Immunogenicity of a 2-Dose Heterologous Vaccination Regimen with Ad26.ZEBOV and MVA-BN-Filo Ebola Vaccines: 12-Month Data from a Phase 1 Randomized Clinical Trial in Uganda and Tanzania. J Infect Dis 2019;220(1):46–56.

246. Mutua G, Anzala O, Luhn K, et al. Safety and Immunogenicity of a 2-Dose Heterologous Vaccine Regimen with Ad26.ZEBOV and MVA-BN-Filo Ebola Vaccines: 12-Month Data from a Phase 1 Randomized Clinical Trial in Nairobi, Kenya. J Infect Dis 2019;220(1):57–67.

247. Hansen F, Feldmann H, Jarvis MA. Targeting Ebola virus replication through pharmaceutical intervention. Expert Opin Investig Drugs [Internet] 2021;30(3):201–26. Available from: https://doi.org/10.1080/13543784.2021.1881061

248. Warren TK, MacLennan S, Mathis A, Giuliano E, Taylor R, Sheridan WP. Efficacy of Galidesivir against Ebola Virus Disease in Rhesus Monkeys. Open Forum Infect Dis 2017;4(suppl_1):S302–S302.

249. Warren TK, Jordan R, Lo MK, et al. Therapeutic efficacy of the small molecule GS-5734 against Ebola virus in rhesus monkeys. Nature 2016;531(7594):381–5.

250. Bixler SL, Bocan TM, Wells J, et al. Efficacy of favipiravir (T-705) in nonhuman primates infected with Ebola virus or Marburg virus. Antiviral Res [Internet] 2018;151(November 2017):97–104. Available from: https://doi.org/10.1016/j.antiviral.2017.12.021

251. Sissoko D, Laouenan C, Folkesson E, et al. Experimental Treatment with Favipiravir for Ebola Virus Disease (the JIKI Trial): A Historically Controlled, Single-Arm Proof-of-Concept Trial in Guinea. PLoS Med 2016;13(3):1–36.

252. Dunning J, Kennedy SB, Antierens A, et al. Experimental treatment of ebola virus disease with brincidofovir. PLoS One 2016;11(9):1–10.

253. Mupapa K, Massamba M, Kibadi K, et al. Treatment of Ebola hemorrhagic fever with blood transfusions from convalescent patients. J Infect Dis 1999;179(SUPPL. 1):18–23.

254. van Griensven J, Edwards T, de Lamballerie X, et al. Evaluation of Convalescent Plasma for Ebola Virus Disease in Guinea. N Engl J Med 2016;374(1):33–42.

255. Kudoyarova-Zubavichene NM, Sergeyev NN, Chepurnov AA, Netesov S V. Preparation and use of hyperimmune serum for prophylaxis and therapy of Ebola virus infections. J Infect Dis 1999;179(SUPPL. 1):218–23.

256. Jahrling PB, Geisbert TW, Geisbert JB, et al. Evaluation of immune globulin and recombinant interferon-α2b for treatment of experimental Ebola virus infections. J Infect Dis 1999;179(SUPPL. 1):224–34.

257. Oswald WB, Geisbert TW, Davis KJ, et al. Neutralizing antibody fails to impact the course of Ebola virus infection in monkeys. PLoS Pathog 2007;3(1):0062–6.

258. Pettitt J, Zeitlin L, Kim DH, et al. Therapeutic intervention of Ebola virus infection in rhesus macaques with the MB-003 monoclonal antibody cocktail. Sci Transl Med [Internet] 2013 [cited 2014 Mar 27];5(199):199ra113. Available from: http://www.ncbi.nlm.nih.gov/pubmed/23966302

259. Qiu X, Wong G, Audet J, et al. Reversion of advanced Ebola virus disease in nonhuman primates with ZMapp. Nature 2014;

260. The PREVAIL II Writing Group for the Multi-National PREVAIL II Study Team. A Randomized, Controlled Trial of ZMapp for Ebola Virus Infection. N Engl J Med [Internet] 2016;375(15):1448–56. Available from: http://www.nejm.org/doi/10.1056/NEJMoa1604330

261. Mulangu S, Dodd LE, Davey RT, et al. A Randomized, Controlled Trial of Ebola Virus Disease Therapeutics. N Engl J Med 2019;381(24):2293–303.

262. Pascal KE, Dudgeon D, Trefry JC, et al. Development of Clinical-Stage Human Monoclonal Antibodies That Treat Advanced Ebola Virus Disease in Nonhuman Primates. J Infect Dis 2018;218(Suppl 5):S612–26.

263. Gaudinski MR, Coates EE, Novik L, et al. Safety, tolerability, pharmacokinetics, and immunogenicity of the therapeutic monoclonal antibody mAb114 targeting Ebola virus glycoprotein (VRC 608): an open-label phase 1 study. Lancet [Internet] 2019;393(10174):889–98. Available from: https://linkinghub.elsevier.com/retrieve/pii/S0140673619300364

264. Ponce L, Kinoshita R, Nishiura H. Exploring the human-animal interface of Ebola virus disease outbreaks. Math Biosci Eng 2019;16(4):3130–43.

265. Walsh PD, Abernethy KA, Bermejo M, et al. Catastrophic ape decline in western equatorial Africa. Nature 2003;422(6932):611–4.

266. Walsh MG, Haseeb MA. The landscape configuration of zoonotic transmission of Ebola virus disease in West and Central Africa: Interaction between population density and vegetation cover. PeerJ 2015;2015(1).

267. Marí Saéz A, Weiss S, Nowak K, et al. Investigating the zoonotic origin of the West African Ebola epidemic. EMBO Mol Med [Internet] 2015;7(1):17–23. Available from: https://www.academia.edu/24080902/Investigating_the_zoonotic_origin_of_the_West_African_Ebola_epidemic

268. Dean NE, Halloran ME, Yang Y, Longini IM. Transmissibility and pathogenicity of Ebola virus: A systematic review and meta-analysis of household secondary attack rate and asymptomatic infection. Clin Infect Dis 2016;62(10):1277–86.

269. Reichler MR, Bangura J, Bruden D, et al. Household transmission of ebola virus: Risks and preventive factors, Freetown, Sierra Leone, 2015. J Infect Dis 2018;218(5):757–67.

270. Bausch DG, Towner JS, Dowell SF, et al. Assessment of the risk of Ebola virus transmission from bodily fluids and fomites. J Infect Dis 2007;196(Suppl 2):S142-147.

271. Vetter P, Fischer WA, Schibler M, Jacobs M, Bausch DG, Kaiser L. Ebola Virus Shedding and Transmission: Review of Current Evidence. J Infect Dis 2016;214(Suppl 3):S177–84.

272. Christie A, Davies-Wayne GJ, Cordier-Lassalle T, et al. Possible Sexual Transmission of Ebola Virus — Liberia , 2015. Morb Mortal Wkly Rep 2015;64(17):479–81.

273. Oduyebo T, Pineda D, Lamin M, Leung A, Corbett CR, Jamieson DJ. A Pregnant Patient With Ebola Virus Disease. Obstet Gynecol 2015;126(6):1273–5.

274. Jamieson DJ, Uyeki TM, Callaghan WM, Meaney-Delman D, Rasmussen SA. What Obstetrician-Gynecologists Should Know About Ebola: A Perspective From the Centers for Disease Control and

Prevention. Obstet Gynecol 2014;124(5):1005–10.

275. Arias A, Watson SJ, Asogun D, et al. Rapid outbreak sequencing of Ebola virus in Sierra Leone identifies transmission chains linked to sporadic cases. Virus Evol 2016;2(1):1–10.

276. Wong G, Qiu X, de La Vega M-A, et al. Pathogenicity Comparison Between the Kikwit and Makona Ebola Virus Variants in Rhesus Macaques. J Infect Dis 2016;214(Suppl 3):S281–9.

277. Mekibib B, Ariën KK. Aerosol transmission of filoviruses. Viruses 2016;8(5):1–16.

278. Madelain V, Baize S, Jacquot F, et al. Ebola viral dynamics in nonhuman primates provides insights into virus immuno-pathogenesis and antiviral strategies. Nat Commun 2018;9(1):1–11.

279. Kuhn JH, Jahrling PB. Clarification and guidance on the proper usage of virus and virus species names. Arch Virol 2010;155(4):445–53.

280. Ansari AA. Clinical features and pathobiology of Ebolavirus infection. J Autoimmun 2014;1–9.

281. Gire SK, Goba A, Andersen KG, et al. Genomic surveillance elucidates Ebola virus origin and transmission during the 2014 outbreak. Science (80-) 2014;345(6202):1369–72.

282. Dudas G, Rambaut A. Phylogenetic Analysis of Guinea 2014 EBOV Ebolavirus Outbreak. PLoS Curr 2014;6:1–11.

283. Grolla A, Mehedi M, Lindsay R, Bosio CM, Duse A, Feldmann H. Enhanced detection of Rift Valley fever virus using molecular assays on whole blood samples. J Clin Virol 2012;54(4):313–7.

284. Demby AH, Chamberlain J, Brown DW, Clegg CS. Early diagnosis of Lassa fever by reverse transcription-PCR. J Clin Microbiol 1994;32(12):2898–903.

285. Lee M, Tan C, Aw L, et al. Real-Time Fluorescence-Based PCR for Detection of Malaria Parasites Real-Time Fluorescence-Based PCR for Detection of Malaria Parasites. J Clin Microbiol 2002;40(11):4343–4345.

286. Dreier J, Störmer M, Kleesiek K. Use of bacteriophage MS2 as an internal control in viral reverse transcription-PCR assays. J Clin Microbiol 2005;43(9):4551–7.

287. Médecins Sans Frontières. Standard Operating Procedures, MSF Ethics Review Board. 2013.

288. Schoepp RJ, Rossi CA, Khan SH, Goba A, Fair JN. Undiagnosed acute viral febrile illnesses, Sierra Leone. Emerg Infect Dis [Internet] 2014;20(7):1176–82. Available from: http://www.pubmedcentral.nih.gov/articlerender.fcgi?artid=4073864&tool=pmcentrez&rendertype=abstract

289. Becquart P, Wauquier N, Mahlakõiv T, et al. High prevalence of both humoral and cellular immunity to Zaire ebolavirus among rural populations in Gabon. PLoS One 2010;5(2):1–9.

290. Boisen ML, Schieffelin JS, Goba A, et al. Multiple Circulating Infections Can Mimic the Early Stages of Viral Hemorrhagic Fevers and Possible Human Exposure to Filoviruses in Sierra Leone Prior to the 2014 Outbreak. Viral Immunol [Internet] 2015;28(1):19–31. Available from: http://online.liebertpub.com/doi/abs/10.1089/vim.2014.0108

291. Leroy EM, Baize S, Volchkov VE, et al. Human asymptomatic Ebola infection and strong inflammatory response. Lancet 2000;355:2210–5.

292. Tong Y-G, Shi W-F, Di Liu, et al. Genetic diversity and evolutionary dynamics of Ebola virus in Sierra Leone. Nature 2015;(302).

293. Olabode AS, Jiang X, Robertson DL, Lovell SC. Ebolavirus is evolving but not changing: No evidence for functional change in EBOV from 1976 to the 2014 outbreak. Virology [Internet] 2015;482:202–7. Available from: http://linkinghub.elsevier.com/retrieve/pii/S0042682215001695

294. World Health Organization (WHO). Factors that contributed to undetected spread of the Ebola virus and impeded rapid containment [Internet]. 2015;Available from: http://www.who.int/csr/disease/ebola/one-year-report/factors/en/

295. Marzi A, Feldmann F, Hanley PW, Scott DP, Günther S, Feldmann H. Delayed Disease Progression in Cynomolgus Macaques Infected with Ebola Virus Makona Strain. Emerg Inf Dis 2015;21(10):1777–83.

296. Jaax NK, Jahrling PB, Geisbert TW, et al. Transmission of Ebola virus (Zaire strain) to uninfected control monkeys in a biocontainment laboratory. Lancet 1995;346(8991–8892):1669–71.

297. Alimonti JB, Leung A, Jones S, et al. Evaluation of transmission risks associated with in vivo replication of several high containment pathogens in a biosafety level 4 laboratory. Sci Rep 2014;4(5824):1–7.

298. Kobinger GP, Leung A, Neufeld J, et al. Replication, pathogenicity, shedding, and transmission of Zaire ebolavirus in pigs. J Infect Dis 2011;204(2):200–8.

299. Weingartl HM, Embury-Hyatt C, Nfon C, Leung A, Smith G, Kobinger GP. Transmission of Ebola virus from pigs to non-human primates. Sci Rep 2012;2(811):1–4.

300. Spengler JR, Chakrabarti AK, Coleman-McCray JD, et al. Utility of Oral Swab Sampling for Ebola Virus Detection in Guinea Pig Model. 2015;21(10):1816–9.

301. Nkoghe D, Padilla C, Becquart P, et al. Risk factors for zaire ebolavirus-specific IgG in rural gabonese populations. J Infect Dis 2011;204(Suppl 3):S768–75.

302. Busico KM, Marshall KL, Ksiazek TG, et al. Prevalence of IgG antibodies to Ebola virus in individuals during an Ebola outbreak, Democratic Republic of the Congo, 1995. J Infect Dis 1999;179(Suppl 1):S102–7.

303. Bower H, Glynn JR. A systematic review and meta-analysis of seroprevalence surveys of ebolavirus infection. Sci Data [Internet] 2017;4(160133):1–9. Available from: http://www.nature.com/articles/sdata2016133

304. Zeng X, Blancett CD, Koistinen KA, et al. Identification and pathological characterization of persistent asymptomatic Ebola virus infection in rhesus monkeys. Nat Microbiol 2017;2:1–11.

305. Akerlund E, Prescott J, Tampellini L. Shedding of Ebola Virus in an Asymptomatic Pregnant Woman. N Engl J Med [Internet] 2015;372(25):2467–9. Available from: http://www.ncbi.nlm.nih.gov/pubmed/26083224

306. Leroy EM, Baize S, Debré P, Lansoud-Soukate J, Mavoungou E. Early immune responses

accompanying human asymptomatic Ebola infections. Clin Exp Immunol 2001;124:453–60.

307. Mire CE, Geisbert JB, Agans KN, Deer DJ, Fenton KA, Geisbert TW. Oral and Conjunctival Exposure of Nonhuman Primates to Low Doses of Ebola Makona Virus. J Infect Dis 2016;214(Suppl 3):S263–7.

308. Nkangu MN, Olatunde OA, Yaya S. The perspective of gender on the Ebola virus using a risk management and population health framework: A scoping review. Infect Dis Poverty 2017;6(1):1–9.

309. World Health Organization (WHO). Ebola outbreak 2014-2015. 2018;

310. World Health Organization (WHO). Ebola Virus Disease Democratic Republic of Congo: External Situation Report 1. Extern Situat Rep 2017;1(May):1–6.

311. World Health Organization (WHO). EBOLA VIRUS DISEASE Democratic Republic of Congo External Situation Report 1. Extern Situat Rep 2018;1(May):1–6.

312. Adepoju P. Ebola returns to Guinea and DR Congo. Lancet 2021;397(10276):781.

313. Mendoza EJ, Qiu X, Kobinger GP. Progression of Ebola Therapeutics During the 2014–2015 Outbreak. Trends Mol Med 2016;22(2):164–73.

314. Scott JT, Sesay FR, Massaquoi TA, Idriss BR, Sahr F, Semple MG. Post-Ebola Syndrome , Sierra Leone. Emerg Infect Dis 2016;22(4):641–6.

315. Carod-Artal FJ. Post-Ebolavirus disease syndrome : what do we know ? Post-Ebolavirus disease syndrome : what do we know ? Expert Rev Anti Infect Ther 2015;13(10):1185–7.

316. Lau MSY, Dalziel BD, Funk S, et al. Spatial and temporal dynamics of superspreading events in the 2014–2015 West Africa Ebola epidemic. Proc Natl Acad Sci 2017;114(9):2337–42.

317. Faye O, Boëlle PY, Heleze E, et al. Chains of transmission and control of ebola virus disease in Conakry, Guniea, in 2014 : an observational study. Lancet Infect Dis 2015;15(March):320–6.

318. Wong G, Liu W, Liu Y, Zhou B, Bi Y, Gao GF. MERS, SARS, and Ebola: The Role of Super-Spreaders in Infectious Disease. Cell Host Microbe 2015;18(4):398–401.

319. Nakayama E, Saijo M. Animal models for Ebola and Marburg virus infections. Front Microbiol 2013;4(September):267.

320. Mitchell SW, McCormick JB. Physicochemical inactivation of Lassa, Ebola, and Marburg viruses and effect on clinical laboratory analyses. J Clin Microbiol 1984;20(3):486–9.

321. Nanclares C, Kapetshi J, Lionetto F, et al. Ebola virus disease, democratic republic of the Congo, 2014. Emerg Infect Dis 2016;22(9):1579–86.

322. Hartley MA, Young A, Tran AM, et al. Predicting Ebola Severity: A Clinical Prioritization Score for Ebola Virus Disease. PLoS Negl Trop Dis 2017;11(2):1–20.

323. Li J, Duan HJ, Chen HY, et al. Age and Ebola viral load correlate with mortality and survival time in 288 Ebola virus disease patients. Int J Infect Dis [Internet] 2016;42:34–9. Available from: http://dx.doi.org/10.1016/j.ijid.2015.10.021

324. Lanini S, Portella G, Vairo F, et al. Blood kinetics of Ebola virus in survivors and nonsurvivors. J Clin Invest 2015;125(12):4692–8.

325. Lanini S, Portella G, Vairo F, et al. Relationship between viremia and specific organ damage in Ebola patients : a cohort study. Clin Infect Dis 2017;1–22.

326. Richard M, Knauf S, Lawrence P, et al. Factors determining human-to-human transmissibility of zoonotic pathogens via contact. Curr Opin Virol 2017;22:7–12.

327. Osterholm MT, Moore KA, Kelley NS, et al. Transmission of Ebola Viruses : What We Know and What We Do Not Know. MBio 2015;6(2):1–9.

328. Brasel T, Comer JE, Massey S, et al. Mucosal challenge ferret models of ebola virus disease. Pathogens 2021;10(3):1–17.

329. Curran KG, Gibson JJ, Marke D, et al. Cluster of Ebola Virus Disease Linked to a Single Funeral — Moyamba District ,. Morb Mortal Wkly Rep 2016;65(8):26–9.

330. Jacobs M, Rodger A, Bell DJ, et al. Late Ebola virus relapse causing meningoencephalitis: a case report. Lancet [Internet] 2016;388:498–503. Available from: http://dx.doi.org/10.1016/S0140-6736(16)30386-5

331. Howlett P, Brown C, Helderman T, et al. Ebola Virus Disease Complicated by Late-Onset Encephalitis and Polyarthritis , Sierra Leone. Emerg Infect Dis 2016;22(1):150–2.

332. Keita M, Diallo B, Mesfin S, et al. High subsequent mortality of Ebola virus disease survivors in Guinea : a nationwide retrospective cohort study. Lancet Infect Dis 2019;XX(XX):XX–XX.

333. Fox JG, Marini RP, editors. Biology and Diseases of the Ferret. 3rd editio. WILEY Blackwell; 2014.

334. Ghosh S, Klein RS. Sex Drives Dimorphic Immune Responses to Viral Infections. J Immunol 2017;198(5):1782–90.

335. Francis ME, Richardson B, McNeil M, et al. Male sex and age biases viral burden, viral shedding, an type 1 and 2 interferon responses during SARS-CoV-2 infection in ferrets. bioRxiv - Prepr 2021;1:1–40.

336. Bissel SJ, Carter CE, Wang G, et al. Age-Related Pathology Associated with H1N1 A/California/07/2009 Influenza Virus Infection. Am J Pathol [Internet] 2019;189(12):2389–99. Available from: http://dx.doi.org/10.1016/j.ajpath.2019.08.017

337. Jaax NK, Davis KJ, Geisbert TW, et al. Lethal experimental infection of rhesus monkeys with Ebola-Zaire (Mayinga) virus by the oral and conjunctival route of exposure. Arch Pathol Lab Med 1996;120(2):140–55.

338. Blaney JE, Marzi A, Willet M, et al. Antibody Quality and Protection from Lethal Ebola Virus Challenge in Nonhuman Primates Immunized with Rabies Virus Based Bivalent Vaccine. PLoS Pathog 2013;9(5):1–13.

339. Reed DS, Lackemeyer MG, Garza NL, Sullivan LJ, Nichols DK. Aerosol exposure to Zaire ebolavirus in three nonhuman primate species: differences in disease course and clinical pathology. Microbes Infect [Internet] 2011 [cited 2014 Jul 31];13(11):930–6. Available from:

http://www.ncbi.nlm.nih.gov/pubmed/21651988

340. Twenhafel NA, Shaia CI, Bunton TE, et al. Experimental Aerosolized Guinea Pig-Adapted Zaire Ebolavirus (Variant: Mayinga) Causes Lethal Pneumonia in Guinea Pigs. Vet Pathol [Internet] 2014 [cited 2014 Jun 11];Available from: http://www.ncbi.nlm.nih.gov/pubmed/24829285

341. Twenhafel NA, Mattix ME, Johnson JC, et al. Pathology of experimental aerosol Zaire ebolavirus infection in rhesus macaques. Vet Pathol [Internet] 2013 [cited 2014 Jul 31];50(3):514–29. Available from: http://www.ncbi.nlm.nih.gov/pubmed/23262834

342. Kapetshi J, Fausther-Bovendo H, Corbett CR, et al. Contribution of Environment Sample-Based Detection to Ebola Outbreak Management. J Infect Dis [Internet] 2018;(Xx Xxxx):1–5. Available from: https://academic.oup.com/jid/advance-article/doi/10.1093/infdis/jiy366/5133070%0Ahttp://www.ncbi.nlm.nih.gov/pubmed/30325435